Order Number 9205854

Tectonic, sedimentary, and volcanic processes associated with rifting of the central Bonin island arc

Brown, Glenn Russell, Ph.D.

University of Hawaii, 1991

U·M·I
300 N. Zeeb Rd.
Ann Arbor, MI 48106

TECTONIC, SEDIMENTARY, AND VOLCANIC PROCESSES ASSOCIATED WITH RIFTING OF THE CENTRAL BONIN ISLAND ARC

A DISSERTATION SUBMITTED TO THE GRADUATE DIVISION OF THE UNIVERSITY OF HAWAII IN PARTIAL FULFILLMENT OF THE REQUIREMENTS FOR THE DEGREE OF

DOCTOR OF PHILOSOPHY

IN GEOLOGY AND GEOPHYSICS

AUGUST 1991

By

Glenn R. Brown

Dissertation Committee:

Brian Taylor, Chairman

William Coulbourn

Patricia Fryer

Alexander Malahoff

George Walker

ACKNOWLEDGMENTS

I learned a great deal during my time in Hawaii and I owe much to the students and staff at the Hawaii Institute of Geophysics. I thank those who made these years a fond part of my memory. In particular I want to mention Paul Anderson, Phil Jarvis, Lynne Rodgers, Sharon Rodgers, Scott Rowland, and Martha Systrom. I thank Nancy Baker and Rick Hagen for helping with administrative matters after my leaving Hawaii. John Smith deserves a special thanks for preparing this work for submission.

Several families in Honolulu made Hawaii seem like home. I thank the Buxtons, Rodgers, Rowlands, and Thielens for the invites to dinner and the American hospitality.

The Marine Division of the Geological Survey of Japan opened their doors for my research. Masato Nohara and Fumitoshi Murakami of the Geological Survey of Japan arranged for me to work with their seismic-reflection data. Keiko and Kohji Fujioka provided a place to stay during my visits to Tsukuba.

Funding for this project was provided by the National Science Foundation **OCE 83-09757** and **OCE 84-10605**. Some maps and figures were drafted by Brook Bays and Nancy Hulbirt.

I was always told that one need not thank the committee in such acknowledgments. But I can't let this pass without praise for the cheerful support I received from my committee members. I also want to acknowledge the long hours spent by Brian Taylor waiting for and reviewing my work. As I sit on the other side of the desk I appreciate Brian's knowledge and the guidance he has provided.

ABSTRACT

When the lithosphere over a subducting slab is stretched, the upper crust at a site near the island arc breaks by asymmetric block-faulting. Areas of subsiding seafloor are quickly covered by tectonically controlled sedimentation and volcanism. Arc rifting is active today in the central Bonin island arc. This dissertation focuses on the morpho-tectonic development of seven semi-isolated basins between 29° and 31°30' N in the Bonin island arc that were surveyed in 1984 with the SeaMARC II sidescan acoustic imagery and bathymetry system. The fundamental physiographic features of the rift segments are the large arc volcanoes, the "active arc" and "proto-remnant arc" margins, and the rift-floor sediment basins. Normal faults, alternating in polarity toward and away from the active arc, appear to have first divided the upper crust into large blocks. Strain on the hanging wall rollovers caused closely-spaced step faults, antithetic but occasionally synthetic to the primary master faults. The master fault zones alternate between the proto-remnant and active arc margins and have a regional orthorhombic pattern analogous to continental rifting. The orthorhombic pattern of the master faults, also observed in older cross-arc normal faults, is thought to be a result of a distributive strain in the upper crust resulting in the development of multiple "simultaneous" slip planes. Sediments, ponded in terraced basins on the walls of the rift and in the main rift-floor depocenters, vary in acoustic facies as a function of depth and distance away from the shallow arc volcano sources. Unconsolidated sediments on the floor of the rifts are reworked by bottom currents, as evidenced by the uniform distribution of 3.5 kHz acoustic facies. Mass wasting on the uplifted walls of the rifts and upper slopes of the arc volcanoes have fed turbidites into young basins. Over 1000 volcanoes were found in the rifted area. The sampled volcanoes are composed of pillowed basalts and dacites which erupted on pre-rift basement highs near rift accommodations zones. Locally, the bimodal volcanism is controlled by the normal faults in the pre-rift and syn-rift section.

TABLE OF CONTENTS

LIST OF ILLUSTRATIONS

Figure **Page**

ABBREVIATIONS AND SYMBOLS

Br	Bedrock
km	kilometers
m	meters
mbsl	meters below sea level
Sp	Prolonged echo-character facies with no subbottom eflectors (BR0 in Chapter II)
Ss	Multiple subbottom reflectors (BR1+ in Chapter II)
SRNB	Sumisu Rift North Basin
SRSB	Sumisu Rift South Basin
STL	Sofu Gan Tectonic Line
Su	Unclassified echo-character facies
TRNB	Torishima Rift North Basin
TRSB	Torishima Rift South Basin
TRWB	Torishima Rift West Basin

(see Appendix for table of symbols and abbreviations used in map figures)

PREFACE

This is a study of the tectonic, sedimentary, and volcanic processes associated with arc volcanism and lithospheric extension in the central Bonin island arc. The work is based on SeaMARC II sidescan acoustic imagery and bathymetry, single-channel seismic reflection data, and 3.5 kHz data collected from the central Bonin island arc, between 29° N and 31°20' N. In the first chapter, I introduce models for island-arc rifting and present an overview of the Bonin island arc. The second chapter deals with detailed morphologies and echo-character mapping in the Sumisu Rift segment. The third chapter focuses on the development of the Sumisu and Torishima rifts in the central Bonin backarc region between 29°50' N and 31°20' N. The fourth chapter looks at the subsidence and uplift in the Sofu Gan segment between 29° N and 29°50' N. SeaMARC II imagery and bathymetry data and a geological map at 1:200,000 are appended to this thesis.

CHAPTER I

Introduction

1.1 Formation of backarc basins

The western Pacific is a mosaic of Tertiary marginal basins and island arcs (Figure 1.1, 1.2). Active "backarc" basins are generally characterized by shallow (<10 km) crustal deformation (e.g. [*Eguchi and Uyeda*, 1983; *Hussong and Sinton*, 1983]). Mature basins appear to have crustal sections analogous to oceanic crust [*LaTraille and Hussong*, 1980; *Bibee et al.*, 1980] and have yielded fresh basalts transitional between island-arc tholeiites and N-type mid-ocean ridge basalts [*Fryer et al.*, 1982].

Several ideas have been proposed to explain the occurrence of the marginal basins in the western Pacific but few of the early models considered the basins to be a product of crustal extension [*Karig* , 1971a]. *Wegener* [1929] came close when he attributed them to wide gaps left behind as arcuate island festoons were abandoned by the westward drift of the Eurasian continent. With new seismic reflection data from the Tonga-Kermadec island-arc system [*Karig*, 1970] and the Mariana Trough [*Karig*, 1971b]. *Karig* [1971a] published the now established model, that basins in the backarc originate by rifting at sites near their frontal arc volcanoes.

Since Karig's early work, the literature on backarc basin geology has flourished, yet few studies have addressed the important nascent stage of the opening process. How the crust in an island arc undergoes extension remains today a key problem in plate tectonics.

To understand the geologic processes that control the growth of backarc basins we need to look at an area where the extensional process is active today and where the opening has not yet advanced to the stage of spreading. There are only a handful of arc-trench systems in the Western Pacific undergoing extension (Figure 1.1, 1.2). This

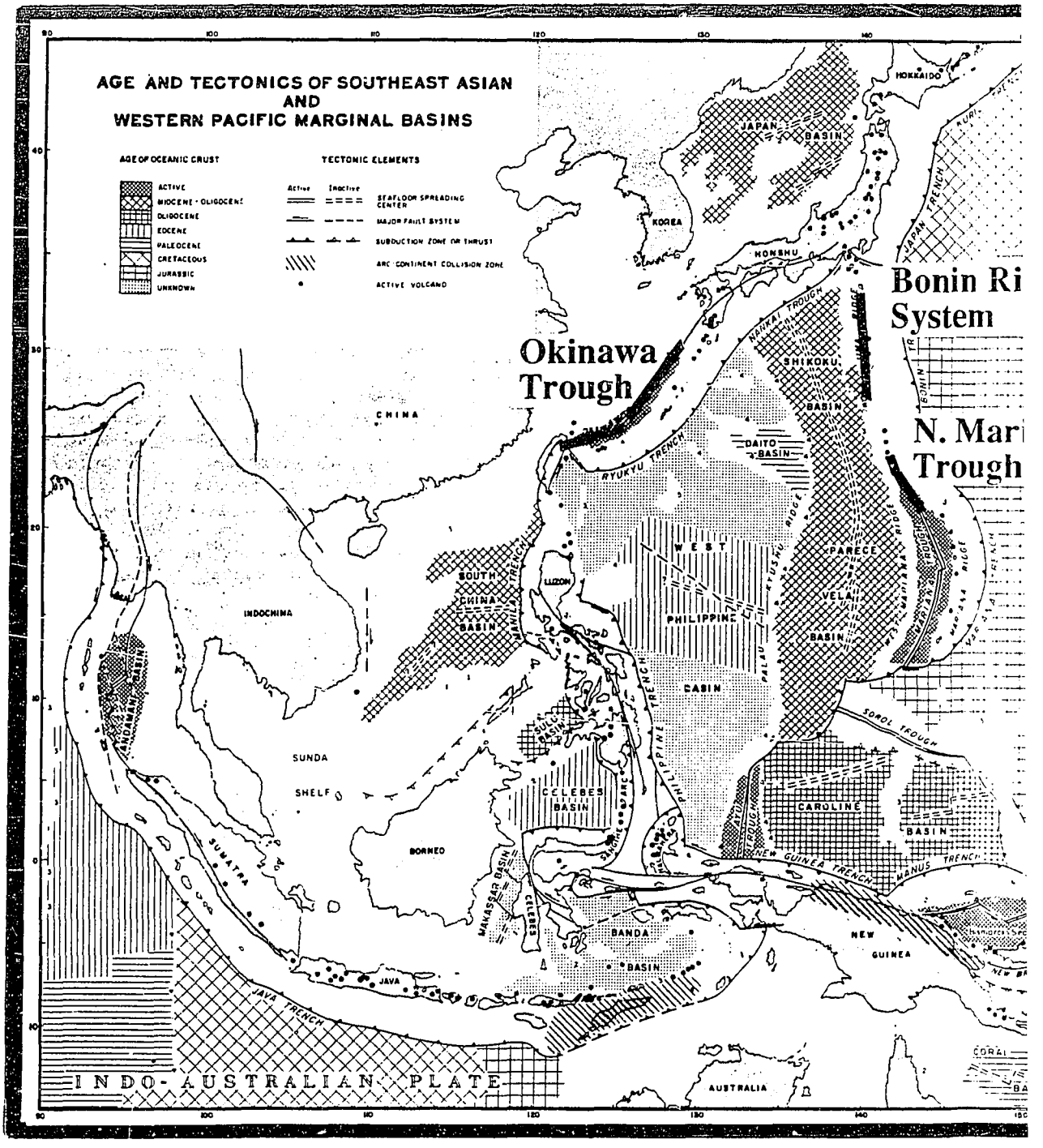

Figure 1.1 The marginal basins of the western Pacific (after *Taylor and Karner* [1983]) showing the approximate age of crust in the basins. Solid lines indicate sites of island arc rifting (without a developed spreading center) above a subducting slab: the **Bonin Rift System** (this dissertation), the **Okinawa Trough** [*Sibuet et al.*, 1987], and the **Northern Mariana Trough** [*Beal*, 1987].

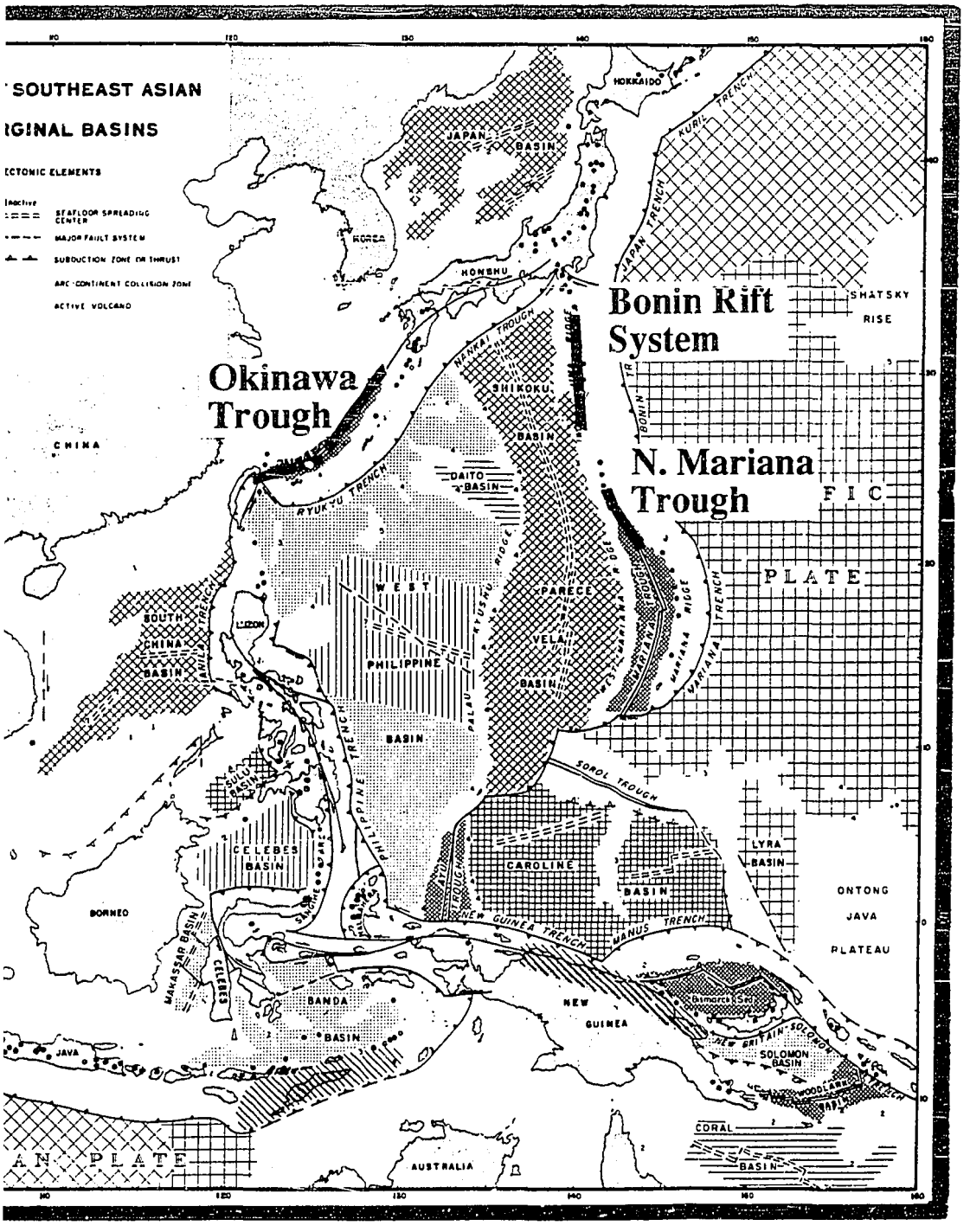

of the western Pacific (after *Taylor and Karner* [1983]) showing the
asins. Solid lines indicate sites of island arc rifting (without a devel-
ubducting slab: the **Bonin Rift System** (this dissertation), the
1987], and the **Northern Mariana Trough** [*Beal*, 1987].

Figure 1.2 The marginal basins of the southwestern Pacific (after *Taylor and Karner* [1983]) showing the approximate age of crust in the basins. Solid lines indicate sites of island arc rifting (without a developed spreading center) above a subducting slab: the **Coriolis Trough** [*Dubois et al.*, 1978], and the **Taupo Rift/Havre Trough** [*Malahoff et al.*, 1982].

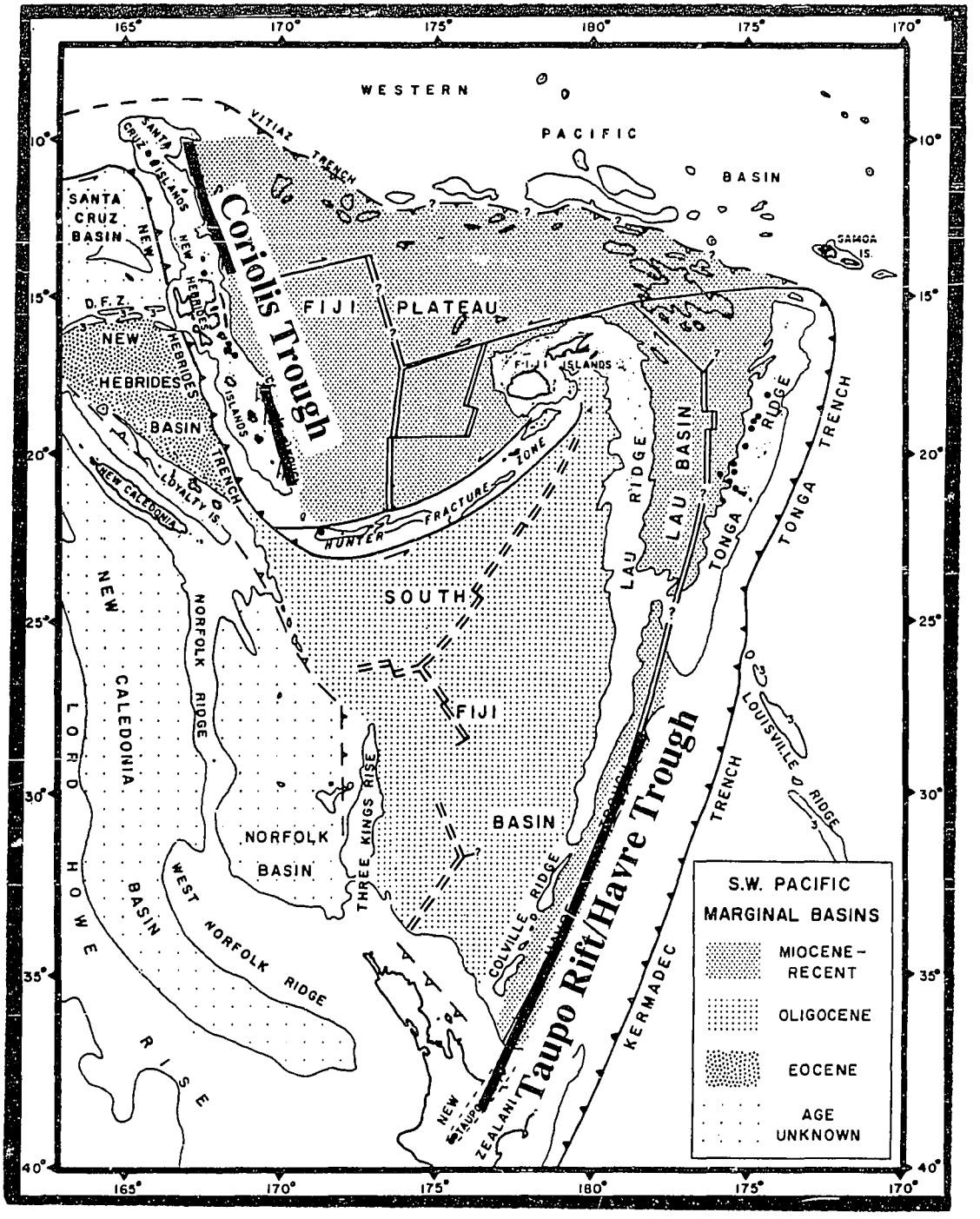
WESTERN
PACIFIC
BASIN
VITIAZ TRENCH
SANTA CRUZ ISLANDS
SANTA CRUZ BASIN
NEW HEBRIDES TRENCH
Coriolis Trough
FIJI PLATEAU
D.F.Z.
NEW HEBRIDES BASIN
NEW HEBRIDES ISLANDS
FIJI ISLANDS
SAMOA IS.
LAU RIDGE
LAU BASIN
TONGA RIDGE
TONGA TRENCH
LOYALTY IS.
NEW CALEDONIA
HUNTER FRACTURE ZONE
SOUTH FIJI BASIN
NEW CALEDONIA BASIN
NORFOLK RIDGE
LORD HOWE RISE
THREE KINGS RISE
NORFOLK BASIN
WEST NORFOLK RIDGE
COLVILLE RIDGE
Taupo Rift/Havre Trough
KERMADEC TRENCH
LOUISVILLE RIDGE
NEW ZEALAND
S.W. PACIFIC MARGINAL BASINS
MIOCENE - RECENT
OLIGOCENE
EOCENE
AGE UNKNOWN
165°
170°
175°
180°
10°
15°
20°
25°
30°
35°
40°

dissertation focuses on the controls and processes of subsidence, uplift, volcanism, faulting and sedimentation, in one of these systems-the central Bonin (*Izu-Ogasawara*) island arc.

Active rifting above a subducting slab

The surface expression of continental extension is characterized by both crustal subsidence and uplift. These phenomena are explained by two groups of models based on the role of the underlying asthenosphere. Extension is thought to occur either from doming and arching, related to a thermal anomaly in the asthenosphere ("active" rifting) or from horizontal stretching of the lithosphere by mechanical tension ("passive" rifting). The classical models for active rifting above a subducting slab use a thermal anomaly in the underlying asthenosphere, but differ in the mechanism to produce the anomaly. Backarc basins were recognized in the late 1960's to be areas of high heat flow [Vaquier et *al.*, 1966], although for inactive basins the heat-flow values are consistent with the age of the crust [*Watanabe,* 1977], and lower lithosphere Sn-wave attenuation [*Molnar and Oliver,* 1969]. *Karig* [1971b] put forward the idea that the opening of arcs is caused by a thermal plume activated by partial melting of the downgoing slab. Karig [1974] postulated that dewatering of the downgoing slab could generate enough heat to perturb convection in the asthenosphere above the slab. A cold sinking slab emplaced into the warm asthenosphere could also induce convection in the asthenosphere [*Sleep and Toksöz*, 1971] and form a thermal anomaly underneath the lithosphere (Figure 1.3A) leading to crustal extension. The major problem with these active models, however, is that they can be expected to affect every subduction zone and so fail to explain why rifting is unique to only certain arcs [*Karig,* 1971b; *Taylor and Karner,* 1983; *Uyeda and Kanamori,* 1986].

Passive rifting above a subducting slab

Models for passive rifting above a subducting slab focus on the dynamic action between the converging plates. Crustal deformation in the overriding plate may be predicted from the kinematics between the two plates [*Dewey*, 1980] (Figure 1.3B). A tensile stress regime is produced as the subducting plate retreats from the overriding plate or *vice versa*. Although models for seaward motion of the trench began to appear in the literature in the early 1970's [*Elsasser*, 1971; *Moberly*, 1972] they generally failed to explain the precise mechanism for retreat. *Molnar and Atwater* [1978] pointed out that an increased age of the subducting lithosphere would accelerate subduction and cause the subducting plate to retreat. *Chase* [1978], in a study of hot spot and relative motions of the plates, found that almost all oceanic subduction zones have absolute motions toward the subducting plate. In the Bonin arc, for example, *Chase* [1978] estimates the Philippine Sea and Pacific plates have a 20 mm/yr difference that is accounted for by rifting in the backarc.

Other models for the mechanical opening of backarc regions attribute extension to unique local features observed in the rifting arc such as the angle of subduction or the geometry of the subducting slab. Backarc opening of the rhomb-shaped grabens in the Okinawa Trough has been attributed to pull-aparts on dextral shears in the overriding continental crust [*Sibuet et al.*, 1987]. Collision of the d'Entrecasteaux Fracture Zone has been suggested as way of opening the backarc troughs in the New Hebrides arc [*Collot et al.*, 1985]. The subducting ridge compresses the central New Hebrides, as evident by uplift along the central arc and the absence of backarc opening opposite the collision zone. Strain in the neighbouring backarc, controls the geometry of the rift basins that straddle either side.

Subduction of a buckled slab and a subsequent acceleration of asthenospheric flow could induce tension in the overriding plate above the warp [*Bayly*, 1982] (Figure 1.3C). Yet this model overlooks the fact that rifting occurs above several subducting

Figure 1.3 Examples of models proposed for the formation of backarc basins. **(A)** Mantle convection activated by the penetration of a cold subducting plate into the hot asthenosphere [*Sleep and Toksöz,* 1971]. **(B)** A kinematic model ([after *Uyeda*, 1983] based on the model by [*Dewey,* 1980]) where backarc opening results from the interaction between plates. The absolute velocity of the arc "platelet" ($\mathbf{V_f}$) is fixed on the "x" axis (perpendicular to the hinge, "h"). The backarc opens when the "x" component of overriding plate absolute velocity ($\mathbf{V_o}$) is positive. **(C)** A cartoon model showing how subduction of a buckled slab and a subsequent change in the velocity of the convecting mantle might allow for a passive opening of the backarc [*Bayly,* 1982].

A

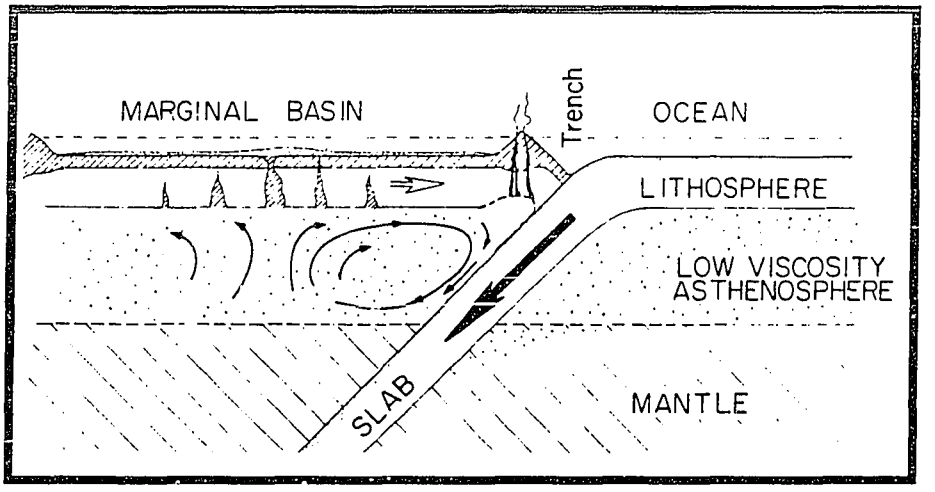
MARGINAL BASIN
Trench
OCEAN
LITHOSPHERE
LOW VISCOSITY
ASTHENOSPHERE
SLAB
MANTLE

B

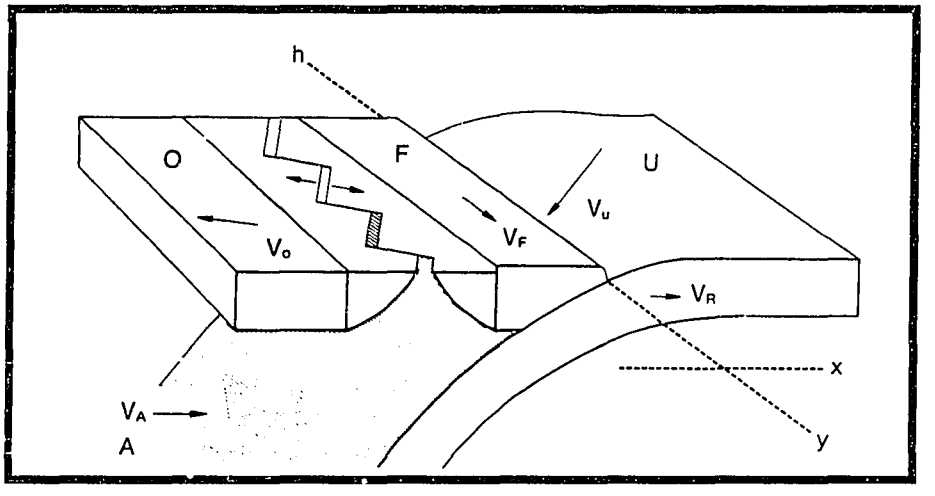
h
O
F
U
V_o
V_F
V_u
V_R
x
y
V_A
A

C

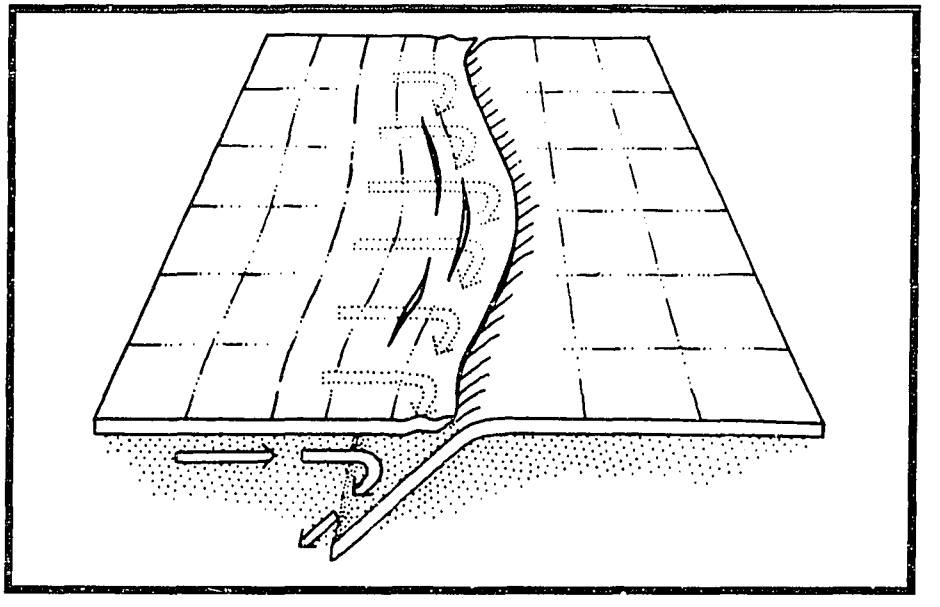

slabs without a central warp (e.g. the Bonin arc, the New Hebrides arc and the Kermadec arc), and that those arcs with a subducting warp and backarc-arc opening have already advanced into a spreading mode (e.g. the Mariana arc and the Scotia arc).

Little is known about the seafloor geology in a rifting island arc and how it relates to the development of a large backarc basin. For example, in the mid-Oligocene the proto-Bonin arc underwent extension that lead to the growth of the Shikoku Basin (Figure 1.4 [*Charmot-Rooke,* 1987]). From anomaly 6C time to anomaly 5B new crust was generated along a southward propagating axis that gives the basin a fan-shaped morphology [*Kobayashi and Nakada,* 1979]. The backarc opening lead to the separation of the Palau-Kyushu ridge, which is a series of bathymetric highs described by *Karig* [1972] as a "remnant arc". A set of NE-trending fracture zones traverse the basin from the old spreading-center to the "Iwo Jima Ridge", where the arc volcanism in the Bonin arc is occurring today. Some of these fractures lie on trend with lineaments in the Iwo Jima Ridge (note wavy contours along the Iwo-Jima Ridge margin in Figure 1.4) and might have been conceived during the earlier rifting event.

1.2 Historic mapping

Isolated from inhabited lands, the Bonin Islands (indicated as "*Malabrigo*" in early maps) and the southern segment of the arc, ("Volcano Islands") were not charted until 1543 when sighted by the early Spanish explorers. Late in the 1500's a Japanese explorer, Ogasawara Sadayori, founded a small settlement on the islands [*Gast,* 1944]. Though they were latter settled by European, American, and Hawaiians in the 19th century, the islands remained unclaimed until Imperial Japan annexed the group in 1878.

The early navigation charts show a variety of names were used for the forearc archipelago and island volcanoes. The place names fall into four groups, (1) original words from the Japanese language (e.g. Ogasawara), (2) Japanese equivalents of foreign words (e.g. Sumisu=Smith Island), (3) foreign words (e.g. Bayonaisse Rocks), and

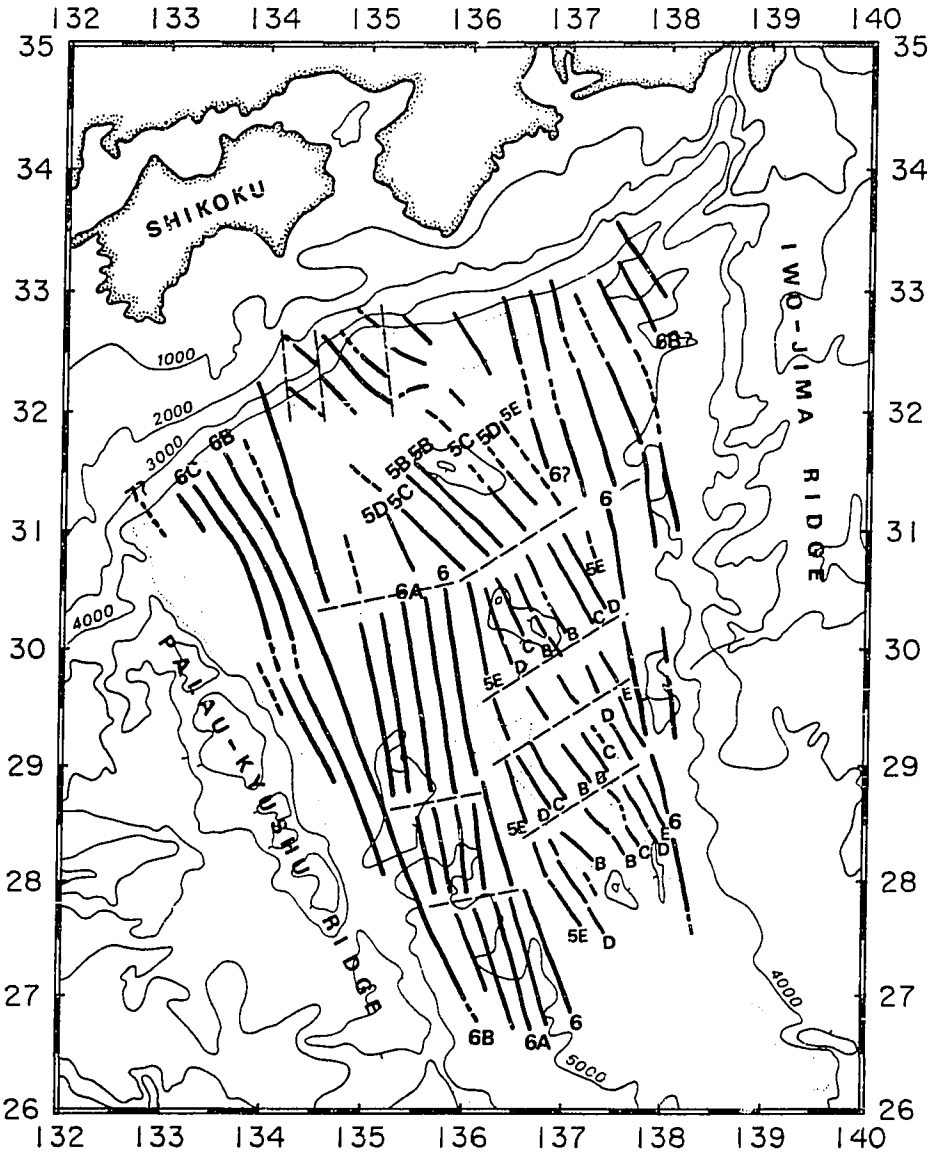

Figure 1.4 Fracture zones and magnetic lineations in the Shikoku Basin identified by *Charmot-Rooke* [1987]. The basin opened by rifting of the proto-Bonin arc before anomaly 6C.

(4) romanized equivalents of Japanese *kanji*. Early Japanese settlers used the *kanji* symbols for "no man", pronounced "*bu nin*" in Japanese, for the islands. This term was later romanized into "bonin" but was restricted in use to the cluster of islands on the forearc.

In the past the Japanese scientific community has used other terms to describe the arc such as "Fuji Volcanic Zone" (as Mt. Fuji is the northernmost volcano on the chain) [*Tsuya,* 1936] and "*Nampo Shoto*" (the seven islands). The Hydrographic Office of Japan now recognizes the term "Ogasawara" for the forearc islands, and "Izu-Ogasawara" for the volcanic islands (*E. Honza,* per comm.). A further discussion on the terminology used in the Bonin area can be found in Chapter III.

In the late 1800's regional echo-sounding maps of the bathymetry around Japan began to appear in the literature. Two early maps, published in *Chigaku Zasshi* [1890, 1895], show the gross morphology of the Bonin Trench and the Iwo-Jima Ridge. The 1890 map (Figure 1.5A) also shows an extra island in the backarc area near Sumisujima. An ephemeral island volcano, mentioned by *Kuno* [1962] existed between the 1870's and 1923 "18 km southwest of Sumisujima". Attempts to verify the historic existence of the island have been unsuccessful and it's now believed that it appeared in the Japanese scientific literature because of an erroneous citation in the early 1900's (*M. Nohara,* pers comm.).

By 1937 the Hydrographic Office of the Imperial Japanese Navy had produced a more detailed bathymetric map (Figure 1.5B) which shows deep water southwest of Sumisujima. No description of the deep appeared until the 1960's (Chapter II). The main bathymetric highs west of the arc line, which we now know correspond to crustal uplifts along the western boundary of the rift system, also appear on this chart.

The entire Bonin arc is part of Japan's 200 km exclusive economic zone. In 1979 the Geological Survey of Japan was commissioned to study possible hydrothermal metal occurrences in these waters. By 1985 the combined ship tracks from the Geological

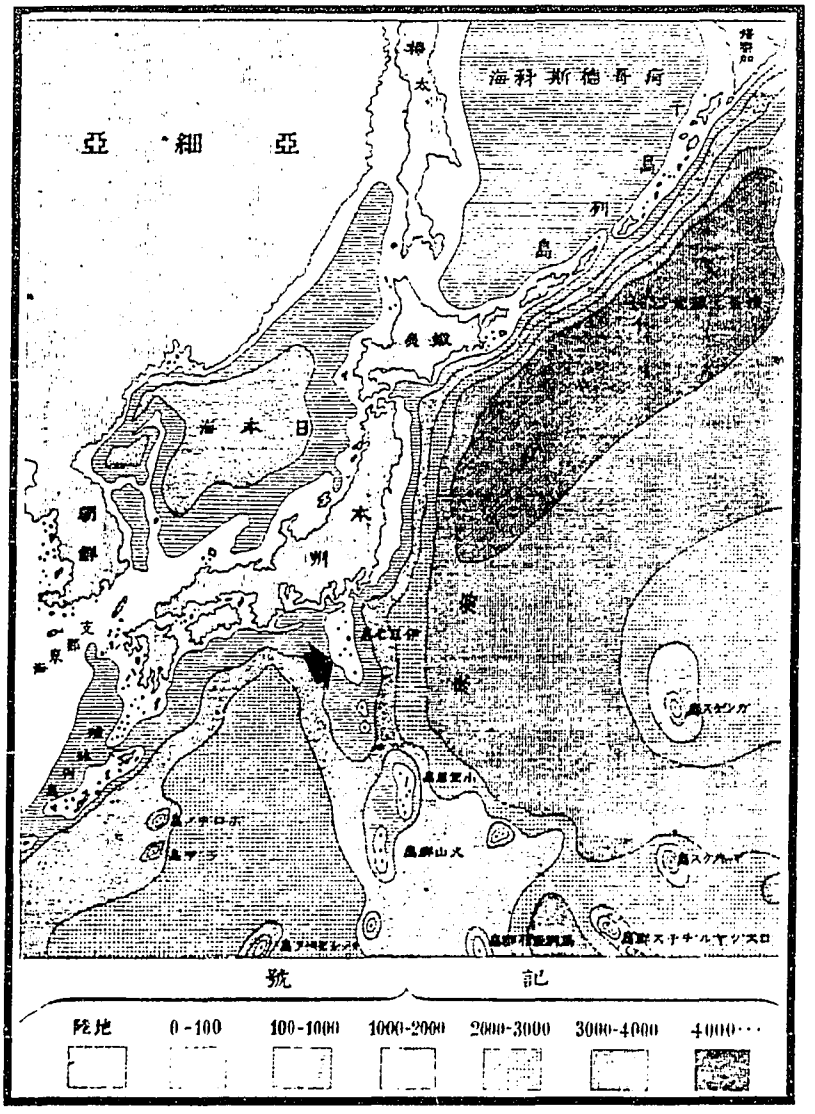

A

Figure 1.5 Historic bathymetry charts of the Bonin arc. **(A)** Published in an 1890 geographical journal, *Chigaku Zasshi* (v.1), this map shows an extra island in the central Bonin arc (indicated with an arrow). Although mentioned in the literature, it's likely that these islands ever existed. The islands forming the arc today have been the main sites of historic eruptions. **(B)** The 1937 chart [*Tsuyu,* 1937] shows the Sumisu Rift (indicated by arrow) and the gross bathymetric features (e.g. the high west of Torishima).

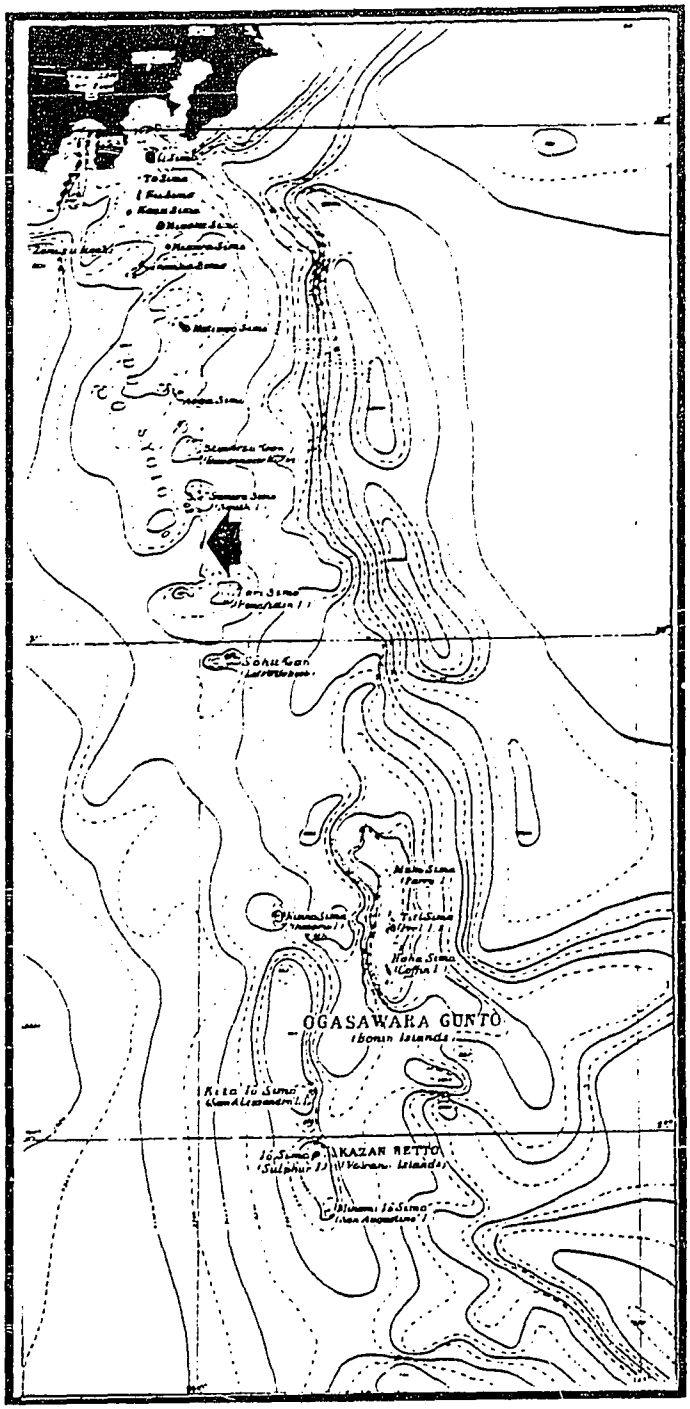
OGASAWARA GUNTO
(Bonin Islands)
KAZAN RETTO
(Volcano Islands)

B

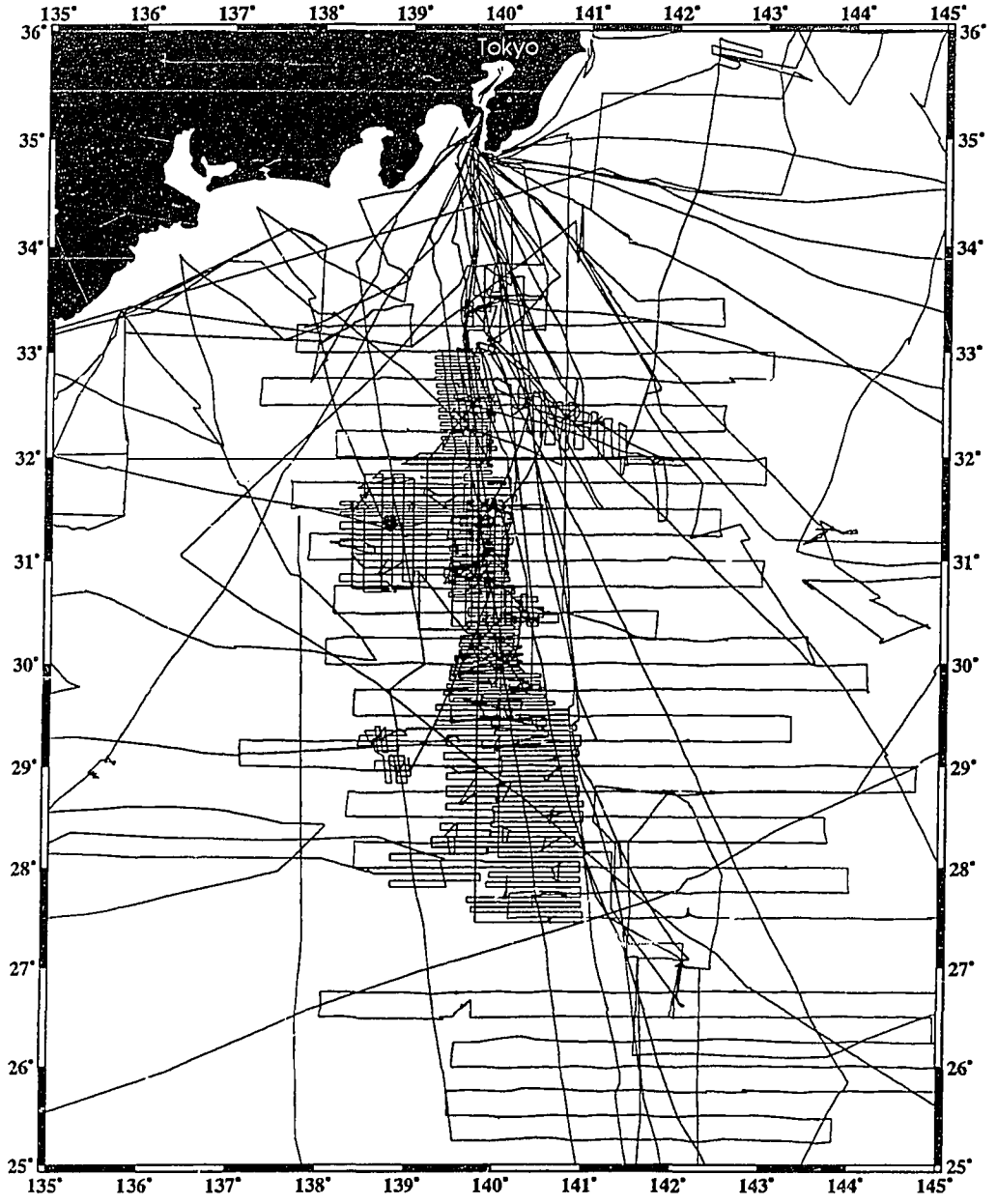

Figure 1.6 Ship tracks in the Bonin area from the Geological Survey of Japan and the Hawaii Institute of Geophysics

Survey of Japan (*R/V Hakurei Maru*) and the Hawaii Institute of Geophysics (*R/V Kana Keoki*) created a dense mesh of geophysical data over the northern arc (Figure 1.6). Parts of these data are used in this thesis to interpret the seafloor geology in the central Bonin backarc.

1.3 Bonin Island Arc

A projected profile of an edifice to edifice line along the arc (Figure 1.7) shows a northward shoaling of the deeps between regularly spaced volcanoes. The deepest point between the volcanoes occurs in the southern arc near a major oblique discontinuity termed by *Yuasa* [1985] the "Sofu Gan Tectonic Line" (Chapter III). With the exception of Nishinoshima, all volcanoes in the southern arc are submarine. To the north, concomitant with shoaling of the arc platform, subaereal volcanoes become more common and often coalesce to form large islands (e.g. Hachijojima, Oshima).

The Bonin arc lies on the northeastern edge of the Philippine Sea plate. Because the Bonin arc forms by oblique subduction of the Pacific Plate beneath the Philippine Sea Plate it can be argued that Hakone and Fuji, in southern Honshu, are the northern part of the chain. The Wadati-Benioff zone beneath the arc has a 45° dip in the north. The slab gradually steepens to near vertical in the south [*Katsumata and Sykes,* 1969]. In the north, the overriding Philippine Sea plate slips beneath Japan's main island of Honshu. The Bonin arc is in collision with this coast and in the past segments of the arc have accreted onto Honshu (Chapter III).

The regional free-air gravity map in the Bonin arc (Figure 1.8) [*Honza and Tamaki,* 1985] shows, that the anomaly over the arc volcanoes typically exceeds +80 mgals. Most seamounts along the arc line have a similar density between approximately 2.5 and 2.7 g/cc [*Ishihara,* 1987]. An outstanding feature in the free-air gravity field is the Bonin Ridge and the Bonin Trough, between 26° and 29.5° N and between 141.5° and 143° E (Chapter IV). Over a distance of 120 km this region experiences the earth's greatest free-air gravity

Figure 1.7 Edifice to edifice profile of the Bonin arc for the area covered in Figure 1.6. There is gentle shoaling of the arc platform north of the Sofu Gan Tectonic Line, toward Honshu.

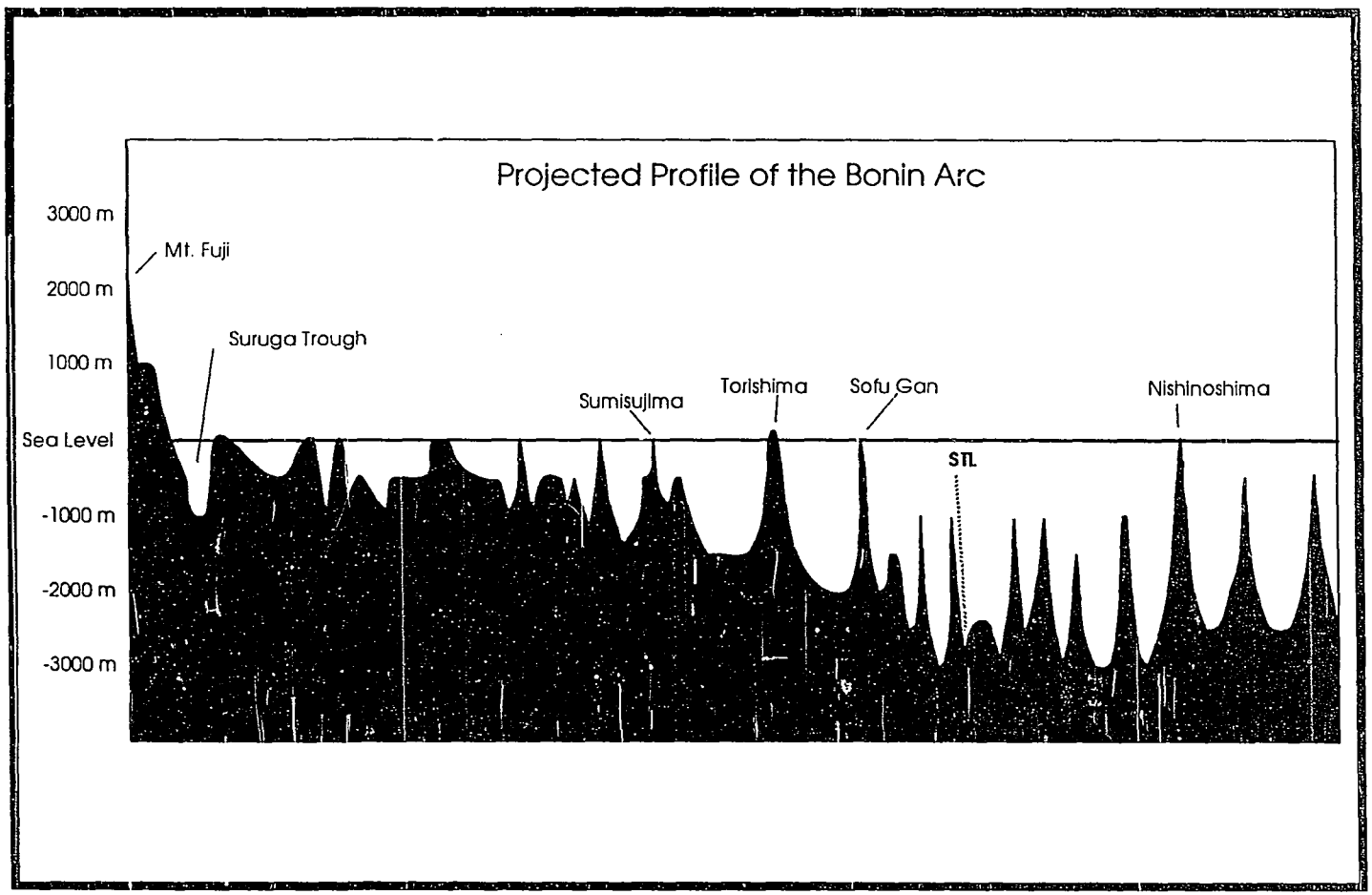
Projected Profile of the Bonin Arc
3000 m
2000 m
1000 m
Sea Level
-1000 m
-2000 m
-3000 m
Mt. Fuji
Suruga Trough
Sumisujima
Torishima
Sofu Gan
STL
Nishinoshima

Figure 1.8 Regional free-air gravity over the Bonin arc compiled by [*Honza and Tamaki,* 1985].

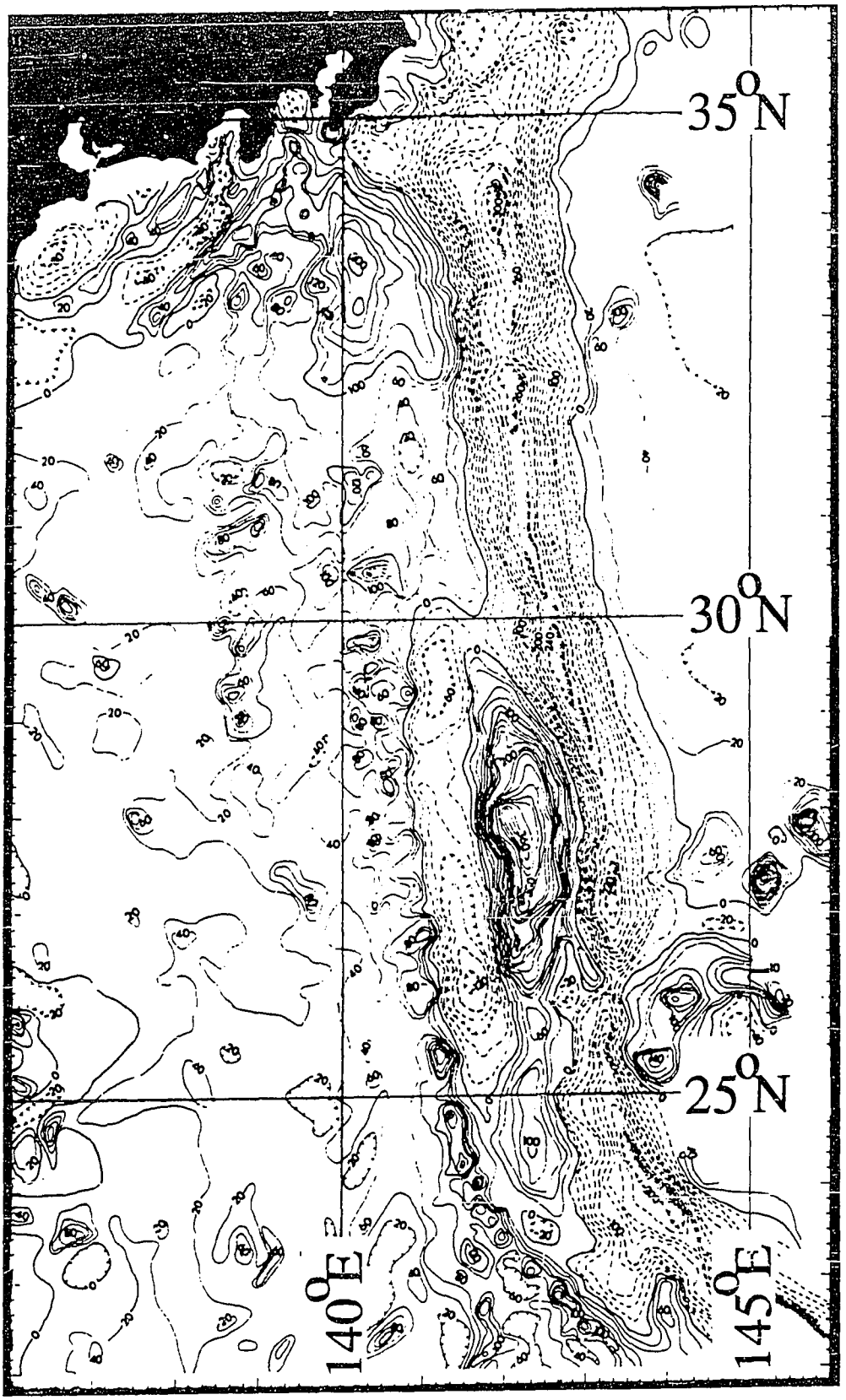
35°N
30°N
25°N
140°E
145°E

variation, between -120 and +380 mgals. The maximum gradient is E-W at 28°N, where the free-air gravity changes from 0 to +300 mgals in 15 nautical miles. The dramatic gradient can be attributed to the deep water and thick sediments in the trough juxtaposed against an uplifted high-density volcanic (boninite and island-arc tholeiite) basement [*Karig and Moore*, 1975].

We know little about the deep crustal structure of the Bonin island arc. A velocity model for the crust at 32°N was prepared by *Hotta* [1970] based on a seismic refraction experiment (Figure 1.9). At this latitude, a high velocity (>6.00 km/sec) layer beneath the arc shoals to within 5 km of the seafloor. The anomaly may represent a rise of mafic material beneath the arc. The thickness of the crust in the central arc is estimated to be on the order of 15 to 20 km as indicated by the depth to the >8.0 km/sec layer.

Figure 1.9 Crustal structure (depth and P-wave velocities) of the central Bonin arc, mainly calculated from a two-ship seismic refraction experiment by *Hotta* [1970].

Crustal Structure of Bonin Arc at 32°N

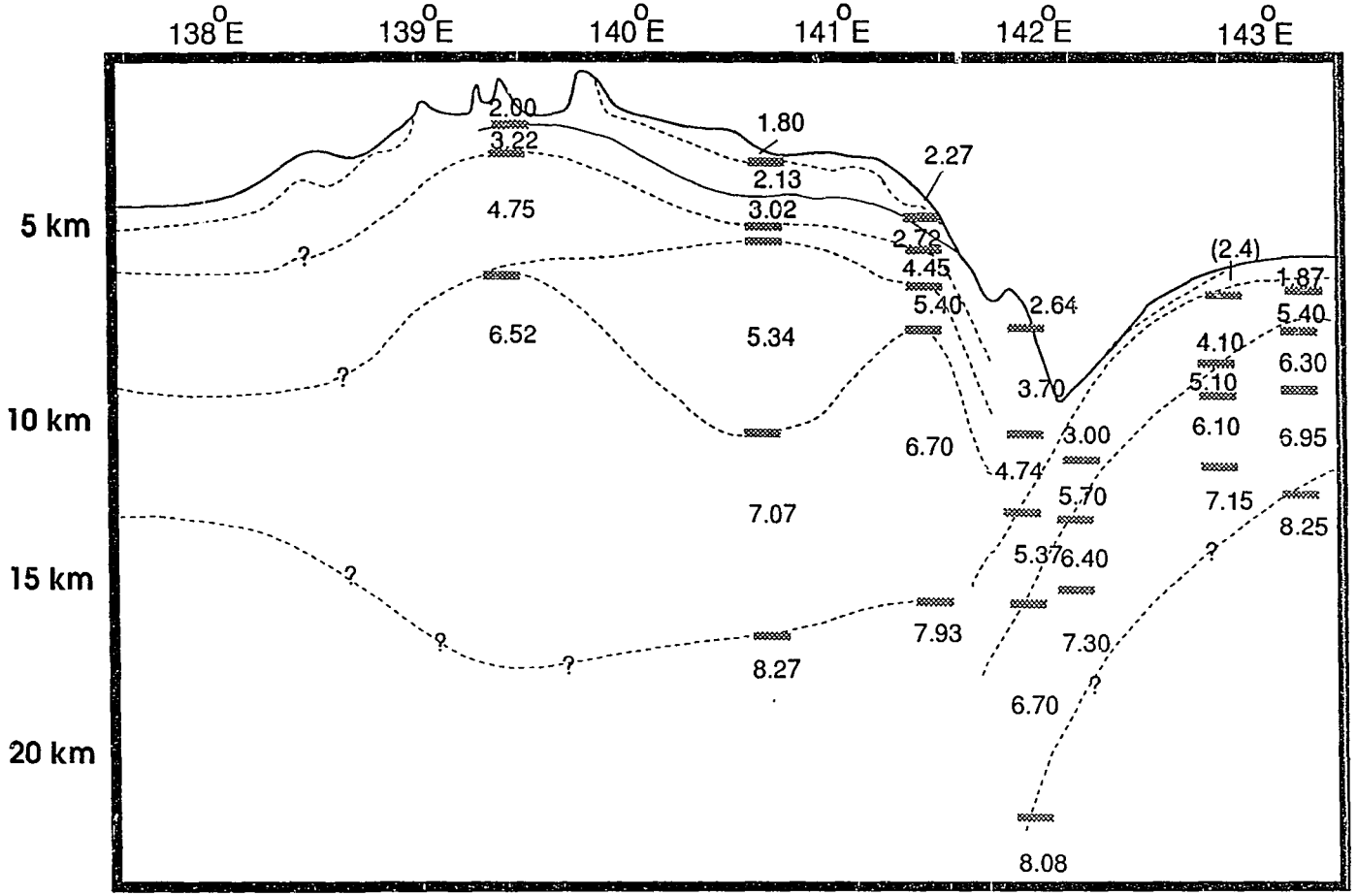

1.4 References

Bayly, B., Geometry of subducted plates and island arcs viewed as a buckling problem, *Geology, 10,* 629-632, 1982.

Beal, K., *The opening of a back arc basin: Northern Mariana Trough,* M.S. thesis, Univ. of Hawaii, Honolulu, 1987.

Bibee, L.D., G.G. Shor Jr., R.S. Lu, Inter-arc spreading in the Mariana Trough, *Marine Geology, 35,* 183-197, 1980.

Chase, C.G., Extension behind island arcs and motions relative to hot spots, *J. Geophys. Res., 83,* 5385-5387, 1978.

Charmot-Rooke, N., V. Renard, and X. LePichon, Magnetic anomalies in the Shikoku Basin: a new interpretation, *Earth Planet Sci. Lett. 83,* 214-228, 1987.

Chigaku Zasshi (in Japanese), Geogr. Soc. of Japan, v.1, 1890.

Chigaku Zasshi (in Japanese), Geogr. Soc. of Japan, v.6, 1895.

Collot, J.Y., J. Daniel and R.V. Burne, Recent tectonics associated with the subduction/ collision of the d'Entrecasteaux zone in the central New Hebrides, *Tectonophysics, 112,* 325-356.

Dewey, J. F., Episodicity, sequence and style at convergent plate boundaries, in *The Continental Crust and Its Mineral Deposits,* edited by Strangway, D.W., Geol. Assoc. of Canada Spec. Paper 20, 553-573, 1980.

Dubois, J.D., F. Dugas, A. Lapouille, and R. Louat, The troughs at the rear of the New Hebrides island arc: possible mechansims of formation, *Can. J. of Earth Sci., 15,* 351-360, 1978.

Eguchi, T., and S. Uyeda, Seismotectonics of the Okinawa Trough and Ryukyu Arc, *Mem. Geol. Soc. China, 5,* 189-210, 1983.

Elsasser, W.M., Sea-floor spreading as thermal convection, *J. Geophys. Res., 76,* 1101-1112, 1971.

Fryer, P., J.M. Sinton and J.A. Philpotts, Basaltic glasses from the Mariana Trough, *Initial Rep. Deep Sea Drill. Proj., 60,* 601-609, 1982.

Gast, R., *Bonin Islands' Story,* Monrovia News-Post, USA, 1944.

Honza, E., and K. Tamaki, Bonin Arc, in *The Ocean Basins and Margins, Vol. 7, The Pacific Ocean,* edited by Nairn, A.E.M., and S. Uyeda, Plenum Press, New York, 459-502, 1985.

Hotta, H., A crustal section across the arc Izu-Ogasawara and trench, *J. Phys. Earth, 18,* 125-141, 1970.

Hussong, D. M. and J. M. Sinton, Seismicity associated with back arc crustal spreading in the central Mariana Trough, in *The Tectonic and Geologic Evolution of Southeast Asian Seas and Islands,* Geophys. Monogr. Ser., vol. 23, edited by Hayes, D. E., 217-235, AGU, Washington DC, 1980.

Ishihara, T., Gravimetric determination of densities of seamounts along the Bonin Arc, in *Seamounts, Islands, and Atolls,* edited by Keating, B., P. Fryer, R. Batiza and G. Boehlert, AGU Geophysical Monograph, 43, Washington D.C., 97-113, 1987.

Karig, D.E., Ridges and basins of the Tonga-Kermadec Island arc system, *J. Geophys. Res., 75,* 239-255, 1970.

Karig, D.E., Origin and development of marginal basins in the western Pacific, *J. Geophys. Res., 76,* 2542-2561, 1971a.

Karig, D.E., Structural history of the Mariana Island arc system, *Bull. Geol. Soc. Am., 82,* 1971b.

Karig, D.E., Remnant arcs, *Geol. Soc. Am. Bull., 83,* 1057-1068, 1972.

Karig, D.E., Evolution of arc systems in the western Pacific, *Annu. Rev. Earth Planet. Sci., 2,* 51-75, 1974.

Karig, D.E. and G.F. Moore, Tectonic complexities in the Bonin Arc system, *Tectonophysics, 27,* 97-118, 1975.

Katsumata, M. and L.R. Sykes, Seismicity and tectonics of the Western Pacific: Izu-Mariana-Caroline and Ryukyu-Taiwan regions, *J. Geophys. Res., 74,* [illegible]3-5948, 1969.

Kobayashi, K. and M. Nakada, Magnetic anomalies and tectonic evolution of the Shikoku inter-arc basin, *Adv. Earth Planet. Sci., 6,* 391-402, 1979.

Kuno, H., Japan, Taiwan, and Marianas, in *Catalogue of the Active Volcanoes of the World, 11,* Int. Volc. Assoc., Rome, 1-132, 1962.

LaTraille, S.L. and D.M. Hussong, Crustal structure across the Mariana Island arc, in *The Tectonic and Geologic Evolution of Southeast Asian Seas and Islands,* Geophys. Monogr. Ser., vol. 23, edited by Hayes, D. E., 209-222, AGU, Washington DC, 1980.

Malahoff, A., R. Feden, and H. Fleming, Magnetic anomalies and tectonic fabric of marginal basins north of New Zealand, *J. Geophy. Res., 87,* 4109-4125, 1982.

Moberly, R., Origin of lithosphere behind island arcs, with reference to the Western Pacific, *GSA Memoir, 132,* 35-55, 1972.

Molnar, P., and T. Atwater, Interarc spreading and cordilleran tectonics as alternates related to the age of subducted oceanic lithosphere, *Earth Planet. Sci. Letters, 41,* 330-340, 1978.

Molnar, P., and J. Oliver, Lateral variations of attenuation in the upper mantle and discontinuities in the lithosphere, *74,* 2648-2660, 1969.

Sibuet, J., J. Letouzey, F. Barbier, J. Charvet, J. Foucer, T. Hilde, M. Kimura, C. Ling-Yun, B. Marsset, C. Muller and J. Stephan, Back arc extension in the Okinawa Trough, *J. Geophys. Res., 92,* 14041-14063, 1987.

Sleep, N.H. and M.N. Toksöz, Evolution of marginal basins, *Nature, 33,* 548-550, 1971.

Taylor, B. and G. D. Karner, On the evolution of marginal basins, *Rev. of Geophys. and Space Physics, 21,* 1727-1741, 1983.

Tsuya, H., On the vulcanism of the Huzi Volcanic Zone, *Bull. Vol., 15,* 217-357, 1937.

Uyeda, S., Comparative subductology, *Episodes, 2,* 21-24, 1983.

Uyeda, S. and H. Kanamori, Back-arc opening and the mode of subduction, *J. Geophys. Res., 84,* 1049-1061, 1979.

Vaquier, V., S. Uyeda, M. Yasui, J. Sclater, C. Corry and T. Watanabe, Heat flow measurements in the northwest Pacific, *Tokyo Daigaku, Jishin Kenkyujo Iho, 44,* 1519-1535, 1966.

Watanabe, T., M. G. Langseth and R. N. Anderson, Heat flow in back-arc basins of the western Pacific, AGU Monograph, 137-162, 1977.

Wegener, A., *The Origin of Continents and Oceans,* translated by Briram, J., 1966, Dover Publications, New York, 246 p., 1929.

Yuasa, M., Sofu Gan Tectonic Line, a new tectonic boundary separating northern and southern parts of the Ogasawara (Bonin) arc, northwest Pacific, in *Formation of Active Ocean Margins*, edited by N. Nasu et al., Terra Scientific Pub. Co., Tokyo, 483-496, 1985.

CHAPTER II

Seafloor Mapping of the Sumisu Rift, Bonin Island Arc

2.1 Introduction

The Bonin (Izu-Bonin, Ogasawara) island-arc is located between Honshu and the Mariana Islands. Several small basins, first described by *Mogi* [1968], are found behind the volcanic line from Hachijoshima to Nishinoshima volcanoes. *Hotta* [1970], in a crustal study in the northern Bonin arc, reported that the small depressions are related to high-angle normal faulting. The nature of the basins was enigmatic until *Karig* [1971,1972] proposed that marginal basins in the Western Pacific were formed by the rifting of island-arcs. *Karig and Moore* [1975a] suggested that the small depressions in the Bonins are incipient back-arc basins. The basins represent a 630 kilometer line of semi-continuous rifting along the central Bonin arc [*Taylor et al.*, 1984]. *Honza and Tamaki* [1985] defined four rift basins (Hachijo, Sumisu, Torishima, and Nishinoshima) which they named after nearby arc volcanoes (Figure 2.1). This paper discusses the physiography and distribution of recent sediments and faults in the Sumisu Rift. The Sumisu Rift lies between 30°30' N and 31°30' N and between 139°20' E and 140°10' E. Although the rift narrows in the south its structures are continuous into the Torishima Rift [*Taylor et al.*, 1984].

Karig and Moore [1975b] and *Carey and Sigurdsson* [1984] have proposed models for sedimentation in marginal basins in which sediments deposited in the early stages of intra-arc basin opening would be dominated by coarse volcaniclastics derived from the proximal arc volcanoes. As the basin matures and widens sedimentation would be influenced more by detritus from marine organisms, montmorillonite clays, and wind-blown continental dust. *Karig and Moore* estimated the rates of sedimentation in young troughs to be much greater than 100 m/m.y..

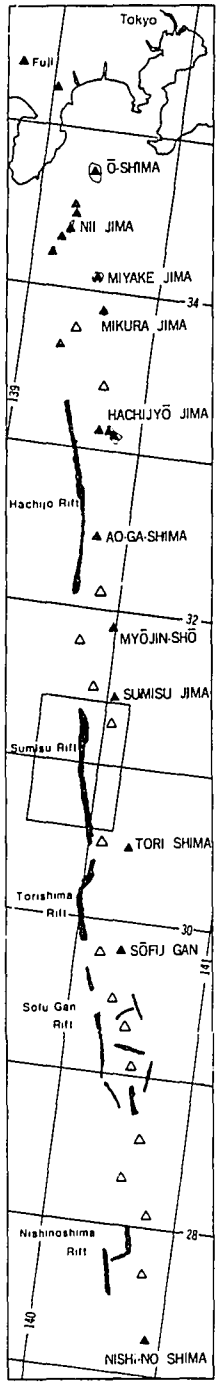

Figure 2.1 Location of the Bonin Rift System (stipled) in the Bonin island-arc [after *Taylor et al.*, 1984; *Honza and Tamaki*, 1985]. The main rift segments are Hachijo, Sumisu, Torishima, Sofu Gan (southern rift segment of the Torishima Rift of *Honza and Tamaki* [1985]), and Nishinoshima. Subaereal arc volcanoes (solid triangles) and submarine arc volcanoes (open triangles) delineate the Bonin arc. The study area is outlined by the rectangle (see also Chapter III).

The thickness of the sediment layer in the Bonin Rifts has been reported by several authors. *Hotta* [1970] observed that the Hachijo Rift has a thin sediment cover except on the western edge of the basin. *Honza and Tamaki* [1985] reported 500 m of sediments in the Nishinoshima Rift and 200 m in the Torishima Rift. Single-channel reflection data from the Hawaii Institute of Geophysics [*Taylor et al.*, 1984] show one second of sediments overlying downthrown blocks in the center of Sumisu Rift. *Honza et al.* [1982] mapped the regional sea-floor sediment distribution in the Bonin arc and reported Quaternary hemipelagic (?) sediments covering the Sumisu Rift, surrounded on the east and west by Quaternary volcaniclastic sediments.

This work is based on 3.5-kHz reflection data and SeaMARC II sidescan imaging and bathymetry data. The 3.5-kHz data were collected by the Hawaii Institute of Geophysics (*R/V Kana Keoki*, 1984) and the Geological Survey of Japan (*R/V Hakurei Maru*, 1979, '80, '84, '85). Track lines are shown in Figure 2.2.

SeaMARC II (Sea Mapping And Remote Characterization) is a shallow-tow sidescan sonar system capable of high resolution sea-floor imaging and bathymetry mapping for five kilometers on either side of the ship's track [*Blackinton et al.*, 1983]. The instrument uses an 11-kHz (port) and 12-kHz (starboard) signal with a fore-aft beam width of 2°. In 1984 the *R/V Kana Keoki* surveyed the Sumisu and Torishima Rifts with the SeaMARC II system. Processed sidescan and bathymetry data for the Sumisu Rift north of 30°35' N is presented in this chapter (Figures 2.3 and 2.4).

2.2 Physiography

The Sumisu Rift is bounded on the east (active arc side) by a 1000-1500 m fault scarp and on the west (remnant arc side) by a stepped,relatively gentie slope with numerous antithetic fault scarps. The contact between regions offset by east-dipping (Sumisu Rift West Fault Zone-SRWFZ) and west-dipping (Sumisu Rift East

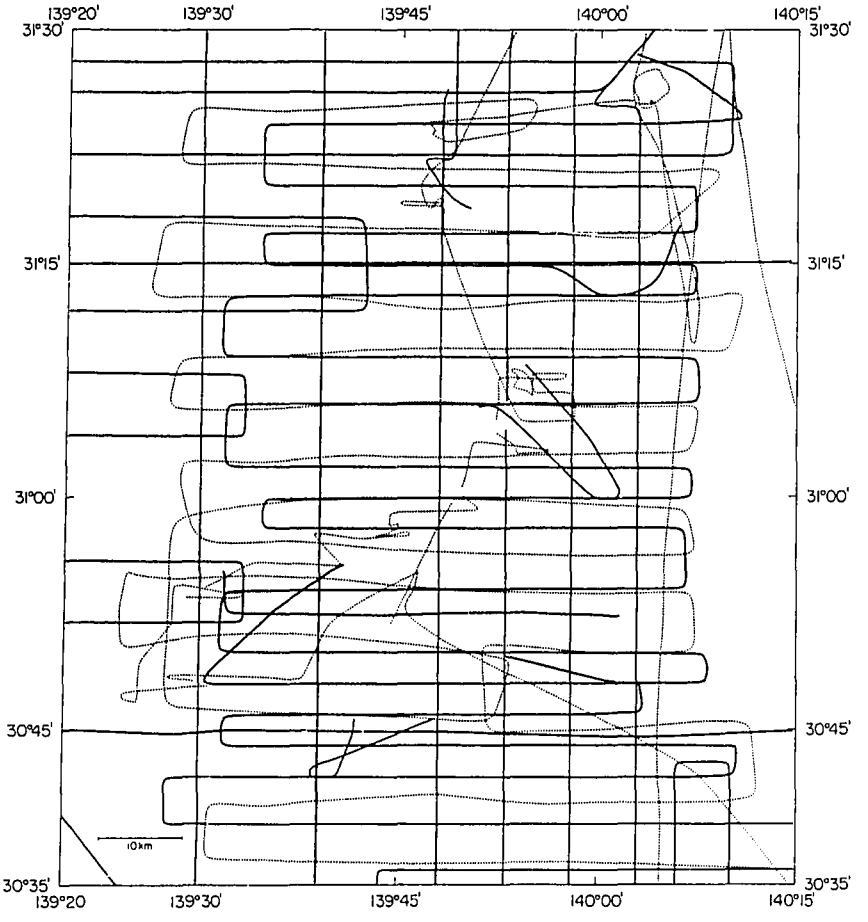

Figure 2.2 Track chart of the Sumisu Rift region showing Hawaii Institute of Geophysics (*R/V Kana Keoki*, dotted lines) and Geological Survey of Japan (*R/V Hakurei Maru*, solid lines) track segments.

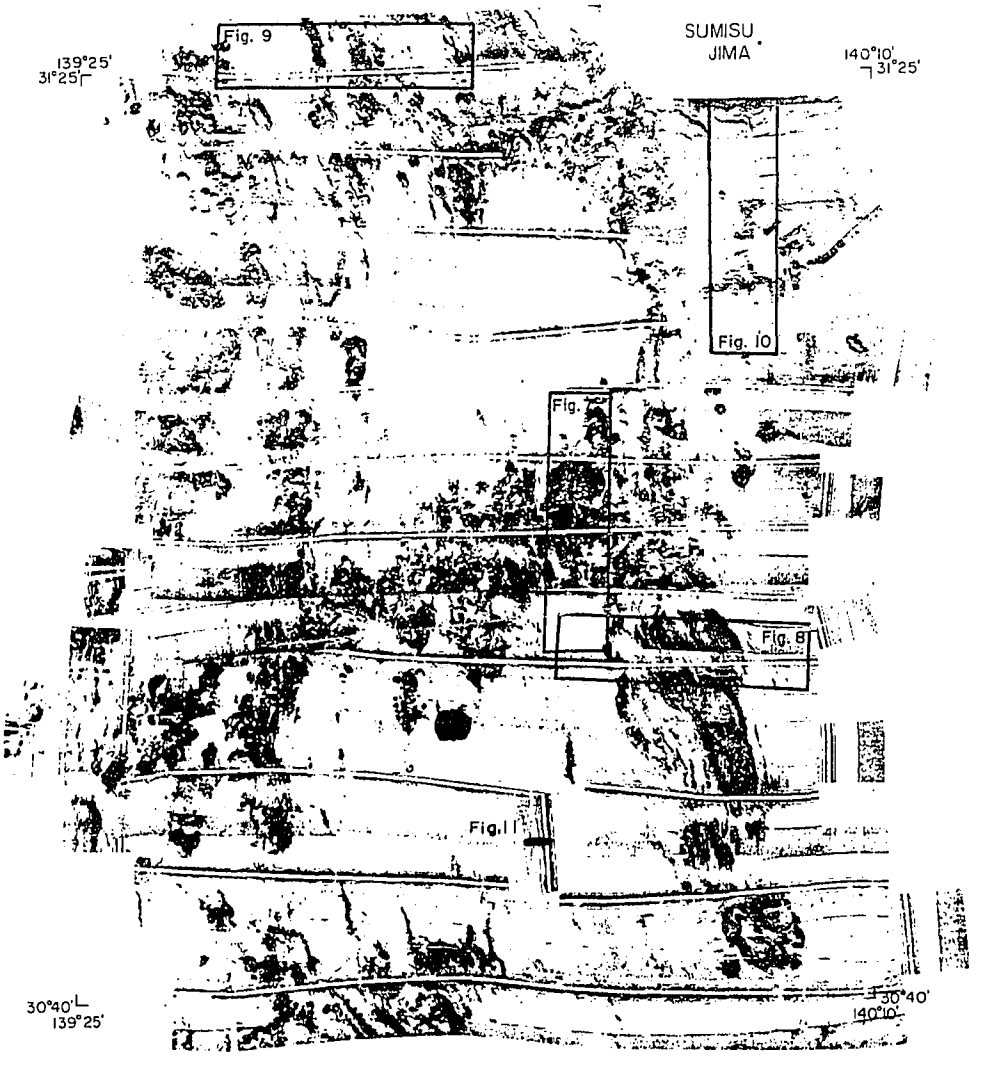

Figure 2.3. Processed SeaMARC II mosaic of the Sumisu Rift. Individual files have been corrected for bottom detect errors and combined to produce the final mosaic. The ship track is shaded with an artificial grey shade. Enclosed areas and line segments refer to Figures 2.7 through 2.11.

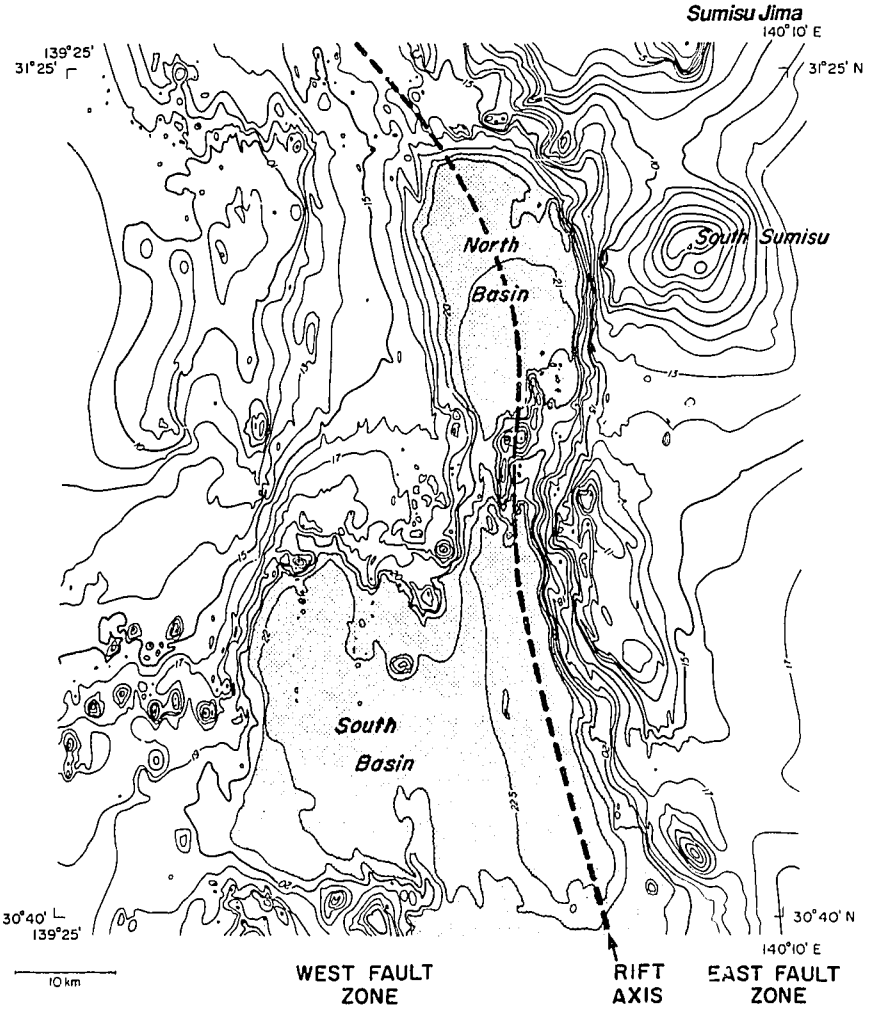

Figure 2.4 SeaMARC II bathymetry of the Sumisu Rift (contour interval 100 m). The South Basin and the deeper part of the North Basin are shaded. The axis of subsidence is indicated by the dashed line.

Fault Zone-SREFZ) faults will be referred to as the Sumisu Rift Axis (Figure 2.4). The rift is asymmetric, with a deep sub-graben on its eastern side. Over 200 volcanic centers are found in the study area (Figure 2.5). The volcanoes average 100-200 m relief, 1-3 km in diameter, and have a composition ranging from tholeiitic basalt to sodic rhyolite [*Fryer et al,* 1985]. Intra-rift volcanoes separate the rift floor into two provinces: the Sumisu Rift North Basin (SRNB) and the Sumisu Rift South Basin (SRSB) (Figure 2.4). The SRSB has a smooth floor which covers a wide area and has an average depth of 2200 m. In contrast the SRNB has two levels: a narrow lower level (shown in Figure 2.4),which is smooth in the south becoming hilly in the north, and an upper level which is part of the faulted west slope of the graben.

Sumisujima is an active island-arc volcano located just to the northeast of the SeaMARC II mosaic. The island is the subaereal tip of a submarine caldera [*Murakami,* 1986]. The southern flank of Sumisujima volcano covers the northeast corner of the mosaic. Twenty kilometers south of Sumisujima volcano is a 350 m deep submarine volcano (hereafter referred to as "South Sumisu"). Torishima, an active subaereal arc volcano, lies southeast of the SeaMARC II mosaic (Figure 2.1).

2.3 Echocharacter and fault mapping

Echo soundings record acoustic returns from the sea floor and the distribution of various echotypes may be systematically mapped [e.g. *Damuth,* 1978; *Damuth,* 1980; *Nemoto and Kroenke,* 1981; *Okamura and Nakamura,* 1981; *Damuth et al.,* 1983]. Echocharacter mapping is limited in its capabilities. Without bottom data (e.g. core samples, bottom photographs) interpretation is qualitative. It is often impossible to determine the genetic origin of echotypes from the echocharacter alone [*Damuth,* 1980], although the echocharacter can be used to study sediment distribution and bottom processes such as turbidity flows and bottom currents [*Damuth,*

Figure 2.5 Echocharacter distribution in the Sumisu Rift based on 3.5-kHz echograms and SeaMARC II sidescan data (BR0—no subbottom reflectors, BR1—1 to 3 subbottom reflectors, BR2—greater than 3 subbottom reflectors, suffix "f"—echotype is interrupted by closely spaced faults, suffix "t"—transparent sediment patches overlay echotype). A combination of echotypes is shown by an overlap of patterns. The distribution is controlled by the proximity of arc volcanoes and the presence of barriers to sediment transport. Contours in the South Basin refer to the thickness of the continuous transparent layer (contour interval is 5 m, assuming 10 msec = 7.5 m).

ECHOCHARACTER SUMISU RIFT

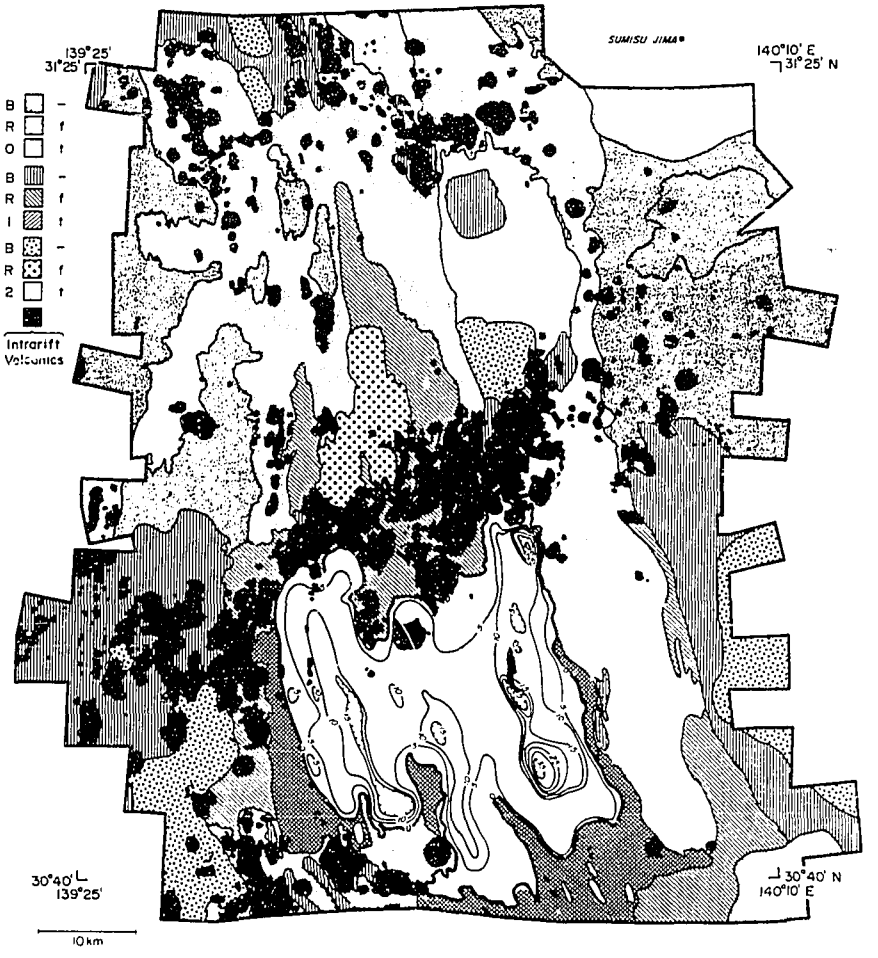

1980; *Embley,* 1980; *Swift,* 1985]. In this study the 3.5-kHz data proved useful in distinguishing differences in sediments, mapping faults, and identifying features on the SeaMARC II sidescan data.

Echograms from the Sumisu Rift were studied and classified based on the nature of subbottom reflectors (a similar to that used by *Damuth* [1980]).Echocharacter types and faults were plotted along the ships' tracks and then compared with the SeaMARC II sidescan mosaic. Normal faults that were identified on the 3.5-kHz records were extrapolated between ships' tracks based on the SeaMARC II sidescan data (Figure 2.6).

In the Sumisu Rift, where arc volcaniclastic sediments dominate, subtle changes in sea-floor sediment type are often more apparent on the deeper penetrating 3.5-kHz records than on the 12-kHz SeaMARC II sidescan. However, areas of the sea floor with a rough bottom and therefore a high backscatter (e.g. coarse volcaniclastics, or exposed rock) and areas with a steep slope facing the ship's track and therefore a high specular reflection (e.g. fault scarps) show significant contrast with flat lying sediments on the SeaMARC II imagery. If a 3.5-kHz echocharacter type is bounded by these features, then the unit can be mapped using the SeaMARC II image. For example, the boundary of the sediment in the SRSB is quite distinct because it is surrounded on the west, north, and east by large fault scarps or intra-rift volcanoes (Figure 2.3).

Echotypes (Figure 2.5) are notated with a prefix "BR" (Bonin Rifts). The number following refers to the order of subbottom reflectors. A suffix "f" denotes that the echotype is not continuous but interrupted by closely spaced (i.e. more than 2 per 5 km) fault scarps (along east-west ships' tracks, perpendicular to the general trend of rifting). A suffix "t" denotes that the unit is overlain by a transparent sediment layer of variable thickness.

Figure 2.6 Normal fault traces and lineations based on 3.5-kHz and SeaMARC II sidescan data. Subsidence of major blocks produces small sags in the overlying sediment pile (e.g. small grabens along the SRWFZ).

NORMAL FAULTS AND LINEAMENTS SUMISU RIFT

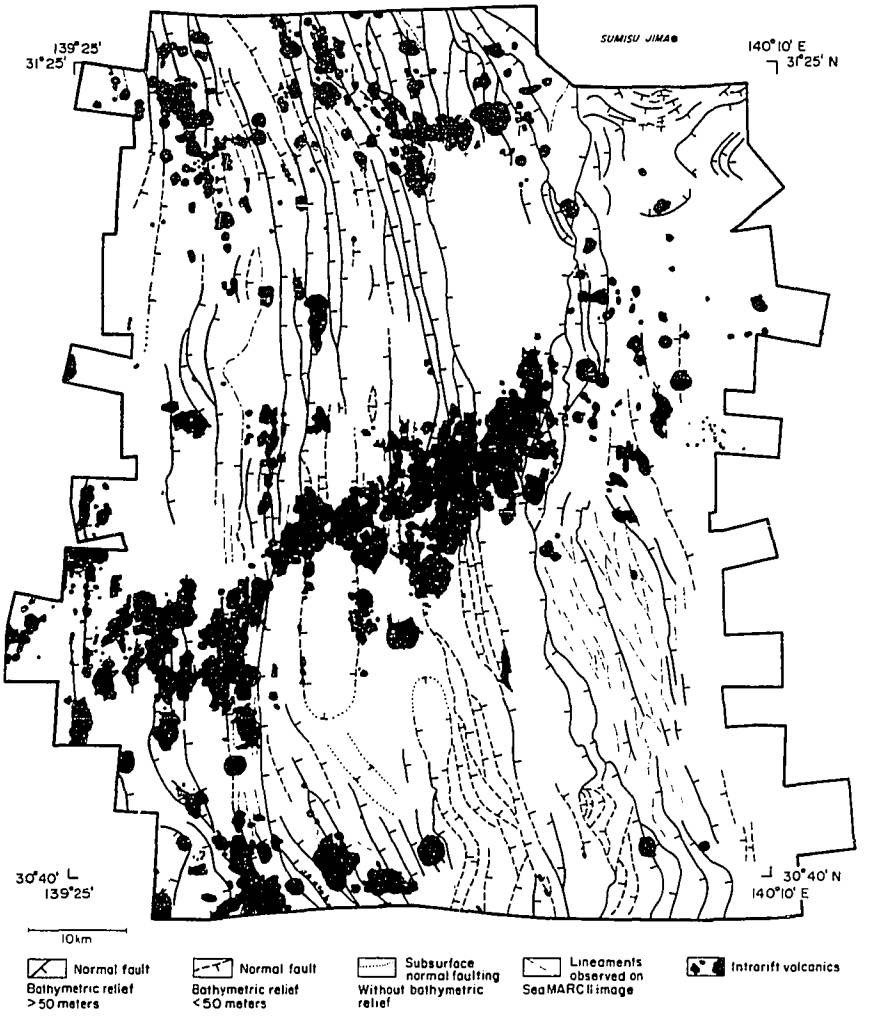

Echotype BR0 (*Damuth,* [1980]: Type IIB) is a prolonged echo with no subbottom reflectors. The sea floor is smooth (BR0) to heavily faulted (BR0f). The bottom reflector amplitude varies from weak to strong. The corresponding SeaMARC II sidescan image is dark to medium grey showing some structural features such as ridges and point reflectors. Echotype BR0 is found on the active island-arc volcanoes, on the remnant arc, on intra-rift volcanoes, and along fault scarps. The prolonged echotype can be associated with two bottom types: exposed rock or coarse terrigenous material (sand/silt sediment) [*Damuth,* 1980].

Echotype BR1 (*Damuth,* [1980]: Type IIA) has a strong bottom reflector,and a somewhat prolonged reflection with 1-3 subbottom reflectors. On 3.5-kHz records the contacts between BR0 and BR1 echotypes are often not distinct. Rather, there is usually a facies change characterized by a gradual increase in the number of subbottom reflectors.

Echotype BR2 (*Damuth,* [1980]: Type IB) has a distinct smooth bottom with multiple (more than 2) continuous subbottom reflectors. Echotype BR2t is characterized by multiple subbottom reflectors overlain by a continuous transparent layer of varying thickness. A strong reflector lies underneath the transparent layer followed by 4 to 6 weaker more discontinuous reflectors. The BR2t echotype is found only in the SRSB. Hemipelagic sediments, composed of fine-grained pelagic organics and silt detritus eroded from the surrounding footwalls, may explain the continuous SRSB transparent layer.

2.4 Discussion

Echocharacter distribution

The small basins along the fault zones vary in echocharacter. Basins above approximately 1300 m depth are dominated by a BR0 echotype. Below 1300 m basins have BR1 and BR2 echotypes. With increasing depth and distance from the

arc volcanoes the change in echocharacter from BR0 to BR2 may represent a facies change from coarse volcaniclastic sediments to sediments with an increased biogenous content similar to the model proposed by *Carey and Sigurdsson* [1984]. Periodic influxes of pyroclastic or epiclastic sediments from volcanic eruptions, debris flows-turbidity currents, or changes in bottom currents may explain the layering.

The transparent echotype is found only in the deepest parts of the graben (Figure 2.5). In the SRSB the transparent layer is smooth and continuous. The even distribution of the sediment layer implies that there are strong currents (relative to the particle size) that sweep across the basin floor. In the northern SRNB transparent sediments fill depressions between hills of BR0 echotype. Northwest of the SRNB transparent sediment is continuous and overlies a BR0 echotype.

Bottom camera photographs and sediment-dispersal studies north of Hachijoshima show that effects of the Kuroshiro geostrophic current are found as deep as 1000 m [*Inouchi and Kinoshita,* 1981]. The Kuroshiro Current flows from the Shikoku Basin into the North Pacific over the Izu Ridge (Bonin arc). *Taft and Freitag* [1979] measured bottom current velocities over the Izu Ridge. They concluded that south of 32°40' N the volume of transport in the northeast direction lessens in favour of flow to the south and recirculation in the Shikoku Basin. Although the Kuroshiro Current has deep-water motion over the Izu Ridge, it may have little effect on the movement of bottom sediments in waters as far south as Sumisu Rift.

Intra-rift volcanoes are shown on Figure 2.5. Reflections on the 3.5-kHz echograms from the volcanoes appear as hyperbolae, the summits being point reflectors. The subbottom echos are prolonged (BR0). The edge of a tilted fault block can appear similar to an intra-rift volcano on the wide beam (30°) echosounder records, but can generally be distinguished with the aid of the SeaMARC II data. The distri-

bution of volcanoes in the rift graben and on the remnant arc is structurally controlled. The volcanoes are usually found at the foot of fault scarps. Except for a few of the large seamounts, the volcanoes are elongated parallel to the north-trending faults, and clusters of aligned vents are common. Most of the eruptions have been from central vents, but a few may be fissure eruptions.

The sea-floor reflector in the SRNB is similar to the undisturbed reflector lying under the transparent layer in the SRSB (Figure 2.7B). The SRNB is over 100 m above the SRSB. The intra-rift volcanoes between the SRNB and the SRSB appear to be a barrier to sediment transport. Sediment cores from the SRNB obtained by the Geological Survey of Japan contain more ash beds and coarse-grained sediments than do cores from the SRSB which are dominated by silt-sized sediments [*Geological Survey of Japan*, 1985]. This may explain the difference in echo-character between the two basins. Sedimentation in the SRNB is dominated by volcaniclastic debris shed from Sumisujima and South Sumisu volcanoes. The intra-rift volcanic ridge between the basins restricts movement of coarse volcaniclastic ash into the SRSB.

Sumisu Rift East Fault Zone

The SREFZ has a complex structure on the sidescan image (Figure 2.8A).On the 3.5-kHz record, rock exposed by normal faulting (footwall rock) has a BR0 echocharacter. The occasional point reflector on the echo record maybe from sediment bedding planes. At the base of the exposed footwall lies the SRSB with a BR2t echocharacter (a). A thicker transparent layer in the SRSB correlates with areas of fault-block subsidence. Terraced basins less than 2 km wide are found along the stepped fault zone (b). These sediment accumulations have white to grey shade on the SeaMARC II sidescan image. The small hyperbolic reflection on the 3.5-kHz record corresponds to a small ridge on the sidescan image. A "v" shaped structure on the SeaMARC II image (c) is formed by the contact between a bedding-plane ledge

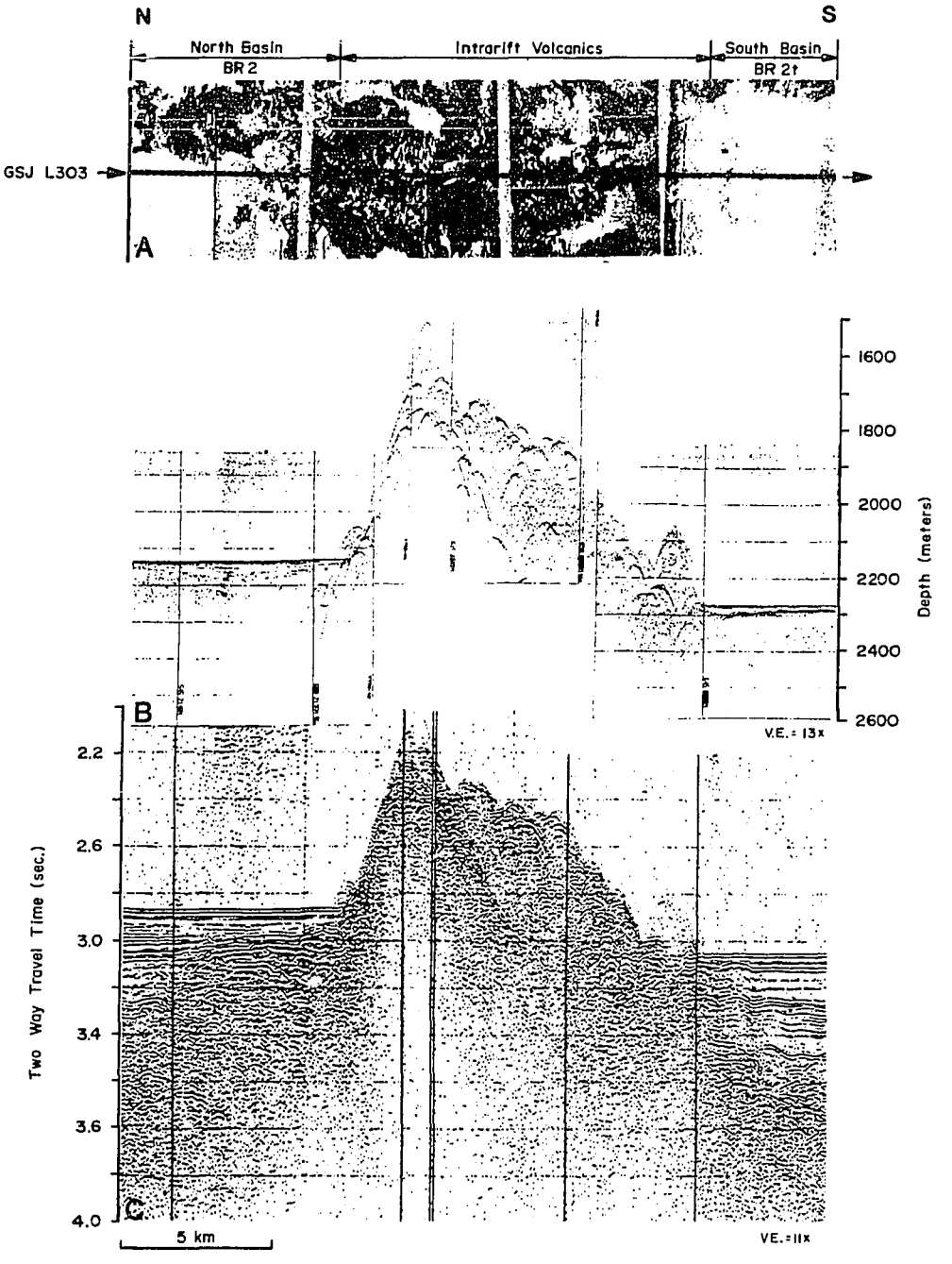

Figure 2.7 Sumisu Rift North Basin (SRNB) and the Sumisu Rift South as in (SRSB) (N-S profile): A. SeaMARC II sidescan image. B. GSJ 3.5-kHz record. C. GSJ single-channel reflection record.

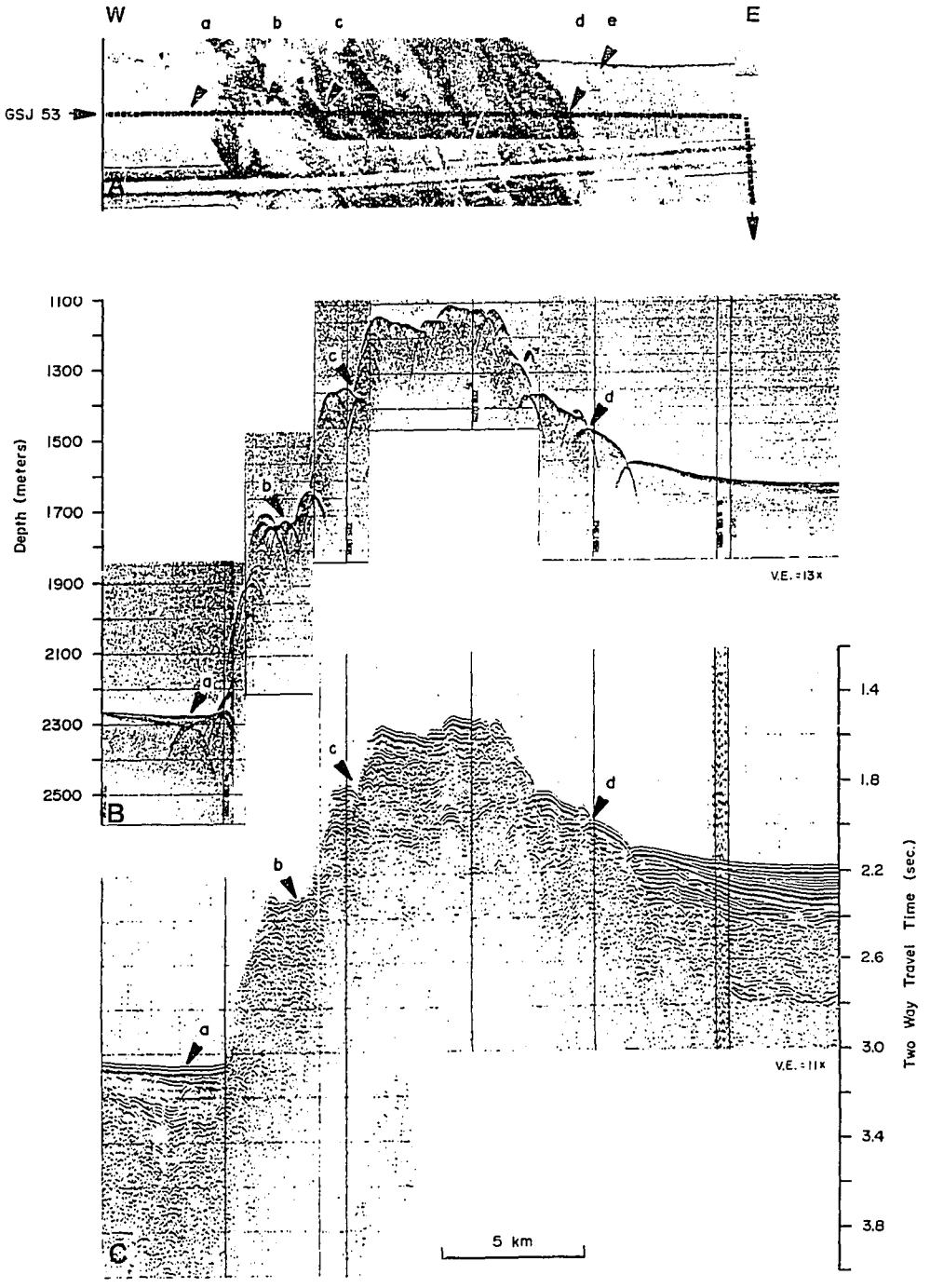

Figure 2.8 Sumisu Rift East Fault Zone (E-W profile): A. SeaMARC II sidescan image. B. GSJ 3.5-kHz record. C. GSJ single-channel reflection record.

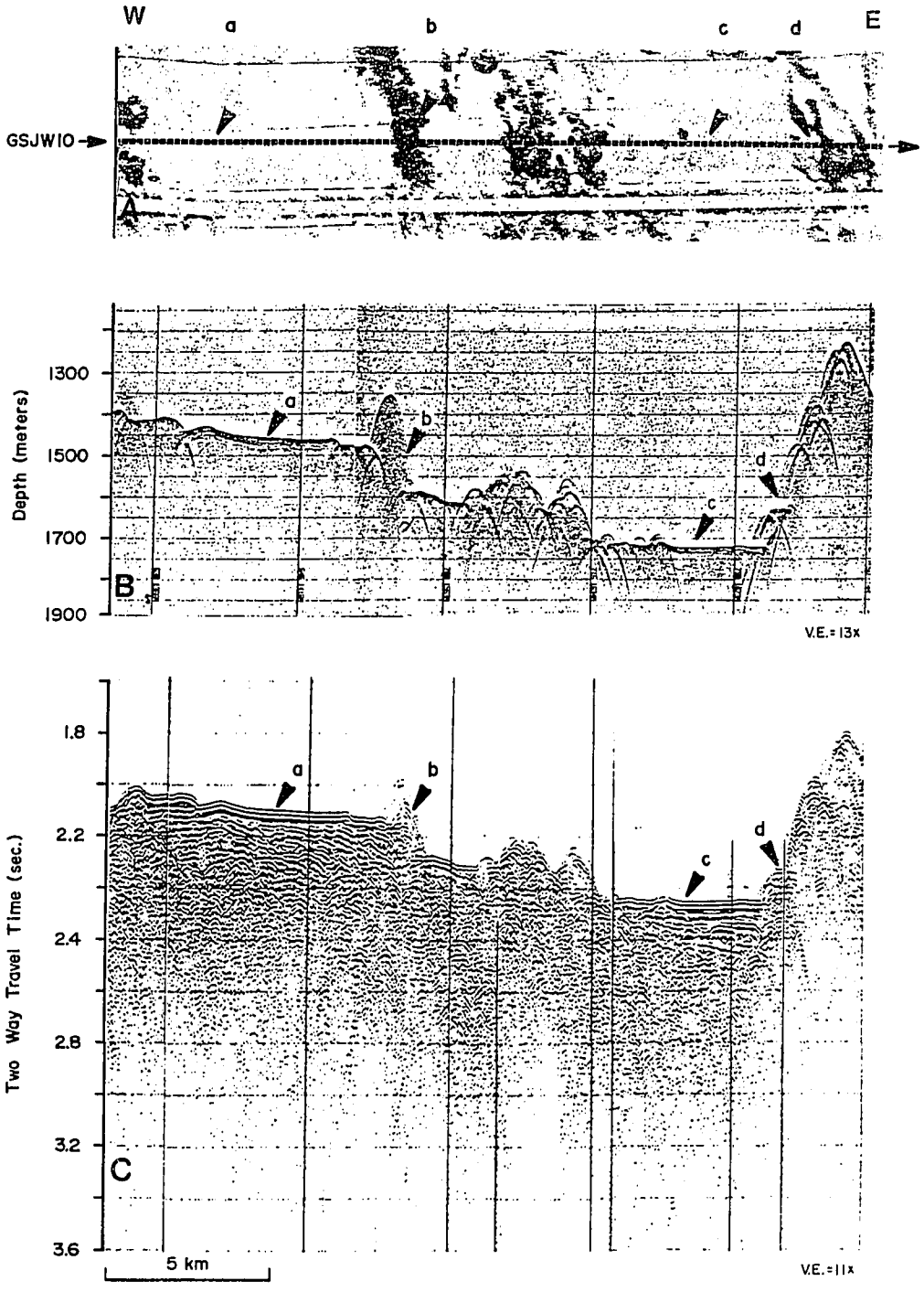

Figure 2.9 Sumisu Rift West Fault Zone (E-W profile): A. SeaMARC II sidescan image. B. GSJ 3.5-kHz record. C. GSJ single-channel reflection record.

and a normal fault. The uplifted block is apparently down-faulted to the east (d). Forearc basin sediments with a BR2 echotype are blanketing the fault-block structures (e).

Sumisu Rift West Fault Zone

Basins along the SRWFZ (Figure 2.9) are much broader than those on the SREFZ. The basin of BR2 echotype (a) is covered on the west by an additional sediment layer. A ridge of intra-rift volcanoes, associated with a fault, (b) separates the BR0 echotype basin from a BR1 echotype basin. The deepest basin (c) is bounded on the east by the SREFZ (d). The basin has a BR0t-echotype and overlies the Sumisu Rift Axis. The variations in sediment echotypes between neighbouring fault-block basins, which are separated by volcanic ridges or fault-block ridges, suggests that the ridges affect the distribution of sediment.

Sumisujima and South Sumisu

Sumisujima and South Sumisu volcanoes have a BR0 echotype (Figure 2.10). The flanks of the volcanoes show evidence of mass-wasting. On the SeaMARC II image, headwall scars of slumps are seen as highly reflective concentric arcs lying around the south edifice of Sumisujima (a). On 3.5-kHZ and single-channel records there are offsets in the sea floor corresponding to the slumps. At (b) a rough area on the SeaMARC II sidescan data is not obvious on the 3.5-kHz data except for a change in slope. This feature is thought to be a debris or lava flow originating near a flank volcano at (c).A region of rough bottom on the summit of South Sumisu is seen on the SeaMARC II image (from (c) to (d)). The summit unit cannot be distinguished on the 3.5-kHz record, except that it corresponds to a change in slope. The summit unit is believed to be either exposed volcanic rock (suggested by single-channel seismic data) or coarse-grained volcaniclastic sediment.

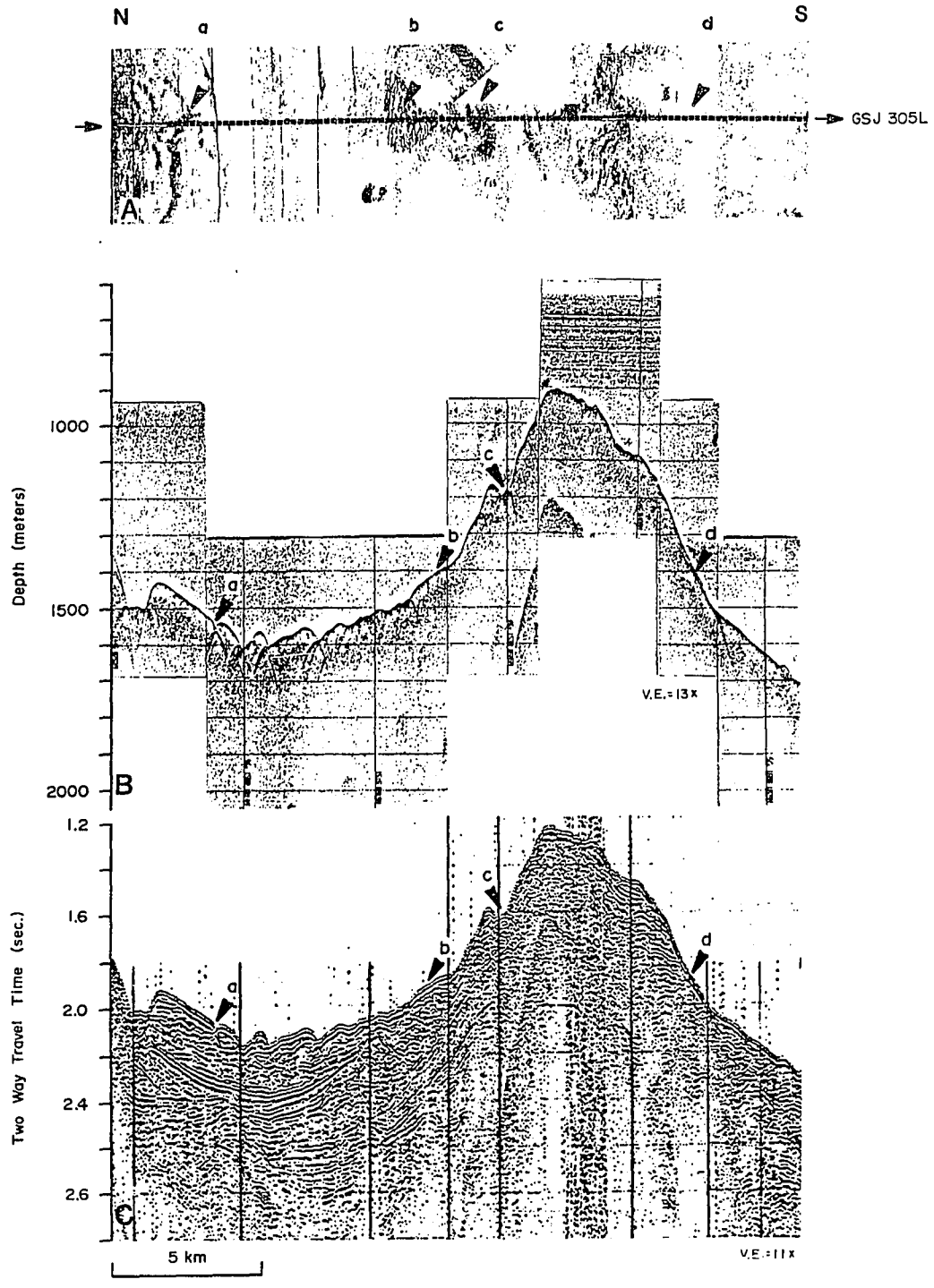

Figure 2.10 Sumisujima and South Sumisu arc volcanoes (N-S profile): A. SeaMARC II sidescan image; B. GSJ 3.5-kHz record; C. GSJ single-channel reflection record.

Normal faults and lineaments

Fault scarps appear black on the sidescan image. In places where the ship track is perpendicular to small faults (<< 50 m bathymetric relief) the scarp appears as subtle discontinuities in the sidescan image on small scale (large size) copies of the sidescan data (e.g. small faults in the SRSB). Small scarps are better imaged when the ship track is parallel to the fault scarp and on the down-dip side of the fault. Lineaments observed on the SeaMARC II sidescan image and mapped on Figure 2.6 maybe bedding planes of exposed rock or unmapped faults.

From the distribution of normal faults in Figure 2.6 it is clear that the rift trend varies in the study area. It trends 345° in the south, shifts to 000° in the center, and returns to 345° in the north. The change is accomplished by bifurcation and bending of the normal faults. Bathymetric relief along the faults is not constant. Relief of some faults lessens by bifurcation into smaller faults (e.g. eastern margin of SRSB).

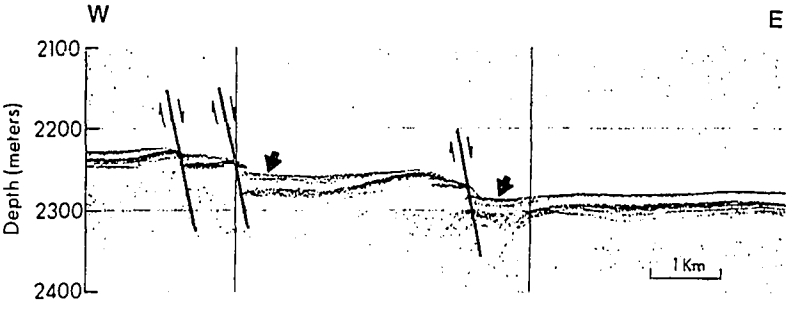

Figure 2.11 GSJ 3.5-kHz record from the South Basin showing small growth faults in BR2t echotype sediment.

Some fault traces are interrupted by the intra-rift volcanic ridge in the center of the rift. Large relief faults north of the volcanics are located to the east of the corresponding fault south of the volcanics. The volcanics may be localized along a right-lateral strike-slip fault which cuts through the center of the rift. Subsidence of fault blocks has formed growth faults in the overlying basins. In the SRWFZ narrow grabens have developed in the fault-block basins. Sediments in the SRSB are being faulted by a similar process. Subsidence of buried fault blocks creates small faults on the seafloor (Figure 2.11). Transparent sediment fills the depressions on the downthrown side of the faults and is sometimes overlain by a thin layer of even more recent sediment (arrow). An isopach map of the transparent layer in the SRSB (Figure 2.5) shows the areas of rapid subsidence in the SRSB.

2.5 Conclusion

The Sumisu Rift is a 120-km long segment of the intra-arc rift system in the central Bonin island arc. Integration of closely spaced 3.5-kHz data and SeaMARC II sidescan imagery allows us to identify sediment types and geologic features, and to determine their distribution. The echocharacter of sea-floor sediments changes from a prolonged reflection to a multilayered reflection with increasing depth and distance from the arc volcanoes. This indicates a change in composition produced by a decrease in the coarse volcaniclastic constituents of the sediment. The change in echocharacter between neighboring intra-rift basins that are separated by volcanic or fault-block ridges suggest that these physical barriers control the distribution of sediment. The distribution of transparent sediment found on the rift floor indicates recent faulting and benthic current motion.

2.6 References

Blackinton, G., D. Hussong, and J. Kosalos, First results from a combination sidescan sonar and sea floor mapping system (SeaMARC II),.In *Proceedings, 15th Annual Offshore Technology Conference, May 2-5,* Houston, Tx., 307-314, 1983.

Carey, S., and H. Sigurdsson, A model of volcanogenic sedimentation, In *Marginal Basin Geology, Geol. Soc. Spec. Publ. no. 16,* edited by Kokelaar, K.P., and M.F. Howells, Blackwell Scientific Publications, Oxford, 37-58, 1984.

Damuth, J.E., Echo character of the Norwegian-Greenland Sea. Relationship to Quaternary sedimentation, *Mar. Geol., 28,* 1-36, 1978.

Damuth, J.E., Use of high-frequency (3.5 - 12 kHz) echograms in the study of near-bottom sedimentation processes in the deep-sea: a review, *Mar. Geol., 38,* 51-75, 1980.

Damuth J.E., R.D. Jacobi and D.E., Sedimentation processes in the Northwest Pacific Basin revealed by echo-character mapping studies, *Geol. Soc. Am. Bull., 94,* 381-395, 1983.

Embley, R.W., The role of mass transport in the distribution and character of deep-ocean sediments with special reference to the North Atlantic, *Mar. Geol., 38,* 23-50, 1980.

Fryer, P., C. Langmuir, B. Taylor, Y. Zhang and D. Hussong, Rifting of the Izu Arc, III: Relationship of chemistry to tectonics, *Trans. Am. Geophys. Un., 66,* 421, 1985.

Geol. Surv. of Japan-Marine Division, Research on exploration methods of heavy metal resources associated with submarine hydrothermal activity, *Report of the 1984 Field Year Cruise, March 1985,* 93 pp., 1985.

Honza, E., K. Tamaki, M. Yuasa, M. Tanahashi and A. Nishimura, Geological Map of the North Ogasawara Arc, *Marine Geology Map Series, 17,* Geological Survey of Japan, Tsukuba, 1982.

Honza, E., and K. Tamaki, Bonin Arc, in *The Ocean Basins and Margins, Vol. 7, The Pacific Ocean,* edited by Nairn, A.E.M. and S. Uyeda, Plenum Press, New York, 459-502, 1985.

Hotta, H., A crustal section across the arc Izu-Ogasawara and trench, *Phys. Earth, 18,* 125-141, 1970.

Inouchi, Y., and Y. Kinoshita, Sea bottom photographs from Shinkurose Bank and its vicinity, *Geological Investigation of the Area Northeast of Hachijoshima Island, Northern Part of Ogasawara Arc* edited by Inoue, E., Cruise Report 16, Geol. Surv. Japan, 53-57, 1981.

Inoue, E., and E. Honza, E., Marine geological map around Japanese Islands, 1:3,000,000, *Marine Geology Map Series 23,* Geol. Surv. of Japan, Tsukuba, 1983.

Karig, D.E., Origin and development of marginal basins in the Western Pacific, *J. Geophys. Res., 76,* 2542-2561, 1971.

Karig, D.E., Remnant arcs, *Geol. Soc. Am. Bull., 83,* 1057-1068, 1972.

Karig, D.E, and G.F. Moore, Tectonic complexities in the Bonin Arc system, Tectonophysics, 27, 97-118, 1975.

Karig, D.E. and G.F. Moore, Tectonically controlled sedimentation in marginal basins, Earth Planet. Sci. Lett., 26, 233-238, 1975.

Mogi, A., The Izu Ridge. in *Fossa Magna* (in Japanese), edited by M. Hoshino, Geol. Soc. Japan, Tokyo, 217-221, 1968.

Murakami, F. and T. Ishihara, Submarine caldera found in northern Ogasawara Arc (in Japanese), *Earth Monthly, 7,* 638-646, 1985.

Nemoto, K., and L.W. Kroenke, Marine geology of the Hess Rise 1. Bathymetry, surface sediment distribution, and environment of deposition. *J. Geophys. Res., 86,* 10734-10752, 1981.

Okamura, Y., and K. Nakamura, 3.5 kHz echo sounder profiling survey in the area northeast of Hachijojima. In *Geological Investigation of the Area Northeast of Hachijoshima Island, Northern Part of Ogasawara Arc,* edited by Inoue, E., Cruise Report 16, Geol. Surv. Japan, 15-19, 1981.

Swift, S., Late Pleistocene sedimentation on the continental slope and rise off western Nova Scotia,*Geol. Soc. Am. Bull., 96,* 832-841, 1985.

Taft, B.A., and P.H. Freitag, On the flow of the Kuroshio over the Izu Ridge, In *Proceedings Fourth CSK Symposium*, Tokyo, 181-200, 1979.

Taylor, B., D. Hussong, and P. Fryer, Rifting of the Bonin Arc (abstract), *EOS Tran. AGU, 65*, 1006, 1984.

Chapter III

Rifting of the Bonin Arc Between 29°50' and 31°20' N

3.1 Introduction

Just as continental rifts are the progenitors of mid-ocean spreading systems, so island-arc rifts are the progenitors of backarc spreading systems. In both continental and arc environments the rifting stage is fundamental to the subsequent structural, thermal, sedimentary, petrological, and overall economic evolution of the resulting passive margins, and also determines the initial geometry of the ridge/transform accreting plate boundary.

Because rifted margins of backarc basins are quickly buried by a thick apron of volcaniclastic sediments, studies of the initial rifting processes may best be undertaken in active intra-arc rifts (prior to backarc spreading). Such rifts include the Okinawa Trough [*Sibuet et al.*, 1987] and Bransfield Strait [*Weaver et al.*, 1979] in continental arcs, and the Havre Trough [*Malahoff et al.*, 1982; *Wright*, 1990a; *Wright et al.*, 1990b], Coriolis Trough [*Dubois et. al.*, 1978], northern Mariana Trough [*Beal*, 1987] and Bonin rifts [*Honza and Tamaki*, 1985] in oceanic arcs. This chapter reports on the results of geophysical mapping of the central Bonin rifts between 29°50' N and 31°30' N and it concentrates on the surficial morpho-tectonic, volcanic and sedimentary features.

Tectonic setting

Subduction of Pacific lithosphere beneath the West Philippine Plate (Figure 3.1) began by the Middle Eocene [*Karig*, 1975; *Kroenke et al.*, 1981], and through the Early Oligocene formed an intra-oceanic volcanic arc and a 200-km-wide forearc of arc volcanic material (tholeiites and boninites) [*Natland and Tarney*, 1981]. The proto-Mariana arc was formed on the edge of the Eocene

Figure 3.1 Tectonic map of the Philippine Sea Plate showing plate boundaries and main bathymetric features. Location of Figure 3.2 is shown by the rectangle. Vector at 30° N indicates the relative plate motion between the Pacific Plate and the Philippine Sea Plate calculated from the angular velocity and pole of rotation derived by *Seno et al.* [1987]. The location of the dashed Honshu/Eurasia plate boundary is from *Seno* [1985]. CBF-Central Basin Fault.

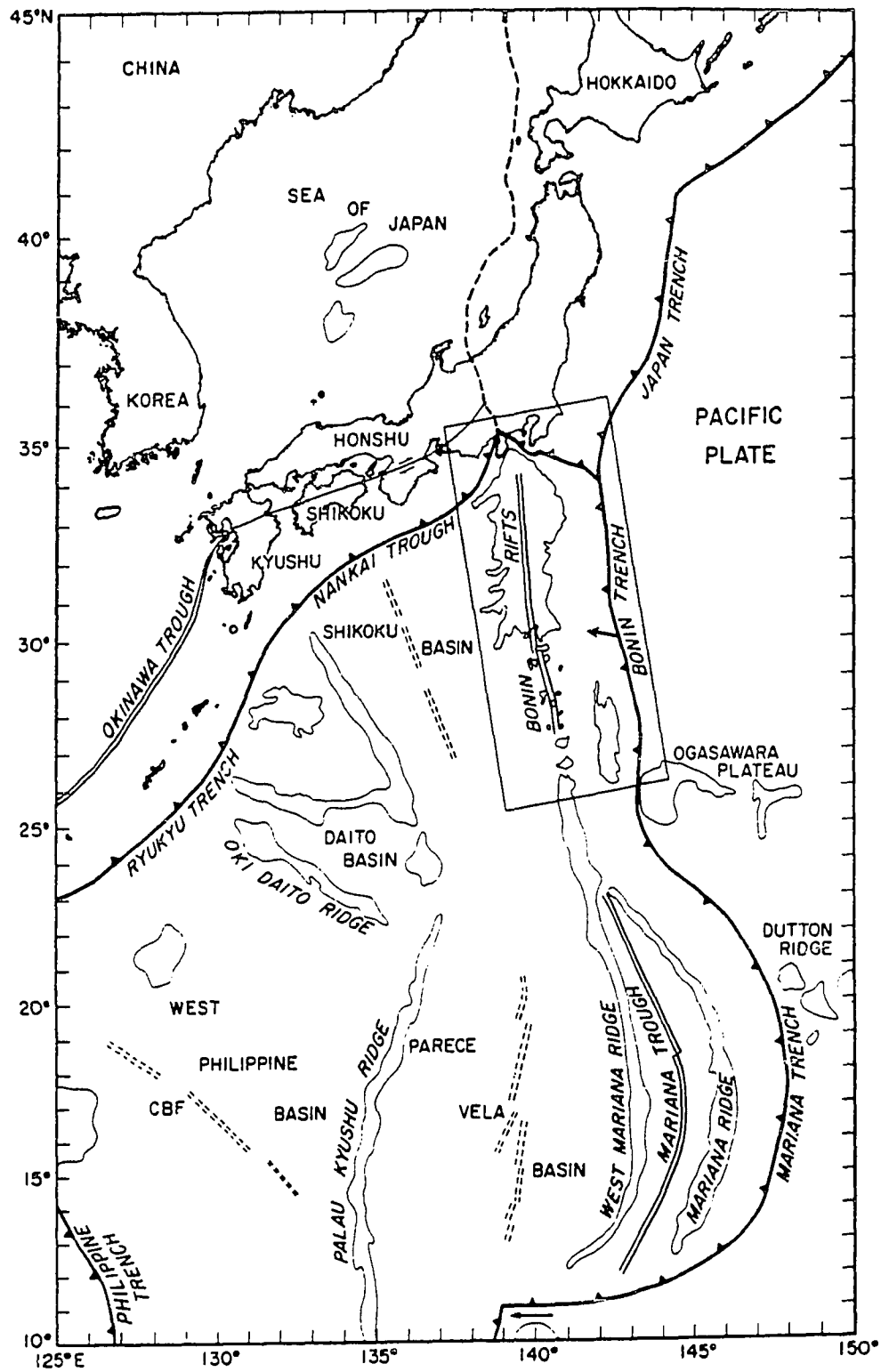
45°N
40°
35°
30°
25°
20°
15°
10°
125°E
130°
135°
140°
145°
150°
CHINA
HOKKAIDO
SEA
OF
JAPAN
KOREA
HONSHU
SHIKOKU
KYUSHU
PACIFIC
PLATE
JAPAN TRENCH
NANKAI TROUGH
OKINAWA TROUGH
RYUKYU TRENCH
SHIKOKU
BASIN
RIFTS
BONIN
BONIN TRENCH
OGASAWARA
PLATEAU
DAITO
BASIN
OKI DAITO RIDGE
DUTTON
RIDGE
WEST
PHILIPPINE
CBF
BASIN
PARECE
VELA
BASIN
PALAU KYUSHU RIDGE
WEST MARIANA RIDGE
MARIANA TROUGH
MARIANA RIDGE
MARIANA TRENCH
PHILIPPINE
TRENCH

West Philippine Basin whereas the proto-Bonin arc was formed on the edge on the Amani-Oki Daito province, a series of island arcs and intervening basins of Santonian to Paleocene age [*Shiki,* 1985]. Mid-Oligocene rifting split the arc and Late Oligocene-Early Miocene backarc spreading in the Parece Vela and Shikoku Basins isolated the remnant arc (Palau-Kyushu Ridge) from the active Bonin-Mariana arc and forearc [*Kobayashi and Nakada,* 1978; *Mrozowski and Hayes,* 1979]. However the initial spreading was not time-synchronous along the length of the Oligocene arc. It began 31 Ma in what became the central Parece Vela Basin and propagated both north and south, giving the basin its bowed out shape [*Mrozowski and Hayes,* 1979]. A second spreading segment began by 25 Ma in the northernmost Shikoku Basin and propagated south [*Kobayashi and Nakada,* 1978]. By 23 Ma the two systems had joined at what is now approximately 23° N and both basins shared a common spreading axis till spreading ceased at 17 to 15 Ma [*Shih,* 1980].

A similar history is being repeated in the Mariana Trough-Bonin rifts. The southern arc split again in the Late Miocene, and 6 to 8 m.y. of new seafloor spreading in the Mariana Trough has isolated the active Mariana arc from, and increased its curvature with respect to, the remnant West Mariana Ridge [*Karig et al.,* 1978; *Hussong and Uyeda,* 1981]. Spreading in the Mariana Trough may be propagating to the north, "unzipping" the Mariana arc from the West Mariana Ridge [*Stern et al.,* 1984] or propagating across the active arc [*Beal,* 1987]. In contrast, the Bonin arc is still in the rifting stage of backarc basin formation. The arc is undergoing extension along most of its length and is not simply rifting apart as the Mariana Trough propagates northward [*Honza and Tamaki,* 1985].

The arc is also being subducted to the north beneath Honshu. Rather than affecting the entire arc [*Karig and Moore,* 1975], deformation of the northern Bonin arc appears to be focussed on the leading edge of the downgoing plate

where subduction-related thrusting at the Nankai Trough is stepping seawards to the south side of Zenisu Ridge, the northernmost en-echelon ridge of the Bonin arc platform [*Le Pichon et al.*, 1987]. Geological data from south central Honshu indicates this process has been occurring over the past 15 My resulting in terrains of Bonin arc crust being accreted onto southern Honshu [*Taira et al.*, submitted]. The Izu Peninsula began accreting onto southern Honshu and deforming the intraplate area in the early Quaternary [*Matsuda*, 1978; *Huchon and Kitazato*, 1985].

Estimates of present motion between the Pacific and Philippine Sea plates are imprecise because of the absence of a spreading-center boundary or hotspot trace on the Philippine Sea Plate. The relative convergence between the two plates, constrained using seismic slip vectors, is estimated at 0.97 to 1.07 °/m.y. with a pole located between 2.1° S to 1.1° N and 133° E to 133.6° E [*Seno et al.*, 1987]. Based on this pole, relative convergence at 30° N is 58 mm/yr along 288° N, making an acute angle of 62° with the trench (Figure 3.1).

Magnetic anomaly lineations, seaward of the subduction zone, range from M11 (125 Ma) at 34° N to M21 (144 Ma) at 25° N [*Nakanishi et al.*, 1989]. The Wadati-Benioff zone dips at an average angle of 45° under the northern arc, steepening to near vertical under the southern arc [*Katsumata and Sykes*, 1969]. In the southern arc the thick Mesozoic Ogasawara Plateau has entered the subduction zone. Opposite the plateau there is a distinct change in the forearc and arc structure [*Honza and Tamaki*, 1985]. However the oblique northward relative motion of the Pacific plate with respect to the forearc means that the Ogasawara Plateau and the province of mid-Pacific seamounts (of which the plateau is the leading northern edge), must have been previously further to the south. As the Bonin Ridge (forearc high) has been at shallow water depths since the Eocene [*Shiki*, 1985] its present elevation cannot be the result of plateau collision alone.

Figure 3.2 Color bathymetry (500 m contour interval, Mercator projection) of the Bonin arc-trench system based on data from the Geological Survey of Japan, Hawaii Institute of Geophysics, Hydrographic Office of Japan, Ocean Research Institute (University of Tokyo), and the U.S. Naval Oceanographic Office.

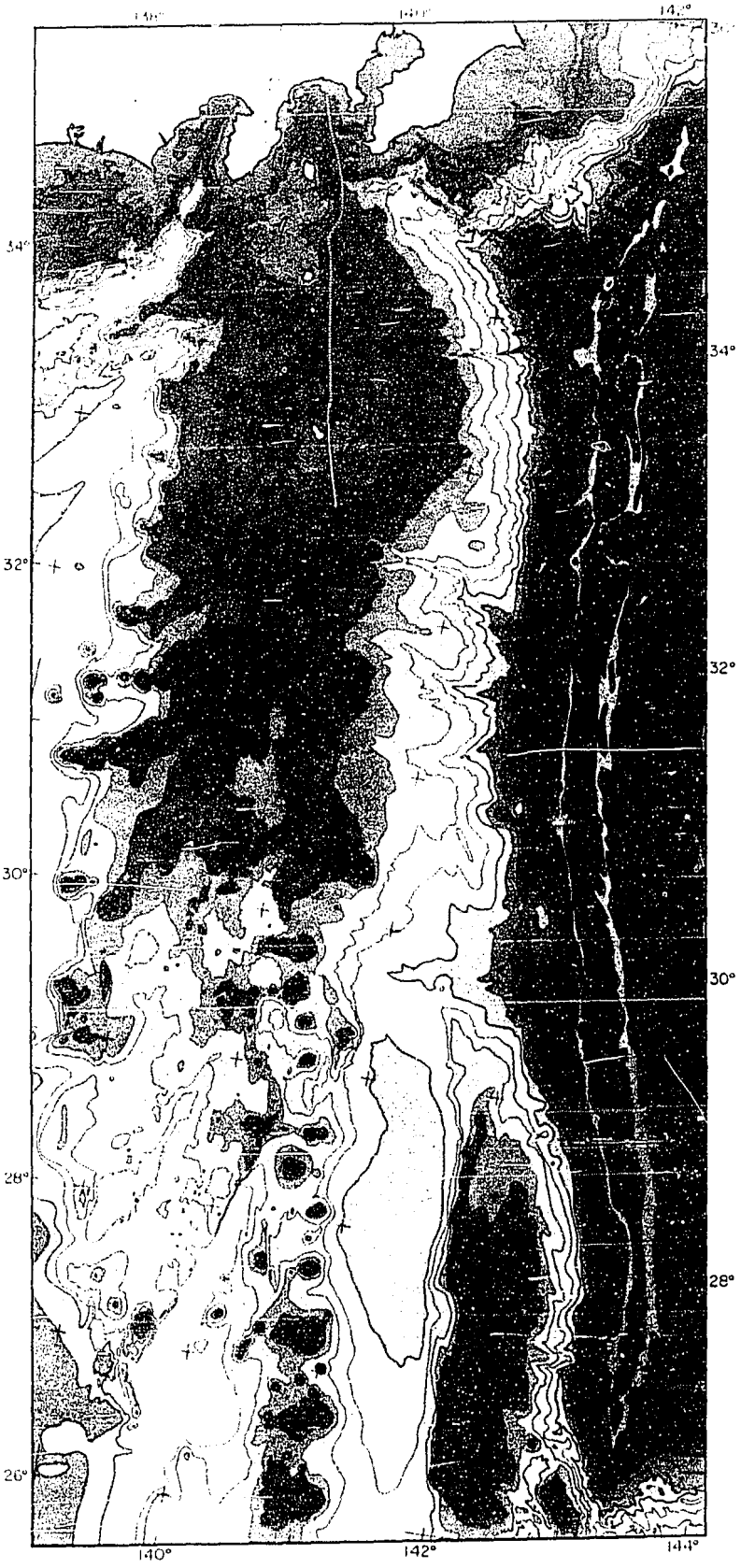
34°
32°
30°
28°
26°
140°
142°
144°

Previous work

A systematic geophysical survey and marine geological investigation of the Bonin and northern Mariana arcs was undertaken by the Geological Survey of Japan in 1979/80 [*Honza et al.,* 1982; *Honza and Tamaki,* 1985]. This provided the first clear delineation of the extent and development of the Bonin rifts. *Tamaki et al.* [1981] described four rift segments between 27° N and 33°20' N, which they named after nearby arc volcanoes (Hachijojima, Sumisujima, Torishima, and Nishinoshima). This thesis modifies their scheme, based on a new bathymetric compilation, to separately identify the Aogashima and Sofu Gan rift segments (Figure 3.3). There are no major rift basins apparent between 27° N and 24° N, the northern Mariana Islands [*Honza and Tamaki,* 1985], although there are small depressions and normal faults near sites of arc volcanism [*Yamazaki and Murakami,* 1987]. *Tamaki et al*. [1981] showed that the rifts are discontinuous along strike, 20 to 60 km wide and have eastern boundaries as little as 10 km west of the active arc. They recognized up to 500 m of volcanogenic sediment in some of the rifts, and sampled fresh basalt from highs within the Sumisu rift.

The seismic reflection profiles published by *Honza and Tamaki* [1985] show the characteristic structural elements of the Bonin arc (Figure 3.4). Above a small accretionary complex at the base of the inner trench wall there is a lower-slope terrace. The terrace is formed by sediments ponding around bathymetric highs spaced 15 to 60 km apart [*Taylor and Smoot,* 1984] (Figure 3.3). Where dredged, the highs consist of serpentinized and chloritized mafics and ultramafics [*Ishii,* 1985]. These protrusions were emplaced as a result of water, given off by the subducting plate, serpentinizing ultramafics in the forearc [*Fryer and Fryer,* 1987; *Ishii et al.,* 1988].

The trench-slope break is formed by an outer forearc basement high which, where exposed to the south in the Bonin Islands, consists of Middle and Late Eocene boninites and island-arc tholeiites [*Shiraki et al.*, 1980; *Tsunakawa et al.*, 1983]. A thick forearc basin sedimentary sequence is observed to lap onto and thin over this outer forearc high. In the southern arc the forearc basin forms the distinct Bonin Trough with sediment thickness greater than 3 km. Major submarine canyon systems with dendritic drainage patterns incise the gentle slopes of the forearc basins north of 29°30' N (Figure 3.3) [*Taylor and Smoot*, 1984]. Discontinuous frontal arc basement highs are present east of the active arc (Figure 3.2) [*Honza and Tamaki*, 1985; *Yuasa and Murakami* 1985]. Eocene fossils have been found in rocks dredged from several of these highs [*M. Yuasa*, pers. comm., 1987].

The Bonin frontal arc volcanoes lie within 10 km of a straight line, bearing 170° N from Oshima to Kaitoku Seamount (Figure 3.3) and south to Iwojima. Historic eruptions have occurred on or near Oshima, Niishima, Myojin Sho, Sumisujima, Torishima, and Nishinoshima [*Simkin et al.*, 1981; *Smoot*, 1988]. Historic volcanism is especially common along the chain of seamounts from 24° N to 25°30' N in the vicinity of the Volcano Islands. Although subaereal volcanoes define a simple chain of islands, the regional bathymetry reveals a broad arc platform with active volcanoes and rift basins on the east and a province of volcanic ridges on the west (Figure 3.3). The latter are arranged in an en-echelon pattern [*Karig and Moore*, 1975a]. The NE- to ENE-trending chains of volcanoes overprint much of the eastern Shikoku Basin older than magnetic anomaly 6A [*Shih*, 1980]. Many of these chains do not extend eastward to the volcanic front. Instead, separate volcanic or tectonic ridges, trending either E-W (e.g. near Sofu Gan) or NNE (e.g. near Torishima and Kaikata Seamount), are found immediately to the west of the volcanic front. Similar chains of volcanoes at a high angle to the volcanic front are found along the active and remnant arcs of the

Figure 3.3 Tectonic map of the Bonin arc-trench system showing the locations of volcanoes (filled circles), frontal arc volcanoes (triangles), backarc rift segments (fault symbols), forearc canyons, and lower forearc ultramafic highs (non-circular filled areas). The main volcanoes are **Fu**-Fuji, **Ha**-Hakone, **Os**-Oshima, **Ni**-Niijima, **Me**-Miyakejima, **Ma**-Mikurajima, **H**-Hachijojima, **A**-Aogashima, **Ms**-Myojin Sho, **S**-Sumisujima, **T**-Torishima, **SG**-Sofu Gan, **N**-Nishinoshima, **Ka**-Kaikata Seamount, **Ku**-Kaitoku Seamount. Named rift segments (sidefacing bold letters) are **H**-Hachijo Rift, **A**-Aogashima Rift, **S**-Sumisu Rift, **T**-Torishima Rift, **SG**-Sofu Gan Rift, **N**-Nishinoshima Rift. Oblique crossarc lineaments are indicated by stipled line segments. Background bathymetry is from Figure 3.2.


138°
140°
142°
36°
34°
32°
30°
28°
26°
144°
HONSHU
Fu
Ha
SURUGA TROUGH
IZU PENN
SAGAMI TROUGH
JAPAN TRENCH
Ob
Ni
Me
Ma
NANKAI TROUGH
ZENISU RIDGE
H
A
Ms
S
SHIKOKU BASIN
T
SG
N
Ka
Ku
BONIN TROUGH
BONIN RIDGE
BONIN TRENCH
OGASAWARA PLATEAU
VOLCANO
FRONTAL ARC VOLCANO
FOREARC CANYON
ULTRAMAFIC HIGH ON LOWER FOREARC
RIFT SEGMENT
CROSSARC LINEAMENT

Mariana system [*Hussong and Fryer,* 1983]. The origin and petrochemistry of these volcanic cross chains are not yet understood in detail. However they are probably related to arc magmas erupting along cross-arc discontinuities and fractures. Contrary to the interpretation of *Karig and Moore* [1975a], our more detailed bathymetry shows that the chains in the Shikoku Basin between 30° N and 33° N parallel early opening flow lines. Several of them are aligned with Shikoku Basin fracture zones proposed by *Shih* [1980].

Previous authors have suggested crossarc structures that control these as well as more NNE-trending bathymetric lineaments on both sides of the arc are strike-slip faults, resulting from Riedal shears associated with oblique motion along the Philippine-Pacific plate boundary [*Kaizuka,* 1973], or collision of the Bonin arc with Japan during the opening of the Japan Sea [*Karig and Moore,* 1975a; *Bandy and Hilde,* 1983]. The most pronounced backarc tectonic lineament occurs in the southern arc, far away from the collision zone at the northern edge of the plate (Figure 3.2 and 3.3). *Yuasa* [1985] suggested the NNE-trending scarp between 26° N and 28°30' N, which he termed the "Sofu Gan Tectonic Line" (STL) resulted from strike-slip motion due to differential opening of the Shikoku and Parece Vela basins.

It is possible to recognize the existence not only of 020°-035° but also of 315°-330° bathymetric lineaments on both sides of the arc (Figure 3.3). A few of the many examples of the latter include the 500 m contour NE of Hachijojima, the offset of the Bonin Ridge near 27° N, and the ridge terminating the south end of the STL at 26°45' N. Together, the two trends form a conjugate pair, which is readily apparent in the 4 km contour on the west side of the Bonin Trough. These bathymetric trends appear to be the surface expression of a basement structural fabric which criss-crosses the Bonin arc (forearc and backarc). This conjugate fabric is approximately bisected by the active arc line and may have originated

Figure 3.4 Line-drawing interpretations of single-channel seismic reflection profiles across the northern Bonin arc between 29° N and 33°30' N collected by the Geological Survey of Japan (modified after *Honza and Tamaki* [1985]). The volcanic front is indicated by short line segments.

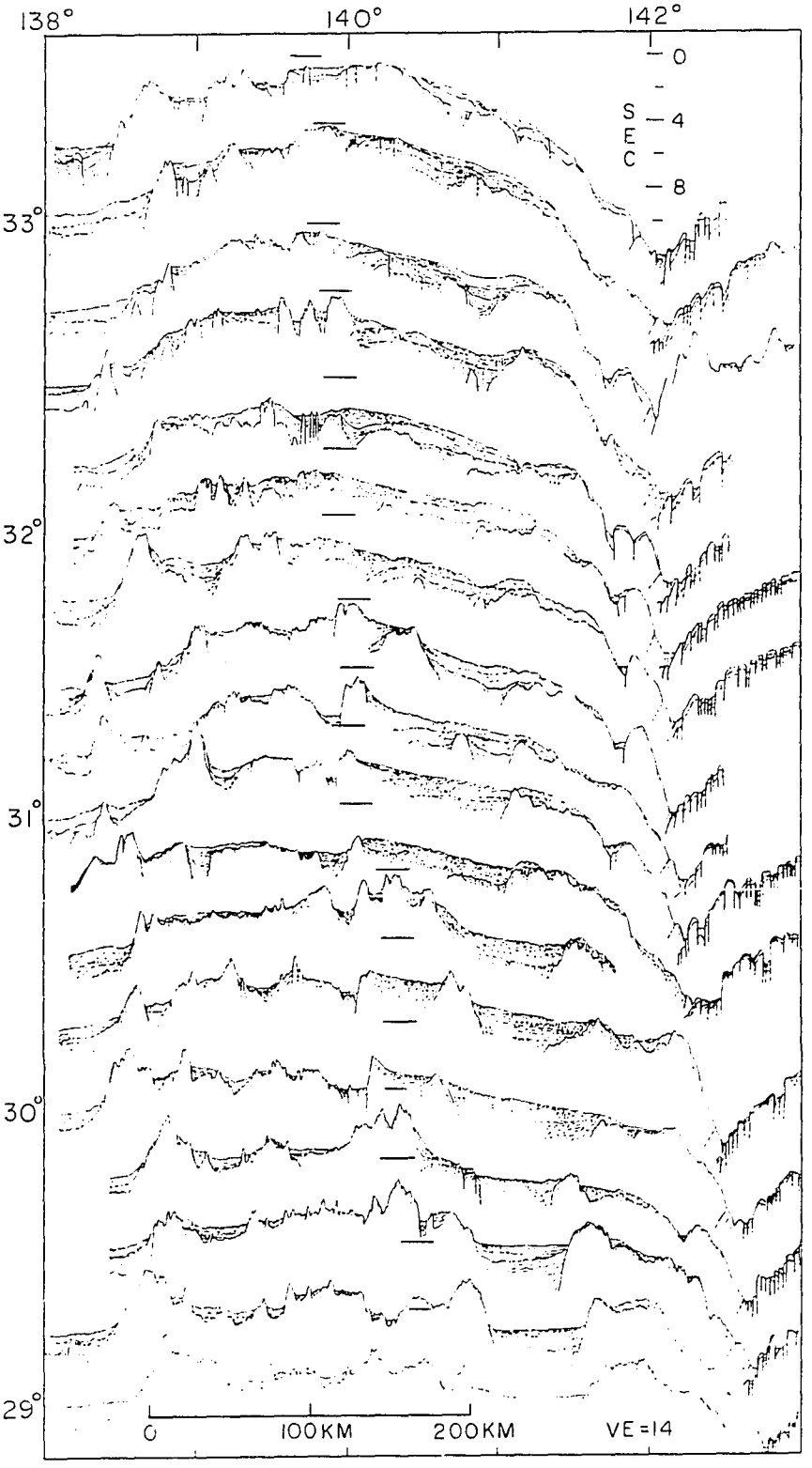
138°
140°
142°
33°
32°
31°
30°
29°
0
S
E
C
4
8
0
100KM
200KM
VE=14

from either arc-parallel compression or arc-orthogonal extension. Recent documentation of extensive mid-Oligocene rifting (*Leg 126 shipboard scientific party*, 1989), both in the forearc and in the backarc suggests these basement trends are an expression of an orthorhombic pattern of normal faulting similar to that found in the active rifts (see below). The importance for our discussion is knowing that the Bonin arc has a pre-rift structural fabric which may be re-activated and/or may influence rift segmentation.

Data

In June of 1984 the Hawaii Institute of Geophysics conducted a survey of the central Bonin arc with the *R/V Kana Keoki* from the Hawaii Institute of Geophysics. Navigation was based on LORAN-C (using the Iwojima, Hokkaido, and Marcus Island network) and transit satellite fixes. During the cruise we surveyed approximately 14,000 km^2 over seven semi-isolated depressions within the central Bonin backarc between 29° N and 31°30' N with the SeaMARC II sidescan acoustic imagery and bathymetry system. This paper presents 10,000 km^2 of this data from the Sumisu and Torishima rifts, north of 29°50' N; the remainder is presented in Chapter IV. SeaMARC II is a shallow-tow instrument capable of mapping 10 km seafloor swaths. The sidescan imagery (Figure 3.5) is presented such that dark areas represent strong returns (from bottom reflectivity and backscatter) and light areas represent weak returns [*Blackinton*, 1986]. The bathymetric data are contoured every 100 m (Figure 3.6). The SeaMARC II imagery and bathymetry for the area discussed in this paper can be found in the Appendix as published by the Geological Survey of Japan at 1:200,000 scale [*Taylor et al.*, 1988]. Analog single-channel seismic reflection data and 3.5 kHz echosounder data were collected simultaneously with the sidescan data. Seismic reflection profiles and corresponding line-drawing interpretations are labelled

from "A" to "X" (Figures 3.7 and 3.8). Horizontal scales have been corrected so profiles have a consistent vertical exaggeration (10x). This study also uses 3.5-kHz echosounder profiles collected by the Geological Survey of Japan with the *R/V Hakurei-Maru* in 1979, '80 and '84.

The combined data sets have allowed us to produce detailed geological maps of the central Bonin rift system (Figure 3.9). A geological map of Sumisu and Torishima rifts has been published in color by the Geological Survey of Japan at the 1:200,000 scale [*Brown et al.*, 1988]. This map shows the distribution of volcanoes, acoustic bedrock, and stratified verses unstratified sediment, inferred from high-frequency geophysical methods (3.5 kHz data). A high density of geophysical data from the Hawaii Institute of Geophysics and the Geological Survey of Japan were used in this study (Figure 3.10). Within the SeaMARC II survey area (perimeter on Figure 3.10), the largest circle which can be inscribed between tracks is under 7.5 km in diameter. Thus, only a handful of features (e.g. faults, volcanoes, or sediment areas) observed on the SeaMARC II imagery could not be located on echo-character profiles.

3.2 Sedimentation

The Bonin rift grabens are floored by syn-rift sedimentary basins and are bounded by "active arc" and "proto-remnant arc" margins on the east and west respectively (Figure 3.11). The active arc margin, comprising the frontal arc volcanoes and eastern rift flank uplifts, separate the rift and forearc basins. The proto-remnant arc margin, between the rift and Shikoku basins, is a broad province of fault blocks and volcanoes, of which we surveyed only the eastern portion.

Of the seven large backarc sediment basins surveyed in 1984, four and the northern branch of one, are described in this paper (Figure 3.11, diagonal lines); the rest are studied in Chapter IV. Sediments are found to accumulate in the rift-

Figure 3.5 SeaMARC II sidescan acoustic imagery mosaic of the Sumisu and Torishima rift segments (1:500,000- Transverse Mercator projection). The data south of 30°40' N has been corrected for near nadir reflections and water-bounce multiples. This data has been published at the 1:200,000 scale [*Taylor et al.*, 1988a].

31° 20' N
30° 40' N
139° 30' E
31° N

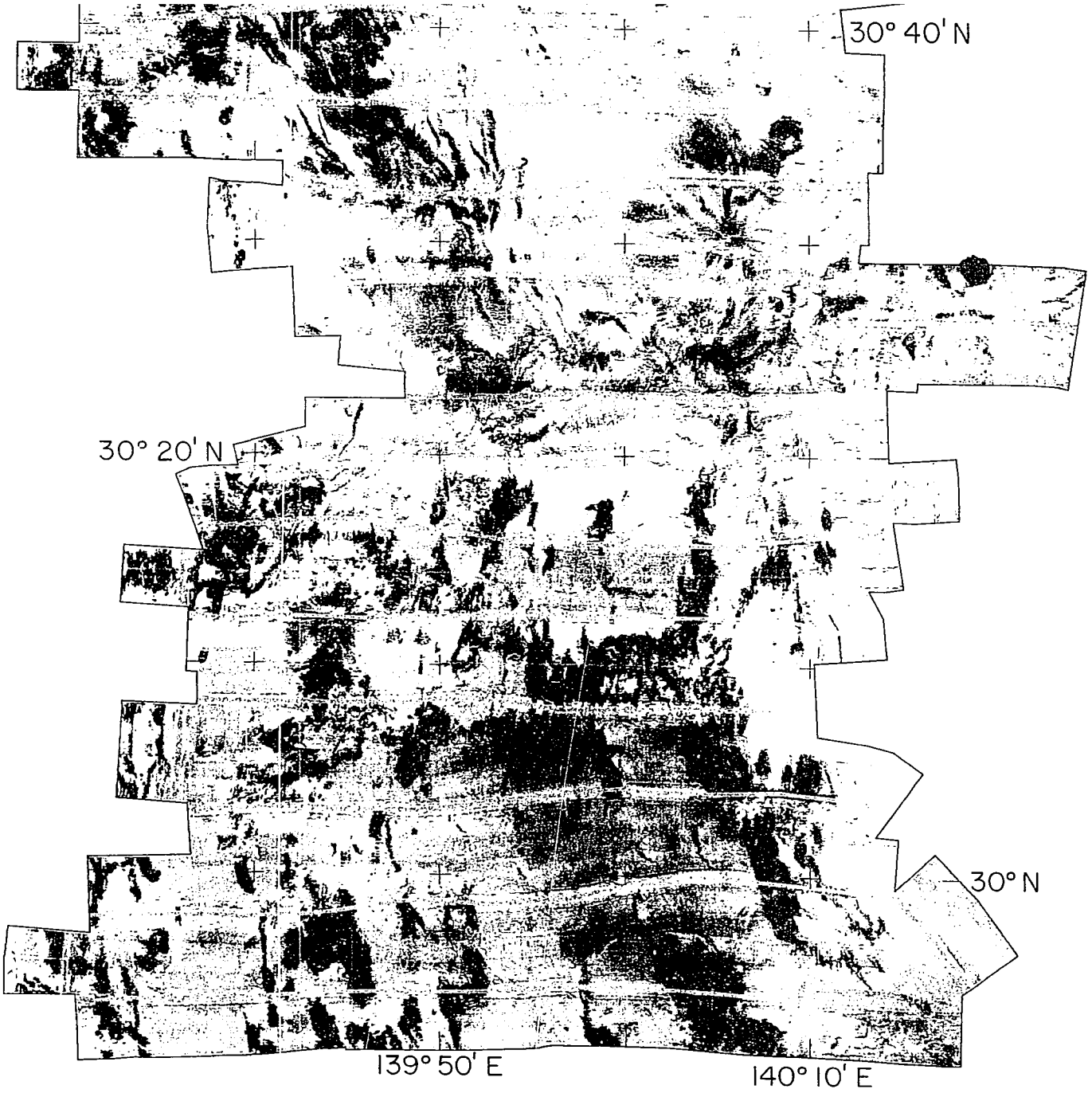
30° 40' N
30° 20' N
30° N
139° 50' E
140° 10' E

Figure 3.6 SeaMARC II bathymetry of the Sumisu and Torishima rift segments (100 m contours, 1:500,000). Contours are dashed in areas with no SeaMARC II coverage. This bathymetry has been published at the 1:200,000 scale [*Taylor et al.*, 1988b].

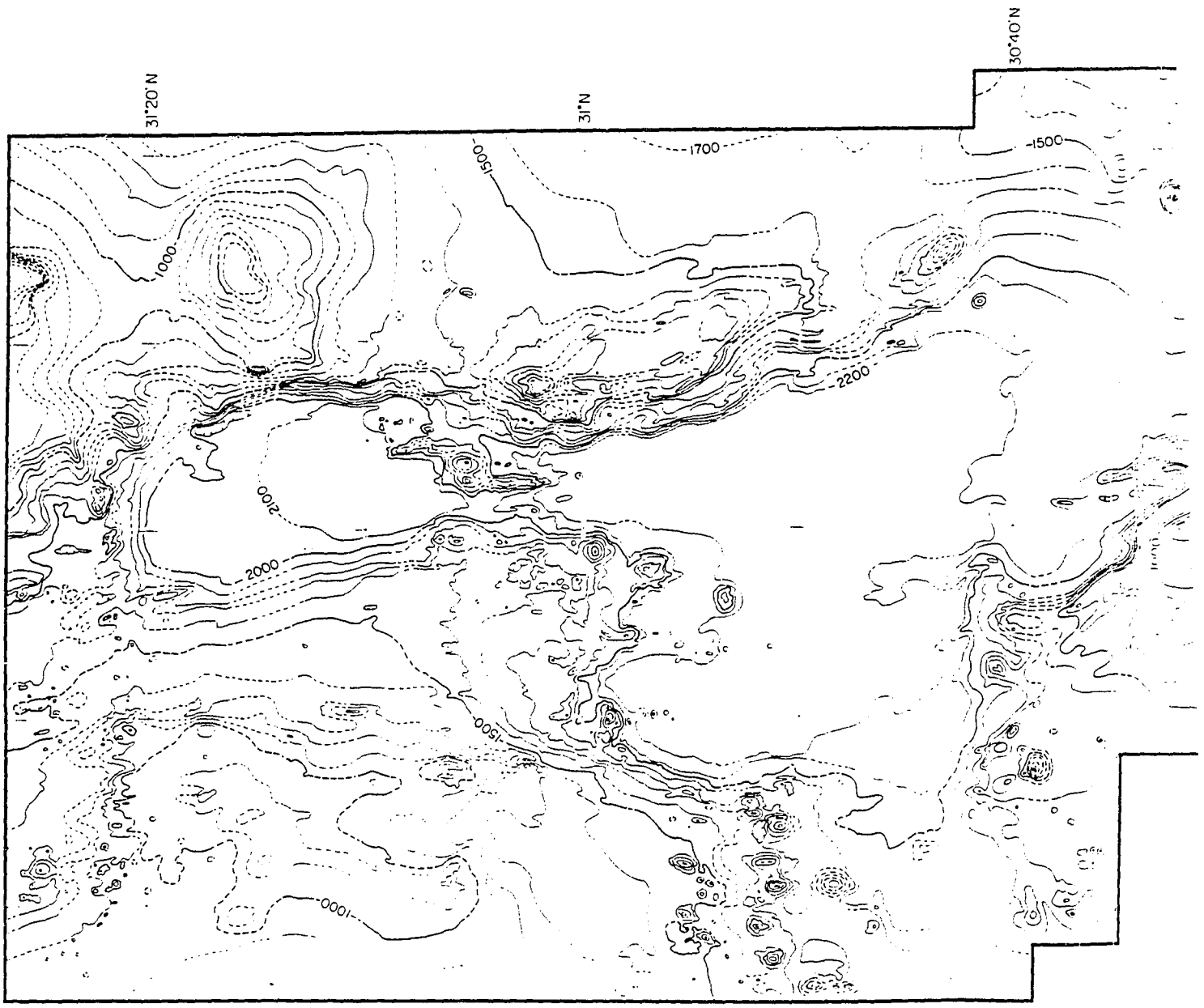
31°20' N
31° N
30°40' N
1700
1500
1000
2200
2100
2000
1500
1000

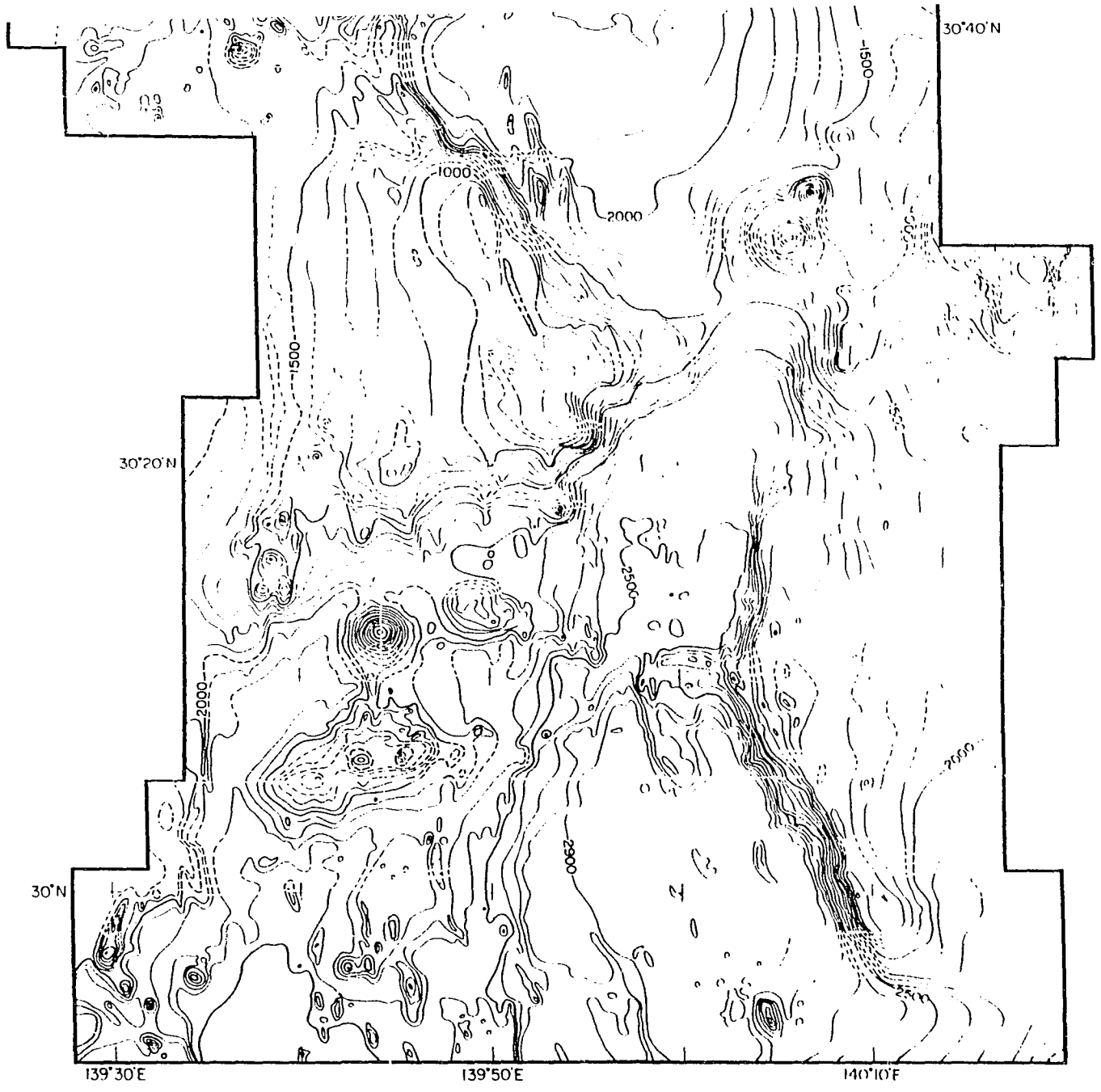
30°40'N
30°20'N
30°N
139°30'E
139°50'E
140°10'E
500
1000
1500
2000
2500
3000

Figure 3.7. Single-channel seismic profiles (**A to M**) and corresponding line-drawing interpretations. The vertical exaggeration on all profiles is 10x. The profiles are centered on 139°50' E. Refer to Figure 3.10 for location.

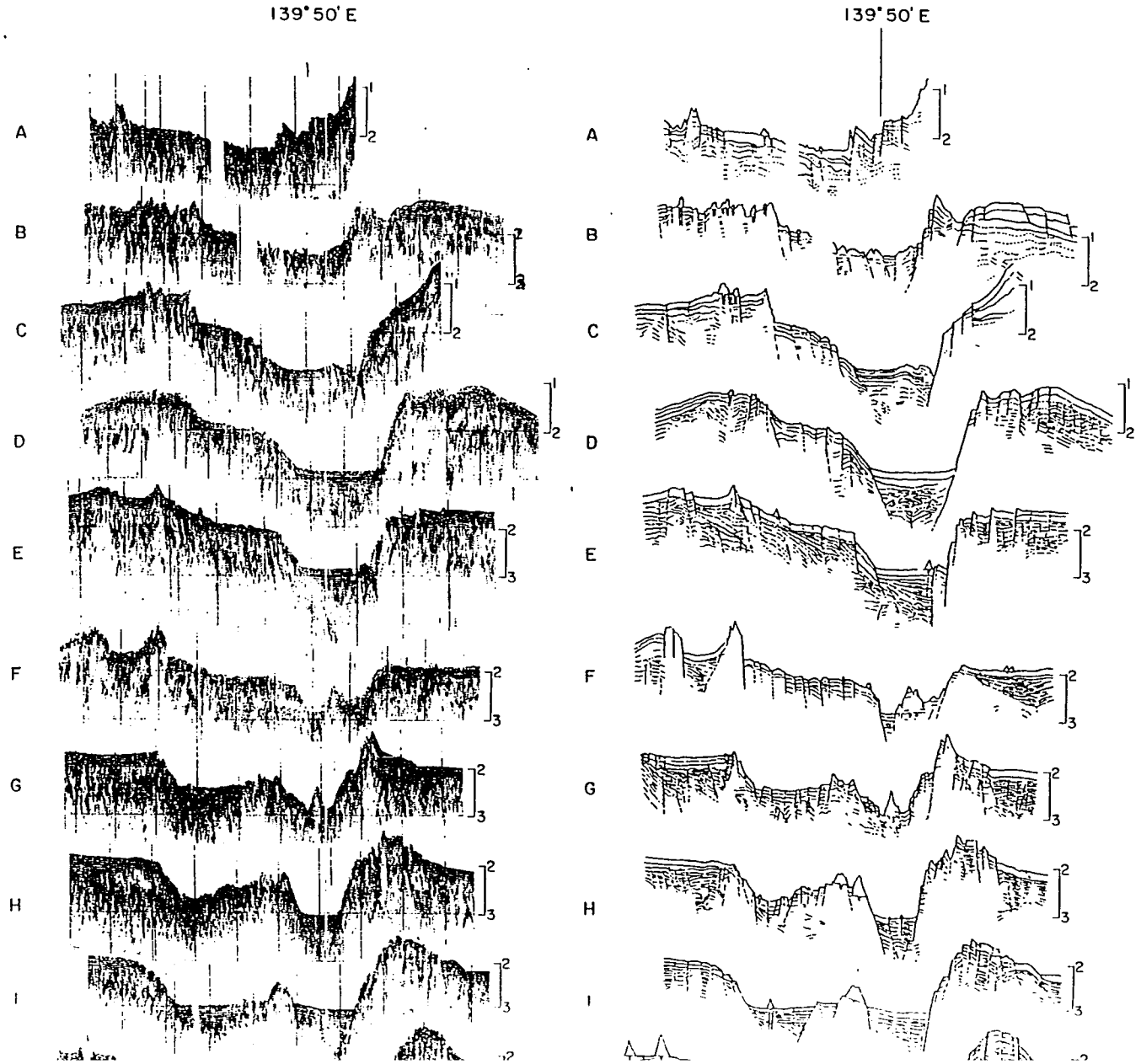
139°50' E
139°50' E
A
B
C
D
E
F
G
H
I

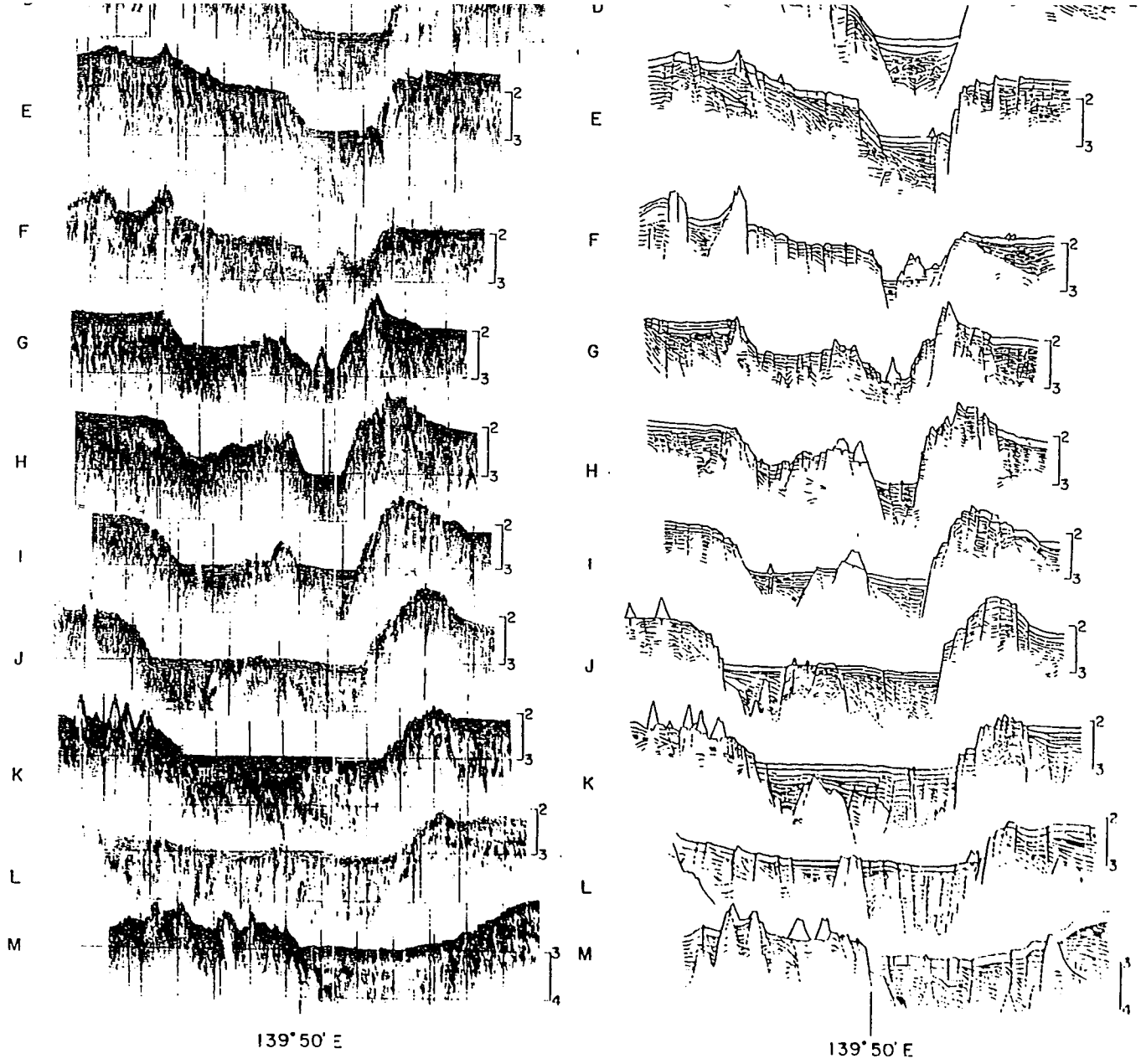
E
F
G
H
I
J
K
L
M
139°50' E
139°50' E

Figure 3.8. Single-channel seismic profiles (**N to X**) and corresponding line-drawing interpretations. The vertical exaggeration on all profiles is 10x. The profiles are centered on 140°00' E. Refer to Figure 3.10 for location.

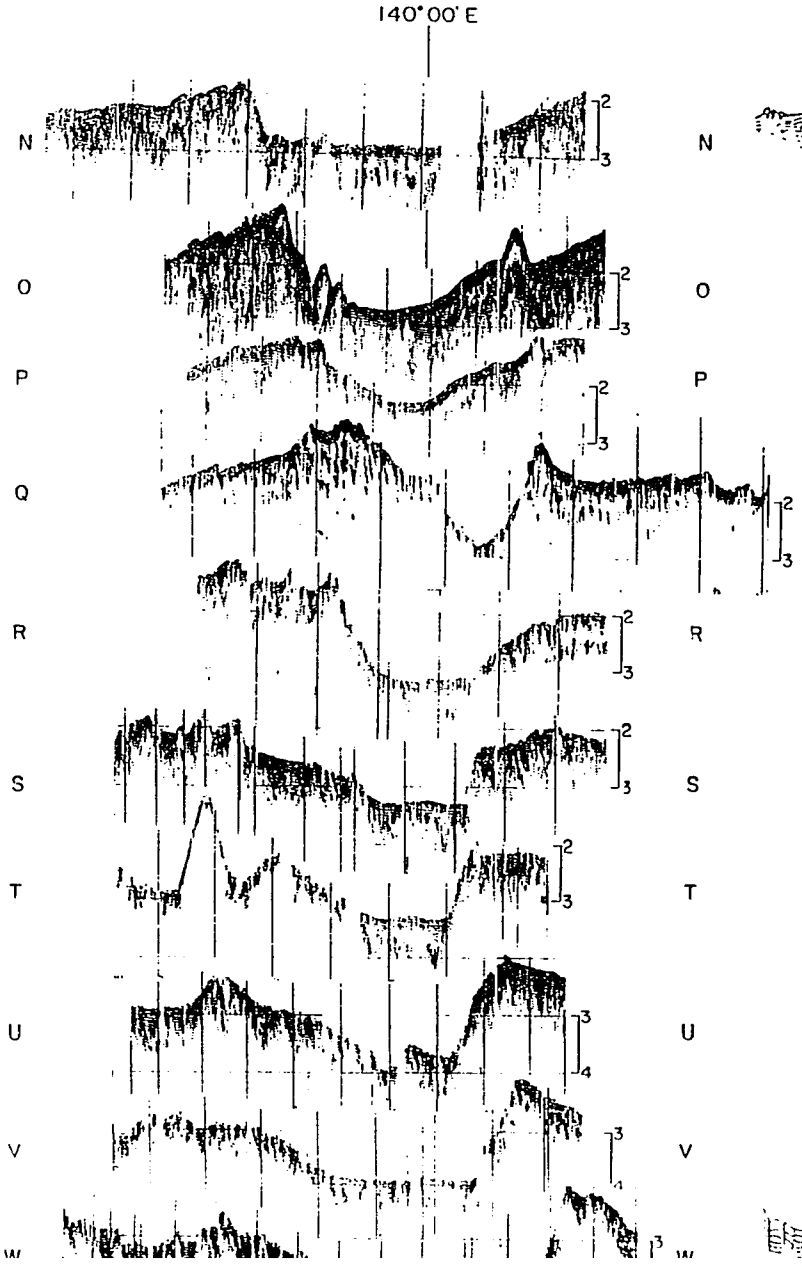
140°00' E
N
O
P
Q
R
S
T
U
V
W

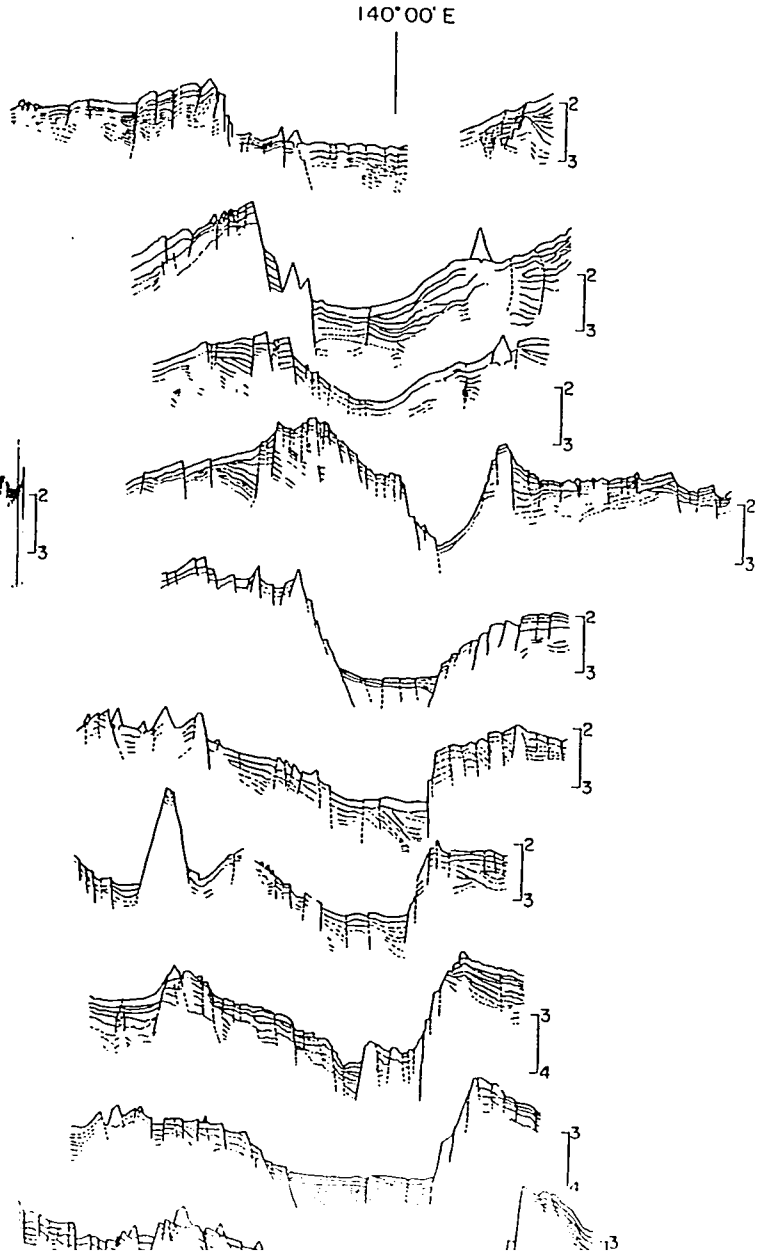
140°00' E
N
O
P
R
S
T
U
V
W

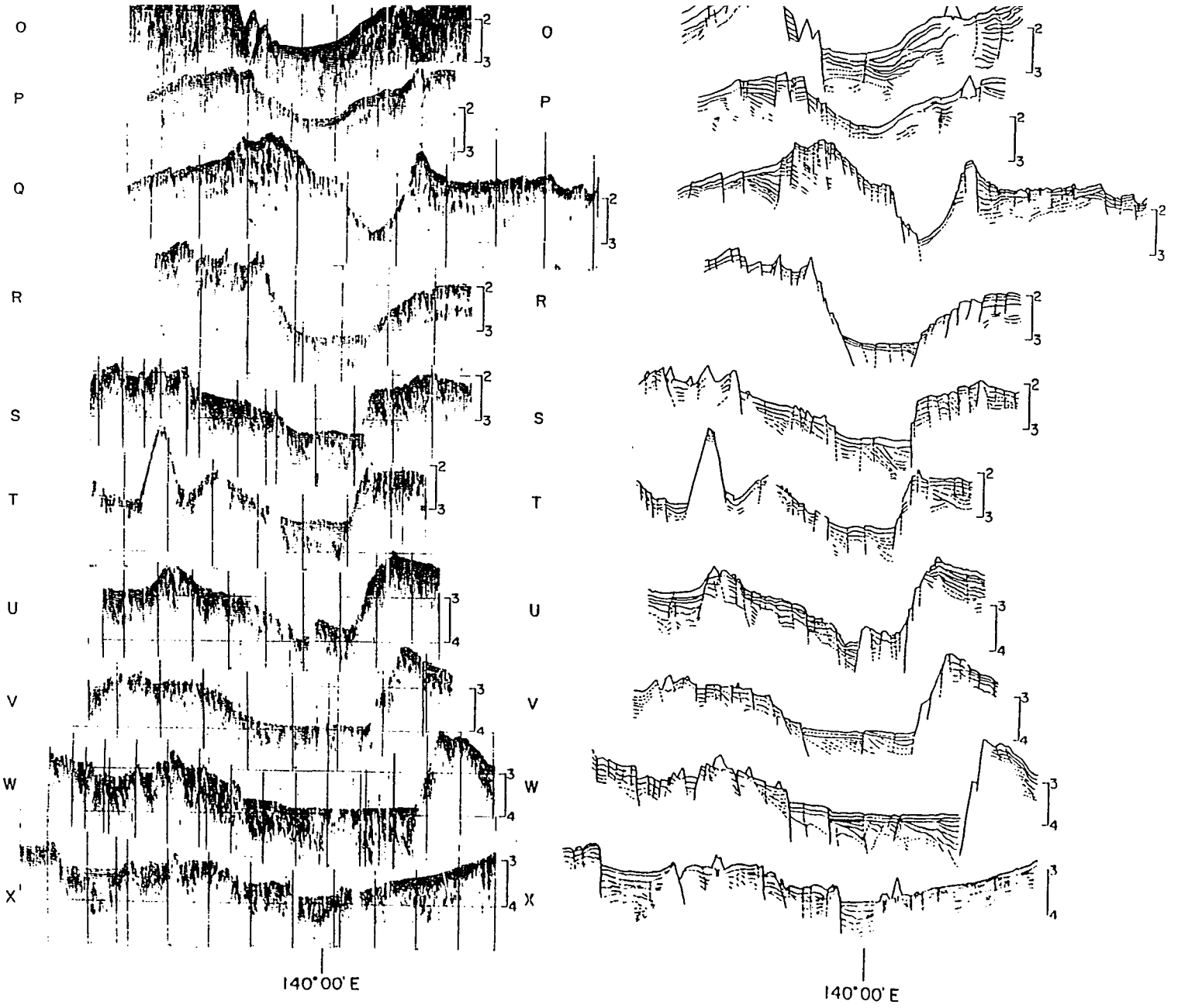
O
P
Q
R
S
T
U
V
W
X'
X
140°00' E
140°00' E

Figure 3.9. Seafloor geological map of the Sumisu and Torishima rifts (1:500,000, Transverse Mercator projection), which has been published in color at 1:200,000 by *Brown et al.* [1988]. The map was based on SeaMARC II data and close-spaced 3.5-kHz data from the Hawaii Institute of Geophysics and the Geological Survey of Japan (see Figure 3.10). Filled areas-extrusive lavas; **Br**-acoustic bedrock (exposures of rock from normal faulting, uplift, or mass-wasting); **Sp** (see Figure 3.12)-unstratified surficial sediments on 3.5 kHz echocharacter records (no subbottom reflectors); **Ss** (see Figure 3.12)-stratified sediment (subbottom reflectors indicative of turbidites); **Su**-unclassified sediment.

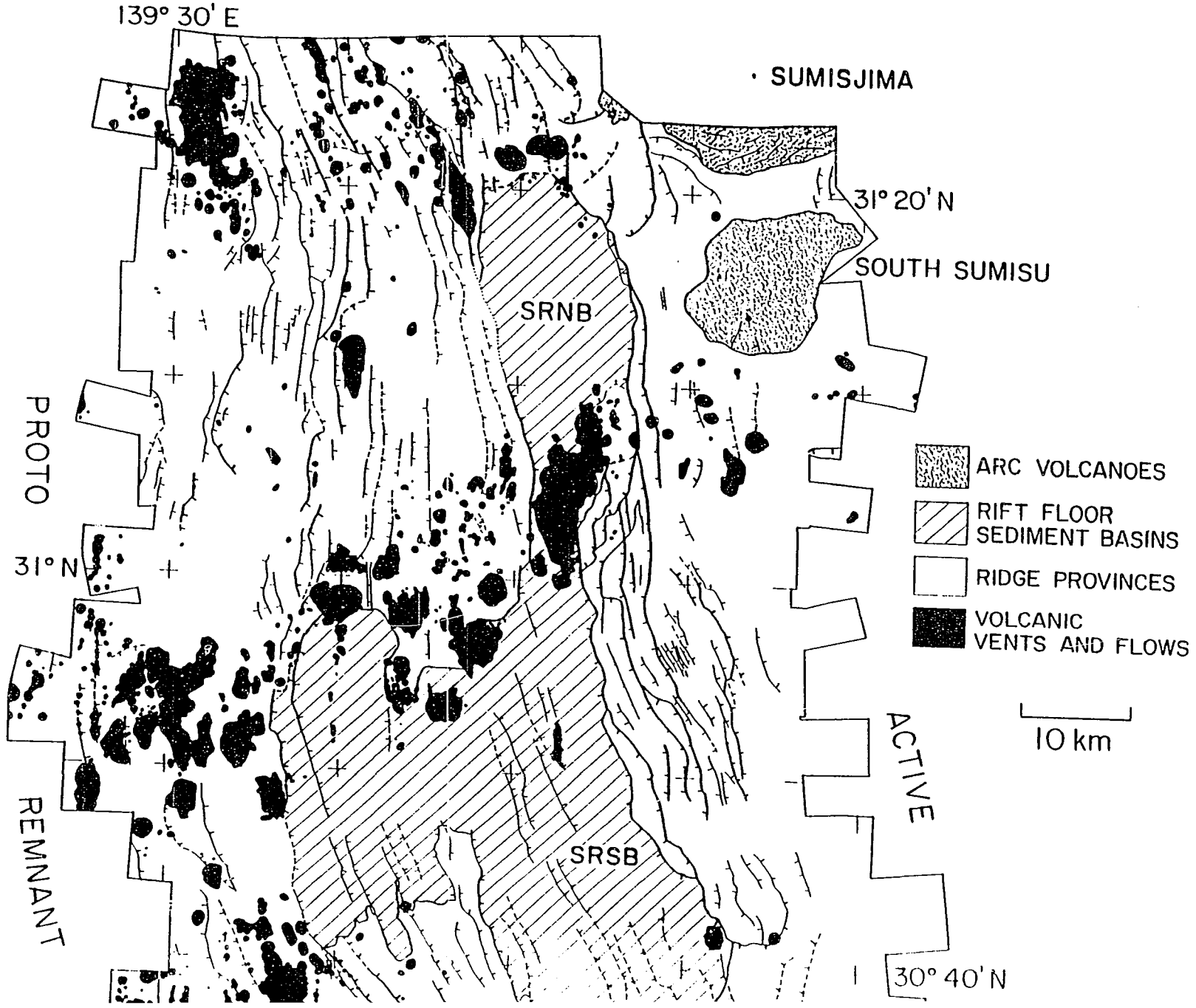
139° 30' E
SUMISJIMA
31° 20' N
SOUTH SUMISU
SRNB
PROTO
31° N
REMNANT
ACTIVE
SRSB
30° 40' N
ARC VOLCANOES
RIFT FLOOR SEDIMENT BASINS
RIDGE PROVINCES
VOLCANIC VENTS AND FLOWS
10 km

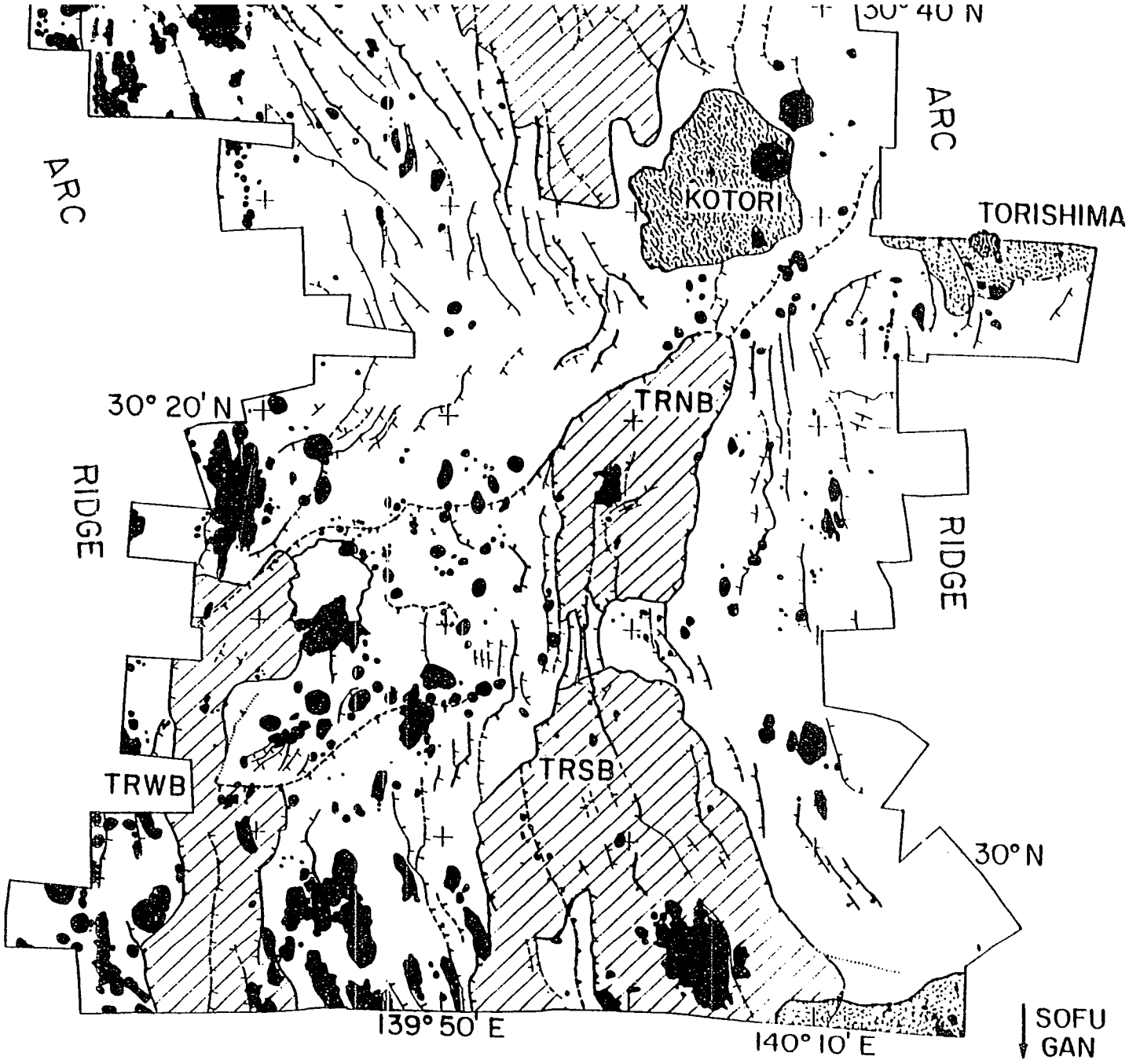
30° 40' N
ARC
ARC
KOTORI
TORISHIMA
30° 20' N
TRNB
RIDGE
RIDGE
TRWB
TRSB
30° N
139° 50' E
140° 10' E
SOFU GAN

Figure 3.10. Hawaii Institute of Geophysics *R/V Kana Keoki* (solid) and Geological Survey of Japan *R/V Hakurei Maru* (dashed) ship tracks from the Sumisu and Torishima rifts. The 3.5 kHz echocharacter data from these cruises was used to interpret and map seafloor geology. Thick solid lines (alphabetized) correspond to single-channel seismic reflection profiles in Figures 3.7 and 3.8. The enclosing line is the perimeter of the SeaMARC II imagery survey area (see Figure 3.5) The location of the seismic profile in Figure 3.13 is indicated by the thicker solid line near profiles V to X.

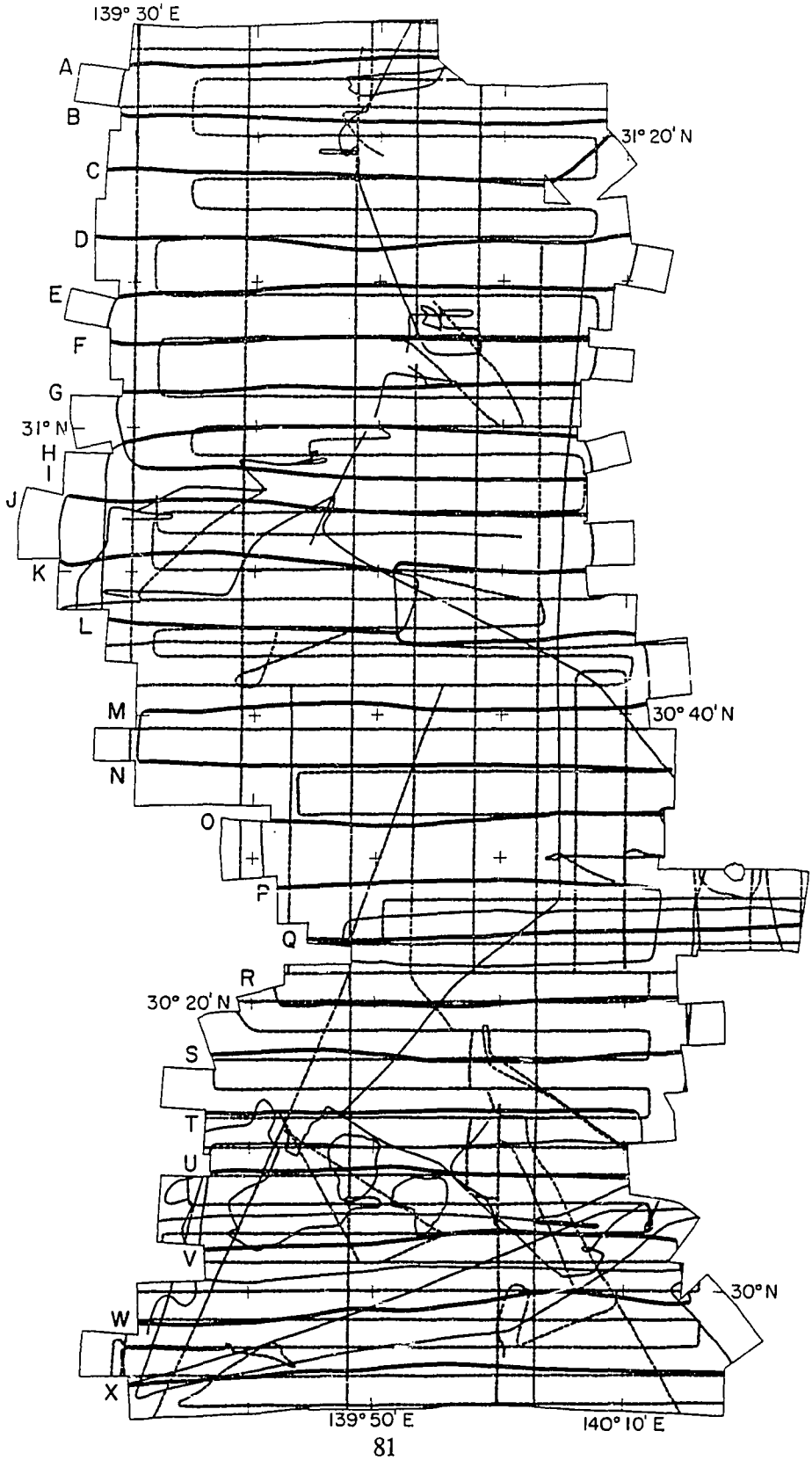
139° 30' E
A
B
C
D
E
F
G
31° N
H
I
J
K
L
M
N
O
P
Q
R
30° 20' N
S
T
U
V
W
X
31° 20' N
30° 40' N
30° N
139° 50' E
140° 10' E

floor basins and fault-block basins, on terraced ledges on the walls of the rifts, and around the slopes of arc volcanoes. Each sedimentary basin (Figure 3.11) has a discrete morphology, structure, and depositional environment. The southern sedimentary basin of Torishima Rift (TRSB) is approximately 25 km east-west and 33 km north-south. The depth of the seafloor approaches 3000 m in the center of the basin, the deepest place in the survey area. The basin's southern margin (just south of the SeaMARC mosaic) lies against the east-west trending volcano-tectonic ridge west of the island of Sofu Gan. South of the data presented in this paper, a narrow branch of TRSB links up with the west basin (TRWB) of Torishima Rift (Figure 3.3, [*Tamaki et al* [1981]). The TRWB, with a width at 30° N of only 10 km, is 30 to 40 km west of the regional axis of subsidence in the TRSB. The basin floor deepens from 2200 m in the north to over 2500 m in the south. The northern sedimentary basin or Torishima Rift (TRNB) is approximately 13 km east-west and 26 km north-south and averages about 2500 m water-depth. The southern basin of Sumisu Rift (SRSB) is 30 km (east-west) by 60 km (north-south). The basin averages 2200 m water-depth with a maximum depth approaching 2300 m along the eastern margin of the basin. The northern basin of Sumisu Rift (SRNB) is 13 km (east-west) by 32 km (north-south) with a maximum depth just below 2100 m. North of SRNB there is a 10 km wide depocenter that continues off of the mosaic for another 15 km on a NNW trend [*Murakami,* 1988].

Heat-flow measurements in the sedimentary basins are locally high but variable, ranging from 38 to 700 mW/m^2 in the SRSB [*Yamazaki,* 1988]. Apparently, extensional deformation allows hydrothermal circulation to continue despite the up to 1500 m thick sedimentary section.

Our knowledge of the composition and distribution of the upper seafloor sediments is based on gravity cores collected by the Geological Survey of Japan, SeaMARC II imagery, and the dense coverage of 3.5 kHz echo-character profiles.

Except at OPD Sites 790 and 791, core samples from rift-floor basins have only been obtained from the top 2 m of sediment [*Nishimura and Murakami,* 1988; *Nishimura et al.,* 1988]. These surficial sediments are hemipelagic and volcanogenic turbiditic silts and clays with layers of both scoriaceous and pumiceous ash. Beneath a thin (5 to 40 cm) brown oxidized layer the sediments are all reduced and grey. Carbonate content is rarely above 12%. Bioturbation is common but the turbidites sometimes retain parallel or cross lamination. *Nishimura and Murakami* [1988]point out that samples from the SRNB tend to have coarser volcanogenic turbidites than those from the SRSB.

Sedimented regions have low reflectance and therefore image light-medium grey on the sidescan (Figure 3.5). Occasionally this low reflectance in the sedimentary basins is interrupted by strong returns from fault-block ridges or volcanic flows.

The sedimented areas are further subdivided based on their acoustic properties as seen on 3.5 kHz echo-sounder data, using a scheme similar to that of *Damuth* [1980] and in Chapter II (Figure 3.12). In sedimented areas, a prolonged unstratified echo indicates coarse grain size. This is inferred from analyses of core samples [*Damuth,* 1980] and from the distribution of this acoustic facies around arc volcanoes (Chapter II). The absence of subbottom reflectors implies rapid deposition with few hiatuses. In general, multiple subbottom reflectors are indicative of episodic depositional events such as from turbidite deposits (Figure 3.12B) [Chapter II, *Nishimura and Murakami,* 1988]. In the deeper parts of the rifts, well sedimented areas (especially in the SRSB) can have an upper transpar-

Figure 3.11. Map of Sumisu and Torishima rifts, showing the main physiographic features, rift and arc volcanoes, faults and rift-floor sediment basins. **SRNB**-Sumisu Rift North Basin, **SRSB**-Sumisu Rift South Basin, **TRNB**-Torishima Rift North Basin, **TRSB**-Torishima Rift South Basin, **TRWB**-Torishima Rift West Basin.

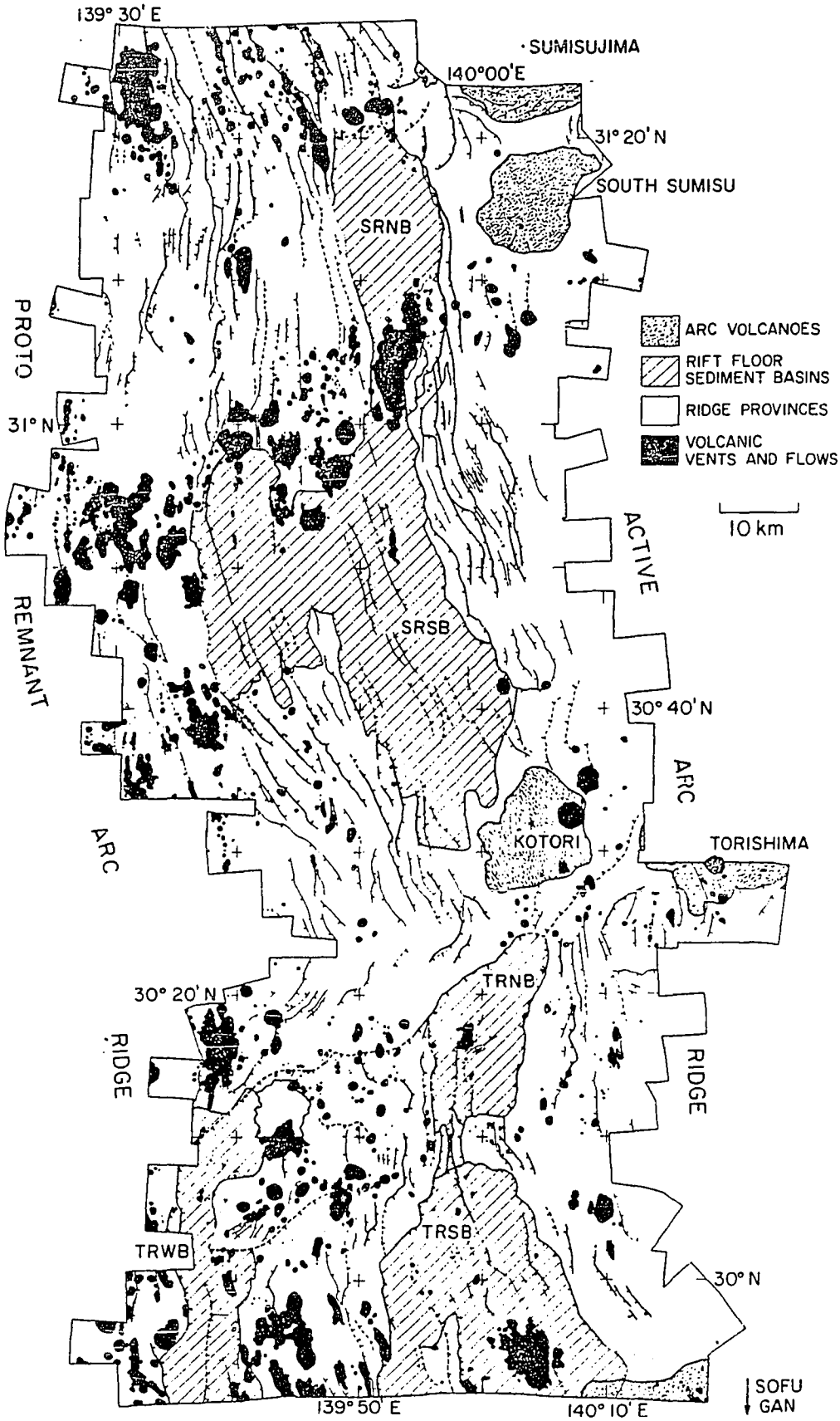
139° 30' E
SUMISUJIMA
140°00'E
31° 20' N
SOUTH SUMISU
SRNB
PROTO
31° N
ARC VOLCANOES
RIFT FLOOR SEDIMENT BASINS
RIDGE PROVINCES
VOLCANIC VENTS AND FLOWS
10 km
ACTIVE
REMNANT
SRSB
30° 40' N
ARC
KOTORI
TORISHIMA
ARC
30° 20' N
TRNB
RIDGE
RIDGE
TRSB
TRWB
30° N
SOFU GAN
139° 50' E
140° 10' E

grained hemipelagic deposition (Figure 3.12C). Drilling at Site 791 showed this layer to be composed dominantly of ash [*Leg 126 Ocean Drilling Program, 1989*].

The SeaMARC II imagery shows few acoustic facies changes within the sedimented areas, whereas, close-spaced echo-character profiles often show abrupt acoustic changes in seafloor sediments not detected by SeaMARC II. In SRNB, for example, there are discrete differences between the northern and southern ends of the basin (see Chapter II). The southern SRNB has a flat bottom with multiple subbottom reflectors (Figure 3.9), but the northern half has a hummocky bottom resulting from gravity flow deposits [*Nishimura and Murakami,* 1988] with isolated packets of flat transparent sediment. The only difference in the sidescan imagery across the basin are minor distortions close to the ships' tracks in the north which appear to be caused by the slight bathymetric changes.

Small scale channelling is common around the submarine arc volcanoes. The slopes of Torishima have several shallow furrows in the upper sediment and a fault-bounded on the south flank of South Sumisu (Figure 3.7D) has been filled in by latter sediments.

At some sites along the active arc margin, erosional features are observed that serve as paths for sediment migration into the basins. A trough approximately 3 km wide with >150 m high walls cuts down an unconformity/fault boundary between the basement backslope and Sumisujima volcano (see Figure 3.7B), and thus provides a direct route between the upper slopes of Sumisujima and the SRNB. Echo-character profiles across the canyon walls have an underlying subbottom hyperbola interpreted by *Nishimura and Murakami* [1988] to be an erosional surface. Near where this canyon meets the northern margin of SRNB

there is a deep erosional scour along the base of the east wall (cut below 2100 m-Figure 3.6, Figure 3.7C) which is possibly carved by currents directed by the canyon into the basin.

Several bathymetric lows occur along the active arc margin between the footwall uplifts and the arc volcanoes, such as at 29°55' N and 30°40' N. These sedimented (low reflectivity, Figure 3.5), structurally controlled saddles allow semi-continuous sedimentation between the forearc and rift-floor basins.

Bottom currents within the basins play an important role in distributing fine-grained sediment around the abyssal floor of the rifts. The surface of the SRSB below 2200 m is a near horizontal sediment plane (Figure 3.6) offset only by active normal faults. Slight perturbations in sub-bottom reflectors on 3.5 kHz data are infilled by the uppermost layers (Figure 3.12C) thereby maintaining the profile of the sediment plane (see Chapter II). It is infered that the plane results from bottom currents reworking the fine-grained hemipelagic sediments. While a continuous transparent layer is not present in other basins [*Brown et al.*, 1988], the unit is present in isolated patches in the lowest parts of the basins as though the material was winnowed from higher levels. Despite the subtle indicators of bottom water motion in the basins, no large amplitude sediment waves are observed on the 3.5 kHz data. In the northern half of SRNB there are depositional hills thought by *Nishimura and Murakami* [1988] to be coarse debris flow deposits supplied by mass-wasting of the surrounding rift walls.

Recent sedimentation in the rift basins is characterized by fine-grained hemipelagic and coarse-grained turbiditic deposition with intermittent layers of ash and pumice. The sediments become more stratified and possibly have a higher pelagic component with increasing depth and distance away from the shallow arc volcanoes. Sediments are deposited in rift basins by episodic distal turbidites started by slumping along the walls of the rift or by volcanic eruptions.

Figure 3.12. Hemipelagic sediment echo-character types mapped in Sumisu and Torishima rifts [*Brown et al.*, 1988]. (**A**) Prolonged echo with no subbottom reflectors (**Sp**, Figure 3.9) interpreted to be primarily volcanogenic (coarse-grained debris). (**B**) Distinct bottom with subbottom reflectors (**Ss**, Figure 3.9) interpreted to be turbidite deposits. (**C**) Overlying transparent layer of variable thickness, interpreted to be fine-grained sediment with a higher pelagic component which is found as a continuous layer only in the SRSB.

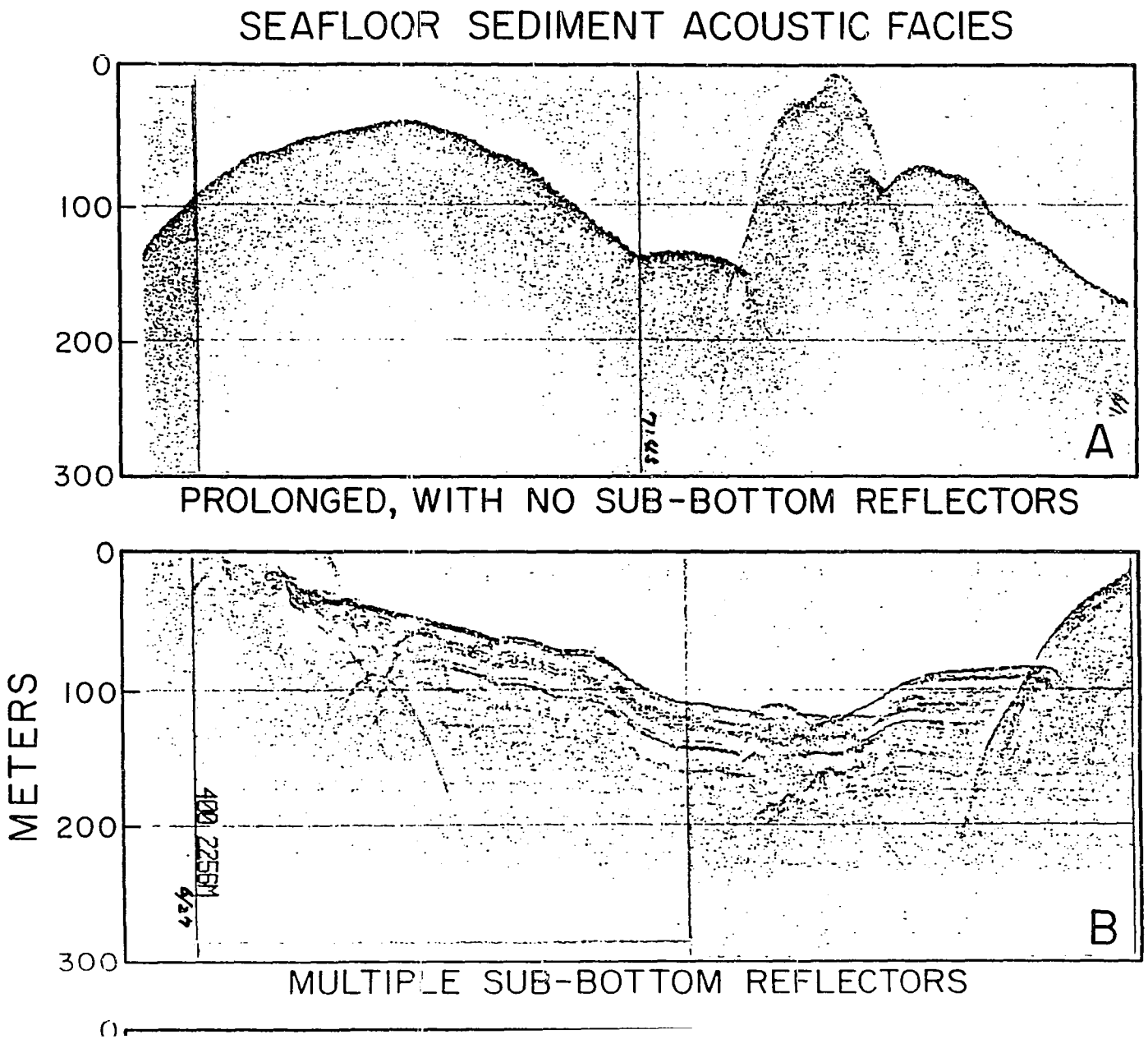
SEAFLOOR SEDIMENT ACOUSTIC FACIES
0
100
200
300
A
PROLONGED, WITH NO SUB-BOTTOM REFLECTORS
METERS
0
100
200
300
400 225FM
B
MULTIPLE SUB-BOTTOM REFLECTORS
0

PROLONGED, WITH NO SUB-BOTTOM REFLECTORS

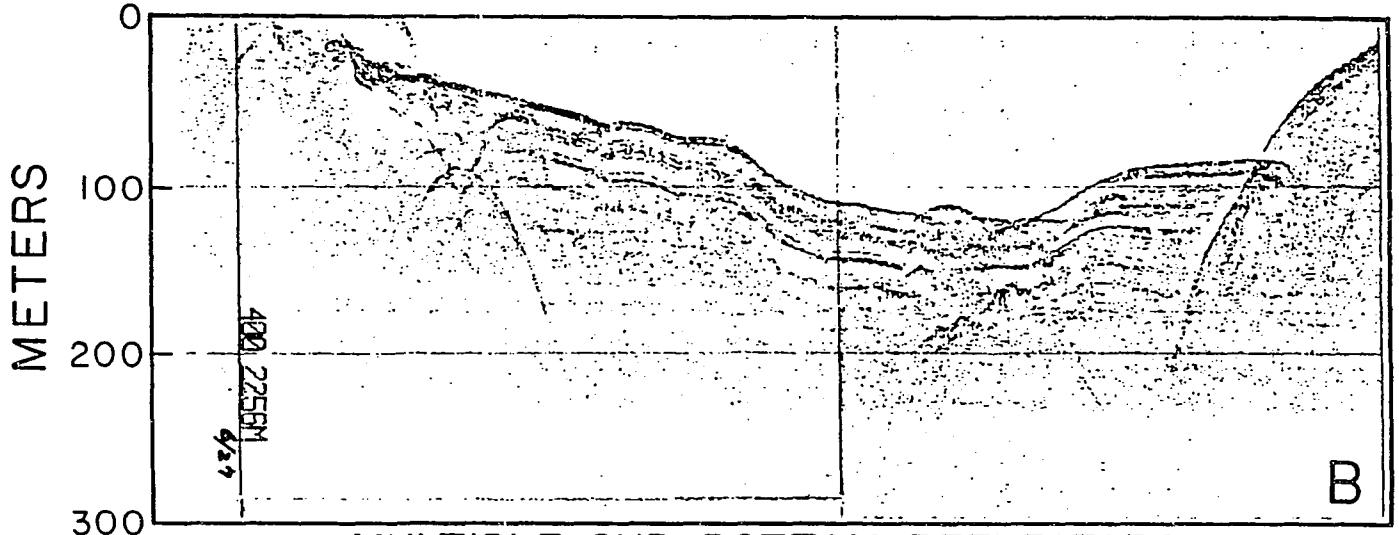

MULTIPLE SUB-BOTTOM REFLECTORS

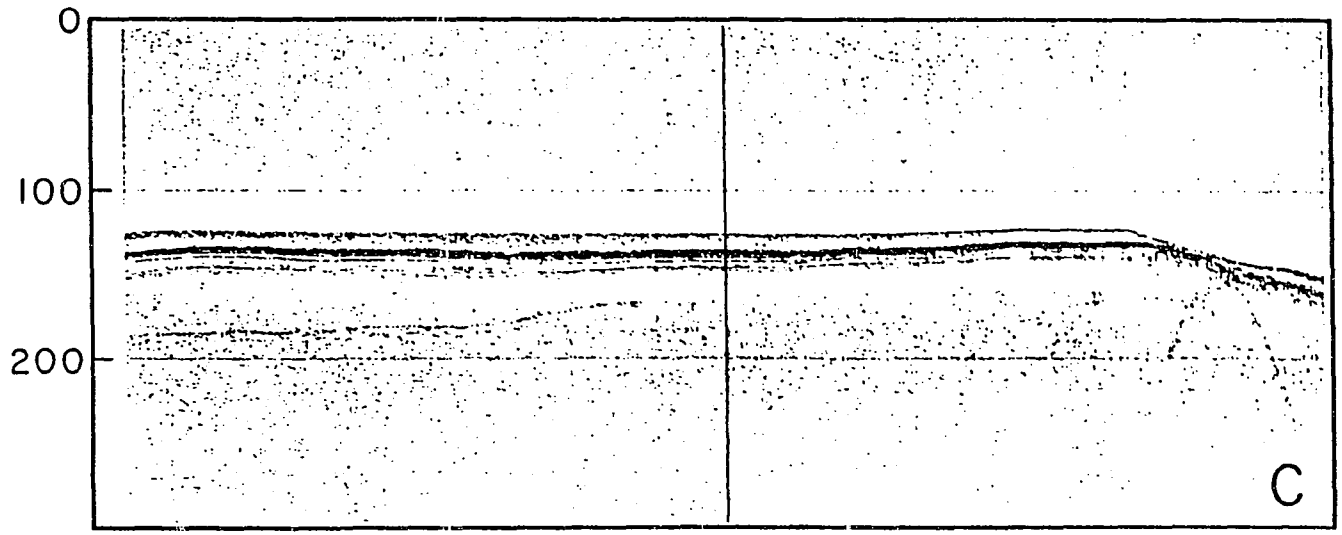

UPPER TRANSPARENT LAYER

Debris from the upper slopes of the volcanoes might migrate directly into the lower basins along channels. Despite the proximity of adjacent rift-floor basins the sedimentation can vary significantly because the local topography strongly affects the distribution of sediments. No bias in sedimentation across the basins, such as that predicted in the model of *Karig and Moore* [1975b], is observed. While the active arc undoubtably controls the supply of sediment during the nascent stages of opening, debris that makes it to the rift-floor basins can be evenly distributed within the basins.

The history of syn-rift sedimentation in the rifts can be inferred from the single-channel seismic data (Figures 3.7 and 3.8, *Murakami* [1988]). In an inter-oceanic island arc, as in the central Bonins, the basement (pre-rift) rock must be old arc volcanics interbedded with hemipelagic sediments. With the inception of subsidence behind the frontal arc, new material flowing into the deeps would have the same composition as the rifting basement. The syn-rift to pre-rift boundary is therefore marked by a simple unconformity and probably does not represent a lithologic contact. On the single channel seismic data the unconformity at the base of the sediment pile can be picked on only a few profiles. The maximum syn-rift sediment accumulation in Sumisu and Torishima rifts occurs in the SRSB. Here, the rifted basement lies underneath 1.5 seconds of fill (Figures 3.7 and 3.8).

The syn-rift sediments accumulated on the surface of the subsiding hanging-wall blocks. Deep reflectors in the basins dip towards the controlling fault indicating a growth fault development (e.g. Figure 3.7I). Despite the tilt on deep reflectors, the surface of the sediment is a horizontal plain. If subsiding areas in the central Bonin arc were starved of sediment then the pre-rift basement rock and structure would be exposed. The differential depth of the basins would indicate total subsidence. On the other hand, if there was continuous sedimentation in the young grabens, such that debris entering the basin quickly fills any slight pertur-

bation from subsidence, then the surface of the sediment pile (the seafloor) maintains a flat profile. In the center of TRSB basement fault-block ridges protrude above the sediment plain (Figure 3.5, linear reflecting areas; Figure 3.8U-W). Yet in SRSB these basement tilt-blocks do not occur except along the unburied margins (Figure 3.7L). In the SRSB the rate of deposition keeps up with and possibly exceeds the rate of subsidence. To the south, the rate of subsidence (and deformation) exceeds the rate of sedimentation. Rift basins south of the Sofu Gan Ridge (at 29°47' N) have thin sediment accumulations and exposures of faulted basement structures create a rough seafloor morphology on the margins of the deep (Chapter IV).

3.3 Volcanism

Four large frontal arc volcanoes were surveyed, including the south and west flanks of Sumisujima, all of the submarine South Sumisu Volcano (*Daisan* 3) except for its summit caldera area, a 10 km wide swath on the southern flank of Torishima and Sofu Gan (the latter is discussed in Chapter IV). The volcanoes are constructed from volcanoclastic sediments and flows. They are characterized by explosive phreato-magmatic eruptions within the shallow (<1000 m) water realm of reduced confining pressure [*Carey and Sigurdson,* 1984]. Pumice and scoria sampled in dredges and cores [*Fryer et al.,* 1990; *Nishimura and Murakami,* 1988], and thick subaereal sections of dike-intruded, bedded tuffs exposed on Torishima, suggest explosive eruptions on this section of the arc are common. Not all eruptions in the central arc generate pyroclastics. In 1939 a basaltic flow erupted from a site near the summit of Torishima and later infilled a bay on the south coast [*Kuno,* 1962]

The flanks of arc volcanoes have light to medium grey tones on the SeaMARC II acoustic sidescan imagery, indicative of weak to moderate reflections and a low backscatter. The imagery often darkens and has an increased number of point-reflectors on the upper slopes of volcanoes. The summit area of South Sumisu, for example, is surrounded by a dark grey area. This was considered in Chapter II to result from a steepening of the slope and a thinning of the sediment cover, but it may also be due to coarse volcaniclastic debris and lavas (especially on the northern slope). Several parasitic cones also occur on the flanks of South Sumisu (Figures 3.5, 3.9). Other small monogenetic volcanoes occur on the arc margin to the south, along strike from a cross-rift volcanic trend.

Slump scars occur in seafloor sediments around the arc volcanoes and arc edifices are incised by normal faulting. On the lower, south slope of Sumisujima, concentric slump scars have broken the sediment (see Chapter II). The saddle between Sumisujima and South Sumisu (31°20' N, 140°15' E), has a pile of chaotic reflectors suggesting long term slumping from the sides. The western margins of South Sumisu and Sumisujima have been heavily fractured by backarc rifting where the SRNB bounding faults down-drops the edge of the arc (Figure 3.7C).

Two other volcanic edifices with greater than 1000 m relief were also surveyed . One of these, hereafter referred to as "Kotori Volcano" occurs 20 km west of Torishima. The other, with a summit depth of less than 900 m, has a 10 km diameter and occurs in the remnant arc margin near 30°16' N, 139°46' E (Figure 3.8T). Both are characterized by radial lineaments on the sidescan imagery (Figure 3.5) which resemble volcaniclastic debris flow paths on subaereal volcanoes.

Eruptions from arc volcanoes and erosion of fault blocks are a major source of the terrigenous sediment found in the study area. As noted above, the echo-character across the slopes of the volcanoes (Figure 3.12A) is prolonged with no subbottom reflectors. With increasing depth and distance away from the arc the echo-character becomes stratified (Figure 3.12B) indicative of less coarse material. Seismic reflection profiles across the lower slope of the arc volcanoes show thick sediment drapes. Volcanogenic sediments (0.25 sec thick) erupted from Kotori have spilled over the east footwall of SRSB (Figure 3.8O).

Sumisu and Torishima rifts contain hundreds of small volcanoes (Figures 3.9, 3.11). Most vents are less than 3 km in diameter and under 400 m in relief. In contrast to the large volcanic edifices these vents have a strong reflectivity and backscatter. They appear as dark, circular to oblate areas on the SeaMARC II acoustic imagery. (The echo-character profile across a small volcano is a symmetric hyperbolae, as the summit is a point reflector.) Dredge samples, collected by the R/V Kana Keoki from vents in the central grabens, yielded fresh and altered, vesiculated fragments of pillowed extrusives ranging in SiO_2 content from 48% to 71%, but dominantly basalts and rhyolites [*Fryer et al.*, 1990; *Nishimura et al.*, 1988].

The historic eruptions in the central Bonin island arc have been attributed to island-arc volcanism [*Kuno*, 1962; *Simkin et al.*, 1981]. Some submarine eruptions detected in the sofar channel with the Pacific hydrophone array may be from rift related volcanism. *Norris and Johnson* [1967] reported on a submarine eruption in the central Bonin arc. Although they associated the event with Torishima, the actual error ellipse lies well into the backarc. If *Norris and Johnson's* locations of the submarine eruptions is accurate, then the event could be from the recent effusion of lava on the floor of the southern Sumisu Rift.

A large unnamed isolated volcano, with 1100 m relief, 10 km in diameter, and a summit depth of 900 m, occurs in the proto-remnant arc margin near 30°16' N and 139°46' E. Similar to arc volcanoes on the active margin, it images with light-grey tones, and has lineaments radiating out from the summit. Echo-character profiles show the volcano to be mantled with sediment acoustically similar to the arc volcanoes on the other side of the rift. These properties indicate that the volcano is mantled by volcaniclastic sediments produced by explosive eruptions, possibly produced by water-rich magmas.

3.4 Tectonic Framework

The axial basins of the Sumisu and Torishima rifts are bounded on at least one margin (active or proto-remnant arc) by an escarpment exceeding 1000 m relief (Figure 3.6). In plan view the escarpments have a "dog-leg" (or "zig-zag") bend with an inside angle of approximately 150° (Figure 3.13). The bounding escarpment or master fault zone is composed of several faulted blocks, some of which now lie under the sediment pile (Figure 3.7I to 3.7L, east "boundary fault"). The individual faults on the escarpment meander and intersect (Figure 3.9) similar to the faulted basement boundary zones of other narrow rifts (e.g. the west boundary fault of the Rhinegraben at the colatitude of Strasbourg [*Illies and Grenier,* 1978]). The pattern is most evident on the SeaMARC II imagery of the east slope of the SRSB where the anastomosing faults create a complex fabric of lineaments (Figure 3.5) (described as the "*East Fault Zone*" in Chapter II). The seismic reflection profiles in Figures 3.7 and 3.8 exaggerate by 10x the dip of the master fault zones. In fact the inclination is shallow, seldom exceeding a 25° dip.

The distinct fault zones are, on the other side of the rift, faced by more gentle slopes with faults dipping into (or "antithetic" to) the master fault zone. This causes an asymmetry best exemplified on the seismic profiles across the

SRNB (Figure 3.7B to 3.7E). Here, the prominent fault lies on the east and is opposed by closely-spaced (approximately 1-2 km) low-relief, antithetic faults. The profiles are remarkably similar to the asymmetric half-graben profiles produced in experimental stretching of homogeneous clay (e.g. *Cloos* [1930] and *Elmohandes* [1981]). It is important to realize though that the east-west seismic profiles can bias sections as they are not always perpendicular to the strike of the master faults [*Rosendahl,* 1987]. A seismic profile, perpendicular to the SRSB master fault zone at the latitude of Figure 3.7L, for example would be symmetric, with the west boundary fault being similar to that in Figure 3.8O.

The master fault zones appear on both sides of the rift basins (Figures 3.6 and 3.13). Between 31°23' N to 30°41' N and 30°25' N to 29°53' N a master fault zone developed on the eastern (active arc) margin. Between 30°42' N and 30°24' N a master fault occurs on the western (proto-remnant) margin. This distribution is similar in geometry to the "flip-flopping" reversals of master fault polarity in the East Africa rifts *Rosendahl* [1987].

A set of faults have developed, perhaps simultaneously, that are homothetic (in the same dip direction) to the dog-leg master fault zones. The faults cut the crust into broad blocks from around 15 to 35 km in width. Figure 3.14 is a key seismic profile perpendicular to the master fault zone on the east boundary of the TRSB. The profile shows a "primary" low-angle master fault "a" (because it is related to the initial rifting rather than as a "secondary" deformation from the interaction or uplift of blocks along the primary faults). Fault "b" is a primary fault that is synthetic to "a". As the sediment pile in the hanging wall basin (TRWB) of fault "b" is comparable in thickness to the axial TRSB, it appears on this profile that slip on fault "b" began near the same time as the maturation of the master fault zone. The primary faults are found at other latitudes. Under the SRSB lies a buried basement block that has primary motion

Figure 3.13 Major faults in the Sumisu and Torishima rifts. Stiple segments are inferred zones of transfer, some of which may be linked to the pre-existing cross arc faults (Figure 3.3). A neck-point between the margins of the rifts occurs where transfer zone intersects the axis of subsidence. The localization of rift-floor basins is controlled by the structures.

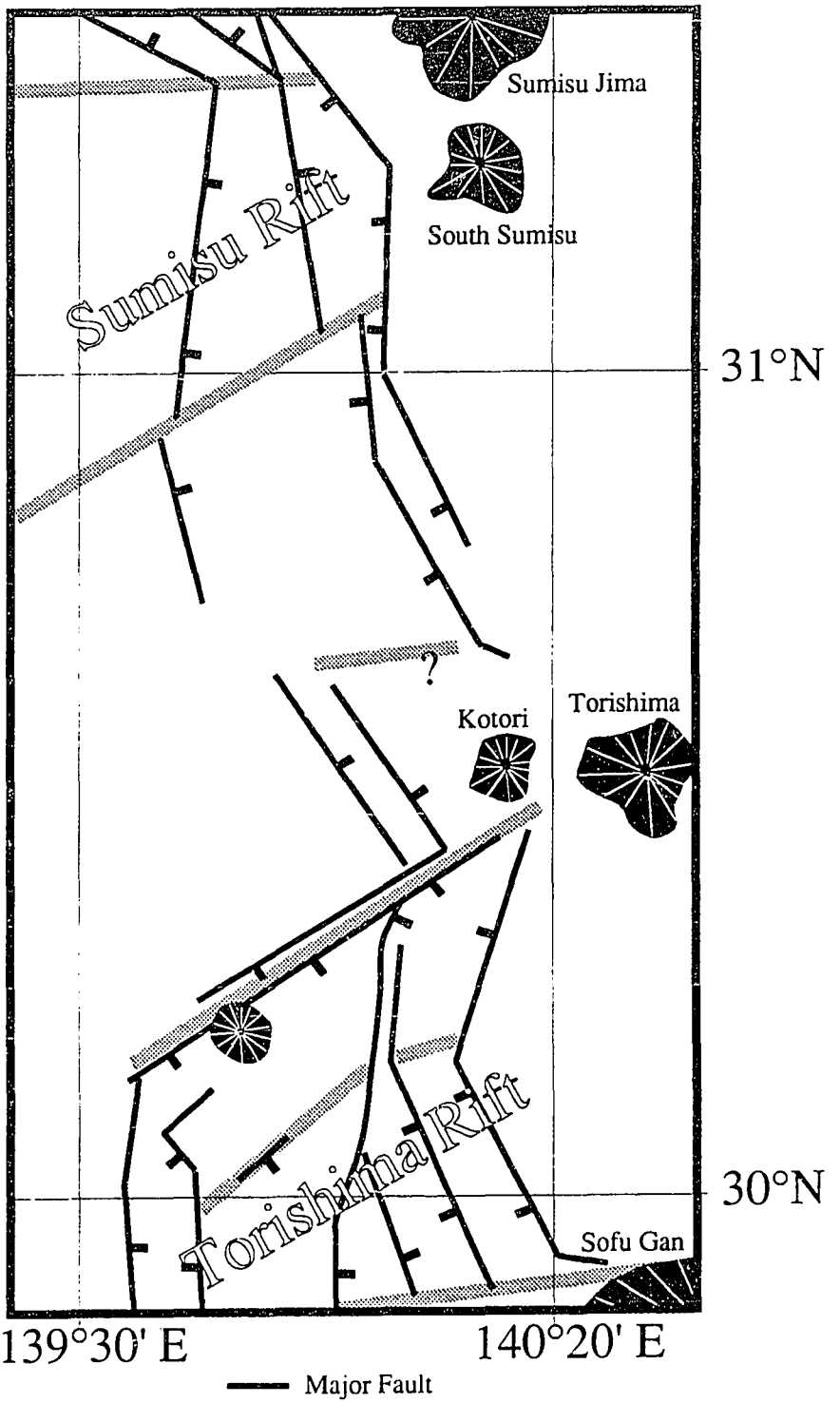
Sumisu Jima
South Sumisu
Sumisu Rift
31°N
?
Kotori
Torishima
Torishima Rift
30°N
Sofu Gan
139°30' E
140°20' E
Major Fault
Transfer Zone

synthetic to the east boundary fault (Figure 3.7H and 3.7I; *Klaus et al.*, 1988). Between Figure 3.7D and 3.7G buried reflectors are also tilted to the east as though the layers were deposited on early faults dipping towards the west (synthetic to the SRNB master fault zone).

The primary synthetic faults are not restricted to the area in front of the master fault. Backslope deformation of the active arc uplifts was initially synthetic to the frontal escarpment (e.g. Figure 3.7E and 3.7G). Later, faults developed in the opposite direction, perhaps as a secondary phenomena from the tilting. The old synthetic faults may still be active. At 30°45' N, on the forearc side of the flexure east of Sumisu Rift (Figure 3.7L), a 5 km wide graben has formed in the 0.50 sec of lower backslope syn-rift sediments. The basement beneath the graben is faulted synthetic to the frontal escarpment.

There is also a secondary mode of faulting either antithetic or synthetic to the master fault zone. Figure 3.14 shows some deformation on the tilted backslope of the block formed by fault "b". The faults at "d" dip antithetic to faults "a" and "b". This class of faults are closely-spaced on seismic profiles (Figures 3.7C to 3.7H) and seem to be absorbing the strain on the upper plate of the low-angle master fault during a hanging-wall roll-over [*Gibbs*, 1984] or bending from the slip on the underlying master fault.

Normal faulting also occurs in the syn-rift sediment pile. The faulting of the sediments is caused by the motion of the buried basement blocks. For example, sediments in the center of the SRSB (Figure 3.7J and 3.7K) are fractured by faults that offset the basement. Some of these small faults must have experienced recent slip. On 3.5 kHz echo-character profiles across the central SRSB a new layer of ash has begun to collect in the hanging-wall moats of low-relief faults that cut the syn-rift sediments (see Chapter II).

Figure 3.14. Single-channel seismic reflection profile on a track line perpendicular to the strike of the east boundary fault across Torishima Rift's south and west basins (see Figure 3.10 for location). Fault "**a**" is the primary master fault. Fault "**b**" is a primary fault synthetic and parallel to the master fault. The gentle sloping platform east of **b** is a gentle backslope from tilting of the crust along **b**. Note that the basement (**c**) dips into fault **b**. The west boundary fault system of the TRSB forms by a secondary (and smaller offset) downfaulting of the lower backslope (**d**). Buried reflectors also incline towards the master fault, although the seafloor in the basin is nearly horizontal (the seismic bubble pulse masks upper reflectors).

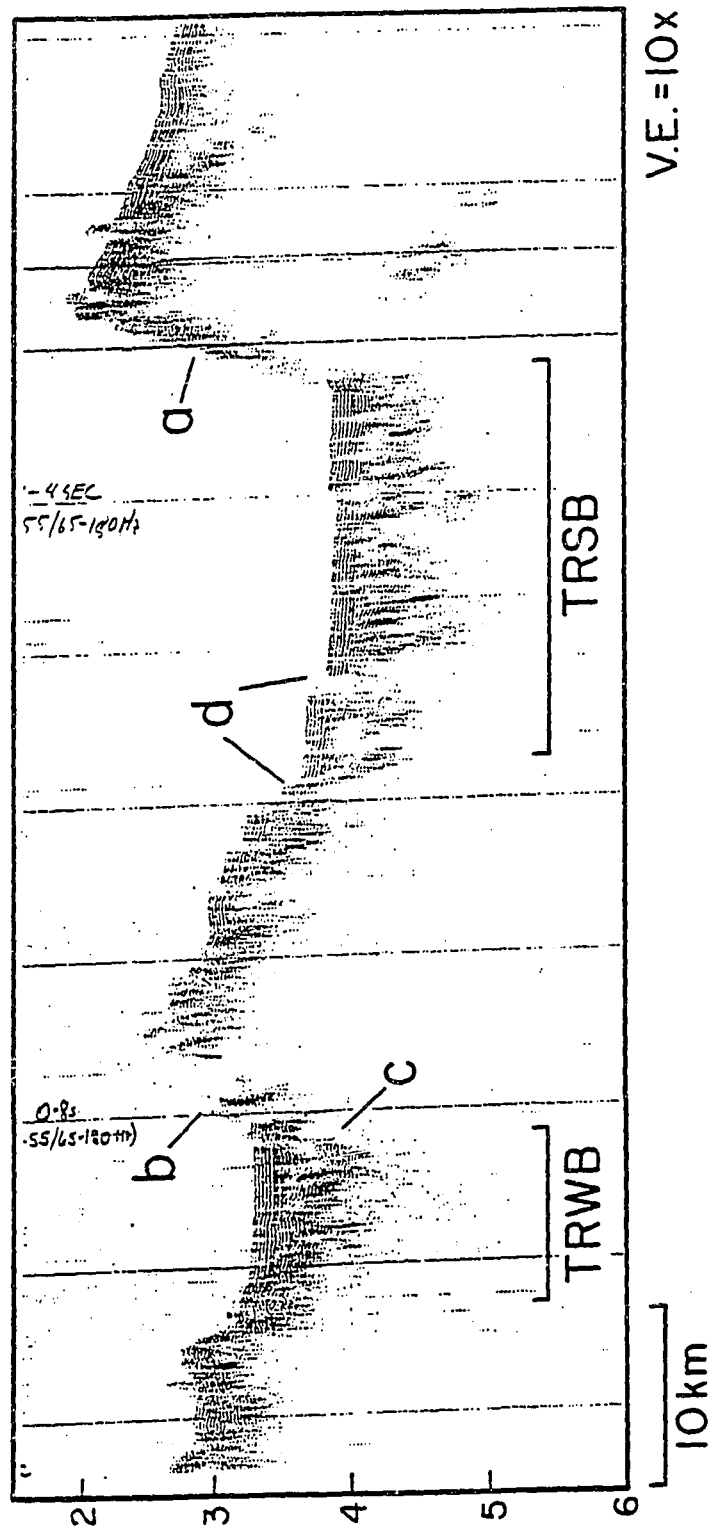
V.E.=10x
a
~4 SEC
55/65-140Hz
d
TRSB
0.8s
55/65-120Hz
b
c
TRWB
10 km
2
3
4
5
6
TWO-WAY TRAVEL TIME (sec)

The master fault "dog-legs", mentioned above, are warped planes that appear to become listric with depth, based on the tilting of reflectors above the hanging wall block. The faulted crust facing the master fault undergoes important adjustments in structure along subtle, rift-oblique zones referred to as an accommodation zones by *Rosendahl* [1987]. The zones allow the faulted basement blocks to jostle position along strike and serve as relays between rift segments with master faults of opposing dip directions. The adjustments are most easy to map on the surveyed portions of the proto-remnant margin although we can often only infer an accommodation zone from salient changes in the strike of faults or from the existence of rift-oblique escarpments (Figure 3.13).

An example of a subtle adjustment in normal faults occurs at the north margin of the SRNB, near 31°20' N (Figure 3.11). The low-relief normal faults in this area are spaced under 1-3 km apart. Between the faults are well-sedimented depocenters (stratified echo-character) (Figure 3.7A, Figure 3.9). The faults change strike by approximately 30° to the NNW [*Murakami*, 1988]. At the latitude of Figure 3.7B, multiple irregularly spaced faults in the proto-remnant margin are antithetic to the opposing master fault zone. The faults (Figure 3.9) appear to terminate or bifurcate towards the NNW trend. Also coincident with this latitude is a 10 km wide swath of volcanic vents. The occurrence of over 50 vents in the area indicates there to be an underlying rift-oblique conduit for the supplying magmas.

Several factors suggest a discontinuity passes through the proto-remnant margin at the northern edge of the SRSB. (1) Structural changes are evident in Figures 3.7G to 3.7H, at the northern edge of the SRSB. Towards the south the predominantly antithetic step-faults develop into a distinct west-boundary fault near Figure 3.7H, where the entire footwall block, west of the SRNB has been covered under the SRSB. (2) In this area a series of en-echelon volcanic ridges

divide the SRNB and inner SRSB (Figure 3.5, 3.9) [Chapter II; *Murakami,* 1988]. Although the individual vents are aligned parallel to the regional trend of normal faults, the vent distribution as a whole is at an oblique angle to the rift structure (Figure 3.11). If the intra-rift volcanic belt is tectonically controlled, deep in the crust, then as the intruding magmas reached the upper crust, the eruptions sites became aligned parallel to the rift normal faults. (3) In 1976 an earthquake occurred at 31° N, 139°30' E at a depth of about 8 km *Moriyama* [1988]. The focal mechanism solution for the quake, determined by *Eguchi* [1985] indicates the motion during the quake was strike-slip with one nodal plane sub-parallel to the northern margin of the SRSB.

The western boundary fault of the SRSB migrates 25 km to the west and becomes less significant in profiles south of Figure 3.7H until there is a conspicuous 10 km wide gap near 30°43' N (Figure 3.9). The proto-remnant margin at this latitude of the SRSB has a gentle, well sedimented slope (low reflectivity on SeaMARC II imagery, Figure 3.5, Figure 3.7L) with numerous volcanic vents. The termination of basement at the northern edge of the block seamount near 30°42' N (Figure 3.5, 3.6), the abrupt uplift of the nearby basement to the south, and the absence of a distinct western boundary escarpment to the north, suggest a crustal discontinuity occurs in this area. The zone may continue to the east under the SRSB and may accommodate the change in structural trend observed between the southern and northern margins of the southern basin (Figure 3.9).

The southwestern area of Torishima rift can be divided into discrete, rotated fault blocks that are synthetic to the east boundary fault zone (Figure 3.14). For 20 km south of the rift-oblique escarpment, marking the northern boundary of the rift segment, the geometry of faulting is more complex (Figure 3.9). Subsidence at the base of the scarp has created a sedimented moat that links up with the TRWB

(Figure 3.11). Several basement highs on the opposite side of the moat trend NNE, parallel to the northern boundary fault. The trend of lineaments in the area suggest that the primary basement deformation (that faulted the south slope) was related to the northern boundary fault rather than to the east boundary fault system.

Seismic profiles (Figures 3.7 and 3.8) show that the shallow bathymetric ridges between the frontal arc volcanoes on the active arc margin, and west of Torishima on the proto-remnant margin (Figure 3.6) are tectonic uplifts along the rift boundary faults. The exposed pre-rift section on the footwall (or "free-face" [*Wallace*, 1977]) and the upper backslope of the tilt-blocks are strong reflectors (dark grey to black tones on the imagery, Figure 3.5) and are mapped as "acoustic bedrock" (Figure 3.9) [*Brown et al.*, 1988]. The backslopes are faulted by normal faults with a 2-3 km spacing and, near the large volcanoes, overlying volcaniclastic sediments can exceed 1.0 second (two-way travel time) in thickness. In Figure 3.7B, for example, a fault-block ridge with a tilted backslope images for at least 1.5 seconds beneath the thick volcanic pile of Sumisu and South Sumisu volcanoes.

Flexural uplift of the footwall blocks leads to faulting and remobilization of sediments around the flanks. For instance, a large, relatively undeformed, basement block between 30°43' N and 30°10' N (Figure 3.7M to 8R) on the proto-remnant margin of the SRSB and TRNB (bounded on the south by the rift-oblique zone mentioned above) has been uplifted on its eastern edge. The seafloor has been depressed at the lower backslope (outside of the sidescan survey area-see Figure 3.2, 2000 m contour west of the block). The free-face escarpments and the upper backslope were imaged with SeaMARC II (Figure 3.5). The exposed area of the northwest-trending branch (Figure 3.8M to 3.8Q) is 2 to 10 km wide with a maximum of 1300 m relief. Normal faults on the wall anastamose and vary in displace-

ment and dip (Figure 3.9). In places the pre-rift section is completely covered by layered sediments (Figure 3.8O, hyperbolae at the base of the escarpment are fault-block ridges, relief on the blocks lessens to the north, Figure 3.5, 3.6).

Mass-wasting of the NNW-trending escarpment has not been uniform. Between 30°34' N and 30°40' N the slope is formed by a narrow fault zone because the lower crustal slices are completely buried by the SRSB sediments (Figure 3.9 shows discontinuous faults along the contact). Terraced basins on the wall are typically under 2 km wide and are infilled with turbidite sequences (stratified echocharacter). Near the easternmost edge of the block, a 5 km wide basement ledge sits half-way down the escarpment (Figure 3.8Q), as though the edge of the orthorhomb was broken and eventually decoupled.

With the uplift of the front of the block, sediment on the backslope has begun to slump toward the west (e.g. faults on Figure 3.8O). These dislocations are mapped in Figure 3.9 with dips towards the west. Echo-character mapping of the backslope shows that recent sediments are deposited on the lower backslope and erosion takes place on the upper areas (hence the upper backslope is mapped as acoustic bedrock, Figure 3.9). This can also be seen from the acoustic imagery (Figure 3.5), which shows an increase in backscatter on the upper backslope area. The submarine erosion (or lack of deposition) at the top the of the tilt blocks was observed during the recent drilling by the Ocean Drilling Program. Site 788 cored into Pliocene sediments beneath a thin (30m) Pleistocene section [*Leg 126 Ocean Drilling Program,* 1989].

3.5 Discussion

Prior to the 1989 drilling of Sumisu Rift [*Leg 126 Ocean Drilling Program,* 1989], the timing of backarc extension could only be estimated. The presence of unfilled basins lying next to arc volcanoes and scarps with about 1 km

relief requires that the basement has subsided recently [*Karig and Moore,* 1975a]. The maximum sediment thickness in the Sumisu Rift (~1500 m) suggests significant subsidence began no earlier than 10 my and probably more like 5 my (300 m/my sedimentation rate).

A further constraint on the age of the grabens is from three K/Ar dates done by the Geological Survey of Japan on volcanics dredged from southern Torishima and central Sumisu rifts by the Hawaii Institute of Geophysics [*Fryer et al,* 1990]. These dates range from 1.96 +/- 0.25 my to 0.21+/- 0.04 my. While the earliest value might be east wall rock of southern Torishima Rift the other two samples are from the syn-rift en echelon ridge of volcanoes in the central Sumisu Rift. If the middle value is accurate then the main phase of subsidence in at least Sumisu Rift must have been prior to 0.34 +/- 0.25 my. The results of ODP drilling indicate that at 31°N the basement in the Sumisu Rift began to subside at 2 +/- 0.5 Ma [*Leg 126 Ocean Drilling Program,* 1989].

The thin sediments (<0.25 sec) in the deepest basins near 29°N (Figure 3.1) suggest a Plio-Pleistocene rift onset at this latitude (see Chapter IV). The amount of extension required to generate the 30-40 km wide rifts, with maximum throw on bounding faults of 2 to 3 km, is quite small, in the range of 2 to 5 km. If the extension is assumed to be accommodated by slip along faults, then the direction of extension can be inferred from the pattern of faulting. In particular, in a region with a dog-leg fault pattern the extension direction bisects the perpendiculars to the two regional fault trends [*Reches,* 1983]. In the case of the Sumisu and Torishima rifts this direction is 075° to 085°, i.e. orthogonal to the regional trend of the frontal arc volcanoes.

Before the recent phase of rifting started there were likely two prevailing structural features on the Bonin platform. (1) The volcanic arc, that has been active since Eocene times, although eruption sites may have been further to the

east in pre-Pliocene times [*Leg 126 Ocean Drilling Program,* 1989], and (2) the regional lineaments (Figure 3.3), described above, developed during an Oligocene rifting event.

The active extension in the Sumisu and Torishima rifts is biased to the backarc (e.g. Figure 3.3), although at latitudes further to the south, recent normal faulting has been observed in the proximal forearc area (Chapter IV). The intimate relationship between arc volcanism and rifting presents a puzzling problem. Does arc volcanism focus the subsidence related to extension or does the extension control the location of the arc? It has been proposed that island arc rifting begins near the arc because the crust is weakest at this position [*Karig,* 1974]. Despite the occurrence of maximum subsidence next to the arc line, extensional deformation can be found over 50 km to the west. The broader zone of synthetic faulting may actually begin near the arc line at a subcrustal detachment beneath the tilted blocks. This model can't be supported from data south of Sofu Gan Island (Chapter IV), however, tilted blocks are homothetic to the east, unless discrete transfers allow a reversal of detachment dip.

The physical presence of arc volcanoes could control the local geometry of rifting. The geographic distribution of individual arc strata-volcanoes is thought to be decided at depth near the subduction zone [*Marsh,* 1979], long before the raising diapirs approach the upper crust. In the central Bonin arc, centers of arc-type volcanism have a regular spacing of about 60 km (Figure 3.3) despite old structural discontinuities and the changes in the geometry of the Wadati-Benioff zone.

It is possible that satellite volcanoes, located near larger seamounts and out of step with the regular volcanic interval, are structurally controlled. Both South Sumisu and Kotori volcanoes lie within 10 km of an extrapolation of proto-remnant arc discontinuities (Figure 3.13). In the case of the former there is little morphologic evidence for the proto-remnant discontinuity continuing through the

active arc although small scale volcanism does traverse the rift axis (Figure 3.11). Both South Sumisu and Kotori lie near subaereal centers (Sumisujima and Torishima respectively). The cross-arc faults could interfere with the magma plumbing beneath the arc volcanoes diverting the magma supply away from the main vent. The result is a volcanic clusters of large arc-type volcanic centers, some of which are structurally controlled.

The geometric relationship between the faulting and the proximal arc volcanoes is difficult to image because of sediment drape supplied by the volcanoes (for example Figure 3.8O-west of Kotori). The crustal tilt-blocks on the active arc margin do tend to shoal in the areas between the centers of arc volcanoes (Figure 3.6). Seismic profiles across South Sumisu volcano (Figures 3.7C and 3.7D) and the neighboring rift depression (SRNB) show that the east escarpment of the rift is suppressed. The repetition of this phenomena (which continues to the south of Sofu Gan Island) indicates a relationship between the locations of arc volcanoes and the block seamounts. Either arc volcanoes control the location of the uplifts or the structure of the upper crust influences the location of arc volcanoes. Because the spacing of arc volcanoes is more or less regular, a kinematic relationship between the rift-related uplifts and arc volcanism must therefore require that the former is dependent on the latter.

A factor in the occurrence of uplifts between the arc volcanoes may be the loading of the crust by the arc volcanoes (Figure 3.15). The loading suppresses uplift, as evident from the shallowest points on the arc margin occurring between the volcanoes (Figure 3.6). Where the arc volcanoes are at a distance from the master fault zones then the footwall block experienced greater uplift. North of 31°20' N, where the strike of the east boundary fault changes to NNW Sumisu volcano rests on the lower backslope. The protruding fault block ridge in Figure 3.7B may be flexed higher because the lower-backslope is loaded.

Figure 3.15 The limbs of tectonic uplifts on the active arc ridge become pinned by mass loading from the large arc volcanoes. Footwall uplifts shoal between the centers of arc volcanism.

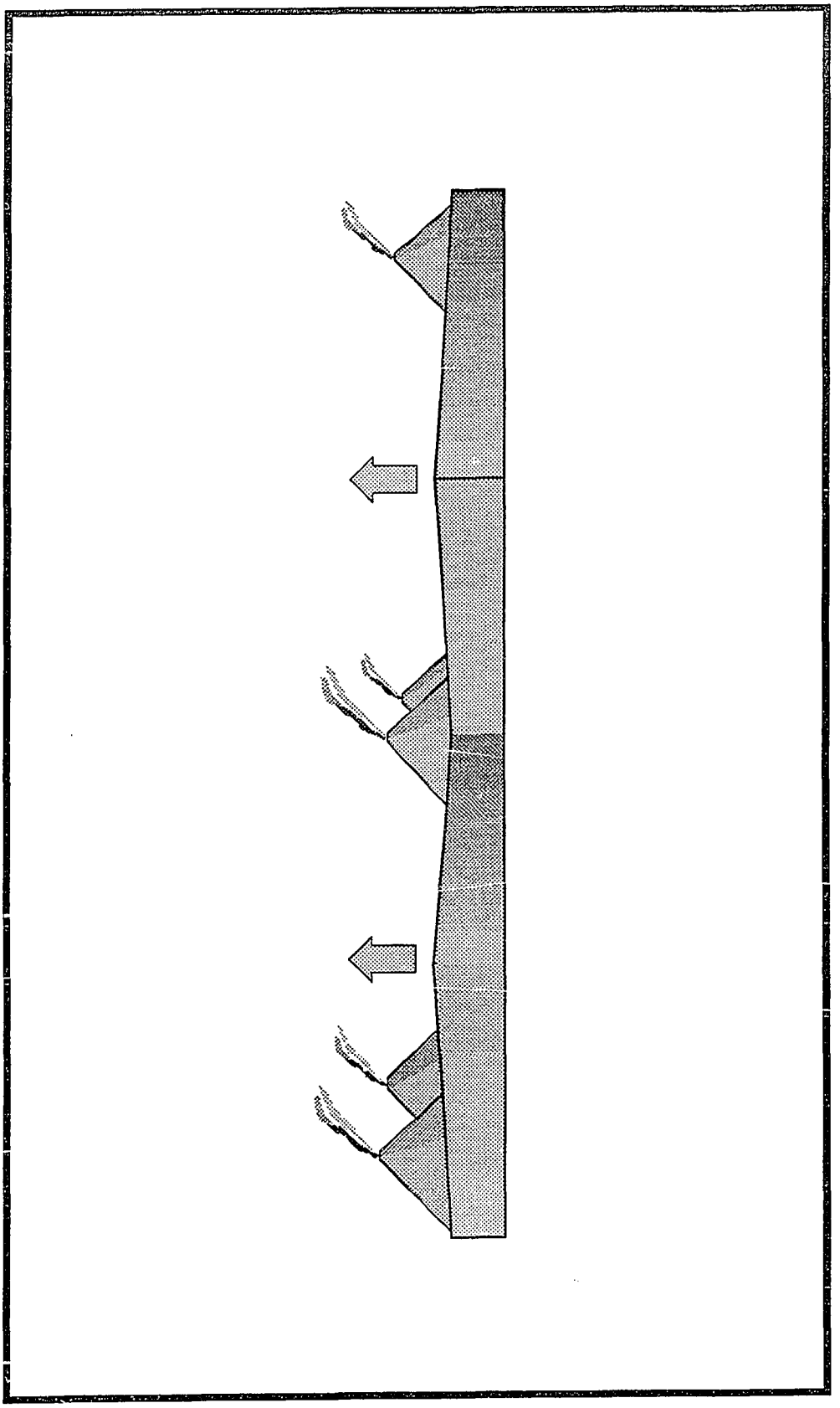

The relationship between tectonic uplifts and arc volcanoes is important to sedimentation in the young rifts. The rising blocks on the active arc margin control the location of debris paths and prevent debris shed east from the arc volcanoes from entering the basins by "daming" the sediments in the forearc. The trough formed between the cuesta at 31°20' N and the arc provides a convenient channel for density currents and turbidites into the SRNB as evident by the erosion in the area [*Nishimura and Murakami,* 1988]. The seafloor in the northeast corner of the SRNB may be scoured at the base of the master fault where the trough reaches the rift-floor (Figure 3.5, inscribed by the 2100m contour).

Faulting associated with continental rifting commonly forms a "dog-leg" or "conjugate" pattern in plan view (e.g. the Rio Grande Rift [*Ramberg et al.,* 1978], the East Africa Rift [*Rosendahl,* 1987] and other rift areas [*Lowell,* 1987]). This fabric has been reproduced using simple clay models (non-rotational, plane-strain) where the plates beneath the clay layer are slowly pulled apart (e.g., [*Freund and Merzer,* 1976]). The experiments duplicate fault patterns similar to those found in the central Bonin backarc. It is also important to realize, however, that the regional orthorhombic fault pattern developed penecontemporaneously. This is in contrast to Anderson-type conjugate faulting, where it is geometrically impossible to have simultaneous slip on the fault sets [*Freund,* 1974]. Polyaxial experiments on rock samples [*Reches and Dieterich* , 1983; Reches, 1983] show that three-dimensional strain is distributed on four sets of orthorhombic faults. As the amount of slip decreases on one fault, it is picked up on another fault. In this same way, as the east master fault system of the SRSB becomes less significant towards the south, the slip required to accommodate extension is picked up on the opposite side (directly perpendicular to the regional trend of opening on a line parallel to the arc) with a reversed polarity of faulting.

The subsidence of basement in the central Bonin island arc occurs by slip on a network of homothetic normal faults that occasionally reverse polarity. In plan-view the master fault zones form an orthorhombic pattern with areas of greatest basement subsidence lying between triangular wedges of uplifted arc crust. While the regional fault pattern is sub-parallel to the volcanic arc there are subtle to distinct adjustments in the orientation and attitude of a rift-forming faults. The rift-floor sediment basins (Figure 3.11) are semi-isolated along strike by either volcanic or tectonic ridges that are controlled by these rift-oblique accommodation zones.

The block faulting in the Torishima Rift (Figure 3.14), homothetic to a master fault, has allowed sediments to accumulate in the hanging-wall basins (the TRSB and TRWB). As the rift matures, the now semi-isolated sediment pockets could merge to form a large basin similar to the SRSB. It is expected that the rift boundary fault on the east of TRSB will experience more slip as the rift takes on a more symmetric mode of subsidence similar to the model presented in Figure 3.16.

3.6 Conclusion

Based on SeaMARC II sidescan imagery and bathymetry and shallow crustal seismic reflection data I have described the active seafloor processes in the central Bonin island arc between 29°50' N and 31°20' N. The following points summarize the development of the Bonin Rift System between these latitudes.

The mid-Oligocene rifting of the paleo-Bonin arc formed regional tilted blocks and an orthorhombic pattern of faulting across the arc platform from the Shikoku Basin to the forearc. The large Quaternary arc volcanoes, constructed in a regular linear trend, subparallel to the trench, overprinted these early structures. A present phase of extension is now active in the mid-section of the Bonin arc. The

Figure 3.16 **A.** During the early stages of rifting opening occurred on synthetic "primary" faults. Syn-rift sediments accumulated in the depressed areas. **B.** With progressive deformation the strain on the hanging-wall fault block creates smaller antithetic faults. There is also deformation in the syn-rift sediment pile as the underlying basement continues to subside. The backslope of footwall uplifts also becomes downfaulted.

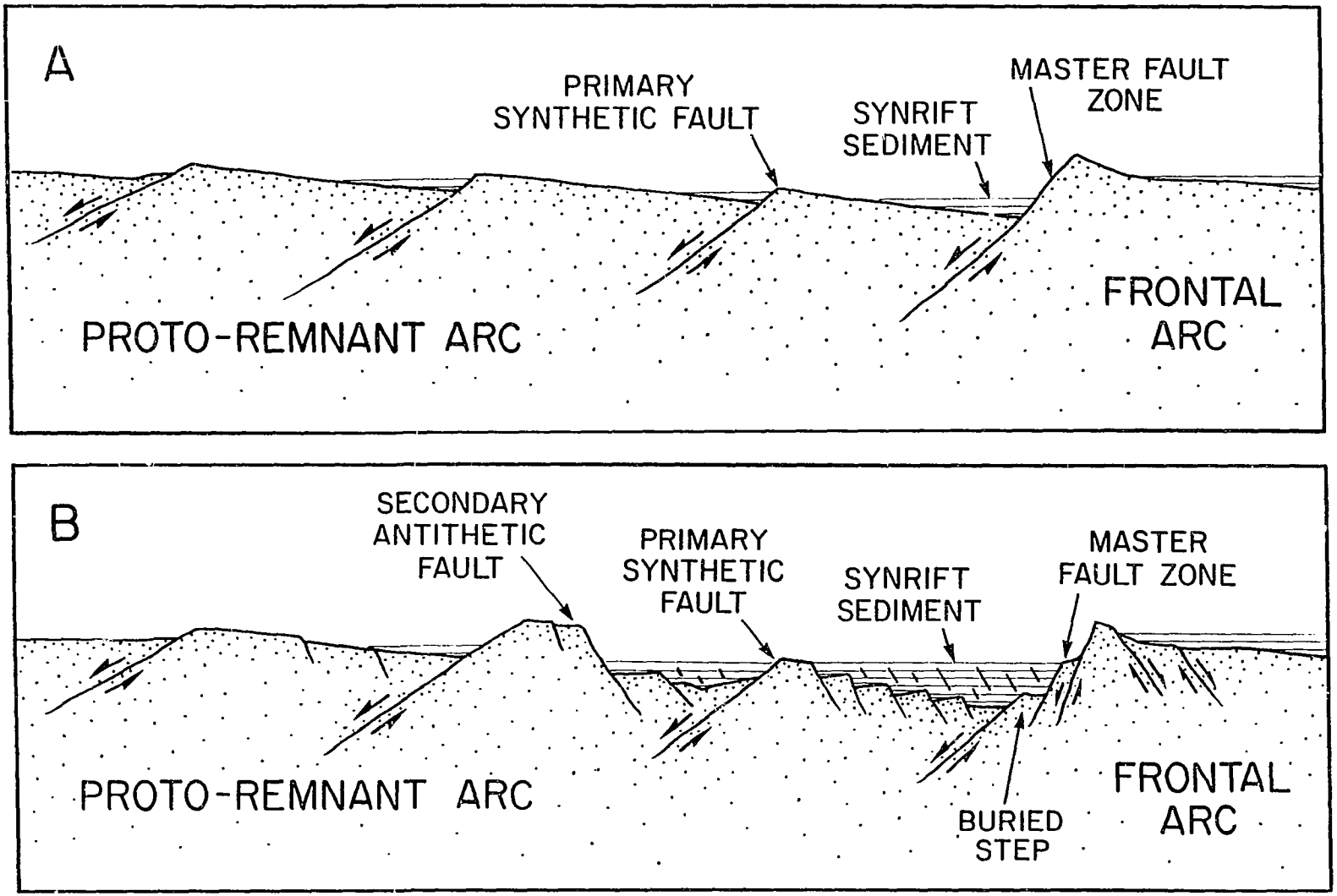
A
PRIMARY
SYNTHETIC FAULT
SYNRIFT
SEDIMENT
MASTER FAULT
ZONE
PROTO-REMNANT ARC
FRONTAL
ARC
B
SECONDARY
ANTITHETIC
FAULT
PRIMARY
SYNTHETIC
FAULT
SYNRIFT
SEDIMENT
MASTER
FAULT ZONE
PROTO-REMNANT ARC
BURIED
STEP
FRONTAL
ARC

Sumisu and Torishima rifts are the manifestations of this extension. The depressions represent upper crustal subsidence within a narrow zone of the proximal backarc.

The architecture of the young island-arc rifts is analogous to areas of continental rifting. The first stage of deformation was a regional synthetic block faulting with rapid subsidence occurring in an asymmetric graben bounded by a master fault zone. The zig-zag pattern of the main boundary faults and a regional pattern of "conjugate" lineaments suggests that the initial fracture pattern developed at the onset of extension into a field of orthorhombic faults similar to *Reches* [1983] experimental models and other rift areas.

Axial basins develop between the orthorhombs, at the base of pre-existing faults or at subtle rift-oblique accommodation zones. Sediments also accumulate in fault-block basins outside the axial areas and in terraced basins around basement highs. The main source of debris appears to be the proximal arc volcanoes and debris eroded from flanking uplifts, although the fine-grained pelagic constituents may increase in isolated depocenters or at distance away from the sources. Sediment "acoustic facies" were mapped and classified based on their 3.5 kHz echocharacter. Sedimentation in rift-floor depocenters is episodic and fines are reworked by bottom currents. These sediments are markedly different in echocharacter compared to the coarse-grained (more diffuse echocharacter) sediments found near the arc volcanoes. The acoustic facies of sediments varies between neighboring depocenters and indicates that currently there is little sediment exchange between the semi-isolated depressions.

Two "modes" of volcanism were found in the central Bonin arc. The sizable arc volcanoes veil the arc active arc margin of the rift system with volcaniclastic output. The flanks are channelled and eruption sites and slump scars on the slopes are common. Within the rift zone there are several hundred

much smaller vents, controlled by the rift normal faults, but concentrated along rift-oblique swaths coincident with subtle shifts in the fault-block geometry. The "intra-rift" volcanism is bimodal and saturated in H_2O and is apparently independent of the arc volcanism [*Fryer et al.*, 1990]. Flexural uplift of rift margins between orthorhombic faults or accommodations leaves triangular "block seamounts". During uplift, deformation and erosion occur on the raised crustal wedges. Flexing of the active arc margin is suppressed by mass-loading from the large arc volcanoes. Together, the extension-related block faulting, which forms areas of subsidence and uplift juxtaposed next to the erupting island arc, creates the complex system of tectonically controlled depocenters.

3.7 References

Bandy, W. and T. Hilde, Structural features of the Bonin arc: Implications for its tectonic history, in *Convergence and Subduction,,Tectonophysics 99,* edited by Hilde, T., and S. Uyeda, 331-353, 1983.

Beal, K., *The opening of a back arc basin: Northern Mariana Trough,* M.S. thesis, Univ. of Hawaii, Honolulu, 1987.

Blackinton, G., *Bathymetric mapping with SeaMARC II: An elevation angle measuring side-scan sonar system,* Ph.D. Diss., Univ. of Hawaii, 145 pp., 1986.

Brown, G., F. Murakami, A. Nishimura, B. Taylor and M. Yuasa, Seafloor Geological Map, Sumisu and Torishima Rifts, Izu-Ogasawara Island Arc, 1:200,000, *Marine Geology Map Series, 31,* Geological Survey of Japan, Tsukuba, 1988.

Carey, S., and H. Sigurdsson, A model of volcanogenic sedimentation, in *Marginal Basin Geology, Geol. Soc. Spec. Publ. No. 16*, edited by Kokelaar, K.P., and M.F. Howells, Blackwell Scientific Publications, Oxford, 37-58, 1984.

Cloos, H., Künstliche Gebirge II, Natur u. Museum, 278-290, 1930.

Damuth, J., Use of high-frequency (3.5 - 12 kHz echograms in the study of near-bottom sedimentation processes in the deep-sea: a review, *Mar. Geol., 38*, 51-75, 1980.

Dubois, J.D., F. Dugas, A. Lapouille and R. Louat, The troughs at the rear of the New Hebrides island arc: possible mechanisms of formation, *Can. J. of Earth Sci., 15,* 351-360, 1978.

Eguchi, T., Seismicity around the Izu-Bonin arc and its tectonic background (in Japanese), *Earth Monthly, 7,* 646-651, 1985.

Elmohandes, S., The central European graben system: Rifting initiated by clay modelling, *Tectonophys., 73,* 69-78, 1981.

Freund, R., Kinematics of transform and transcurrent faults, *Tectonophys., 21,* 93-134, 1974.

Freund, R., and A. Merzer, The formation of rift valleys and their zigzag fault patterns. *Geol. Mag., 113,* 561-568, 1976.

Fryer P., and G. Fryer, Origins of nonvolcanic seamounts in a forearc environment, in *Seamounts, Islands, and Atolls,* edited by Keating, B., P. Fryer, R. Batiza and G. Boehlert, AGU Geophysical Monograph, 43, Washington D.C., 61-69, 1987.

Fryer P., Petrology and geochemistry of lavas from the Sumisu and Torishima backarc rifts, *Earth Planet. Sci. Lett., 100,* 161-178, 1990.

Gibbs, A.D., Structural evolution of extensional basin margins, *J. Geol. Soc.London, 141,* 609-620, 1984.

Hess, H.H., Major structural features of the Western North Pacific, *Geol. Soc. Am. Bull., 59,* 417-446, 1948.

Honza, E., K. Tamaki, M. Yuasa, M. Tanahashi and A. Nishimura, Geological Map of the North Ogasawara Arc, *Marine Geology Map Series, 17,* Geological Survey of Japan, Tsukuba, 1982.

Honza, E., and K. Tamaki, Bonin Arc, in *The Ocean Basins and Margins, Vol. 7, The Pacific Ocean,* edited by Nairn, A.E.M., and S. Uyeda, Plenum Press, New York, 459-502, 1985.

Hotta, H., A crustal section across the arc Izu-Ogasawara and trench, *Phys. Earth, 18,* 125-141, 1970.

Huchon, P., and H. Kitazato, Collision of the Izu block with central Japan during the Quaternary and geological evolution of the Ashigara area, *Tectonophys., 110,* 201-210, 1985.

Hussong , D., and P. Fryer, Back-arc seamounts and the SeaMARC II seafloor mapping system (abstract), *EOS Tran. AGU, 45,* 627-632, 1983.

Hussong, D., and S. Uyeda, Tectonic processes and the history of the Mariana arc: a synthesis of the results of Deep Sea Drilling Project Leg 60, in *Init. Repts.of the DSDP, 60,* edited by Hussong, D.M., and S. Uyeda, U.S. Govt. Printing Office, Washington D.C., 909-929, 1981.

Ishii, T., Dredged samples from the Ogasawara forearc seamount or "Ogasawara Paleoland"-"forearc ophiolite", in *Formation of Active Ocean Margins,* edited by Nasu N., et al., Terra Publ., Tokyo, 307-342, 1985.

Kaizuka, S., A tectonic model for the morphology of arc trench systems, especially for the echelon ridges and mid-arc faults, in *IXth INQUA Congress,* Christchurch, 9-28, 1973.

Karig, D.E., Origin and development of marginal basins in the Western Pacific, *J. Geophys. Res., 76,* 2542-2561, 1971.

Karig, D.E., Evolution of arc systems in the Western Pacific, *Annual Rev. Earth Planet. Sci., 2,* 51-75, 1974.

Karig, D.E., Basin genesis in the Philippine Sea, in *Init. Repts.of the DSDP, 31*, edited by Karig D.E., et al., U.S. Govt. Printing Office, Washington, 857-879, 1975.

Karig, D.E, and G.F. Moore, Tectonic complexities in the Bonin Arc system, *Tectonophys., 27,* 97-118, 1975a.

Karig, D.E., and G.F. Moore, Tectonically controlled sedimentation in marginal basins, *Earth Planet. Sci. Lett., 26*, 233-238, 1975b.

Karig, D.E., R. N. Anderson and L.D. Bibee, Characteristics of backarc spreading in the Mariana Trough, *J. Geophys. Res., 83,* 1213-1226, 1978.

Katsumata, M., and L.R. Sykes, Seismicity and tectonics of the western Pacific: Izu-Mariana-Caroline and Ryukyu-Taiwan region, *J. Geophys. Res., 74,* 5923-5948, 1969.

Klaus, A., B. Taylor, M. MacKay and G. Moore, Rifting of the Bonin arc: Preliminary results from multichannel seismic data (abstract), *EOS Tran. AGU, 69*, 1442, 1988.

Kobayashi, K., and M. Nakada, Magnetic anomalies and tectonic evolution of the Shikoku inter-arc basin, *J. Phys. Earth, 26*, 391-402, 1978.

Kroenke, L.W., R.B.Scott, et al., in *Initial Reports of the Deep Sea Drilling Project, 59*, U.S. Government Printing Office, Washington D.C., 1981.

Kuno, H., Japan, Taiwan, and Marianas, in *Catalogue of the Active Volcanoes of the World, 11*, Int. Volc. Assoc., Rome, 1-132, 1962.

Leg 126 Shipboard scientific party, 1989, Arc volcanism and rifting, *Nature*, in press.

LePichon, X., T. Iiyama, H. Chamley, J. Charvet, M. Faure, H. Fujimoto, T. Furuta, Y. Ida, H. Kagami, S. Lallemant, J. Leggett, A. Murata, H. Okada, C. Rangin, V. Renard, A. Taira and H. Tokuyama, The eastern and western ends of Nankai Trough: results of Box 5 and Box 7 Kaiko survey, *Earth Planet. Sci. Lett., 83*, 199-213, 1987.

Lowell, J.D., Structural styles in petroleum exploration, Oil and Gas Consultants Int., Tulsa, Okla, 490 pp., 1985.

Malahoff, A., R. Feden, and H. Fleming, Magnetic anomalies and tectonic fabric of marginal basins north of New Zealand, *J. Geophy. Res., 87*, 4109-4125, 1982.

Mammerickx, J., R. Fisher, F. Emmel, S. Smith, *Bathymetry of the East and Southeast Asian Seas*, Scripps Inst. of Oceanography, 1976.

Marsh, B., Island-arc volcanism, *Am. Sci., 67*, 161-172, 1979.

Matsuda, T., Collision of the Izu-Bonin arc with central Honshu-Cenozoic tectonics of the Fossa Magna, Japan, *J. Phys. Earth, 26*, s409-s421, 1978.

Mogi, A., The Izu Ridge, in *Fossa Magna* (in Japanese), edited by Hoshino, M., Geol. Soc. Japan, Tokyo, 217-221, 1968.

Moriyama, T., *Focal mechanisms and depths of the earthquakes in the Bonin arc and their tectonic implications,* M.S. thesis, Univ. of Tsukuba, Ibaraki, Japan, 1988.

Mrozowski, C.L., and D.E. Hayes, The evolution of the Parece Vela Basin, Eastern Philippine Sea, *Earth Plan. Sci. Lett., 46*, 49-67, 1979.

Murakami, F., Structural framework of the Sumisu Rift, Izu-Ogasawara arc, *Bull. Geol. Surv. of Japan, 39*, 1-21, 1988.

Murakami, F., and T. Ishihara, Submarine caldera found in northern Ogasawara Arc (in Japanese), *Earth Monthly, 7*, 638-646, 1985.

Nakanishi, M., K. Tamaki and K. Kobayashi, Mesozoic magnetic anomaly lineations and seafloor spreading history of the northwestern Pacific, *J. Geophys. Res., 94,* 15437-15462, 1989.

Natland, J., and J. Tarney, Petrological evolution of the Mariana arc and back-arc basin system-a synthesis of drilling results in the South Philippine Sea, in *Init. Repts. of the DSDP, 60*, edited by D.M. Hussong, and S. Uyeda, U.S. Govt. Printing Office, Washington D.C., 877-908, 1981.

Nishimura A., and F. Murakami, Sedimentation of the Sumisu Rift, Izu-Ogasawara arc, *Bull. Geol. Surv. of Japan, 39*, 39-61, 1988.

Nishimura A., T. Yamazaki, M. Yuasa, N. Mita and S. Nakao, Bottom Sample and Heat Flow Data of Sumisu and Torishima Rifts, Izu-Ogasawara Arc, 1:200,000, *Marine Geology Map Series, 31,* Geological Survey of Japan, Tsukuba, 1988.

Norris, R..A., and R.H. Johnson, Submarine volcanic eruptions recently located in the Pacific by SOFAR hydrophones, *J. Geophy. Res., 74*, 650-664, 1969.

Ramberg, I.B., F.A. Cook and S.B. Smithson, Structure of the Rio Grande rift in southern New Mexico and West Texas based on gravity interpretation, *Geol. Soc. Am. Bull., 89,* 107-123, 1978.

Reches, Z., Analysis of faulting in three-dimensional strain field, *Tectonophys., 47,* 109-120, 1978.

Reches, Z., and J.H. Dieterich, Faulting of rocks in three-dimensional strain fields I. Failure of rocks in polyaxial, servo-control experiments, *Tectonophys., 95,* 111-132, 1983.

Reches, Z., Faulting of rocks in three-dimensional strain fields II. Tectonic analysis, *Tectonophys., 95,* 133-156, 1983.

Rosendahl, B., Architecture of continental rifts with special reference to East Africa, *Ann. Rev. Earth Planet. Sci., 15,* 445-503, 1987.

Seno, T., Is north Honshu a microplate?, *Tectonophys., 115,* 177-196, 1985.

Seno, T., T. Moriyama, S. Stein, D. Woods, C. Demets, D., Angus and R. Gordon, Redetermination of the Philippine Sea Plate motion (abstract), *EOS Tran. AGU, 68*, 1474, 1987.

Shih, T., Marine magnetic anomalies from the western Philippine Sea implications for the evolution of marginal basins, *AGU Monograph 23*, 1980.

Shiki, T., *Geology of the Northern Philippine Sea,* Tokai Univ. Press, Tokyo, 1985.

Shiraki, K., N. Kuroda, H. Urano and S. Maruyama, Clinoenstatite in boninites from the Bonin Islands, Japan, *Nature, 285*, 31-32, 1980.

Sibuet, J., J. Letouzey, F. Barbier, J. Charvet, J. Foucer, T. Hilde, M. Kimura, C. Ling-Yun, B. Marsset, C. Muller and J. Stephan, Back arc extension in the Okinawa Trough, *J. Geophys. Res., 92*, 14041-14063, 1987.

Simkin, T., L., Siebert, L., McClelland, D. Bridge, C. Newhall and J. Latter, *Volcanoes of the World. A regional directory, gazetteer, and chronology of volcanism during the last 10,000 years*, Smithsonian Institute, Washington D.C., 232 pp., 1981.

Smoot, N.C., The growth rate of submarine volcanoes on the South Honshu and East Mariana ridges, *Jour. Vol. Geotherm. Res., 35* , 1-15, 1988.

Steckler, M.S., Uplift and extension at the Gulf of Suez: Indications of induced mantle convection, *Nature, 317*, p.135-139, 1985.

Stern, R.J., N.C. Smoot and M. Rubin, Unzipping of the Volcano Arc, Japan, in *Geodynamics of back-arc regions, Tectonophys., 102*, edited by R.L. Carlson and K. Kobayashi, 153-174, 1984.

Tamaki, K., E. Inoue, M. Yuasa, M. Tanahashi and E. Honza, On the possibility of active back-arc spreading of Ogasawara arc (in Japanese), *Earth Monthly, 3,* 421-431, 1981.

Tamaki, K., Two modes of back-arc spreading, *Geology, 13,* 475-478, 1985.

Taylor, B., and N.C. Smoot, Morphology of Bonin fore-arc submarine canyons, *Geology, 12,* 724-727, 1984.

Taylor, B., G. Brown, D. Hussong and P. Fryer, SeaMARC II Sidescan Acoustic Imagery, Sumisu and Torishima Rifts, Izu-Ogasawara Island Arc, 1:200,000, *Marine Geology Map Series, 31,* Geol. Surv. of Japan, Tsukuba, 1988.

Taylor, B., G. Brown, D. Hussong and P. Fryer, SeaMARC II Bathymetry, Sumisu and Torishima Rifts, Izu-Ogasawara Island Arc, 1:200,000, *Marine Geology Map Series, 31,* Geol. Surv. of Japan, Tsukuba, 1988.

Taylor, B., D. Hussong, and P. Fryer, Rifting of the Bonin Arc (abstract), *EOS Tran. AGU, 65*, 1006, 1984.

Taira, A., H. Tokuyama, and W. Soh, Accretion tectonics and evolution of Japan, (submitted).

Tsunakawa, H., K-Ar dating on volcanic rocks in the Bonin Islands and its tectonic implication, *Tectonophys., 95,* 221-232, 1983.

Wallace, R.E., Profiles and ages of young fault scarps, north-central Nevada, *Geol. Soc. Am. Bull., 88,* 1267-1281, 1977.

Weaver, S.D., A.D. Saunders, R.J. Pankhurst and J. Tarney, A geochemical study of magmatism associated with the initial stages of back-arc spreading: the Quaternary volcanics of the Bransfield Strait, South Shetland Islands, *Contrib. Mineral. Petrol., 68,* 151-169, 1979.

Weissel, J., and G. Karner, Flexural uplift of rift flanks due to tectonic denudation of the lithosphere during extension, *J. Geophys. Res.,* in review.

Wood, D.A., N.G. Marsh, J. Tarney, J. Joron, P. Fryer and M. Treuil, Geochemistry of igneous rocks recovered from a transect across the Mariana Trough, Arc, Forearc, and Trench, Sites 453 to 461, Deep Sea Drilling Project Leg 60, in *Init. Repts. DSDP, 60,* edited by D.M. Hussong, and S. Uyeda, U.S. Govt. Printing Office, Washington D.C., 611-645, 1981.

Wright, I.C., Late Quaternary faulting of the offshore Whakatane Graben, Taupo Volcanic Zone, New Zealand, *N.Z. J. Geol. Geophys., 33,* 245-256, 1990.

Wright, I., L. Carter and K. Lewis, Gloria survey of the oceanic-continental transition of the Havre-Taupo back-arc basin, *Geo-Marine Letters, 10*, 59-67, 1990.

Yamazaki, T., Heat flow in the Sumisu Rift, Izu-Ogasawara arc, *Bull. Geol. Surv. of Japan, 39*, 63-70, 1988.

Yamazaki, T., and F. Murakami, Heat flow and structure in the back-arc area of the Izu-Ogasawara Arc (abstract) (in Japanese), *Autumn meeting SSJ*, 204, 1987.

Yuasa, M., Sofu Gan Tectonic Line, a new tectonic boundary separating northern and southern parts of the Ogasawara (Bonin) arc, northwest Pacific, in *Formation of Active Ocean Margins*, edited by N. Nasu et al., Terra Scientific Pub. Co., Tokyo, 483-496, 1985.

Yuasa, M., and F. Murakami, Geology and geomorphology of the Ogasawara arc and the Sofu Gan Tectonic Line (in Japanese), *Earth Monthly, 94*, 47-66, 1985

Chapter IV

Rifting of the Bonin Arc between 29° and 29°50' N

4.1 Introduction

Backarc basins open by rifting near the sites of arc volcanism. Hanging-wall subsidence and footwall uplift occurs across master normal-fault zones that reverse polarity (dip direction) along strike. The early forming primary faults grow into a regional orthorhombic pattern by distributing slip simultaneously. Strain on the hanging-wall rollover induces sets of closely-spaced step-faults that are predominantly antithetic to the primary master fault zone. The crustal blocks shaped by the orthorhombic pattern of faulting are free to rise along the flanks of the grabens unless loaded by large volcanic masses (Chapter III).

The Sumisu and Torishima rift segments (Figure 4.1) are analogous to early asymmetric stages of narrow continental rifts with prominent flexural uplifts, exceeding 1 km in relief, that flank well sedimented rift basins. The axis of subsidence is parallel with the volcanic front and partial to the proximal retroarc. Blocks of crust "seesaw" along the axis and undergo adjustments at rift-oblique accommodation zones. The basement in the Sumisu Rift south of 31° N began to subside in the mid-Pliocene. Since this time >1200 m of sediments have filled the graben [*Leg 126 Scientific Drilling Party*, 1989]. Because the thick sediments partly cover fault blocks in the axial area (Chapter III) a study of the three- dimensional basement structure in the Sumisu and Torishima rifts is difficult. This chapter looks at rift development and related processes in the central Bonin arc between 29° N and 29°50' N (Figure 4.2). In this area there are important rift structures in the basement that are not yet buried by syn-rift sediments. The available data set covers an area within approximately 80 km of the proximal backarc and 35 km of the proximal forearc (south of 29°30' N).

Figure 4.1 The main tectonic elements and bathymetry of the Bonin island arc, from Chapter III. The contour interval is 500 m. Stipled box shows the location of Figure 4.2. The main volcanoes in the central Bonin arc are S-Sumisujima, T-Torishima, SG-Sofu Gan, N-Nishinoshima, Ka-Kaikata Seamount, Ku-Kaitoku Seamount. The previously named rift segments (sidefacing bold letters) are H-Hachijo Rift, A-Aogashima Rift, S-Sumisu Rift, T-Torishima Rift, SG-Sofu Gan Rift, and N-Nishinoshima Rift. Pre-Pliocene (?) lineaments, oblique to the arc, are indicated by stipled line segments. Background bathymetry is based on data from the Geological Survey of Japan, Hawaii Institute of Geophysics, Hydrographic Office of Japan, Ocean Research Institute (University of Tokyo), and the U.S. Naval Oceanographic Office.

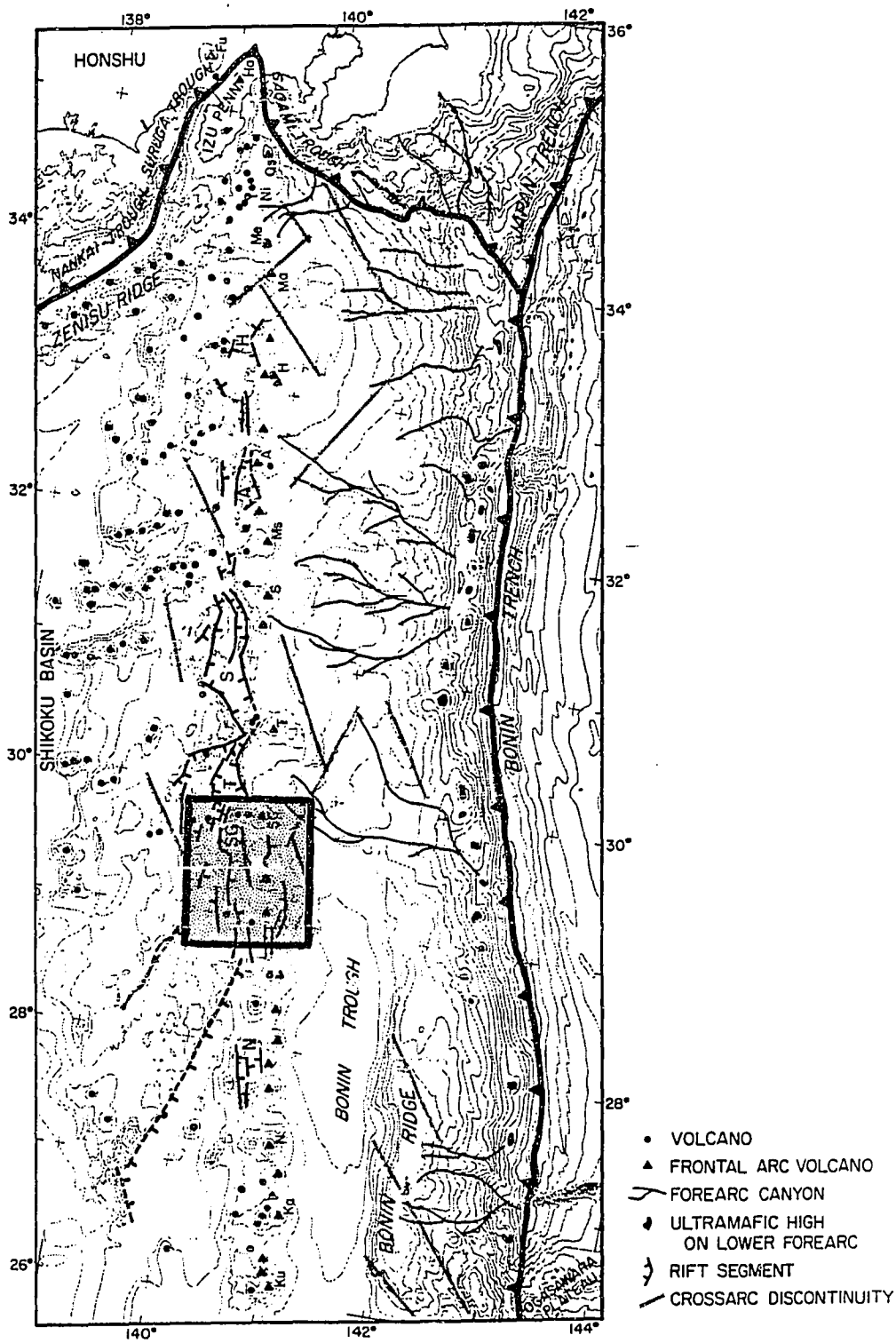
138°
140°
142°
36°
34°
32°
30°
28°
26°
144°
HONSHU
IZU PENINSULA
SURUGA TROUGH
NANKAI TROUGH
ZENISU RIDGE
SHIKOKU BASIN
JAPAN TRENCH
BONIN TRENCH
BONIN TROUGH
BONIN RIDGE
OGASAWARA RIDGE
VOLCANO
FRONTAL ARC VOLCANO
FOREARC CANYON
ULTRAMAFIC HIGH ON LOWER FOREARC
RIFT SEGMENT
CROSSARC DISCONTINUITY

Figure 4.2 The location of the Sofu Gan survey area, the focus of this chapter, between 29° and 29°50' N. The proposed names for seamounts south of Sofu Gan Island are shown. Stipled pattern indicates the locations of extension-related basement subsidence near the sites of arc volcanism. The most significant of the older faults (solid lines) is the Sofu Gan Tectonic Line of *Yuasa* [1985].

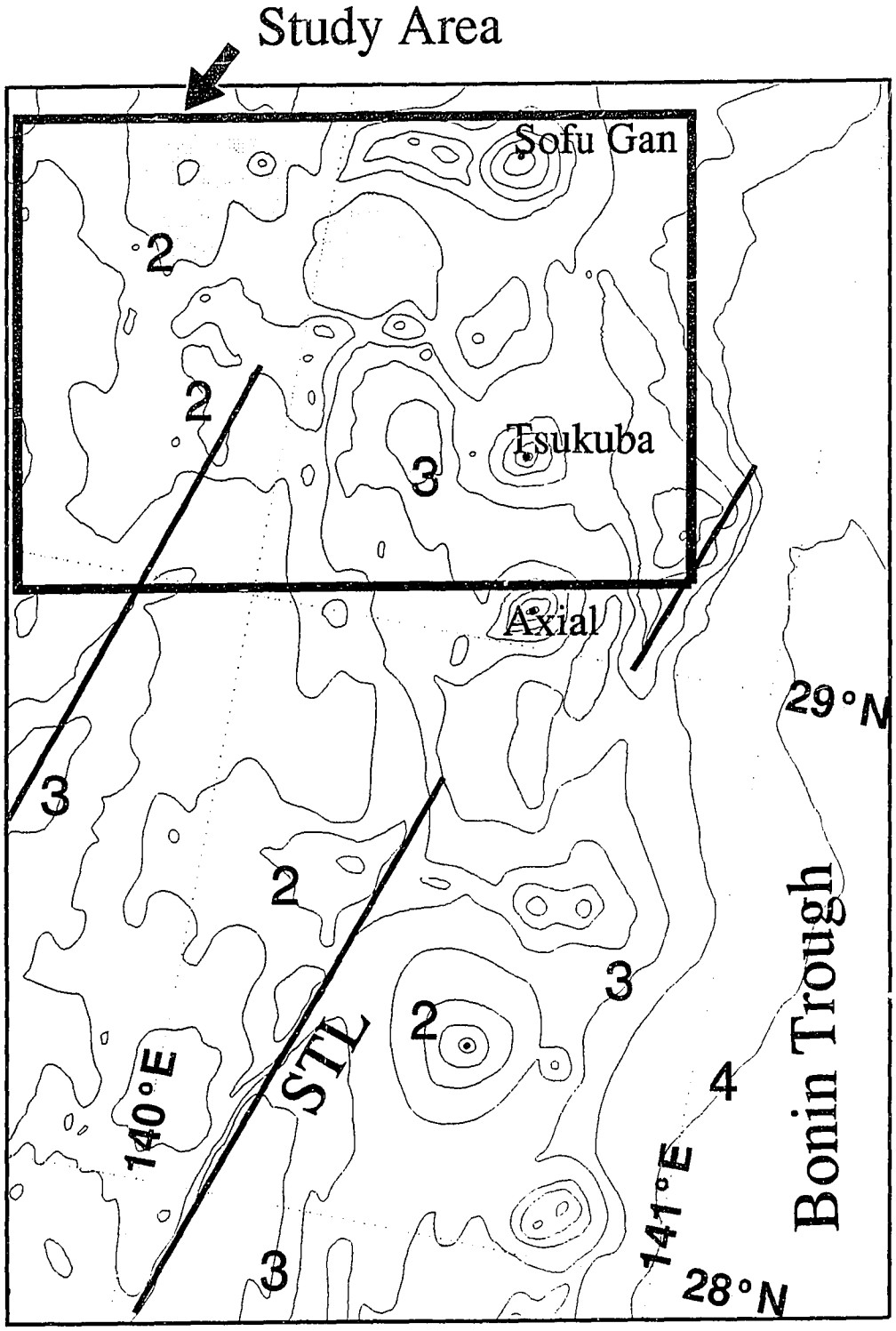
Study Area
Sofu Gan
Tsukuba
Axial
29°N
28°N
140°E
141°E
STL
Bonin Trough
2
2
3
3
2
3
2
3
4

The regional geology of the central Bonin arc was discussed in the previous chapter. The linear chain of island and submarine volcanoes, constituting the "arc", begins at Mt. Fuji on Honshu and deepens southwards (Figure 4.3). North of Sofu Gan Island, at 29°47' N, many of the arc volcanoes are subaereal. The subaereal exposures are either rock pinnacles at the edge of a submarine caldera (e.g. Sumisujima), individual volcanic edifices (e.g. Torishima), or coalesced edifices (e.g. Hachijojima). There are numerous submarine calderas and satellite edifices in this northern segment (e.g. South Sumisu). For approximately 350 km south of Sofu Gan Island the tops of frontal arc volcanoes are deeper than 500 mbsl (meters below sea level) until Nishinoshima near 27°15' N. The best studied submarine volcano south of Sofu Gan is the summit caldera of Kaikata Seamount at 27°40' N where hydrothermal vent sites have been investigated by the Geological Survey of Japan [*Nakao et al.*, 1989].

South of Sofu Gan Island the large frontal arc volcanoes are located on or near rifted lithosphere. The slopes of three arc volcanoes were surveyed between 29° and 29°50' N. To aid the discussion in this chapter the unnamed volcanoes (Figure 4.2) will be refered to as "Tsukuba Volcano" (after the location of the Geological Survey of Japan) and "Axial Volcano" (as it lies in the axis of the young rift system).

In order to learn more about the processes associated with early stages of backarc opening, we surveyed the central Bonin rift system between 29° N and 31°20' N with the SeaMARC II sidescan imagery and bathymetry system, single-channel (analog) seismic reflection and conventional shipboard geophysics using the *R/V Kana Keoki* from the Hawaii Institute of Geophysics. This study also uses closely-spaced 3.5 kHz echo-character data collected prior to 1985 by the Geological Survey of Japan with the *R/V Hakurei-Maru*. Seabeam data collected in 1987 on the *R/V Atlantis II* west of Sofu Gan are also integrated into the bathymetry.

Figure 4.3 A profile of the Bonin frontal arc volcanoes (within 25 km of the arc line) showing the location of the study area for this chapter. The high south of Sofu Gan is tectonic uplift. There is a shoaling of the "arc platform" between the study area and Honshu.

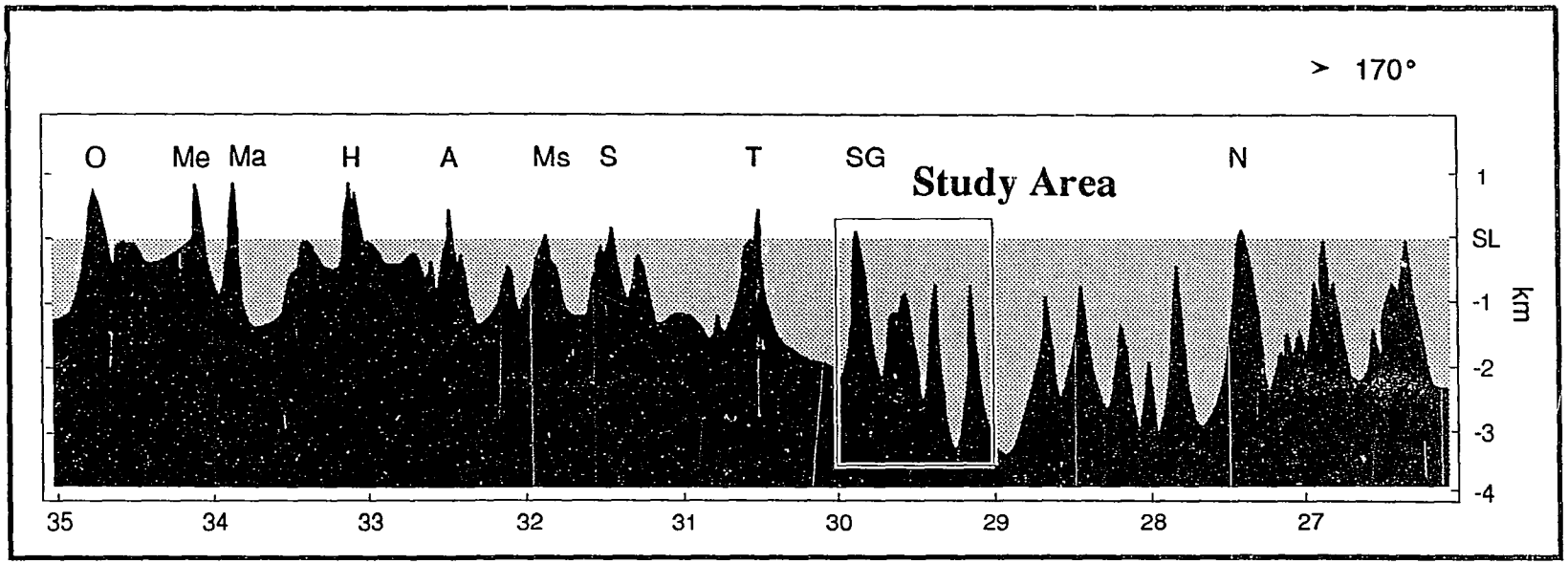
> 170°
O
Me
Ma
H
A
Ms
S
T
SG
Study Area
N
1
SL
-1
-2
-3
-4
km
35
34
33
32
31
30
29
28
27

The SeaMARC II acoustic imagery (Appendix) and bathymetry (solid lines-Figure 4.4) data were recorded in irregularly spaced 10 km wide swaths across the arc and approximately 80 km into the backarc. SeaMARC II imagery is processed from the bottom reflectivity and backscatter. Dark tones correspond to areas of high reflectivity (slopes facing the instrument or areas with a rough bottom such as lava flows). Light tones correspond to areas of low reflectivity (sedimented surfaces, shadowed areas). A description of mapping with SeaMARC II in the Sumisu and Torishima rifts can be found in Chapter II and III.

The bathymetry was compiled from the afore-mentioned SeaMARC II data together with data from systematic surveys by the Geological Survey of Japan. Bathymetry collected during these surveys (prior to 1985) was visually adjusted to account for the differences in the beam width between 3.5 kHz systems (15^{o} around ship) and the SeaMARC II data.

Echo-character data (3.5 kHz) from the Geological Survey of Japan and the Hawaii Institute of Geophysics were studied to assist in the interpretation of seafloor morphologies and map their distribution. The analog single-channel seismic reflection data collected by the *R/V Kana Keoki* were used to interpret the shallow crustal structure in the area. Seismic profiles (labelled "Y" through "JJ", Figure 4.5) are aligned to match with those from Chapter III. Several single-channel seismic reflection profiles were also provided by the Geological Survey of Japan. The lines have an average spacing of 5 km and cover a wider east-west area than the SeaMARC II data set (Figure 4.6). The key GSJ seismic profiles, discussed in this Chapter (GSJ 89, 92 and 100), are shown in Figure 4.7.

The central Bonin island arc is characterized by great variations in relief caused by the juxtaposition of juvenile subsidence, uplift, and arc volcanism (Figures 4.4, 4.5). For example, in the SeaMARC II survey area the maximum depth of the seafloor is 3600 mbsl (meters below sea level) but within 7 km of this deep the seafloor shoals to above

Figure 4.4 Bathymetric map (100 m contour interval) of the Bonin arc between 29° N and 29°50' N. Based on a compilation of SeaMARC II sidescan bathymetry, 3.5 kHz depth recording data from the Hawaii Institute of Geophysics and the Geological Survey of Japan, and 1987 *R/V Atlantis II* Seabeam data west of Sofu Gan Island.

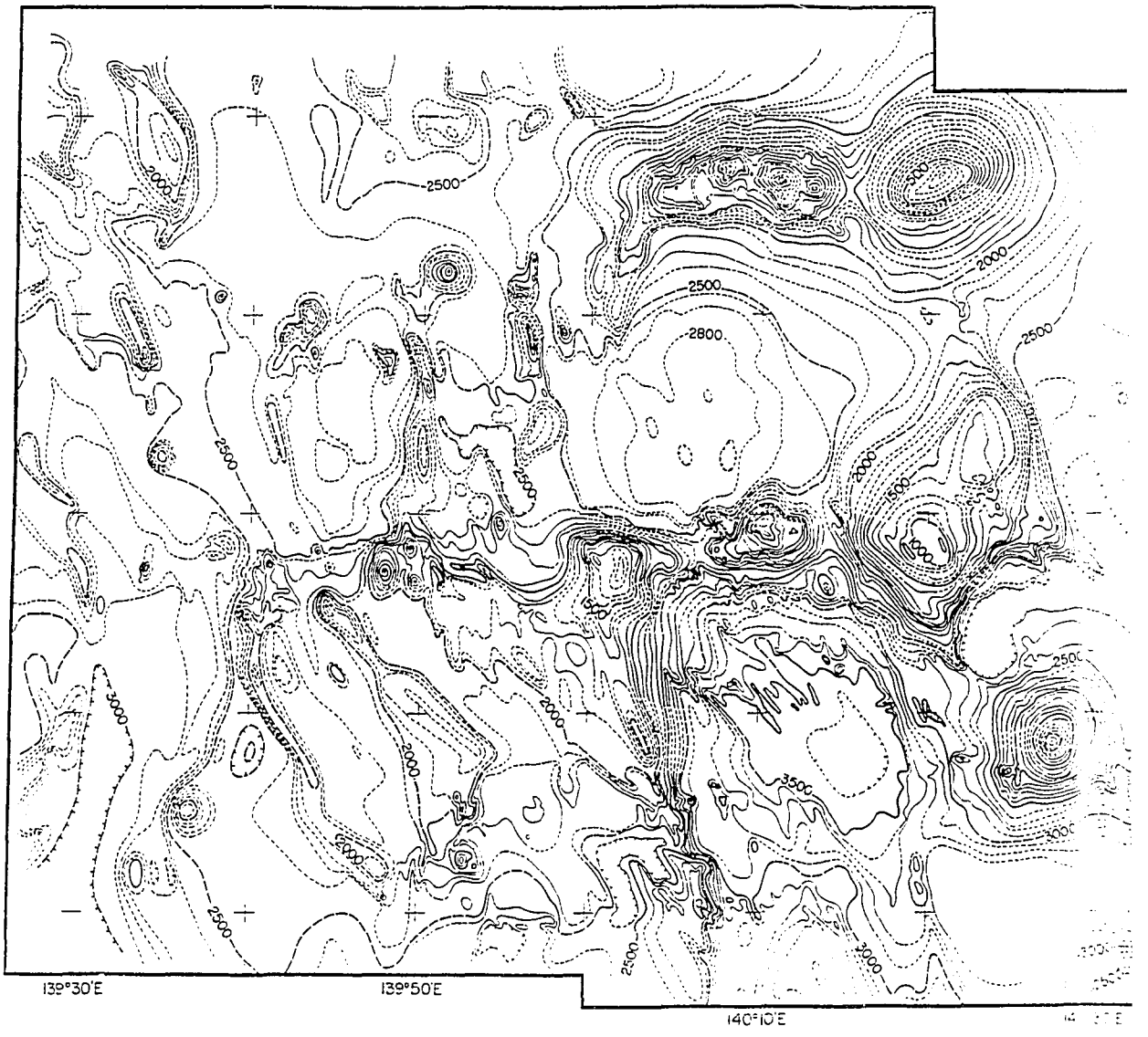
2500
2000
2800
3500
3000
1500
139°30'E
139°50'E
140°10'E

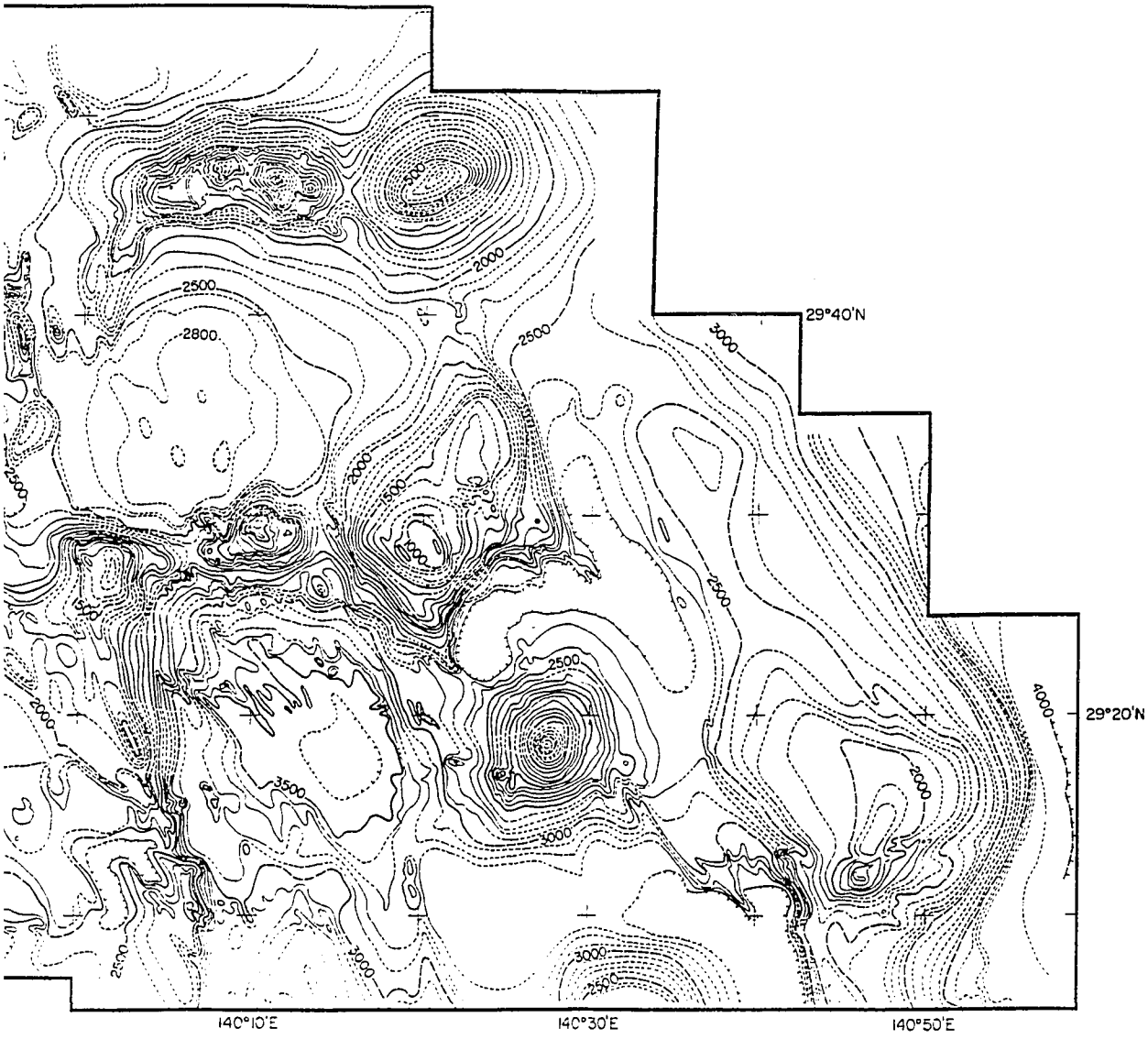
29°40'N
29°20'N
140°10'E
140°30'E
140°50'E
2000
2500
2800
3000
3500
4000

Figure 4.5 Single-channel seismic reflection profiles, labelled "Y" through"JJ". Refer to Figure 4.6 for location. This series of profiles appends onto Profiles "A" to "X" from Chapter III. The vertical exaggeration is 10x.

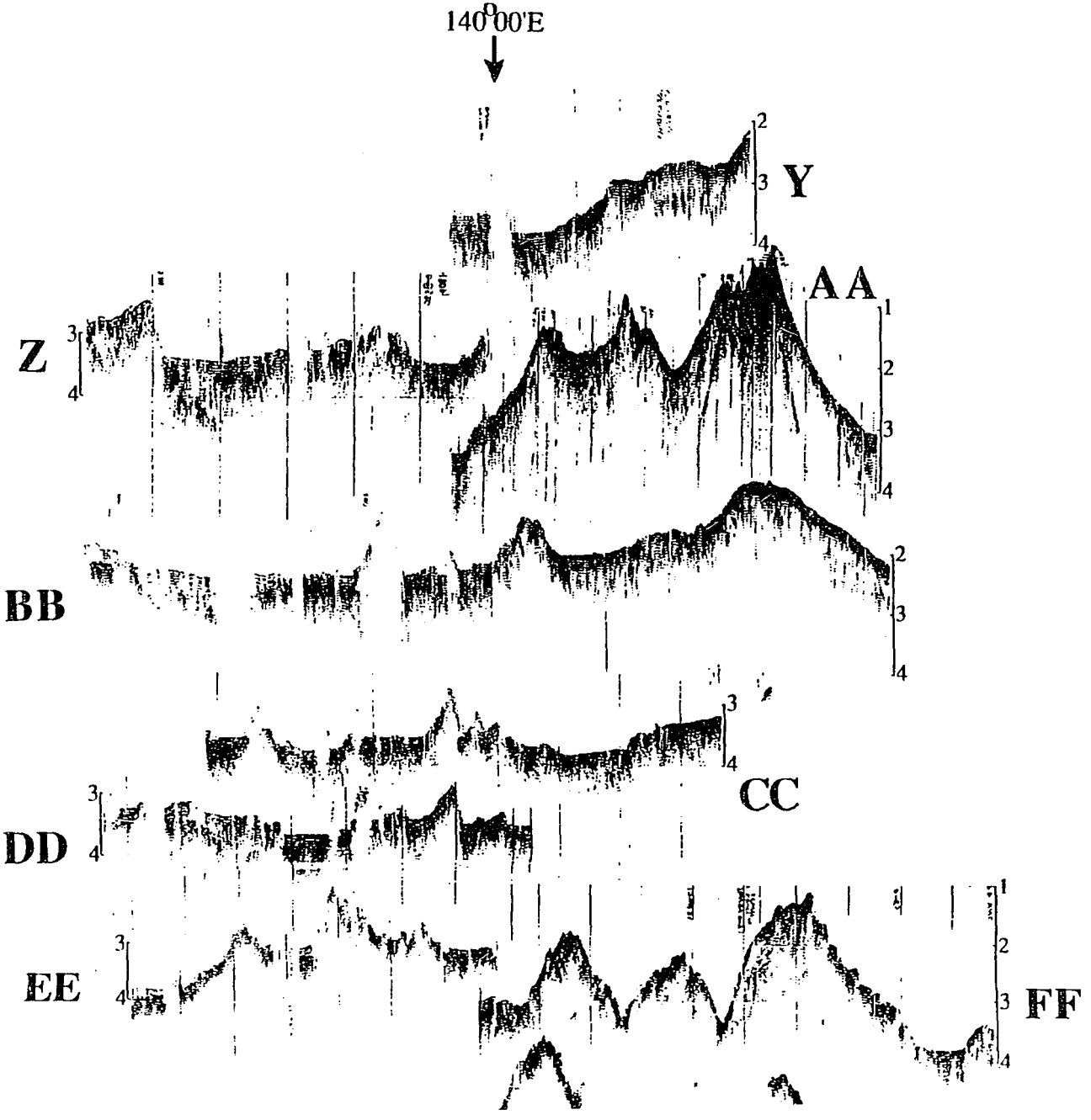
140°00'E
Y
AA
Z
BB
CC
DD
EE
FF

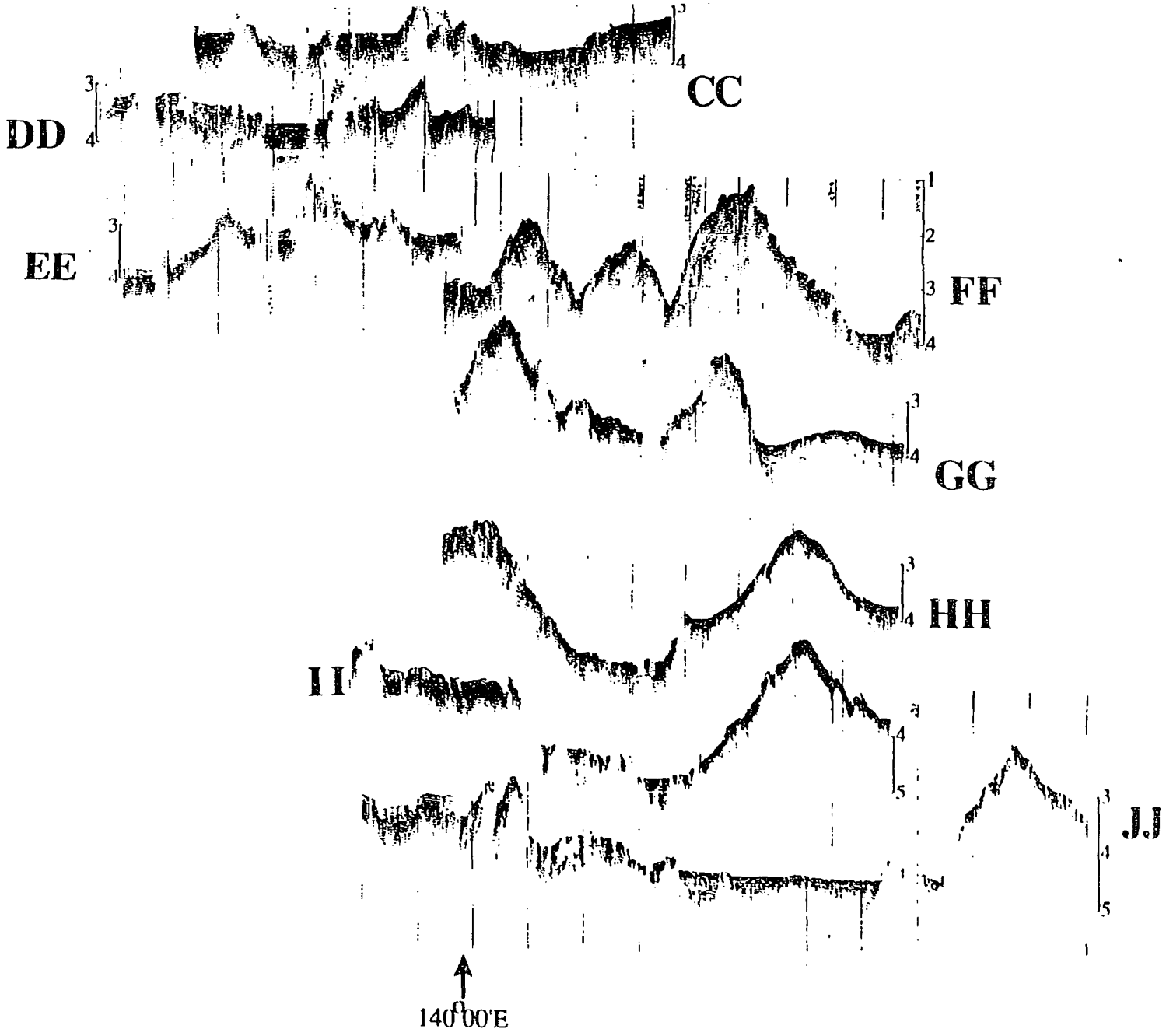
CC
DD
EE
FF
GG
HH
II
JJ
140°00'E

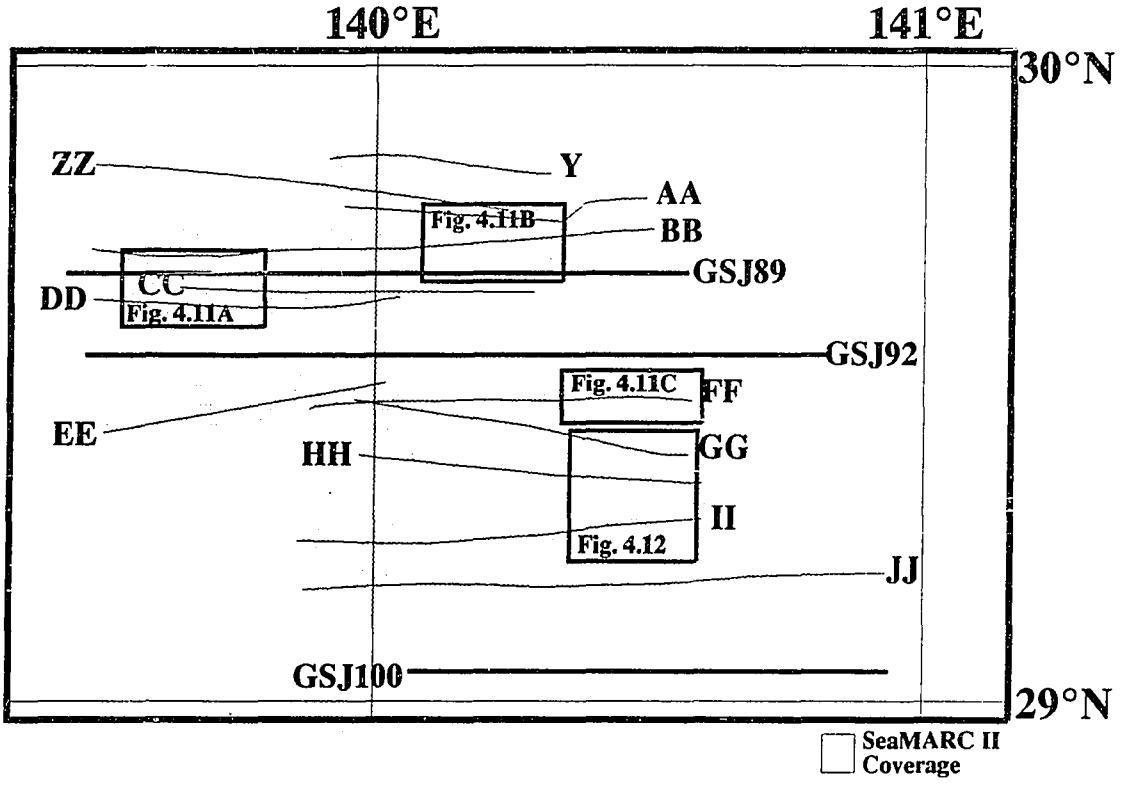

Figure 4.6 The location of the seismic profiles used for this study in the area between 29° N and 29°30' N. Lettered profiles correspond to the sidescan swaths and the single-channel seismic data in Figure 4.5. The numbered seismic lines (shown in Figure 4.7) are from the Geological Survey of Japan. The stiple indicates the coverage of SeaMARC II imagery (Appendix). Boxes show the location of subsequent figures.

Figure 4.7 Single-channel seismic reflection profiles from the Geological Survey of Japan. Refer to Figure 4.6 for location.

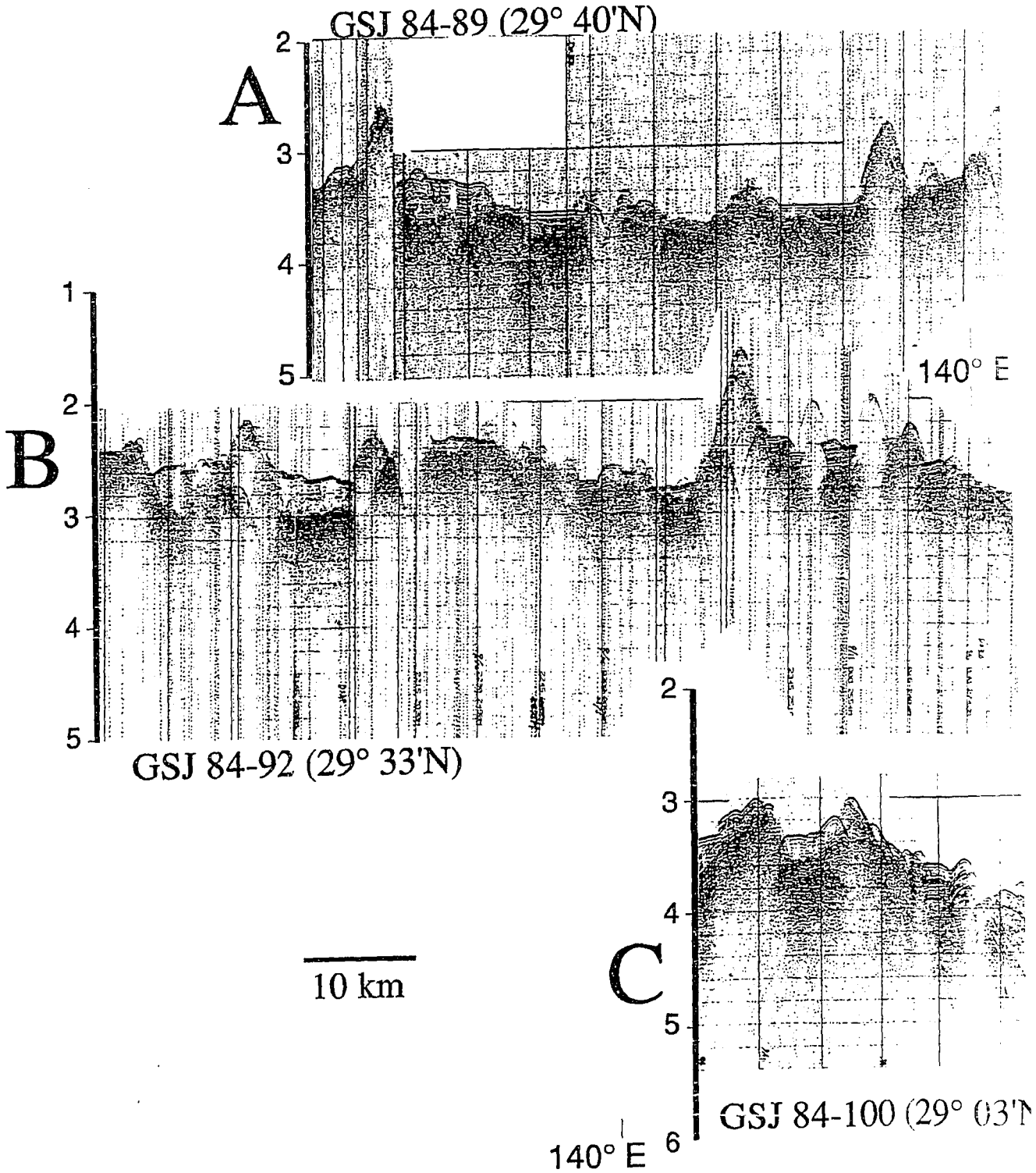
GSJ 84-89 (29° 40'N)
A
2
3
4
5
140° E
1
2
B
3
4
5
GSJ 84-92 (29° 33'N)
10 km
2
3
4
C
5
6
140° E
GSJ 84-100 (29° 03'N

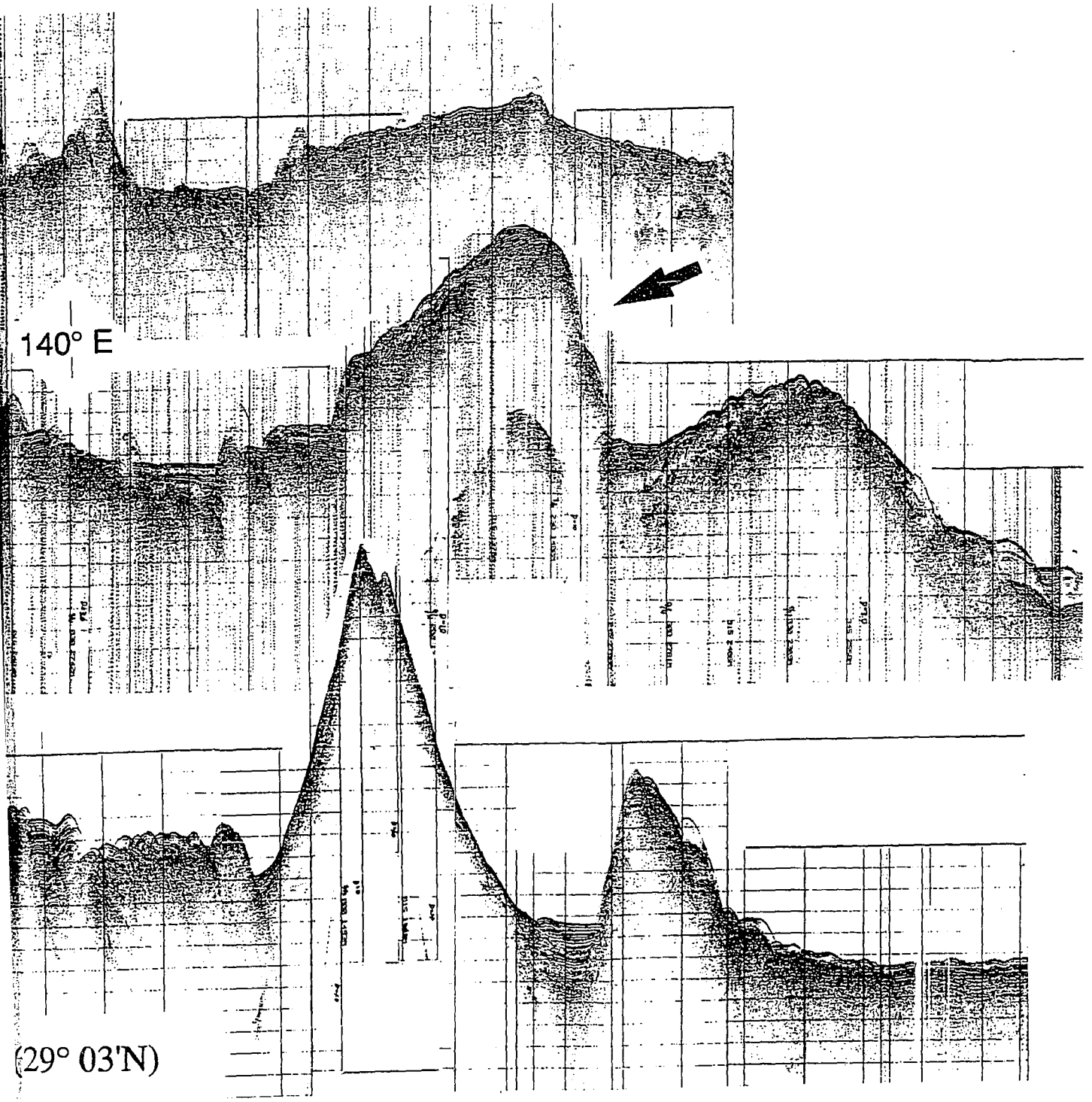
140° E
(29° 03'N)

800 mbsl. The subsiding crust forms a series of basins that are separated by basement (pre-rift) highs. As in the basins to the north (forming Sumisu and Torishima rifts) there is usually one boundary fault, termed the master fault, which controls the morpho-tectonic evolution of the basin. A dominant master fault can give a rift basin an asymmetric profile. A boundary fault invariably opposes (or is antithetic to) the master fault zone but it appears to develop as "secondary" displacement, with less slip than the master fault (Chapter III).

In general, the subsided crust in the proximal Bonin backarc forms a discontinuous trough that parallels the arc line. The basin segments of the rift system were named after the nearby arc volcanoes (see also Chapter III). The basins which lie on trend with this regional axis of subsidence, near the active arc margin (to the east) will be refered to as "axial basins". The basement exposures west of the axial basins and north of 29°50' N were described in Chapter III as the "proto-remnant arc margin". This term becomes less accurate in areas of broader asymmetric deformation as it implies that the present axis of subsidence is destined to become the axis of a future backarc basin. In this chapter the term is used loosely to describe the area outside and west of the active deformation zone.

4.2 Fault geometry

Relict faults

Prior to the present rifting, the Bonin arc experienced a deformation event that led to a regional orthorhombic or rectilinear pattern of normal fault sets (Figure 4.1, Chapter III). Large faulted blocks of tilted basement crust were created by this event. Because the old faults are common in the south-central arc platform it is important to describe these structures first in order to fully understand the Quaternary rifting.

Two significant tectonic features occur near the zone of the active rifting in the south-central Bonin arc: the Bonin Trough and the Sofu Gan Tectonic Line (Figure 4.2). East of the study area and opposite the volcanic front, the 100 km wide Bonin Trough is a forearc basin that separates the partially uplifted, Eocene-age basement of the Bonin Islands [*Shiraki et al.*, 1980] from the active island arc (Figures 4.1 and 4.2). The trough exceeds 4000 mbsl and has sediment thicknesses in excess of 4.0 sec [*Honza and Tamaki*, 1985]. A seismic refraction study in the central Bonin Trough measured an increase in P-wave velocities from an average of 3.6 km/sec to an average of 6.5 km/sec at approximately 4 km below the sea floor [*Kato et al.*, 1990]. This contact may mark the top of the buried Eocene volcanic basement beneath the sediment pile. The -120 mgal free-air gravity anomaly in the south-central trough and a nearby +365 mgal anomaly over the Bonin Ridge forms the highest gravity gradient on earth [*Karig and Moore*, 1975]. The negative anomalies continue to the north as far as 32° N suggesting that the forearc sedimentary basin actually extends north of its morphologic limit near 30° N. The east boundary fault on the Bonin Trough has an approximately 10° dip towards the west which is considerably steeper than the trench side (Figure 4.1). Basement subsidence in the trough varied along strike. Near 29°30' N the greatest subsidence was along the west margin of the trough, as indicated by buried reflectors that are later covered by onlapping sediments (Figure 4.8, third profile from bottom). Near 28°40' N the greatest basement subsidence was along the east (Bonin Ridge) margin [*Japanese DELP Research Group*, 1989].

Opposite the volcanic arc, at approximately the same latitude as the central Bonin Trough, is the Sofu Gan Tectonic Line ("STL", Figure 4.2), a 1200 m high backarc normal fault trending 020° [*Yuasa*, 1985]. At the base of the STL is a wide hanging-wall basin which narrows to the north near an unusually large volcano behind the volcanic front. The STL crosses the arc near the deepest point along the entire volcanic front (Figure 4.3). It appears to be a relict structure, perhaps the product of mid-Oligocene rifting that led to

subsidence in the Bonin Trough and the dog-leg cross-arc lineaments found throughout the platform to the north (Chapter III). The hanging-wall basin has flat-lying undisturbed sediments with deep underlying reflectors inclined steeply toward the escarpment and in places (especially in the west) the escarpment has been incised by erosional features that subsequently were infilled with sediment. Note, for example, the 3500 m contour that crosses the escarpment twice near 27°30' N in Figure 4.1. Sometime after the development of the hanging-wall sediment basin, several arc-sized seamounts, part of a large province of extinct volcanoes west of the northern arc ("knoll zone" of *Honza and Tamaki* [1985]), were emplaced at the base of the STL escarpment. These seamounts (and STL) probably pre-date the Quaternary rifting of the arc. Volcanic clasts dredged by *R/V Hakurei Maru* from some of these seamounts were completely encrusted with 2 cm of manganese. Similar seamonts, in the distal backarc to the north, have yielded K/Ar ages of greater than 2 Ma [*Ishihara,* 1988]. Although not conclusive these relationships suggest that the backarc seamount province and the STL are older than the Pleistocene.

The forearc Bonin Trough and the backarc STL are probably related to the same tectonic event in the mid-Tertiary. The present line of arc volcanoes and the effects of arc perpendicular tension overprinted the sedimentary basins and intervening horst blocks that were once bounded by the Bonin Ridge on the East and the STL on the West. The regionally deformed basement platform in the northern Bonin arc stops at the STL (near 29° N at the active arc). The transition from the old platform to the STL-Bonin Trough basin can be see in the Figures 4.1 and 4.3. The northern arc volcanoes are mostly subareal. The southern arc volcanoes are mostly submarine. South of the STL the active arc has built a linear ridge with only minor Quaternary rift deformation of the proximal backarc north of Nishinoshima [*Yamazaki and Murakami,* 1987] and no Eocene-age basement exposures have been found in the vicinity of the arc.

Figure 4.8 Line-drawing interpretations of single-channel seismic reflection profiles across the northern Bonin arc between 29° N and 30°30' N collected by the Geological Survey of Japan (modified after *Honza and Tamaki*, [1985]). The volcanic front is indicated by the horizontal line above each profile. The arrow in the upper profile points to the west boundary fault of the Torishima Rift. The arrow on the lower profile points to the exposure of Eocene basement that separates the juvenile rift basins from the older Bonin Trough (to the east).

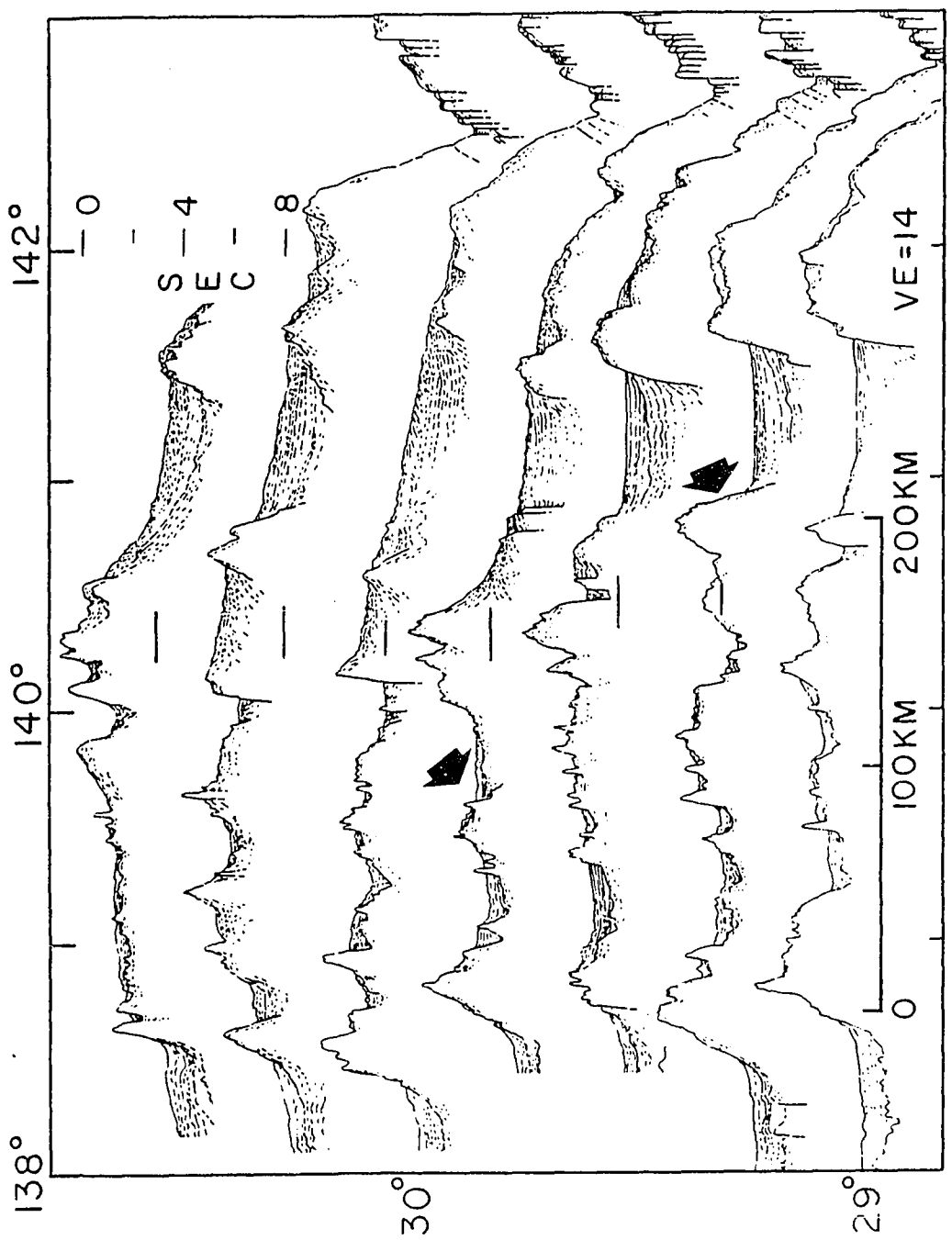
138°
140°
142°
30°
29°
0
100KM
200KM
VE=14
SEC-8
4
0

In the south-central arc the pervasive relict faults intersect the rift system and have left arc proximal exposures of basement. An example is the massive block north of 29° N, between the frontal arc and the Bonin Trough (Figure 4.2). This block is faulted on both sides although primary faulting was to the east as indicated by the regional seismic profiles in Figure 4.8 (2nd from bottom, basement high on west side of the Bonin Trough). The eastern slope forms the margin to the Bonin Trough and the trend of the southern limb matches that of the STL. Sediments sampled from the surface of the block yielded a late Eocene fossil assemblage *(Asterocyclina sp.* and *Biplanispira sp.* [*Ishihara* , 1988]), contemporaneous with the age of sediments on the Bonin Ridge [*Shiraki et al.*, 1980].

Active Faulting

A major problem in interpreting the tectonics in this arc segment is assessing the earlier deformation's control on the fault-block architecture in the active rift system. The distinctions between the two events are cross-cutting relationships and differences in fault trends-the older phase being especially clear in the 29° N area. Active faults were identified by seafloor offsets and by an inward dip of reflectors in the hanging-wall basin. The main faults mapped between 29° and 29°50' N vary in relief and spacing and although some may be reactivated from the earlier event, nearly all cut across the older trends.

Figure 4.4 and the bathymetry perspective in Figure 4.9 shows the relative subsidence and uplift effects of recent high-displacement normal faulting. The semi-isolated depressions in the seafloor are separated by fault-block ridges or volcanic highs. The morphologic depressions in the study area are described below:

(1) A broad basin (40 km in east-west width) in the northwest quarter, defined by the 2500 m contour, was mapped as part of the Torishima Rift by *Tamaki et al.* [1981]. The Torishima Rift has three rift-floor sediment basins. The north and south basins are segments of the arc-parallel zone of subsidence west of a master fault zone at the active

Figure 4.9 Shaded perspective view (looking southwest) of the study area based on 3.5 kHz bathymetry data from the Hawaii Institute of Geophysics and the Geological Survey of Japan. The color changes every 100m. Shading is on the southeast flank of bathymetric highs.

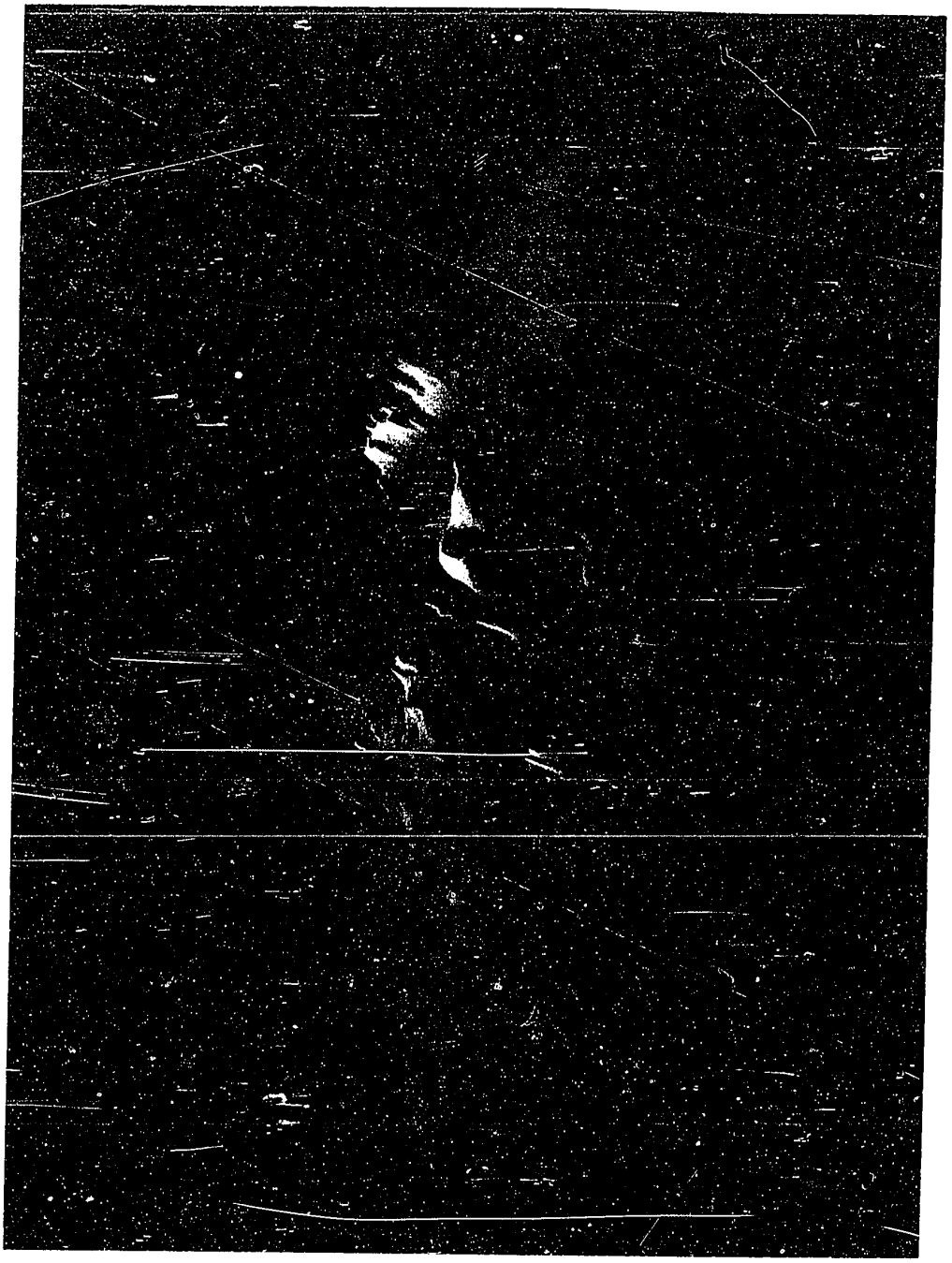

arc margin. The sedimented fault-block basin near the western boundary fault (Figure 4.7A) was refered to as the Torishima Rift West Basin (TRWB) in Chapter III. It is this basin which continue to the south (Figure 4.10). (2) A small deep southwest of Sofu Gan, defined by the 2500 m contour, refered to as the "Sofu Gan Rift" in this chapter. (3) A group of basins surround Tsukuba Volcano, defined by the 3000 m contour, and refered to as the "Tsukuba Rift" in this chapter. (4) A small basin in the forearc north of Tsukuba Volcano defined by the 2600 m contour.

The main tectonic highs in the study area are: (1) A hook-shaped ridge west of Sofu Gan Island, refered to as the "Sofu Gan Ridge". (2) A footwall uplift west of Tsukuba Rift. (3) An east-west basement ridge, separating the axial basins at 29°30' N. (4) An uplift on the arc line between Sofu Gan and Tsukuba volcanoes. (5) A large forearc basement exposure in the southeast corner of the study area, that separates the young rift system from the Bonin Trough (described above).

The structure of the Bonin Rift System was found in Chapter III to be the result of a distribution of arc orthogonal strain between sets of boundary faults. As the displacement diminishes on a boundary fault it can be "picked-up" by one on the other side of the graben. The lateral motion caused by the normal faulting is accounted for by rift-oblique zones of displacement "transfer" [*Gibbs*, 1984]. The main graben boundary faults and the transfer zones, found in the study area, from the latest rifting event are shown in Figure 4.10. There are no observed rift-oblique fault structures in the study area. Rather, the transfer zones are characterized by an interdigitating termination of faults across a bathymetric slope. The growth and decline of the fault scarps, a function of the total slip, can be seen in the serial single-channel seismic lines in Figures 4.5 and 4.7. An exposure of heavily intruded pre-rift basement separates the subsiding basement in the southern Torishima Rift (Chapter III). Near 29°50' N the master fault zone, bounding the east side of the Torishima Rift, is transfered 35 km to the west (Figure 4.10). The transfer zone marks the north side of the Sofu Gan Ridge. The nature of the transfer zone is masked by

Figure 4.10 The tectonic and volcanic features of the central Bonin arc between 29° N and 29° 50' N, showing the rift grabens discussed in the text. The geological interpretation, A to A', is based on the seismic line GSJ 89 (Figure 4.7) and the SeaMARC II imagery (Figure 4.11A, B and Appendix). Dashed fault lines indicate a basement fault beneath faulted or unfaulted sediments. Major faults are those that divide the crust in blocks of greater than 10 km width, can be mapped on the surface or below sediments for over 10 km along strike, and have vertical offsets greater than 100 meters. Where high displacement faults are next to each other (a "zone") the lower fault observed in the data is mapped as the "major fault".

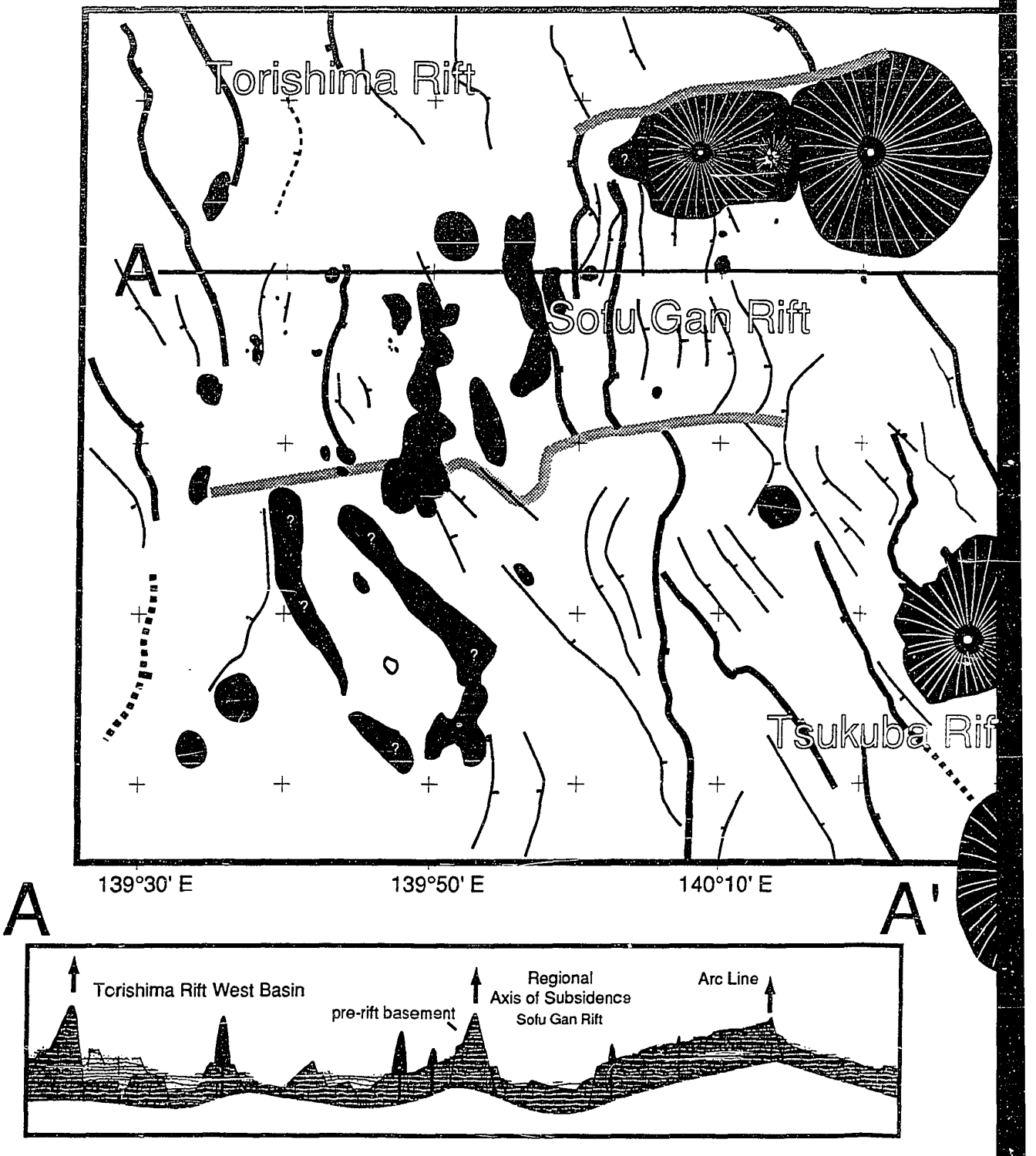
Torishima Rift
A
Sofu Gan Rift
Tsukuba Rif
139°30' E
139°50' E
140°10' E
A
A'
Torishima Rift West Basin
pre-rift basement
Regional
Axis of Subsidence
Sofu Gan Rift
Arc Line

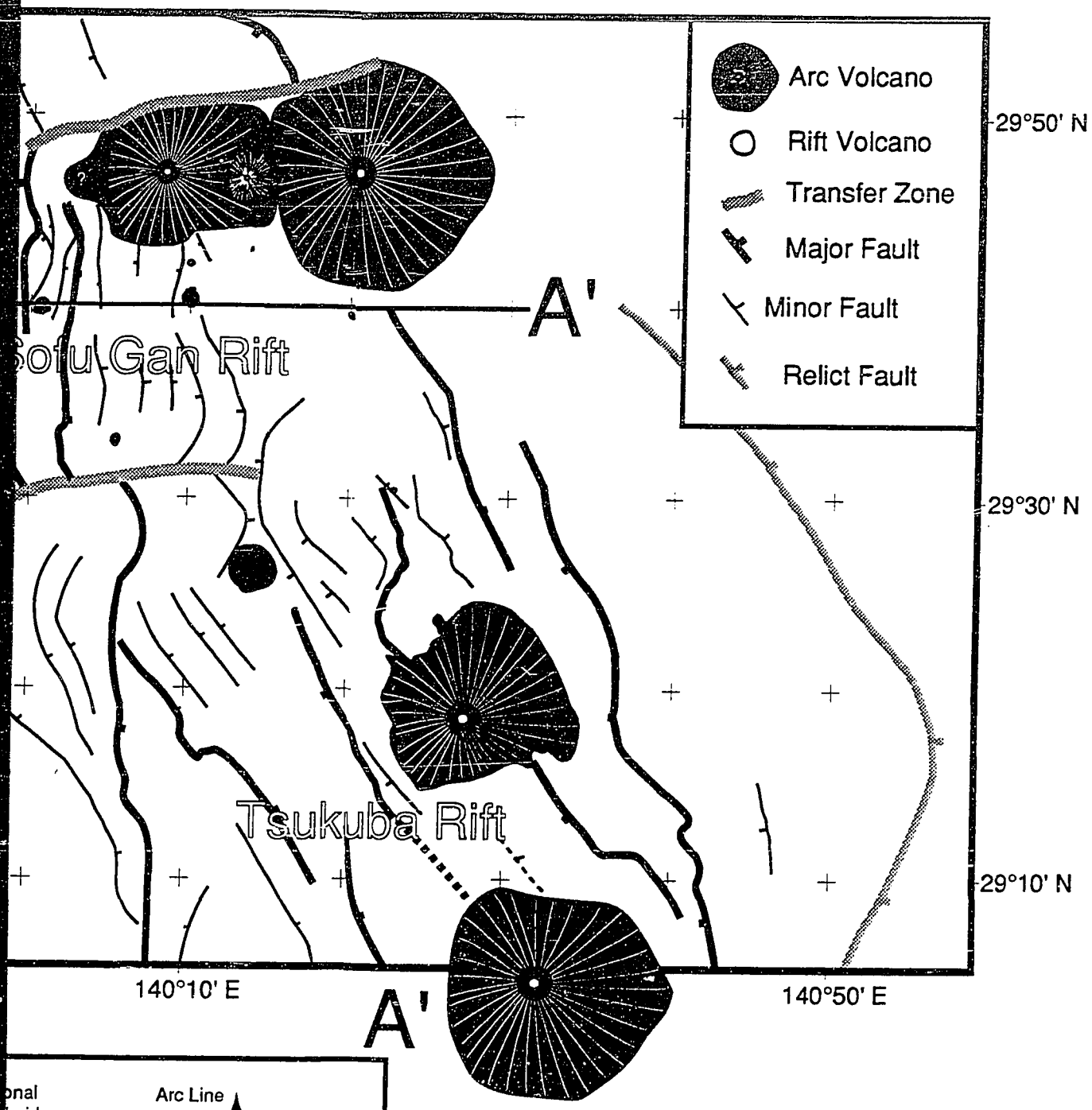
Arc Volcano
Rift Volcano
Transfer Zone
Major Fault
Minor Fault
Relict Fault
29°50' N
29°30' N
29°10' N
140°10' E
140°50' E
A'
A'
Sofu Gan Rift
Tsukuba Rift

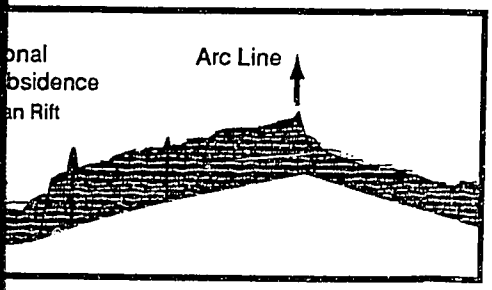
onal
bsidence
an Rift
Arc Line

volcanogenic sediments from the volcanic portions of the ridge, although a faulted basement exposure and the westernmost high of the active arc margin, can be seen in Figure 4.5Y and Figure 4.5AA respectively. Other step-faults developed on the escarpment (Figure 4.5AA) and these allow sediments to pond near the crest of the Sofu Gan Ridge. The eastern half of the ridge was built from volcanic activity, with Sofu Gan as the largest single contributor. A series of smaller cones trail away to the west from the frontal arc volcano.

North of 29°50' N the major rift normal faults dip to the West (Chapter III). In the distant backarc, a low relief fault with an east dip marks the western boundary of the Torishima Rift. From 29°50' N to 29°30' N the fault becomes more dominant (Figure 4.4 and Figure 4.5Z, 4.7A). Between these latitudes, basement subsidence shifts to the west. Within a few km south of 29°30' N fault structures in the TRWB terminate on a distinct east-west trending transfer zone (Figure 4.11). The zone is nearly orthogonal to the axis of rifting and parallel to the direction of opening. The basement ridge (Figure 4.5FF), associated with the transfer zone near the arc line, divides the two axial basins (Sofu Gan and Tsukuba rifts).

The maximum basement subsidence in the TRWB can be found near 29°45' N. Here, the basement lies under approximately 1.0 sec. of syn-rift sediment fill in narrow growth-fault basin (Figure 4.7A, 4.11A). The seafloor exceeds 2600 mbsl in this part of the basin. The syn-rift sediments are offset by the motion of the deep basement faults.

The master faults that control subsidence in the basins can form on the apparent backslope of neighboring fault-block. Tilting of the western edge of the Sofu Gan Ridge is evident in Figure 4.5AA. The narrow tilt-block ridge trends north-south, giving the Sofu Gan Ridge a characteristic hooked shape (Figure 4.4). At the latitude of Figure 4.5BB the ridge is found to be down-faulted on both the east and west sides. The fault on the west side bounds the TRWB, the fault of the east side bounds the Sofu Gan Rift. The ridge terminates abruptly to the south near 29°40' N and the controlling motion for this

margin of the Sofu Gan Rift is passed to a similar structure a few km to the west (Figure 4.10). Whereas the Sofu Gan Rift is bounded on the west by a en-echelon fault zone with a footwall of >500 m relief, it is bounded on the east by a low-relief fault zone, formed in the lower backslope of the arc margin uplift that tilts away from the forearc (Figure 4.7A-B).

Despite the proximity to the Sofu Gan volcano and the enclosed shape of the basin, the Sofu Gan Rift contains only a thin sediment layer. Only the edges of the Sofu Gan Rift were mapped with the SeaMARC II system. The central parts of the basin were mapped with close-spaced 3.5 kHz profiles from the Geological Survey of Japan. The basin is a circular deep surrounded by tectonic and volcanic highs. Sedimented troughs, controlled by faults, along the north margin channel debris off the Sofu Gan Ridge (Figure 4.11).

The 10 km wide basement ridge between the two axial basins (Figure 4.4) is broken into large fault-blocks (Figure 4.5FF, 4.7). The easternmost block occurs on the arc line between Sofu Gan and Tsukuba volcanoes (Figure 4.4, 4.9) similar to the position of the rift-shoulder uplifts on the active arc margin of Sumisu and Torishima rifts (Chapter III). Because the block has a equidimensional trapazoid shape, and is positioned on the arc line, it could be easily mistaken for a volcanic edifice (note that the feature shows on the arc profile as the first high south of Sofu Gan in Figure 4.3). The block was initially downfaulted on the forearc side (Figure 4.5FF, 4.5GG, 4.7B). The subsidence and sedimentation rates on the forearc side of the block were high. Reflectors in the hanging-wall basin (in the forearc) slope toward the fault, indicative of a growth-fault basin. A maximum sediment thickness of 0.8 sec. was found north of Tsukuba Volcano (Figure 4.11). This may be attributed to preferential deposition from the nearby source. The east boundary fault of the Sofu Gan and Tsukuba rifts occurs in the lower

Figure 4.11 The SeaMARC II imagery and local structure of **(A)** Torishima Rift West Basin and **(B)** Sofu Gan Rift and **(C)** piedmont step-faults on the southern flank of the arc-line footwall uplift (see Figure 4.6 for location). The interpretations are based on seismic reflection (single channel and 3.5 kHz) profiles and SeaMARC II sidescan imagery data.

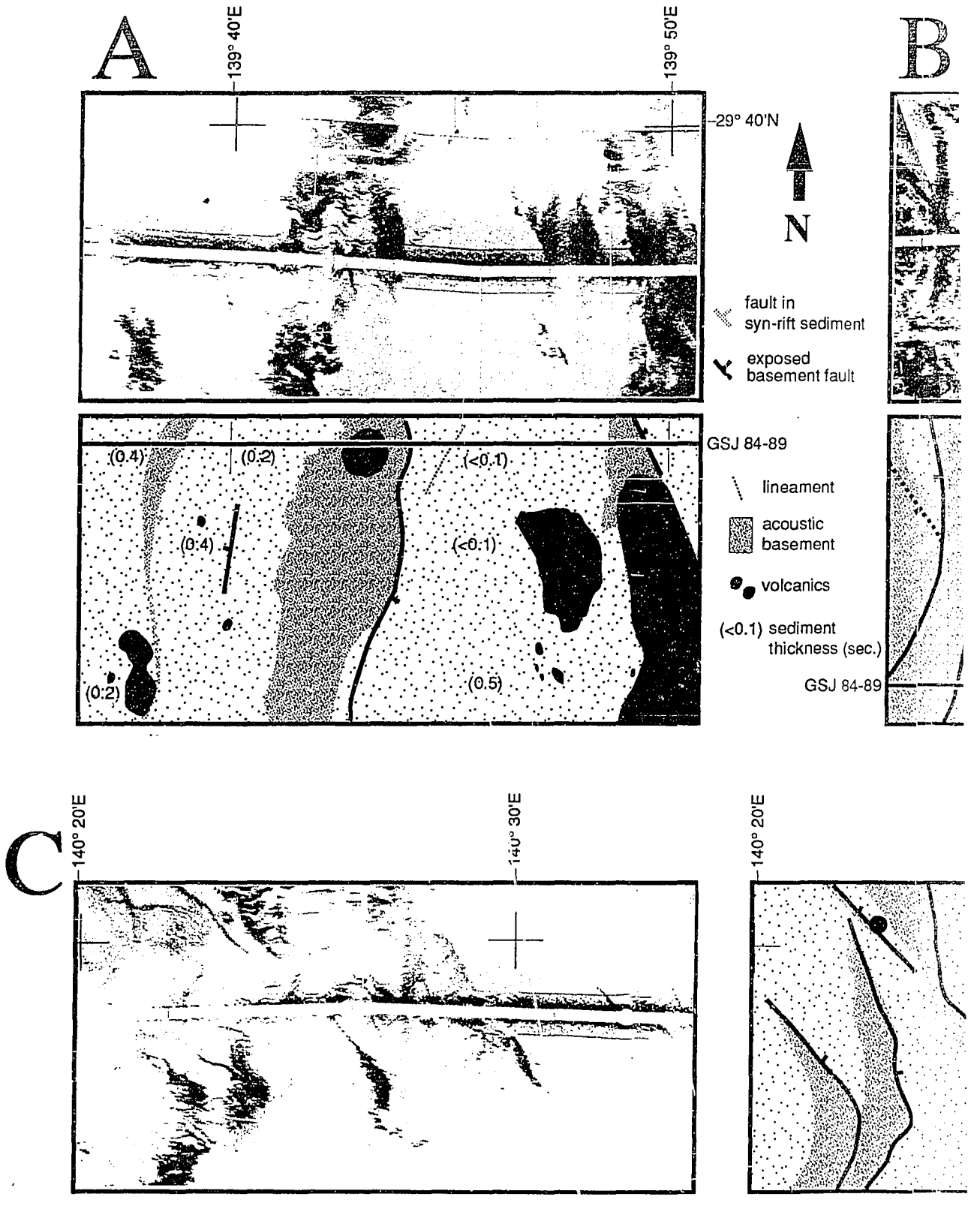
A
139° 40'E
139° 50'E
29° 40'N
N
fault in
syn-rift sediment
exposed
basement fault
GSJ 84-89
(0.4)
(0.2)
(<0.1)
(0.4)
(<0.1)
(0.2)
(0.5)
lineament
acoustic
basement
volcanics
(<0.1) sediment
thickness (sec.)
GSJ 84-89
B
C
140° 20'E
140° 30'E
140° 20'E

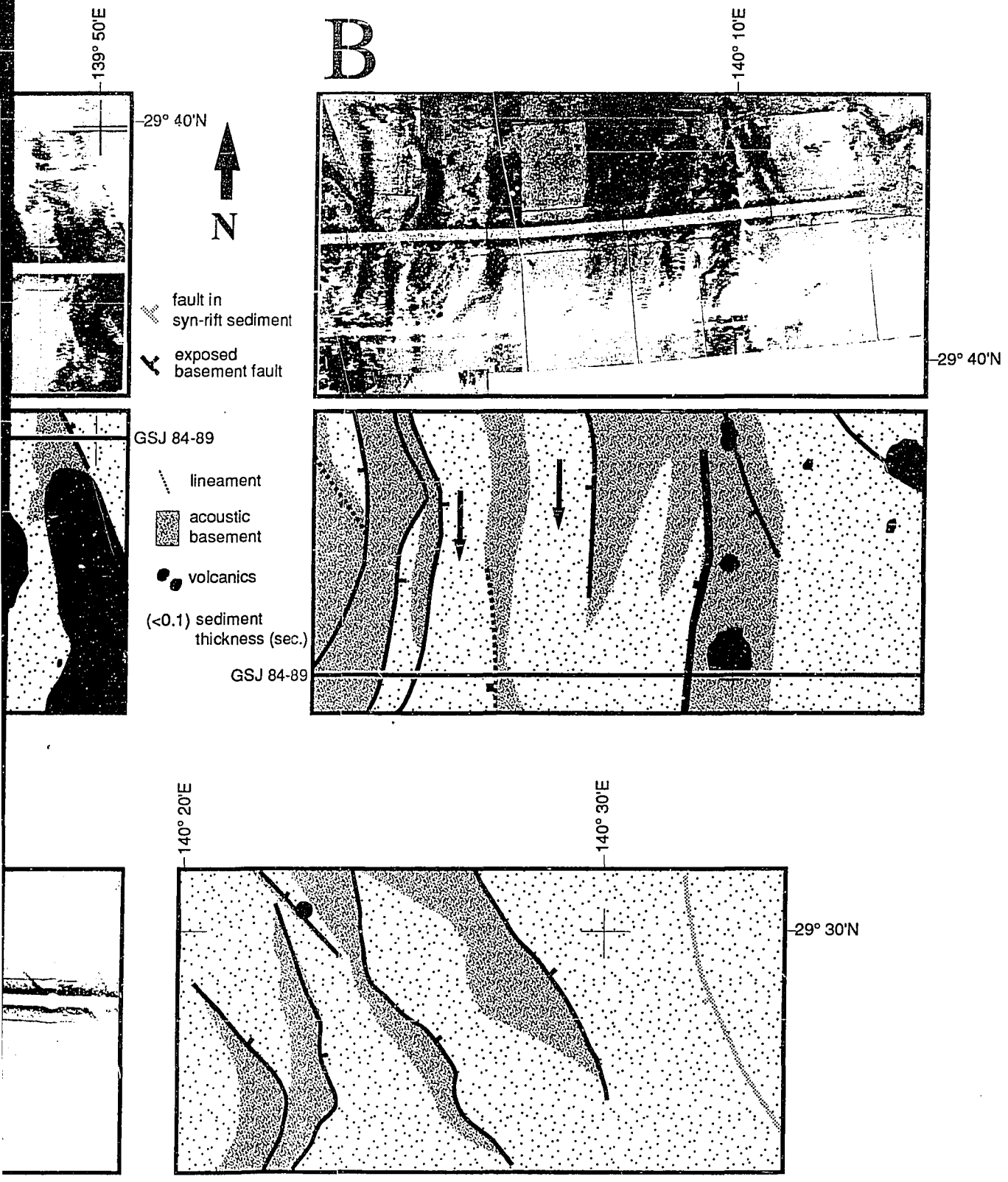
B
139° 50'E
140° 10'E
29° 40'N
29° 40'N
N
fault in
syn-rift sediment
exposed
basement fault
GSJ 84-89
lineament
acoustic
basement
volcanics
(<0.1) sediment
thickness (sec.)
GSJ 84-89
140° 20'E
140° 30'E
29° 30'N

backslope of this crustal block (Figure 4.7B). As we move southward along the active arc margin of the Sofu Gan Rift the block emerges from the forearc. This is matched by a growth in the slip on the west-dipping boundary fault zone to the axial basins.

Faulting of the forearc side of the tectonic uplift left an anastomosing pattern of closely-spaced "secondary" faults (Figure 4.11C). The southern flank of the basement block has sunk underneath Tsukuba Volcano. The thick sediment wedge fills the gap between the two highs. The step faults are en echelon in this area. Erosional debris channels may be present on the escarpments although point reflectors were elongated parallel to the instrument tow-direction (Figure 4.11C).

The block seamount on the active arc is key to understanding the development of the island arc rift system. For here, active normal faulting was originally synthetic to the west boundary faults of the axial basins. Based on the thickness of syn-rift sediment in the narrow forearc basin, the forearc faulting began before the axial basins start to collect sediments (assuming a similar rate). As the system matured, secondary faults developed on the lower backslope of a tilt-block opposing the master fault zone. A similar history of basin development was described for the Torishima Rift except in the opposite direction. It's interesting to note the forearc tilt-block is coincident with the basement ridge across the proto-remnant margin. It's possible that the fault zone on the east side of the high is absorbing most of the strain at this latitude. The original basement surface behind it (to the west) is "shadowed" by motion of the forearc fault. There is no need for this band of crust to fail except where broken by faults propagating from the south. The basement ridge is broken into several highs but only where large faults have come in from the south (Figure 4.10).

Just south of the 29° 30' N transfer zone the west-boundary fault becomes the dominant master fault to the Tsukuba Rift (Figure 4.5II). An east-boundary fault zone may lie due west of Tsukuba Volcano (Figure 4.12), where basement ridges crop out on the flank of the volcano. But these features are down strike from the forearc block's ridge

and seafloor offsets confirm that primary faulting is of the same polarity (to the west-see interpretation Figure 4.12). Further south and 10 km to the east, an emerging fault zone cuts the west side the basement exposure at the edge of the Bonin Trough (shown in Figure 4.8). At the 29° 30' N there are no west-dipping faults in the basement of this forearc ridge, although there are some slump-like faults in the overlying sediments (Figure 4.7B). Near 29° 20' N the west slope of the ridge steepens. At 29° N the block is clearly faulted, as two basement offsets can be identified in the seismic data (Figure 4.5JJ). Between these latitudes the Tsukuba Rift opens into a full symmetric graben that straddles the arc, with boundary faults on both margins (Figure 4.10).

In the Bonin Rift System rift-flanking uplifts achieve a maximum relief near the intersection of two fault sets (Chapter III). The west-boundary fault of the Tsukuba Rift begins at 29°30' N in the north and can be mapped with few interuptions until it intersects the STL in the south, at 28°50' N. The angle of the backslope and amount of relief on the exposed fault decreases to the south, matching the growth of the east boundary fault zone (Figure 4.5HH-JJ). Further south, the footwall to the west-boundary fault zone shoals again (in the absence of a distinct east boundary fault zone) to 1000 mbsl at the intersection with the STL (Figure 4.2).

Minor (low displacement, spaced 1-2 km) faults are common in exposures of pre-rift basement. On tectonic slopes, such as the footwall uplift described above or the flank uplift on the southwest margin of Sumisu Rift (Chapter III), these faults resemble gravity slides. This mode of faulting can also be found on margins with low slopes. The northern Tsukuba Rift (Figure 4.4) is 3600 m deep with less than 0.25 sec of sediment fill. Tectonic "slivers" on the basin's margin were well-imaged by the SeaMARC II system (Figure 4.10), as individual scarps cause a specular reflection and image with dark tones (Appendix). These structures indicate that rift-related stresses can lead to fine breaks in the arc crust. The faults may be similar to the secondary antithetic faults opposite the master fault in the northern basin of Sumisu Rift (Chapter III)

4.3 Volcanism and Sedimentation

Arc volcanism

The upper tip of the Sofu Gan strata-volcano rises to 99 m above sea level near 29°48' N. Its submarine pyroclastic apron extends for a radius of over 10 km around the island (Figures 4.4, 4.10). The sedimented slopes are incised by thin radiating debris flow channels similar to those found on the stratified arc volcanoes to the north (Chapter III) and in the Mariana arc [*Hussong and Fryer,* 1983]. Sofu Gan is the largest volcano on the east end of the 60 km long volcano-tectonic ridge, discussed in the previous section. Arc-type volcanism appears to continue further to the west of Sofu Gan along the segmented ridge opposite a narrow saddle near 140°15' E at the 1500 m contour. The breaks in the ridge can be observed in Figure 4.5AA and in the perspective view shown in Figure 4.9. The ridge shoals to 400 mbsl at approximately 16 km west of Sofu Gan Island and then it tapers to the west. The western segment of the ridge is enclosed by the 1500 m contour and consists of four bathymetric highs three of which are shallower than 1000 mbsl. The western-most high is slightly shallower than 1100 mbsl and is separated from the others by a 2 km wide, 200 m deep trough. The southern slope on the ridge has a darker reflectivity (see SeaMARC II imagery mosaic, Appendix), either from specular reflections or because of bedrock exposures, in contrast to the northern slope which has a lower reflectivity with essentially the same angle of slope implying that the north slope is mantled by sediment. Monogenetic volcanoes in other segments of the Bonin backarc typically have high reflectivity on the SeaMARC II imagery (Chapter II), however the bathymetric highs on the crest of Sofu Gan Ridge are noted by an absence of distinct reflectivity (Appendix), perhaps indicating that the features are blanketed by arc-derived tuffaceous sediments.

The position of Tsukuba Volcano, 50 km south of Sofu Gan at 29°19' N can be related to basement faulting (Figure 4.12). With a summit depth of less than 800 m the slopes of the volcano have had several flank eruptions, some of which have supplied flows. Tsukuba Volcano actually sits in the rift system. The volcano is emplaced over the hanging-wall block of the east boundary fault zone. The lower basement block of the east fault zone in Figure 4.5JJ emerges to the north (Figure 4.4). A basement protrusion is apparent on the lower east-flank of the volcano (Figure 4.5II). The SeaMARC II imagery shows debris flow paths diverted southward by the rise of the basement ridge (Figure 4.12). Figure 4.5HH shows the volcano resting on the backslope of a footwall block. In the south the block subsided well below the level of sediment fill (Figure 4.5JJ).

Intra-rift volcanism

Monogenetic volcanism is common during the early stages of backarc basin formation. In Sumisu and Torishima rifts over 600 volcanoes have been identified (Chapter III). Nearly all of the individual volcanoes are less than 3 km in diameter and have under 600 m relief. Dredge and dive samples from an en echelon ridge of pillows and talus [*Fryer et al.*, 1990] in the axis of Sumisu Rift at 31° N yielded vesiculated basalts to rhyolites with a petrogenesis typical of back arc basin basalts. The small volcanic vents in the Sumisu and Torishima rifts rest on basement exposures near the rift-oblique transfer zones. On a local scale the individual vents are aligned sub-parallel to the axis of rifting. This was thought to indicate that magma ascends along lower crust weaknesses that strike oblique to the arc. When passing into the upper crust, the magma is reoriented along faults produced by arc orthogonal extension (Chapter III). Perhaps a more important relationship though, is the intimacy between "intra-rift" volcanoes and the basement. While there are numerous lava mounds in the axial basins nearly all sit on

Figure 4.12 (A) SeaMARC II imagery and (B) geological interpretation of the conical "Tsukuba Volcano". The radiating lineaments are debris channels. The eastern flank is heavily faulted by slip on an underlying basement fault that crops out south of the volcano. Indications of east boundary of Tsukuba Rift were found further to the west on the lower slope. If continued on strike to north the fault under the east flank would need to reverse polarity under the center of the vent. SeaMARC II imagery (Figure 4.4) show lineaments bend into the center of the cone from this fault as though the volcano has been emplaced over an offset in the east-boundary fault.

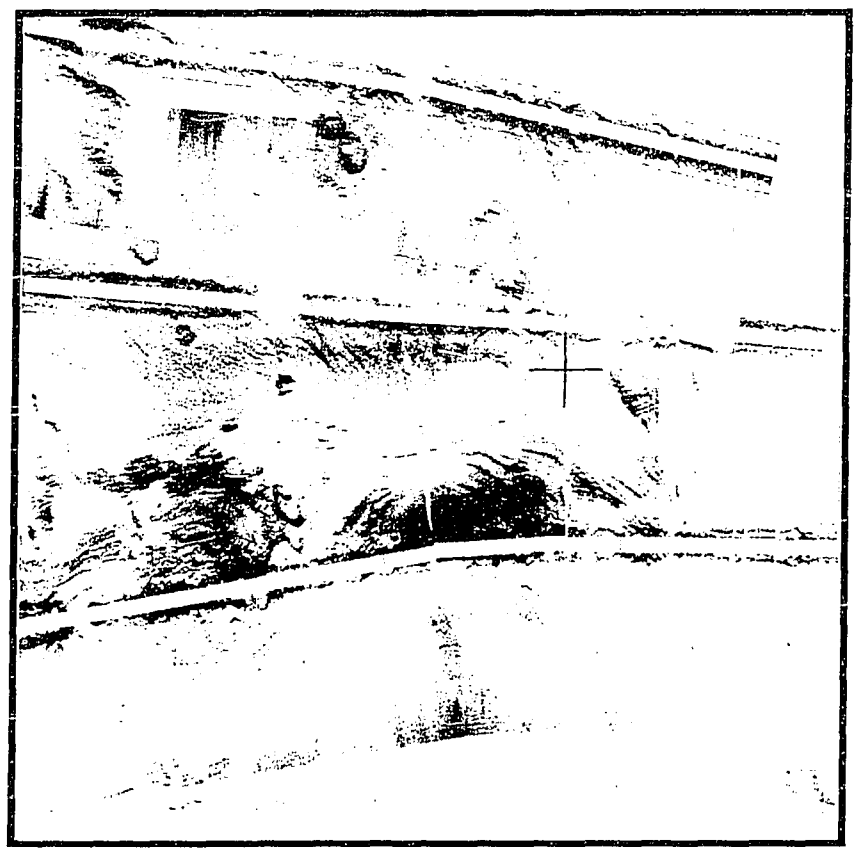

N

0 5 10

kilometers

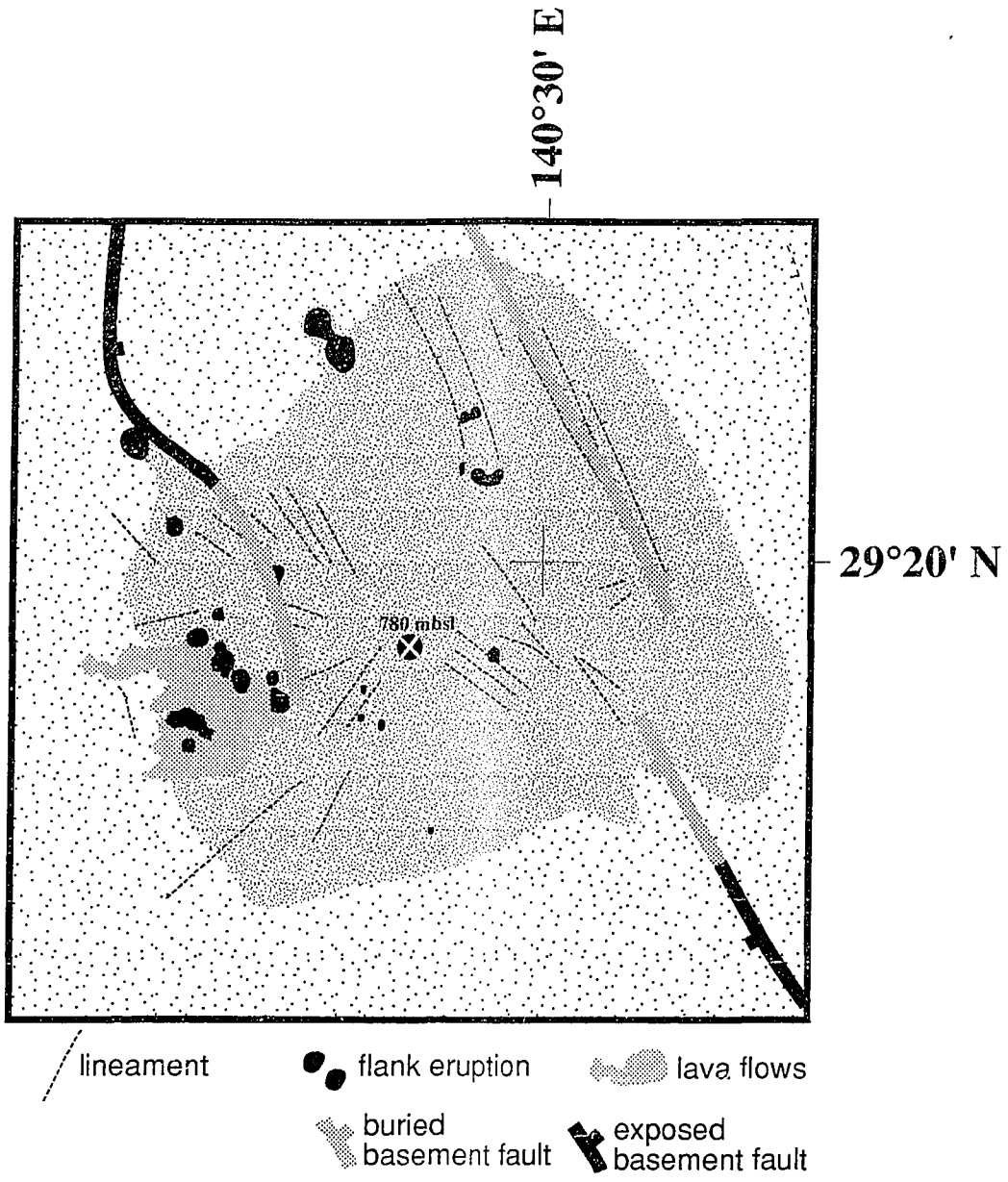
140°30' E
29°20' N
780 mbsl
lineament
flank eruption
lava flows
buried
basement fault
exposed
basement fault

basement or on shallow basement. There were only a few isolated cases, typically near faults (e.g. Shadow Mountain in southern Sumisu Rift [*Taylor et al.*, 1990]), where magma erupted through the thick sediments.

In the study area intra-rift volcanism was found scattered over the shallow basement on the distant proto-remnant margin, similar to the volcanics on the basement highs on the proto-remnant margin of Torishima Rift (Figure 4.10). The numerous vents in TRWB image with dark tones in the SeaMARC II data (Appendix). Closely-spaced intrusive bodies are evident on the corresponding seismic profiles across the TRWB (Figure 4.5, 4.7). In the southern TRWB voluminous outpourings of flows along fissures have built 20 km long sinuous ridges. The chains of volcanic vents are distinguishable from the narrow fault-block ridges that occur in the northern basin, because they are highly reflective on the SeaMARC II imagery and have a symmetric hyperbola on 3.5 kHz profiles with no change in the level of the seafloor on either side or signs of displacement on the seismic reflection profiles (Figure 4.10).

The concentration of volcanism away from, or at an oblique angle to, the regional structural axis has ramifications for the development of the backarc. The occurrences of axial volcanism have been considered as the nascent stage of seafloor spreading along the rift axis [*Hochstaedter et al.*, 1990; *Murakami*, 1988]. In this chapter and in Chapter III the structural axis is assumed to be the future axis of spreading. But will organized spreading evolve along the structural axis or along independent rift-oblique (or off-axis) volcanic segments? If the young rifts mature someday into a backarc basin then the organized spreading center might evolve along the volcanic axis away from, and at an oblique angle to, the structural axis. Some mature backarc basins that are actively opening, like the Lau Basin, are characterized by diffuse magnetic anomalies [*Lawver and Hawkins*, 1978] and short offset spreading centers [*Parson et al.*, 1990]. Perhaps this pattern of speading can be explained if the initial rise of the aesthenosphere was not continuous along the structural axis.

Sedimentation

Recent sedimentation was studied based on it's acoustic response to 3.5 kHz sound. The echo-character profiles in the Bonin arc fall into two catagories. Those without sub-bottom reflectors and those with sub-bottom reflectors. The former was found to correspond with the slopes of arc volcanoes and areas of pre-rift basement exposure (acoustic bedrock). The diffuse echo-character type is thought to be returned from coarse-grained volcanogenic sediments or compacted sediments (Chapter II). The latter was found on the surface of the sediment fill in the main depocenters. The multiple sub-bottom echo-character type is related to the episodic deposition of turbidites (Chapter II). The seafloor sedimentation in the Sofu Gan area is analogous to the depositional systems in Sumisu and Torishima rifts. One important difference though is that seafloor sediments throughout the TRWB have numerous (ten to fifteen) sub-bottom reflectors. The frequency of the reflectors may be an indicator of the importance of pelagic and distal turbidite deposition in the basin. The isolated TRWB is the farthest rift basin from the active arc volcanoes. The continuity of the echo-character (from the NNE transfer zone in the central rift to the east-west transfer zone at the southern margin) indicates the depositional environment is consistent across the basin (much like the transparent layer in the Sumisu Rift). Some elevated point-reflectors on the 3.5 kHz data (matching with volcanoes and fault block ridges inferred from the SeaMARC II data) have thin sub-bottom reflectors. This is the only place in the central rift system where acoustic sediments were found on the surface of intra-rift volcanoes. Either the volcanism in this area is older than other areas or the erosional effects of bottom currents on the sediments deposited on elevated features is less than in the inner rift basins.

In the Bonin rift basins sediments migrate downslope to the growing depocenters unless the flow is restricted by tectonic or volcanic ridges (Chapter II and III). It is possible to estimate the relative rates of sedimentation and subsidence based on the profile of

the basin and the nature of seismic reflectors. If the sedimentation rate in an active basin exceeds the subsidence rate then the basin can maintain a flat seafloor profile and deep refectors will be inclined toward the controlling fault. If the subsidence rate is greater than the sedimentation rate then the seafloor will slope into the fault (the fault will have a "moat"). The south basin of the Sumisu Rift is an example of an area where the sedimentation rates are high and bottom currents are active. The basin keeps a flat profile as perturbations in the bottom are infilled by fresh sediments (Chapter II). Some non-faulted (by boundary faults) margins to the axial basins in the study area have rates of sedimentation lower than the subsidence rate. The northern margins of Sofu Gan Rift (Figure 4.7A, 4.11) and the northwestern margin of Tsukuba Rift have profiles indicative of low sedimentation rates. In both cases, close-spaced normal faults have broken into an exposed basement ridge which slopes toward a depocenter. In the case of Tsukuba Rift we can see the local fracturing of the basement on the SeaMARC II imagery. Bottom currents moving downslope may transport fine sediments downslope, towards the south, eventually to a settling point in the large depocenter around Axial Volcano, where sediments from the nearby arc strata-volcanoes (Tsukuba and Axial, both of which sit in the graben) completely cover the rift structures (Figure 4.7C).

The fast subsiding basins near arc volcanoes should have thick sediment accumulations. In southern Sumisu Rift, near arc volcanoes, the pre-rift basement lies at approximately 3400 mbsl with 1200 m of syn-rift sediment fill [*Leg 126 Scientific Drilling Party*, 1989]. In the Sofu Gan and Tsukuba rifts, also near the arc, basement is significantly deeper, with a sediment cover less than 0.20 sec. In places, such as the northwest Tsukuba Rift, basement is unsedimented even though the arc is nearby. The contrast in the thicknesses of accumulated syn-rift sediments along the rift system may be a function of age (Sumisu Rift is older) or bottom currents (debris from Tsukuba Volcano migrates

east). It might be related to the number of volcanoes nearby. The south basin of Sumisu Rift has direct access to two arc volcanoes (Torishima and Kotori, Chapter III). The northern axial basin of Tsukuba Rift has one volcano (Tsukuba).

Perhaps its not the physical presence of arc volcanoes that makes the difference but the amount of volcaniclastic debris generated by eruptions. Almost all arc volcanoes north of Sofu Gan are shallower than 100 mbsl (Figure 4.3). The northern rift basins are characterized by thick accumulations of sediment. At the latitude of Hachijo Rift, graben structures are filled with sediments. The shallow volcanoes are capable of supplying large amounts of debris to the neighboring basins as they tend to have more explosive, ash producing eruptions.

4.4 Conclusions

The structural elements in the Bonin arc between 29° and 29°50' N are the result of two tectonic events overprinted by Quaternary arc volcanism. Sometime in the Oligocene or Miocene (?), perhaps during the southward propagation of the Shikoku Basin [*Chamot-Rooke,* 1987], the south-central Bonin arc underwent extension. In it's wake the deformation left a network of faults across the Bonin arc platform.

A new phase of arc volcanism and extension cut through this older deformation zone. Quaternary crustal extension of the central Bonin arc platform produced multiple sets of homothetic normal faults that are adjusted along strike by transfer zones. South of Sofu Gan Island, several basement deeps are developing in the proximal backarc at the lower backslope of a crustal wedge. The lack of sediment in the basins, despite the nearby arc volcanism and eroded uplifts, implies that these basins are younger than the axial basins of Sumisu and Torishima rifts to the north. The latest phase of rifting in the Bonin Arc is thought to have begun further to the north, at the mid-section of the arc.

Why rifting begins near the volcanic line and spreading begins in the backarc is a key problem in plate tectonics. The following points are important to keep in mind when considering this problem.

(1) Arc volcanoes appear to control the structural framework of the incipient rift system. The rapid emplacement of large volumes of lava and ash can load the fractured crust and reduce footwall uplift (Chapter III). The large rift basins in the central Bonins lie between the arc volcanoes. If the strain normal to the central arc is uniform then the crust near arc volcanoes such as Sumisujima must somehow be accommodating the strain observed in the intervening rift segments. The nature of the crust under the arc volcanoes is unknown. In areas of eroded paleo-arcs, such as the Sierra Nevada Mountains, the crust below the volcanoes was filled with large batholiths. It is possible that there is non-brittle accommodation of strain beneath the volcanoes and this keeps the surface of the crust from failing.

(2) There can be large uplifts of the footwall block of the rift boundary faults. The uplifts in the central Bonins are within 700 meters of sea level (for example between Sumisujima and Torishima, Chapter III). For example, the recent rifting of the Coriolis Trough has led to a footwall uplift that is well above sea level. The island of Futuna, Vanuatu is capped with Pleistocene reef [*Carney and Macfarlane*, 1979] that may have formed as the footwall crust pushed through the photic zone.

The uplifts are significant in that they explain the nature of the remnant arc. Some of the bathymetric features may be tectonic features, remnants of the old margin of the rift system rather than arc volcanism. Active arc are generally within a 180 to 200 km distance from their trench [*Taylor and Karner*, 1983]). As the rift system matures to full-fledged spreading and the generation of new crust) the footwall uplifts on the proto-remnant margin migrate away from the arc-trench relationship.

In the Sumisu and Torishima rifts flexural uplifts were found similar to those along the margin of continental rifts. The shoulder uplift phenomena has been used historically to support models that attribute rifting to an aesthenosphere thermal anomaly or rift induced secondary convection. South of the Sofu Gan Ridge uplift is observed on the west shoulder of Tsukuba Rift and on the active arc margin. The tectonic block on the active arc margin, exposed at 29°30'N, does not flank the axial rifts as would be expected. Instead, uplift faces to the east away from the axial basins toward an area with no rift-related volcanism. Because of this and the lack of volcanism in the axial areas, compared with the TRWB, it is doubtful that fault block rotations were caused by a thermal anomaly. The uplift may be explained however by an isostatic adjustment due to the removal of mass on its hanging-wall [*Karner and Weissel,* 1989]. The block faulting and volcanism in the south-central Bonin arc suggests that the rifting is driven by a mechanical force within the underlying lithosphere and that the underlying rise of the aesthenosphere is secondary. If this is correct then models that attribute the formation of backarc basins to a subduction-induced thermal anomaly will need to be reevaluated.

(3) Island-arc rifts are charaterized by bimodal extension-related (rather than arc-related) volcanism (Chapter III). There are over 1000 small volcanoes (<3 km in diameter) in the central Bonin Rift System. The eruption sites are concentrated near the transfer zones of the rift segments. But a more important point is that the volcanoes are most commonly found on exposures of the pre-rift basement. Of all the rift-related volcanoes mapped in this study only a handful lie in the axial sedimentary basins. The occurence of basalts on basement at the base of the sediment pile in Sumisu Rift [*Leg 126 Scientific Drilling Party*, 1989], and the early Quaternary age-dates determined by the Geological Survey of Japan (Chapter III) suggest that there were voluminous volcanic eruptions during the initial break-up of the arc crust. There may still be active rift-related volcanism in the grabens today (based on bottom camera observations [*Smith et al.*, 1990], the freshness of basalts [*Fryer et al.*, 1990], and historic eruptions located by *Norris and*

Johnson [1967]). Perhaps concentrated volcanism on the sedimented floors of the grabens was not observed because the ascending magma, intruded into the base of the sediment pile, spreads laterally as sills. Only where the rising magma has a clear path through the fractured sediment (e.g. Shadow Mountain in the South Basin of Sumisu Rift) will it erupt on the seafloor.

(4) As with the rifting of continents, the rifting of arcs is a lithosphere phenomena. The deformation observed on the seafloor is the effect of stresses with the lithosphere. During the "rifting of arcs" it's not the arc that rifts but the underlying lithosphere, or in the case of the central Bonin arc, the old-arc crust. Nearby normal-faulting and transfer zones can affect the morphology and location (e.g. Tsukuba Volcano) of the arc volcanoes and it may affect the locations of small satellite eruption sites (e.g. Sofu Gan Ridge). The juvenile master fault zones can begin in both the forearc and backarc crust. The regional subsidence, however, is focussed in the proximal backarc, often on faults that appear later than those from the initial break-up.

4.5 References

Brown, G., F. Murakami, A. Nishimura, B. Taylor and M. Yuasa, Seafloor Geological Map, Sumisu and Torishima Rifts, Izu-Ogasawara Island Arc, 1:200,000, *Marine Geology Map Series, 31*, Geological Survey of Japan, Tsukuba, 1988.

Carney, J.N and A. Macfarlane, Geology of Tanna, Aneityum, Futuna and Aniwa, *New Hebrides Govern. Geol. Surv. Reg. Rept.*, 71p, 1979.

Fryer, P., B. Taylor, C.H. Langmuir and A.G. Hochstaedter, Petrology and geochemistry of lavas from the Sumisu and Torishima backarc rifts, *Earth Planet. Sci. Lett., 100*, 161-178, 1990.

Gibbs, A.D., Structural evolution of extensional basin margins, *J.Geol. Soc.London, 141*, 609-620, 1984.

Hochstaedter, A.G., J.B. Gill, and J.D. Morris, Volcanism in the Sumisu Rift II. Subduction and non-subduction related components, *Earth Planet. Sci. Lett., 100*, 195-209, 1990.

Honza, E., and K. Tamaki, Bonin Arc. in *The Ocean Basins and Margins, Vol. 7, The Pacific Ocean*, edited by Nairn, A.E.M. and S. Uyeda, Plenum Press, New York, 459-502, 1985.

Hotta, H., A crustal section across the arc Izu-Ogasawara and trench, *Phys. Earth, 18*, 125-141, 1970.

Hussong , D. and P. Fryer, Back-arc seamounts and the SeaMARC II seafloor mapping system, *EOS Tran. AGU, 45*, 627-632, 1983.

Ishihara, T., Gravimetric determination of densities of seamounts along the Bonin Arc, in *Seamounts, Islands, and Atolls*, edited by Keating, B., P. Fryer, R. Batiza and G. Boehlert, AGU Geophysical Monograph, 43, Washington D.C., 97-113, 1987.

Japanese DELP Research Group on Back-arc Basins, Report on DELP 1987 cruises in the Ogasawara area, Parts 1-VII, *Bull. Earthq. Res. Inst., Univ. Tokyo, 64*, 119-254, 1989.

Karig, D.E, and G.F. Moore, Tectonic complexities in the Bonin Arc system, *Tectonophysics, 27,* 97-118, 1975.

Karig, D.E. and G.F. Moore, Tectonically controlled sedimentation in marginal basins, *Earth Planet. Sci. Lett., 26,* 233-238, 1975.

Kato, H., R. Hiro, H. Kinoshita and S. Nagumo, Crustal structure of the Bonin Trough, *Tectonophysics, 181,* 345-356, 1990.

Lawver, L.A. and J.A. Hawkins, Diffuse magnetic anomalies in marginal basins: Their possible tectonic and petrologic significance, *Tectonophysics, 45,* 323-339, 1978.

Leg 126 Scientific Drilling Party, Arc volcanism and rifting, *Nature, 342,* 36-38, 1989.

Murakami, F., Structural framework of the Sumisu Rift, Izu-Ogasawara arc, *Bull. Geol. Surv. of Japan, 39,* 1-21, 1988.

Norris, R..A., and R.H. Johnson, Submarine volcanic eruptions recently located in the Pacific by SOFAR hydrophones, *J. Geophy. Res., 74,* 650-664, 1969.

Parson, L.M., J. Pearce, B. Murton, R. Hodkinson and RRS Charles Darwin Scientific Party, Role of ridge jumps and ridge propagation in the tectonic evolution of the Lau back-arc basin, southwest Pacific, *Geology, 18,* 470-473, 1990.

Shiraki, K., N. Kuroda, H. Urano and S. Maruyama, Clinoenstatite in boninites from the Bonin Islands, Japan, *Nature, 285,* 31-32, 1980.

Smith, J.R., B. Taylor, A. Malahoff and L. Petersen, Submarine volcanism in the Sumisu Rift, Izu-Bonin arc, *Earth Planet. Sci. Lett., 100*, 148-160, 1990.

Taylor, B., G. Brown, P. Fryer, J.B. Gill, A.G. Hochstaedter, H. Hotta, C.H. Langmuir, M. Leinen, A. Nishimura and T. Urabe, ALVIN-Seabeam studies of the Sumisu Rift, Izu-Bonin arc, *Earth Planet. Sci. Lett., 100*, 127-147, 1990.

Usui, A., T. Mellir, M. Nohara, M. Yuasa, Structural stability of marine 10Å manganates from the Ogasawara (Bonin) arc: Implications for low-temperature hydrothermal activity, *Marine Geology, 86,* 41-56, 1989.

Yamazaki, T. and F. Murakami, Heat flow and structure in the back-arc area of the Izu-Ogasawara Arc. *Autumn Meeting of the Seismological Society of Japan,* p. 204, 1987.

Yuasa, M., Sofu Gan Tectonic Line, a new tectonic boundary separating northern and southern parts of the Ogasawara (Bonin) arc, northwest Pacific, in *Formation of Active Ocean Margins*, edited by N. Nasu et al., Terra Scientific Pub. Co., Tokyo, 483-496, 1985.

Appendix A

海 洋 地 質 図 31
MARINE GEOLOGY MAP SERIES 31

Vb

火山　溶岩；玄武岩質～流紋デイサイト質．新鮮なものも変質したものも含まれる．
Volcanoes　Extrusive lavas; dredged sites yield basaltic to rhyodacitic compositions, fresh and a

Br

岩盤　SeaMARC II 画像，3.5kHz 反射記録及び反射法地震探査記録に基づく露岩．一部は数mの厚さの
われている．正断層の下盤，隆起斜面あるいはマス・ウェイスティングや侵食によって堆積物が除去され
出している．
Bedrock　Exposures of rock based on Sea MARC II imagery, 3.5-kHz echograms and seismic
records. Some areas may be covered with several meters of sediment. Bedrock exposures oc
footwall block of normal faults, on uplifted backslope areas, and in areas of recent sediment r
mass-wasting and erosion.

Sp

非成層堆積物　3.5kHz サブボトムプロファイラの記録上で，海底下の反射や成層を示さず，海底反射が
引くような特徴をもつ堆積層．
Unstratified sediment　Sediment with a prolonged acoustic echo-character without subbottom re
stratification apparent on 3.5-kHz profiles.

Sp

大規模火山体　1000m以上の起伏のある火山体．粗粒の火砕岩片で覆われている．SeaMARC II 画像上で反
Large volcanic edifice　Volcanic edifice has over 1000 meters relief, is mantled with coarse volc
debris, and is of low reflectivity on the SeaMARC II imagery.

Ss

成層堆積物　3.5kHz サブボトムプロファイラの記録上で，1枚以上の成層した反射面がみられる堆積層．
Stratified sediment　Sedimented areas with one or more subbottom reflectors on 3.5-kHz echo
profiles.

Ss

上部に音響的透明層を伴う堆積物分布域　内部反射のない音響的透明層が連続する．海底は滑らかで平らで
Sedimented area with overlying transparent layer　The acoustically transparent layer is continuou
internal reflectors.

Su

未区分堆積物
Unclassified sediment

火山島
Volcanic island

正断層　断層崖の比高が100m以上あるもの．
Normal faults　Exposure of footwall block has greater than 100 meters relief.

スミスリフ

GEOLOGIC
TORISHIMA R

G. ブラウン※・村上文敏・西村　昭・B. テイラー※・湯浅真人
※ハワイ大学

ons, fresh and altered.

部は数mの厚さの堆積物に覆
堆積物が除去された場所に露

ms and seismic reflection
k exposures occur on the
ent sediment removal by

ず，海底反射が下方へ尾を

t subbottom reflectors or

RC II 画像上で反射率が低い.
with coarse volcaniclastic

みられる堆積層.
n 3.5-kHz echocharacter

は滑らかで平らである.
yer is continuous with no

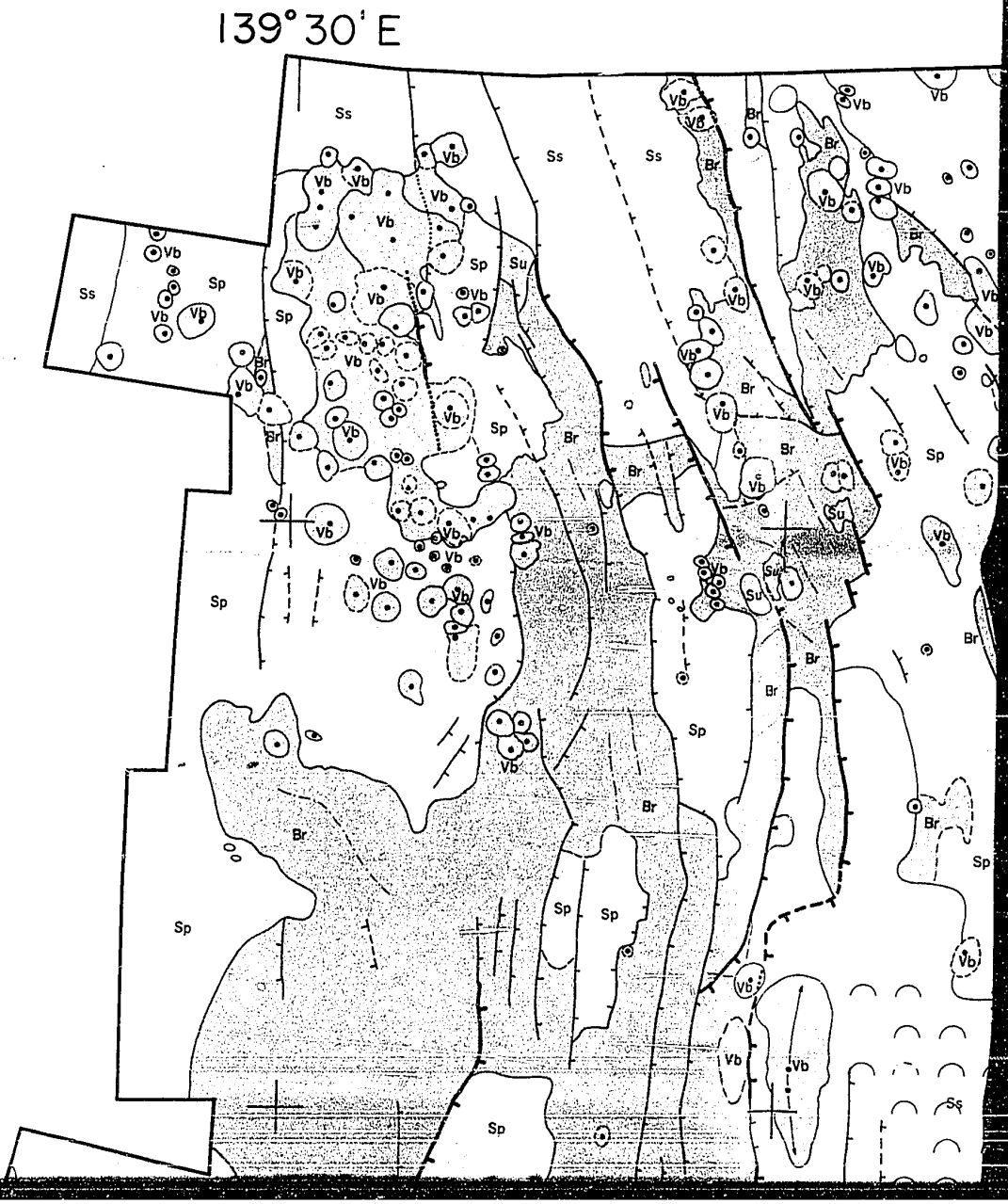

及び鳥島リフト海底地質図

MAP OF SUMISU AND TS, IZU-OGASAWARA ARC

1 : 200,000

Glenn BROWN,※ Fumitoshi MURAKAMI, Akira NISHIMURA, Brian TAYLOR※ and Makoto YUASA
※ Hawaii Institute of Geophysics, University of Hawaii

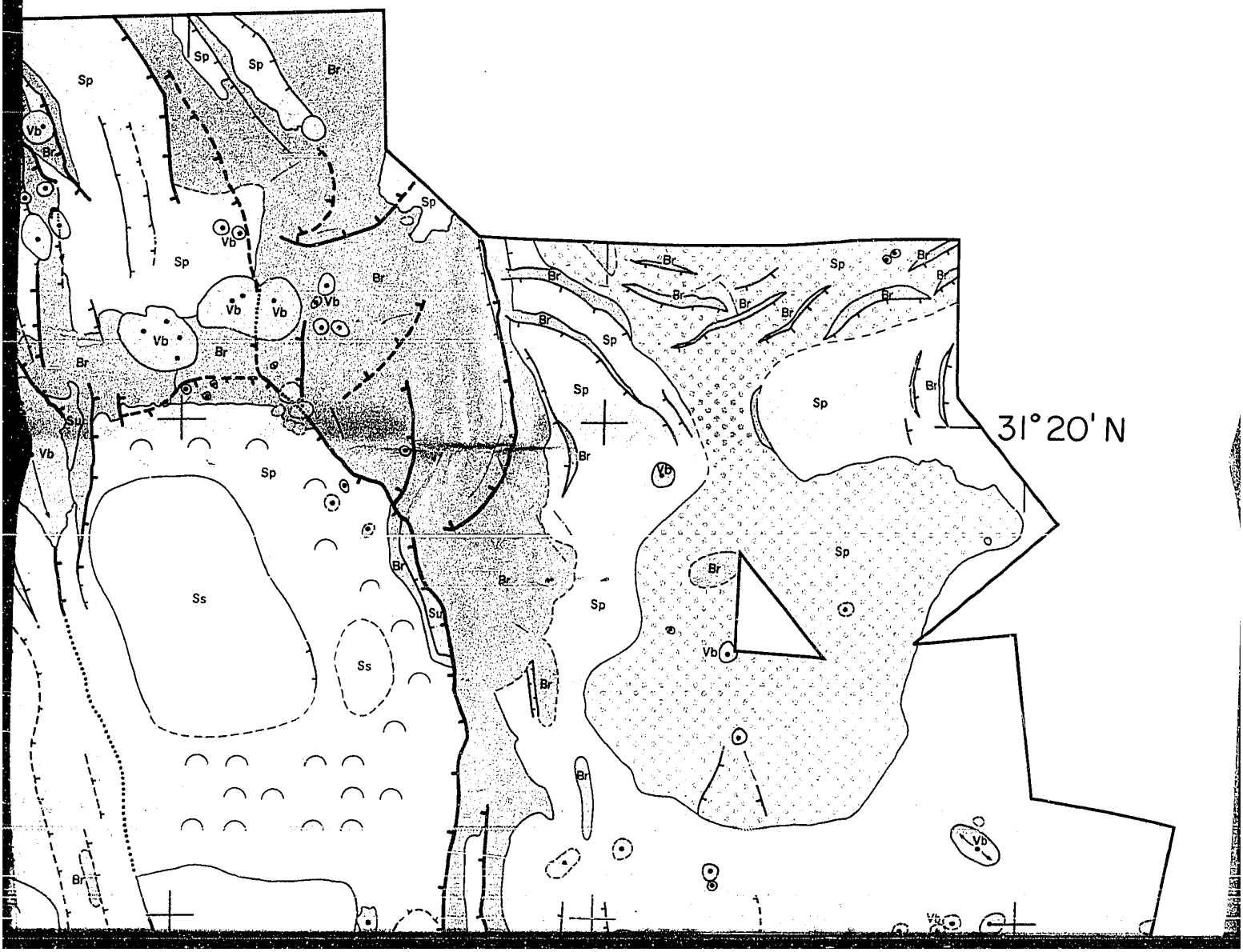

Ss

Sedimented area with overlying transparent layer The acoustically transparent layer is continuou
internal reflectors.

Su

未区分堆積物
Unclassified sediment

火山島
Volcanic island

正断層　断層崖の比高が100m以上あるもの.
Normal faults　Exposure of footwall block has greater than 100 meters relief.

正断層　断層崖の比高が100m以下のもの.
Normal faults　Exposure of footwall block has less than 100 meters relief.

リニアメント　SeaMARC II画像で観察される線状構造. 3.5kHzサブボトムプロファイラ記録上では観察さ
されても不明瞭なものである.
Lineaments　Observed on SeaMARC II imagery; no data or ambiguous on 3.5-kHz profiles.

推定断層
Location of fault is uncertain

伏在断層
Buried fault

火山の中心　噴火の中心あるいは山頂火道の位置. 海底地形, SeaMARC II 画像あるいは3.5kHzサブボ
ァイラ記録上で盛り上った点反射の頂部に基づいて決定した.
Center of volcano　Indicates the center of eruption or summit volcanic vent. Based on bathymet
SeaMARC II imagery, or apex of elevated point-reflectors on 3.5-kHz profiles.

線状火山の軸　割目噴火あるいは断層トラフを埋めて形成されたと考えられる線状火山地形の軸部分を示す
Axis of linear volcano　Feature is linear volcano possibly formed by fissure eruptions or fillin
troughs.

海底に小起伏のみられる地域
Area of rolling/hiliy sea floor

トラフ軸　海底地形に基づいて描いたトラフの軸. 堆積物の移動は多分この軸に沿って行われたと思われ
Trough axis　Axis of trough based on bathymetry. Possible path of sediment migration.

付　　記

スミス及び鳥島リフトは，伊豆ー小笠原弧内にみられるリフティテングの初期の型を示している (Taylor et al., in prep.). この地質図は, HIG及びGSJの調査により得られたSeaMARC II 画像とエアガン地震探査, 3.5kHz SBP記録に基づいて作成されたものである. 航走測線は，別図に示したように，SeaMARC II 曳航は2～4マイル間隔, エアガン曳航及び3.5kHz PDRの測線は2及び3マイル間隔，で東西に配置した.

火山の中心は，SeaMARC II 画像上で反射率の高く盛上った円ないし偏円状区域として識別された. 3.5kHz PDRによるデータのある海域では，火山の存在をそれで確認した. 火道の多数ある火山の場合には，個々の火道は画像あるいは地形図で輪郭が明瞭なものだけを記した.

岩盤の露出は，正断層の下盤と隆起斜面，マス・ウェイスティングや侵蝕によって最近の堆積物が除去された場所，

Notes

Sumisu and Torishima rifts are incipient isla
rifts in the Izu-Ogasawara (Izu-Bonin) island arc (
et al., in prep.). The Geological Map is ba
SeaMARC II sidescan imagery and bathymetr
single-channel seismic reflection and 3.5-kHz echo
ing profiles, from Hawaii Institute of Geophysic
and the Geological Survey of Japan. Navigation
rived from SeaMARC II sidescan imagery (S
Seafloor geomorphology in the rift segments is
duct of volcano-tectonic and sedimentary proce

Volcanic centers were identified on the SeaM
imagery as circular/oblate high-reflectivity are
positive bathymetric relief. Where data were av

is continuous with ac

録上では観察されないか,

profiles.

3.5kHz サブボトムプロフ

on bathymetry,

の軸部分を示す.
tions or filling of fault

られたと思われる.
ation.

incipient island-arc
n) island arc (Taylor
Map is based on
d bathymetry, and
l 3.5-kHz echosound-
of Geophysics (HIG)
Navigation was de-
imagery (Sheet 3).
segments is a pro-
entary processes.
on the SeaMARC II
flectivity areas with
data were available,
Hz records. Indivi-

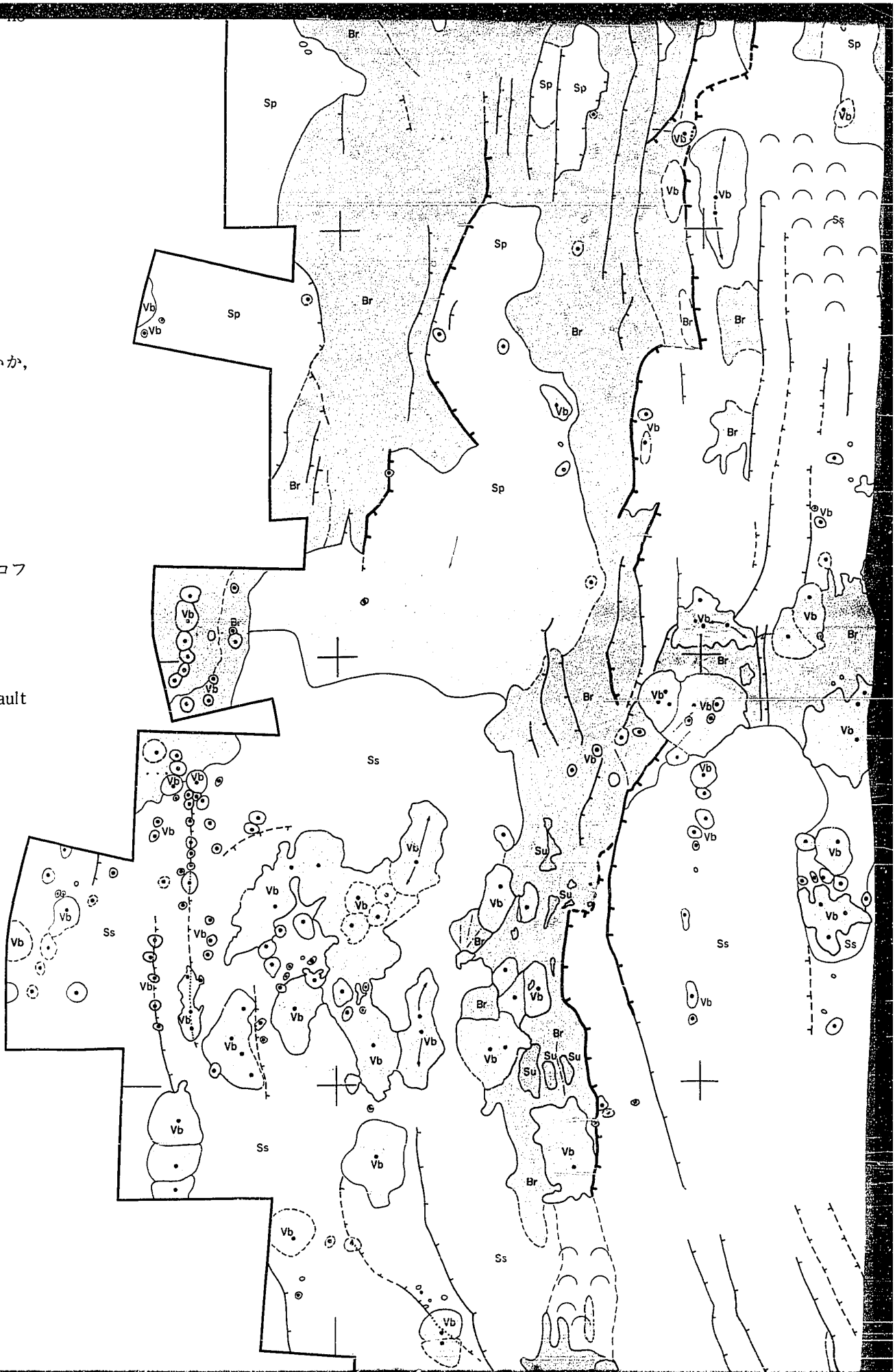

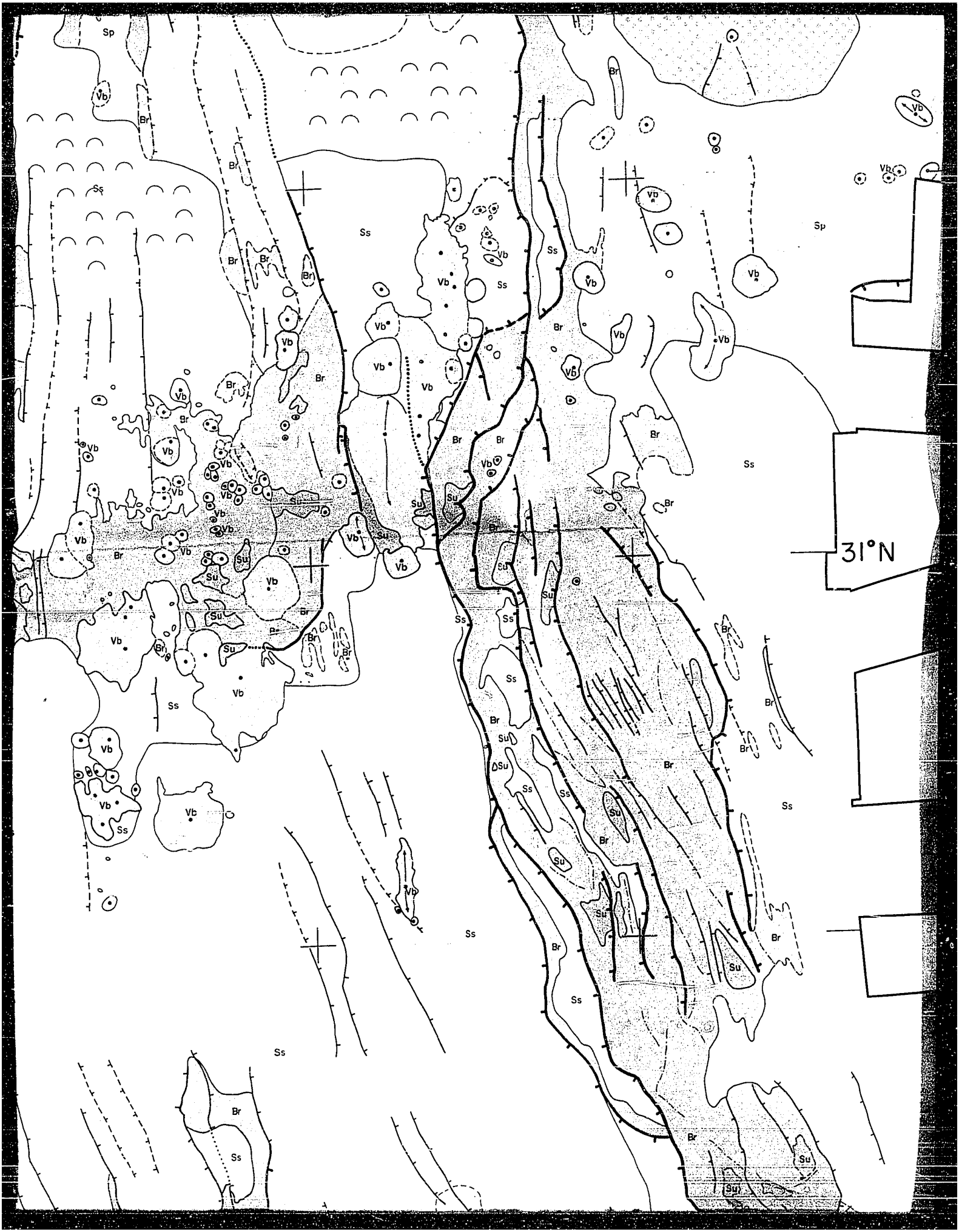
31°N
Sp
Vb
Br
Ss
Su

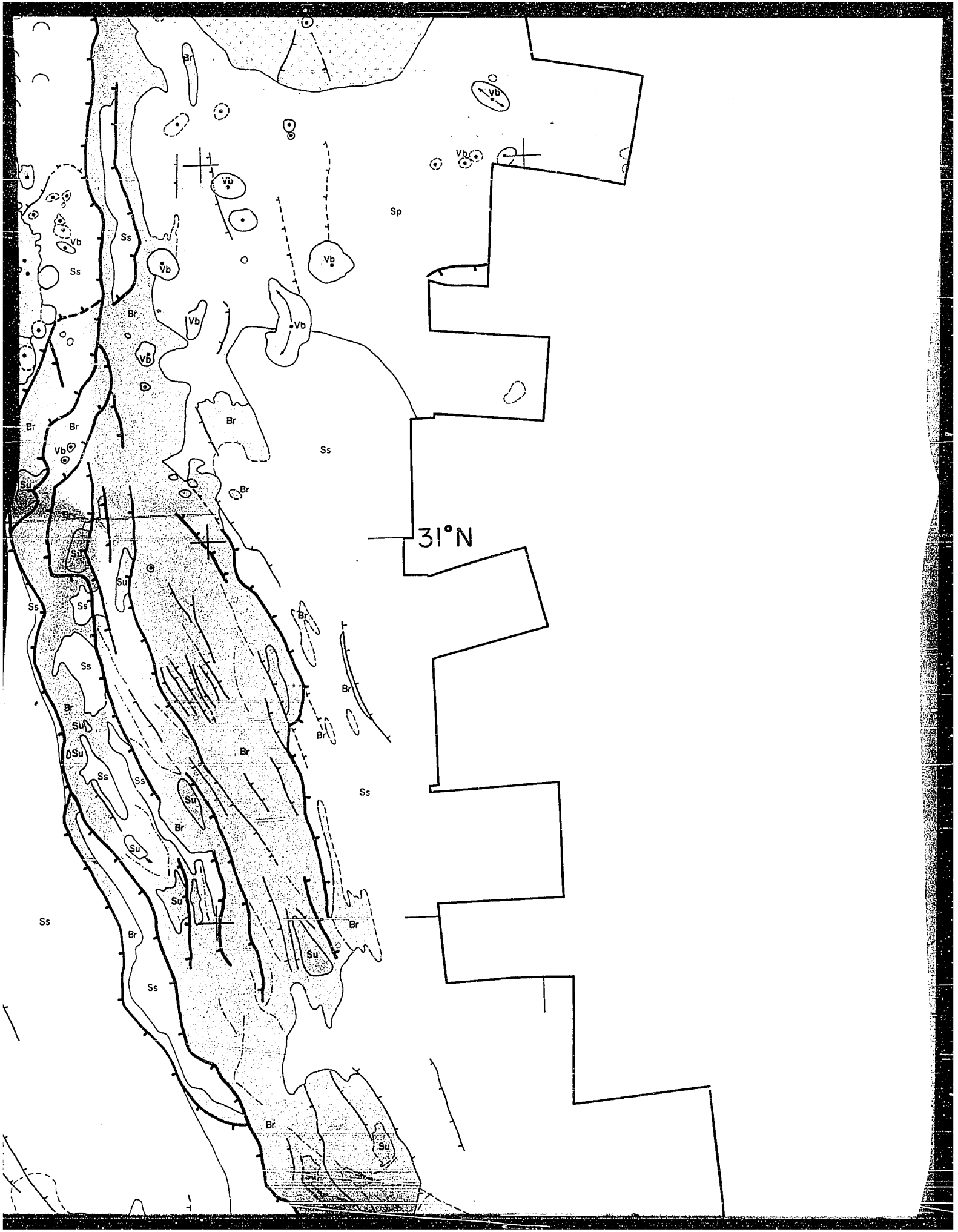
31°N
Br
Vb
Sp
Ss
Su

た．火道の多数ある火山の場合には，個々の火道は画像あるいは地形図で輪郭が明瞭なものだけを記した．

岩盤の露出は，正断層の下盤と隆起斜面，マス・ウェイスティングや侵蝕によって最近の堆積物が除去された場所，あるいは，大規模な島弧火山の上部斜面にみられる．岩盤分布域は強い反射を起こす急傾斜地であり，したがって，SeaMARC II 画像上では黒く見える．また，岩盤分布域は，3.5kHz PDR上で海底が多数の双曲線からなる．その海底反射は明瞭であり，海底下の反射はない．

堆積相は，反響記録のタイプによって分類されている (Brown and Taylor, 1988; Nishimura and Murakami, 1988)．この地質図では，非成層及び成層堆積物の分布を示した．非成層堆積物は水深の小さな島弧火山の周辺にみられる．一方，成層堆積物は断層盆地，リフト底，あるいは海底崖下部斜面のテラス状盆地に普通にみられる．10枚以上の海底下反射面をもち成層の発達する堆積物が本海域の南西隅を覆っている．しかしながら，海域の大半では海底下反射面が1～4枚で，成層はあまり発達しない．成層堆積物はタービダイトであると解釈される．

反響データがないか，あるいはあっても不明瞭なもので，SeaMARC II 画像で識別された小規模な堆積物分布域は別分類とした．このほか，地球物理的観測に基づく堆積作用の中心を示した．なお，火山岩あるいは岩盤分布域とした所も薄い堆積物が覆っている可能性はある．

なお，この地質図を含み同番号の図(海洋地質図31, 1～4)はすべてWGS-72測地座標系に基づき，国際横メルカトール図法で描かれている．

References

BROWN, G. and TAYLOR, B. (1988) Seafloor mapping of the Sumisu Rift, Izu-Ogasawara (Bonin) Island Arc. *Bull. Geol. Surv. Japan*, vol. 39, p. 23-38.

MURAKAMI, F. (1988) Structural framework of the Sumisu Rift, Izu-Ogasawara Arc. *Bull. Geol. Surv. Japan*, vol. 39, p. 1-21.

NISHIMURA, A. and MURAKAMI, F. (1988) Sedimentation of the Sumisu Rift, Izu-Ogasawara Arc. *Bull. Geol. Surv. Japan*, vol. 39, p. 39-61.

TAYLOR, B., BROWN, G., HUSSONG, D., and FRYER, P. (in prep.) Rifting of the Bonin Island Arc.

YAMAZAKI, T. (1988) Heat flow in the Sumisu Rift, Izu-Ogasawara (Bonin) Arc. *Bull. Geol. Surv. Japan*, vol. 39, p. 63-70.

duct of volcano-tectonic and sedimentary process

Volcanic centers were identified on the SeaMA imagery as circular/oblate high-reflectivity areas positive bathymetric relief. Where data were avai volcanoes were confirmed on 3.5-kHz records. I dual vents forming multi-vent volcanic fields mapped only if outlines were clear on imager bathymetry.

Bedrock exposures occur on the footwall blo normal faults, on uplifted backslope areas, in are recent sediment removal by mass-wasting and ero and upper slopes of large arc volcanoes. Bedrock generally have a steep slope which produces a st specular reflection and hence appears darke SeaMARC II imagery. Bedrock areas on 3.5-kHz files have bottom hyperbolae, a distinct bottom refl and no subbottom reflectors.

Sediment facies are classified by echo-char type (Brown and Taylor, 1988, Nishimura and Mura 1988). This map shows the distribution of unstra and stratified sediment. Unstratified sediment is f on and around the flanks of shallow arc volca Stratified sediments are common in fault-block ba rift floor basins, and terraced basins on the lower sl of escarpments. Well-stratified deposits with more 10 subbottom reflectors cover the southwest corne the study area. Most areas mapped however are orly stratified with 1 to 4 subbottom reflec Stratified sediments are interpreted as turbidites.

Small sediment patches identified on SeaMA imagery with no available echo-character data or are ambiguous have been classified separately. map shows the distribution of sediment depoce based on geophysical observations. A thin sedi cover may be present on areas mapped as vol and bedrock.

All maps under this number (Marine Geology Series 31, 1～4) were drawn based on the geodetic sy "WGS-72" and UTM (Universal Transverse Merca Projection.

地質調査所による音波探査(エア・ガン及び3.5kHz PDR)測線
GSJ seismic (air-gun) and 3.5kHz PDR survey tracks

tary processes.
n the SeaMARC II
ctivity areas with
ta were available,
records. Indivi-
anic fields were
on imagery or

footwall block of
areas, in areas of
sting and erosion,
es. Bedrock areas
produces a strong
pears darker on
s on 3.5-kHz pro-
ct bottom reflector

y echo-character
ra and Murakami,
on of unstratified
sediment is found
w arc volcanoes.
fault-block basins,
n the lower slopes
ts with more than
thwest corner of
however are po-
ottom reflectors.
s turbidites.
on SeaMARC II
ter data or which
separately. This
ment depocenters
A thin sediment
pped as volcanic

ine Geology Map
e geodetic system
verse Mercator)

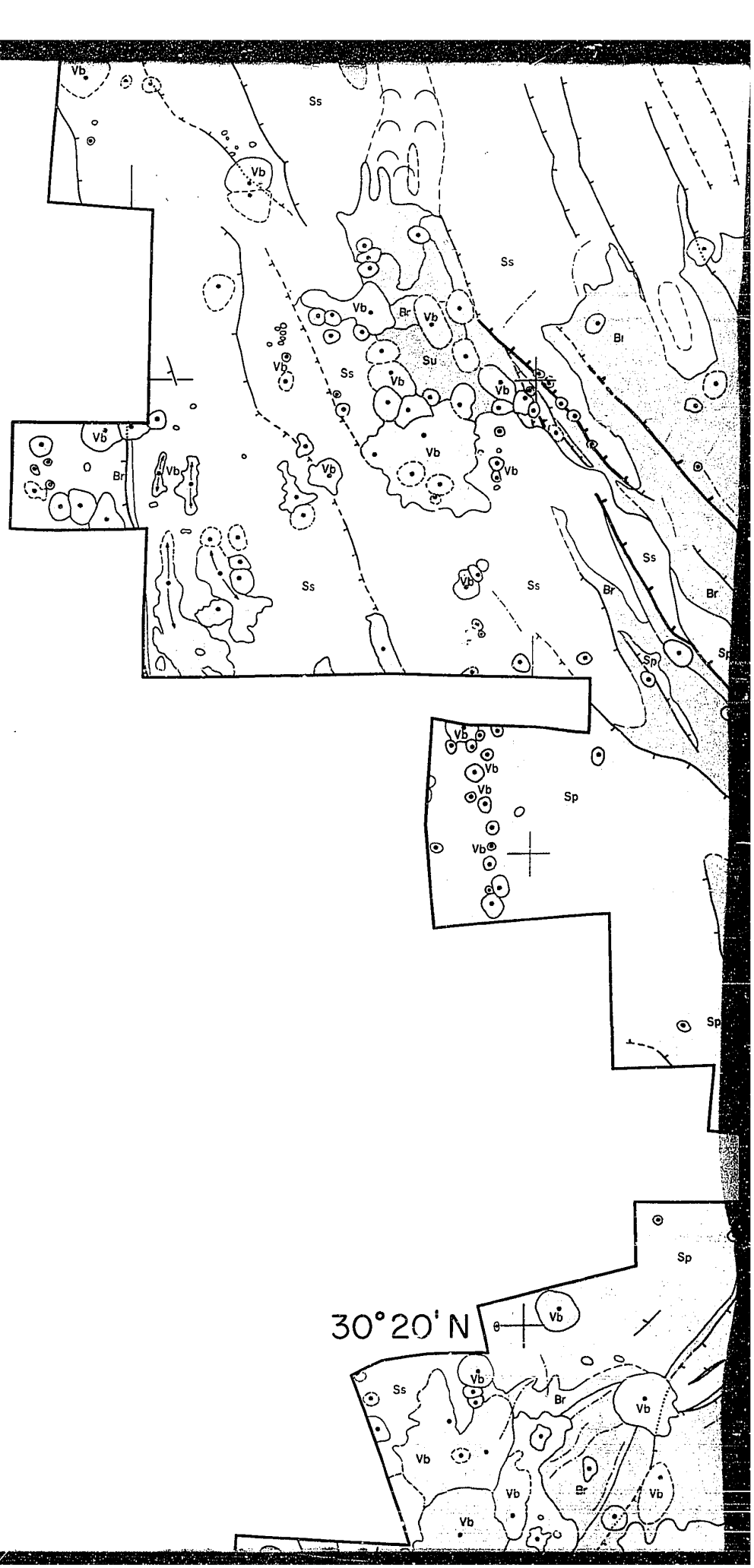

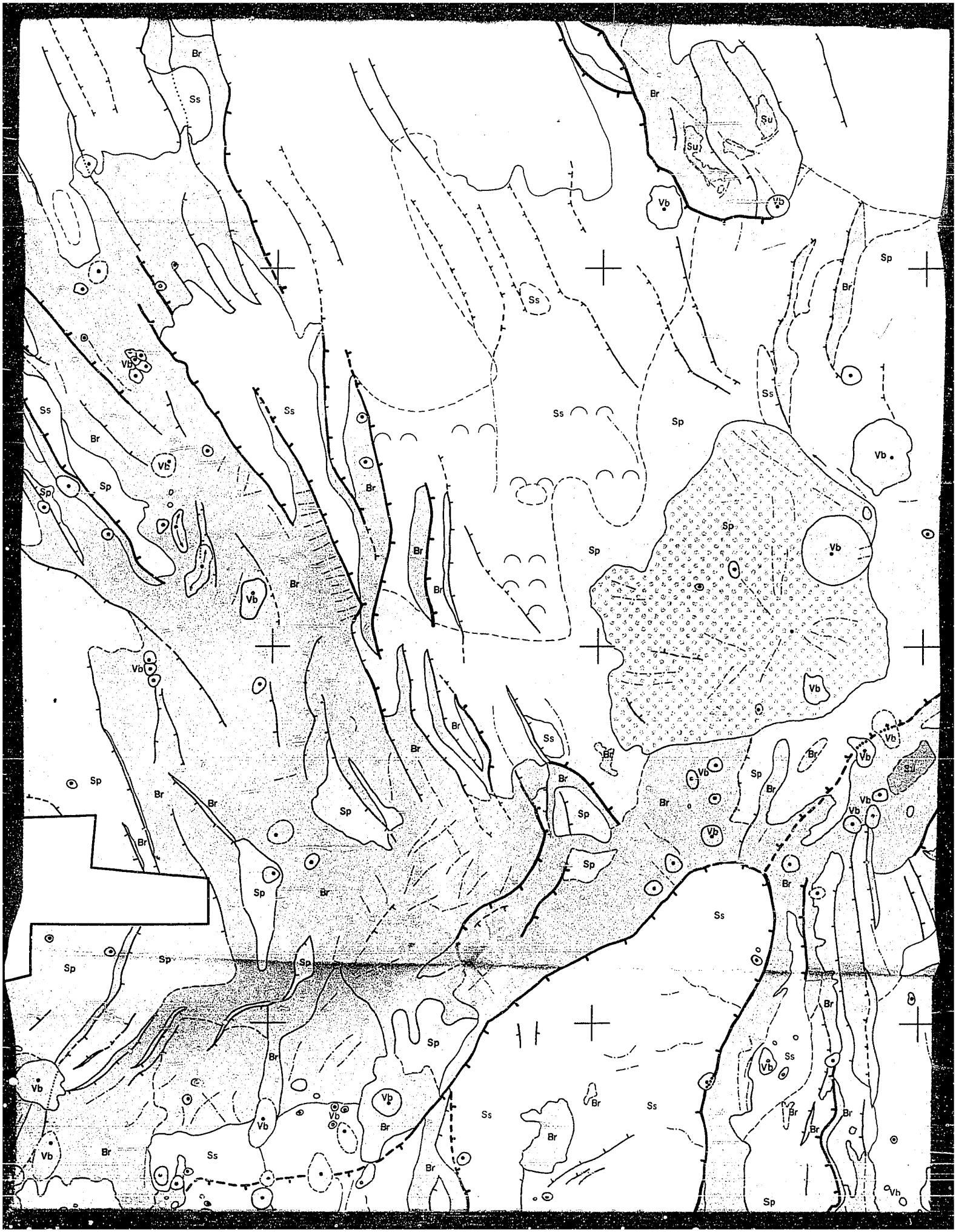
Br
Ss
Su
Vb
Sp

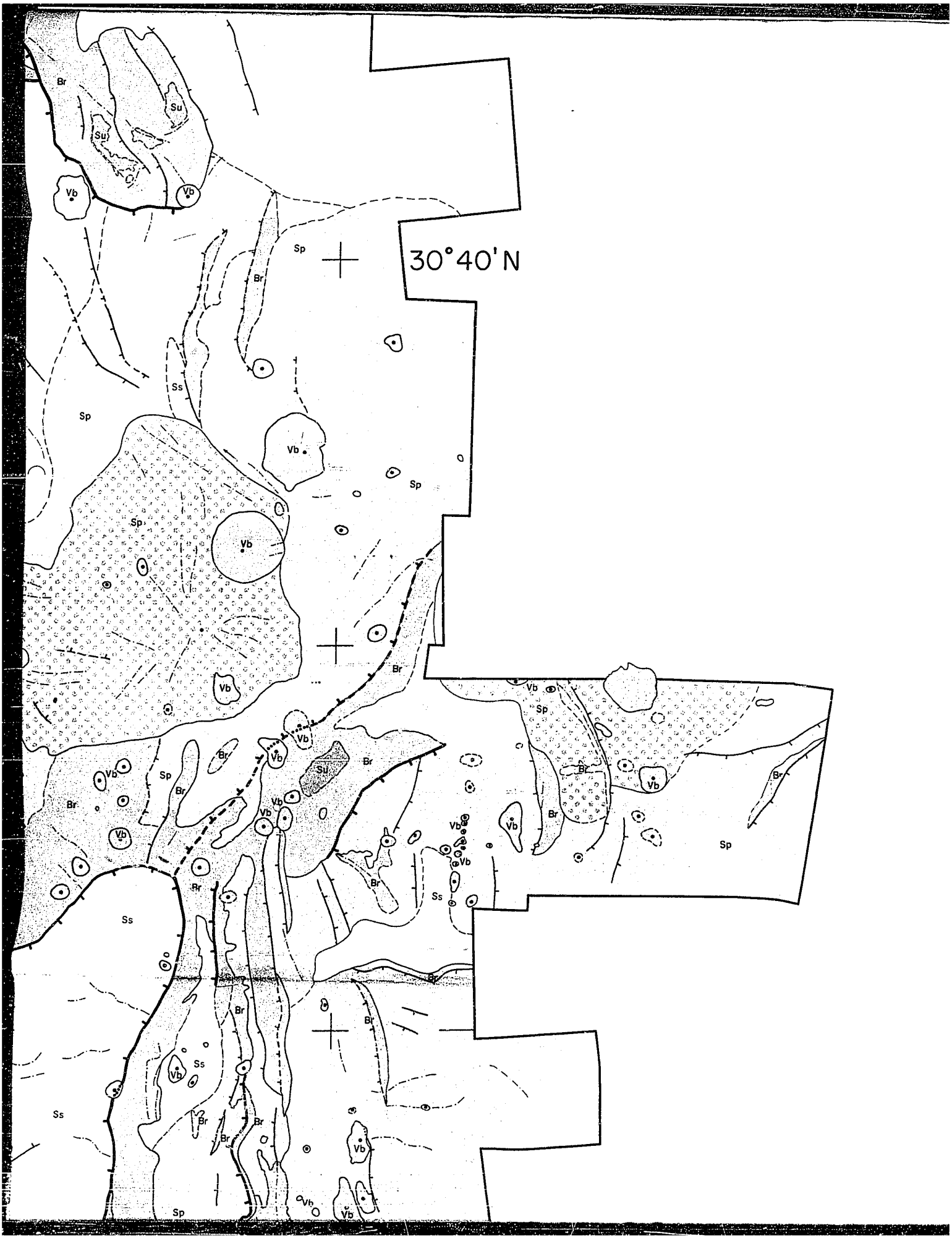
30°40'N
Br
Su
Vb
Sp
Ss

vol. 39, p. 63-70.

Series 31, 1–4) were drawn based on the geodetic system "WGS-72" and UTM (Universal Transverse Mercator) Projection.

地質調査所による音波探査(エア・ガン及び3.5kHz PDR)測線
GSJ seismic (air-gun) and 3.5kHz PDR survey tracks

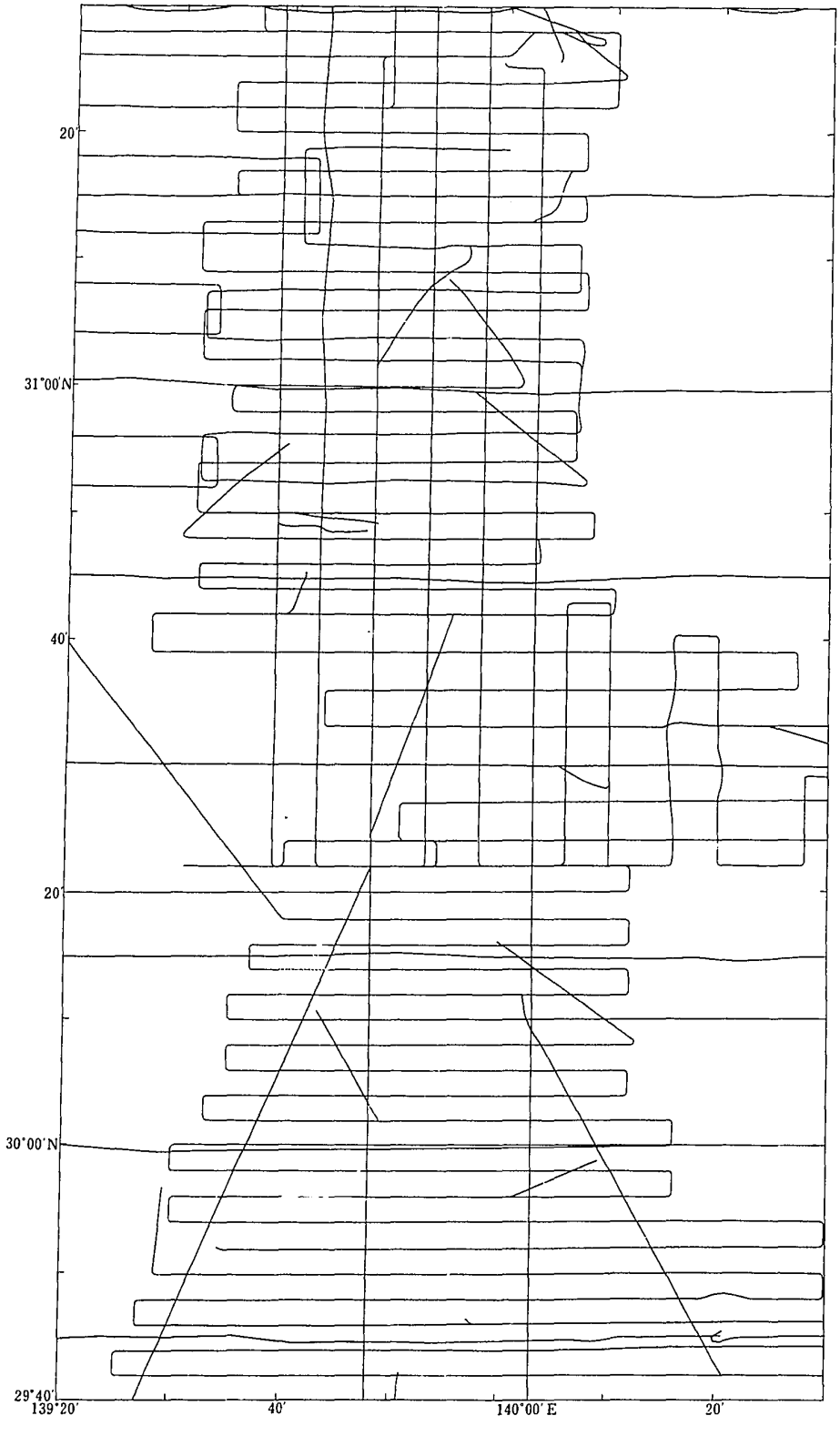

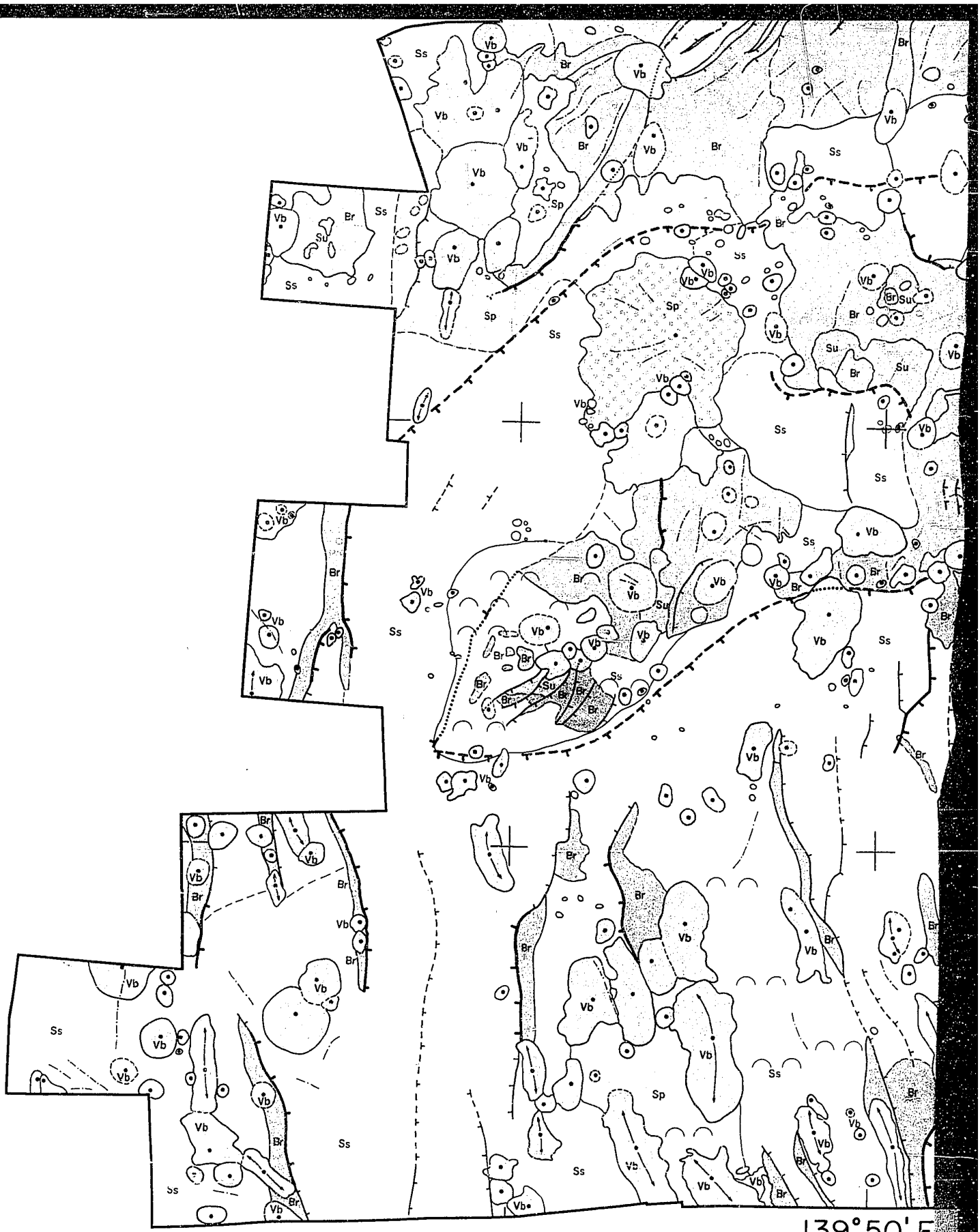

国土地図株式会社印刷（7色刷）

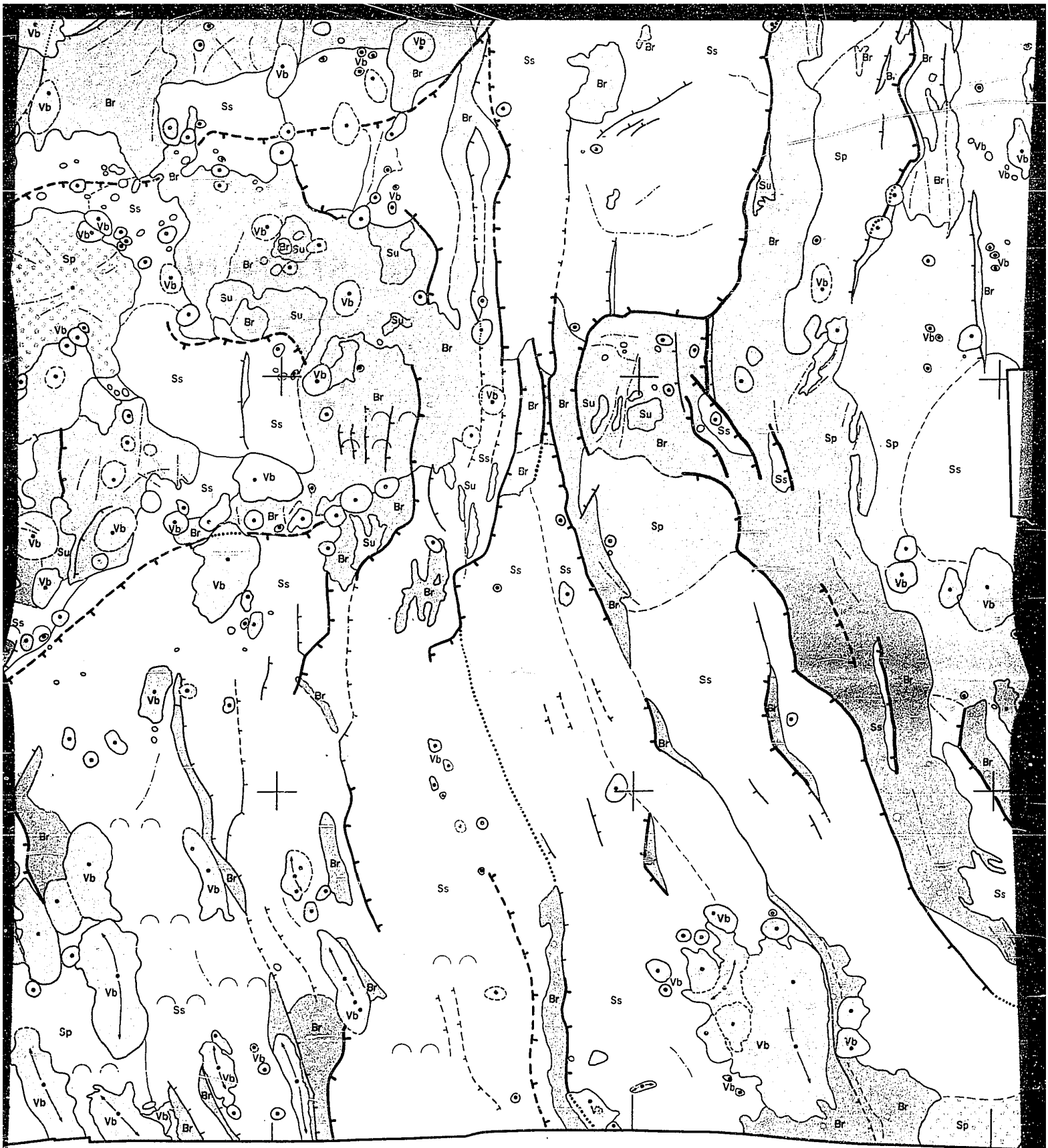

GEOLO

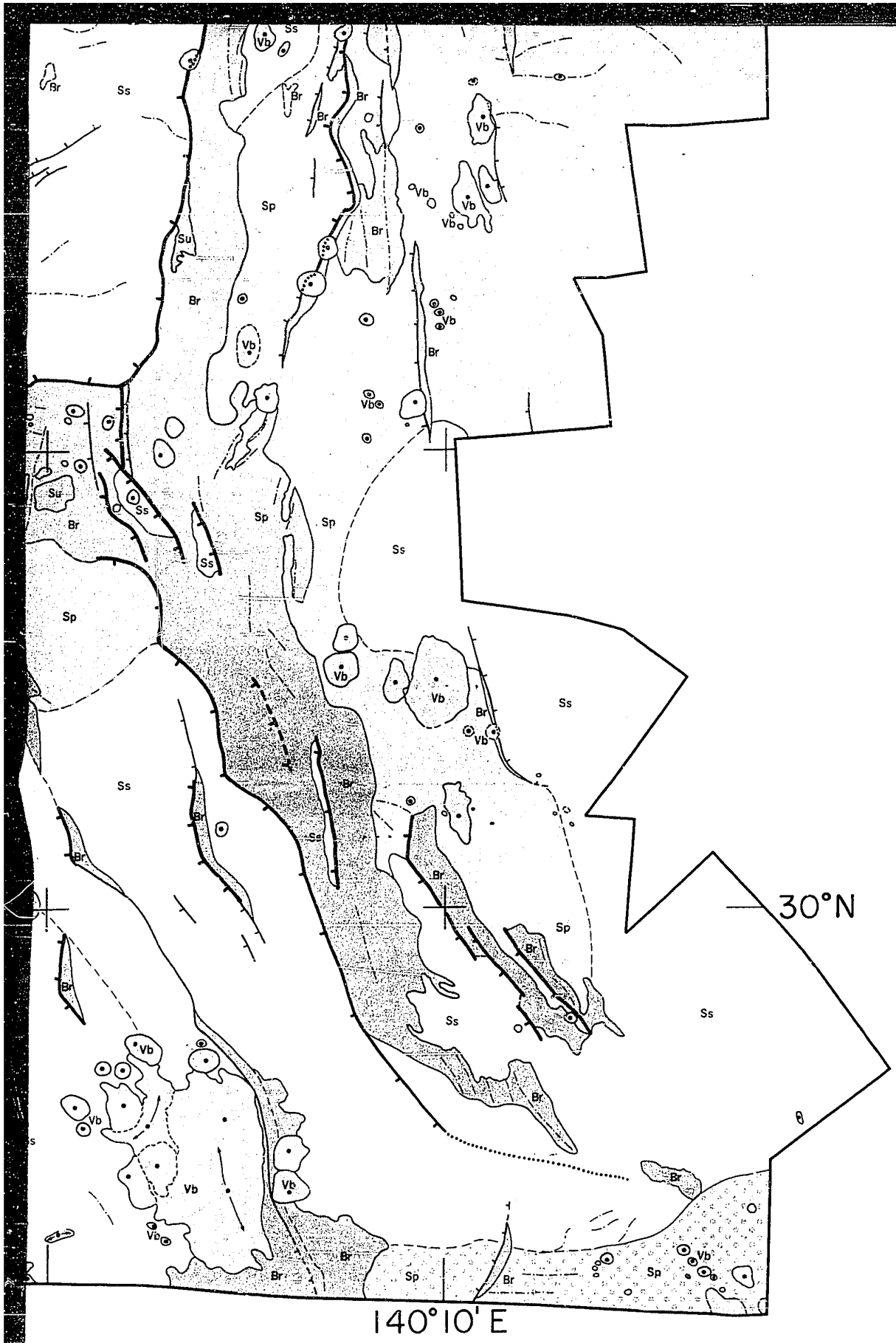

PLEASE NOTE:

Oversize maps and charts are filmed in sections in the following manner:

LEFT TO RIGHT, TOP TO BOTTOM, WITH SMALL OVERLAPS

The following map or chart has been refilmed in its entirety at the end of this dissertation (not available on microfiche). A xerographic reproduction has been provided for paper copies and is inserted into the inside of the back cover.

Black and white photographic prints (17" x 23") are available for an additional charge.

University Microfilms International

Appendix B

Sea

海 洋 地 質 図 31
MARINE GEOLOGY MAP SERIES 31

B. テイラー・G. ブラウン・D. ハッソン・P. フライヤー
ハワイ大学

スミスリフト及び鳥島リフト
SeaMARC II サイドスキャン音響画像
SeaMARC II SIDESCAN ACOUSTIC IMAGERY OF SUMISU AND TORISHIMA RIFTS IZU-OGASAWARA ARC

1：200,000

・P. フライヤー

Brian TAYLOR, G
Hawaii Institute

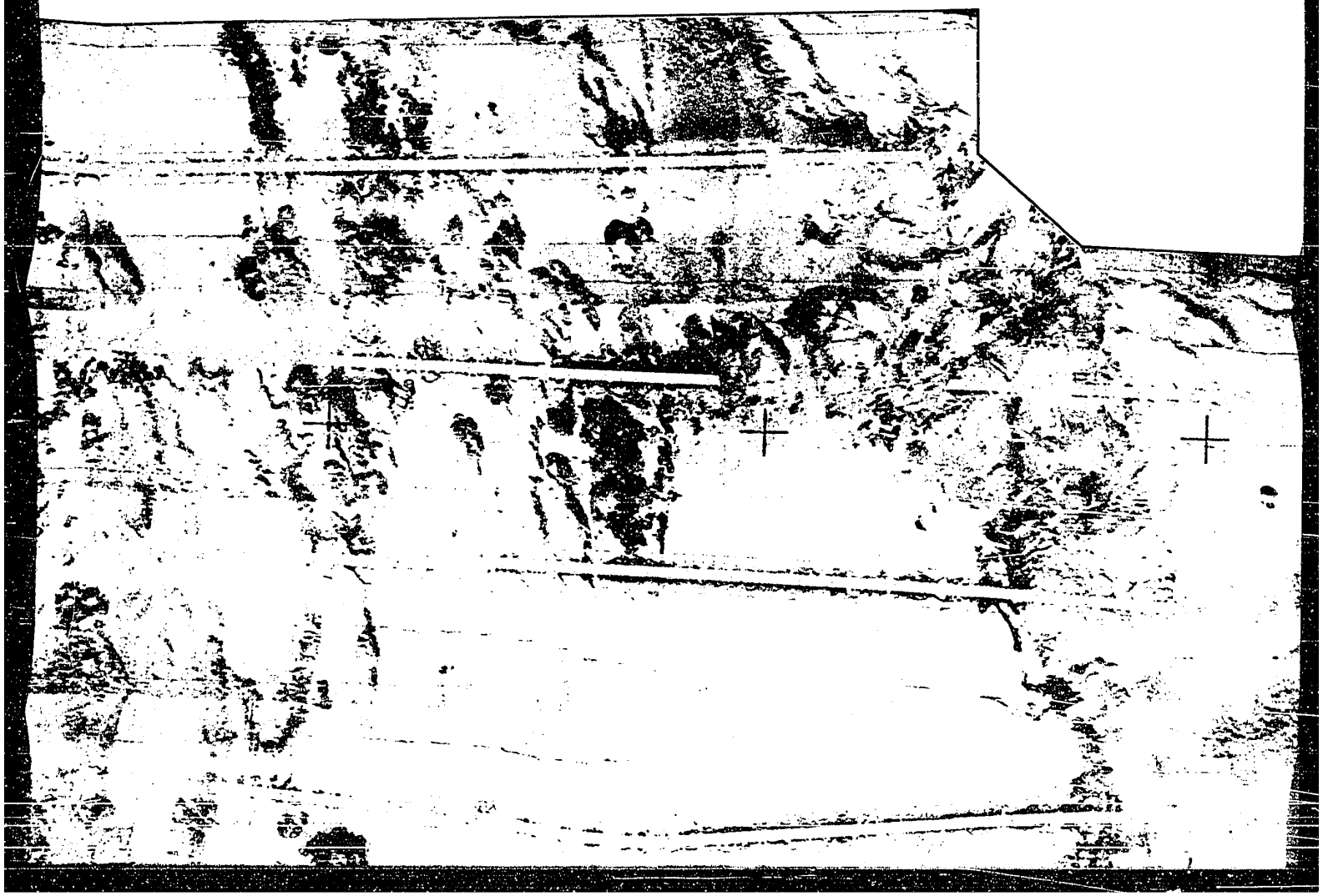

及び鳥島リフト
スキャン音響画像図

ACOUSTIC IMAGERY
TORISHIMA RIFTS,
WARA ARC

0,000

Brian TAYLOR, Glenn BROWN, Donald HUSSONG and Patricia FRYER
Hawaii Institute of Geophysics, University of Hawaii

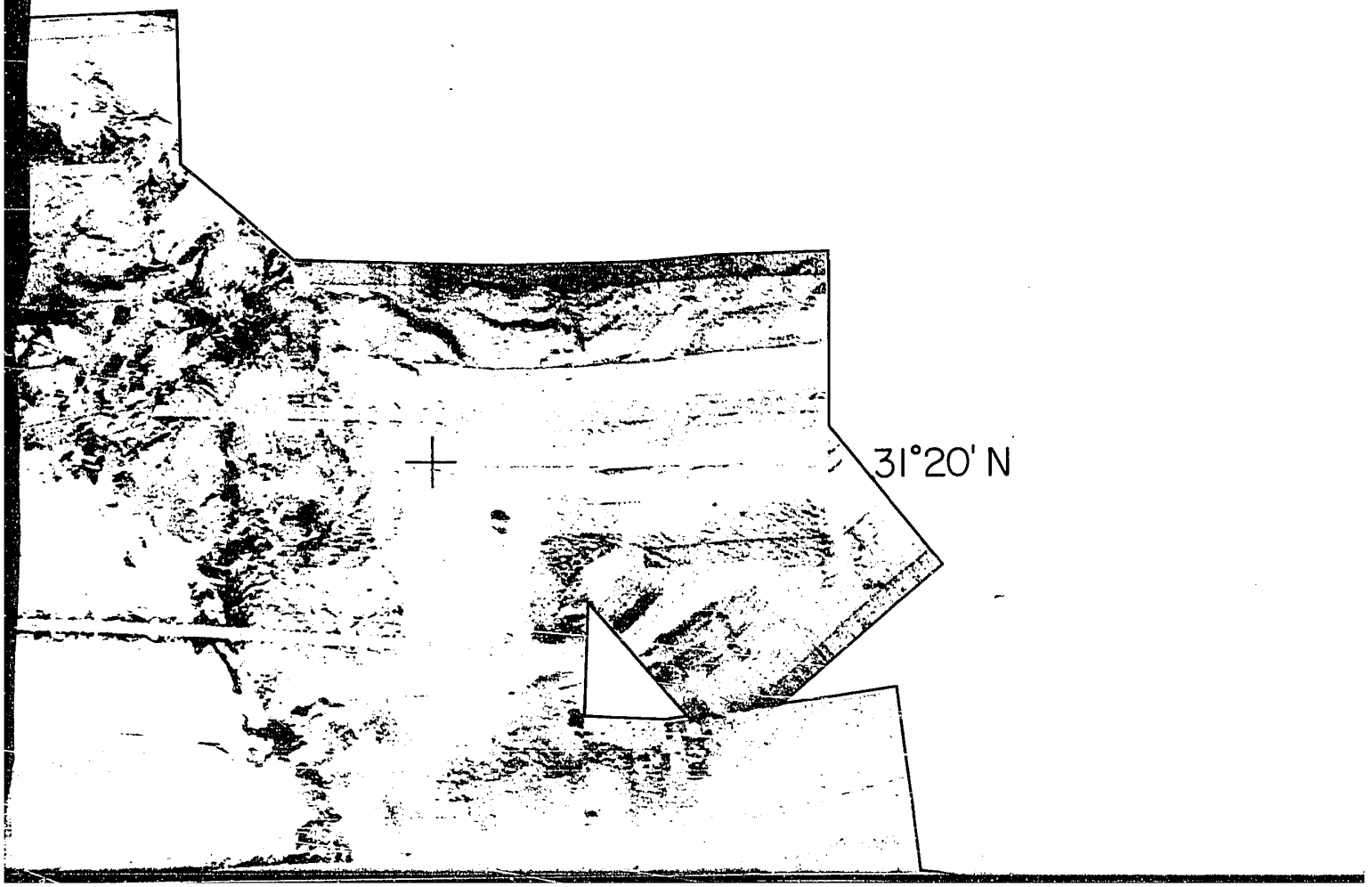

付　　記

SeaMARC II は曳航式の海底マッピング装置で，両舷各5kmの幅の海底を一度に探査することができる．この図は，1984年にハワイ大学所属の調査船カナケオキ号により観測されたSeaMARC II イメージの画像モザイクである．船位は，人工衛星航法とロランC航法とを併用して決定し，曳航体の位置は画像形態の整合性をもとに補正してある．画像モザイクは，縮尺1:78,740で，北緯30度40分以北では東経141度線を，同じく以南では東経139度線を中央経線とする横メルカトール図法で調整した．北緯30度40分以南のデータについては，海面反射及び測線直下からの反射は除去され，また，測線に沿っての利得調整は行われていない．

Notes

SeaMARC II is a shallow-tow sidescan sonar capable of mapping 5 km on either side of the ship's track. Imagery is processed from bottom reflectivity. There are two classes of bottom reflectors (Blackinton, 1986); macro-reflectors and micro-reflectors. Macro-reflectors are specular reflections from average slopes of areas. Micro-reflectors are backscatter from rough bottoms occurring when surface roughness is close to the wave-

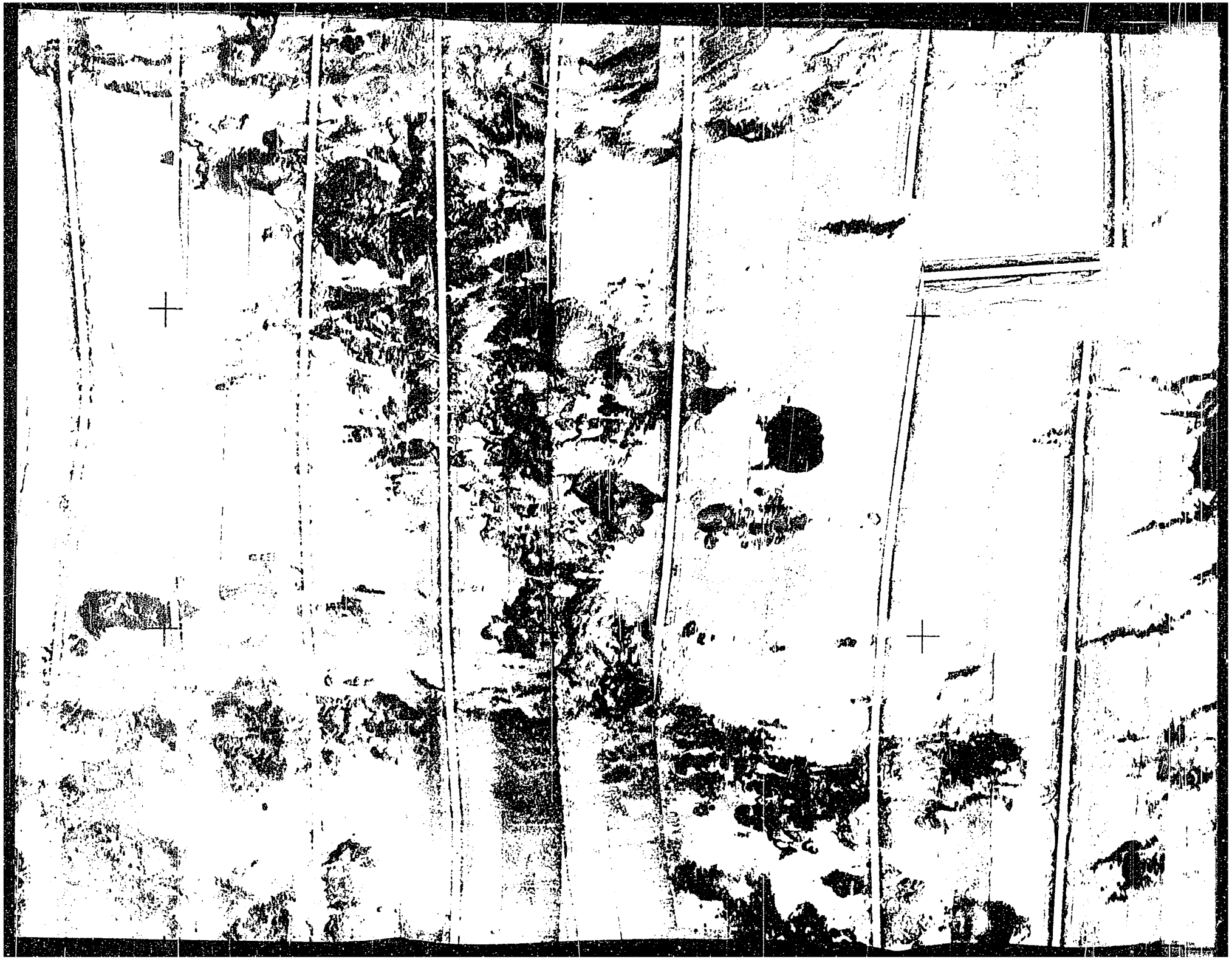

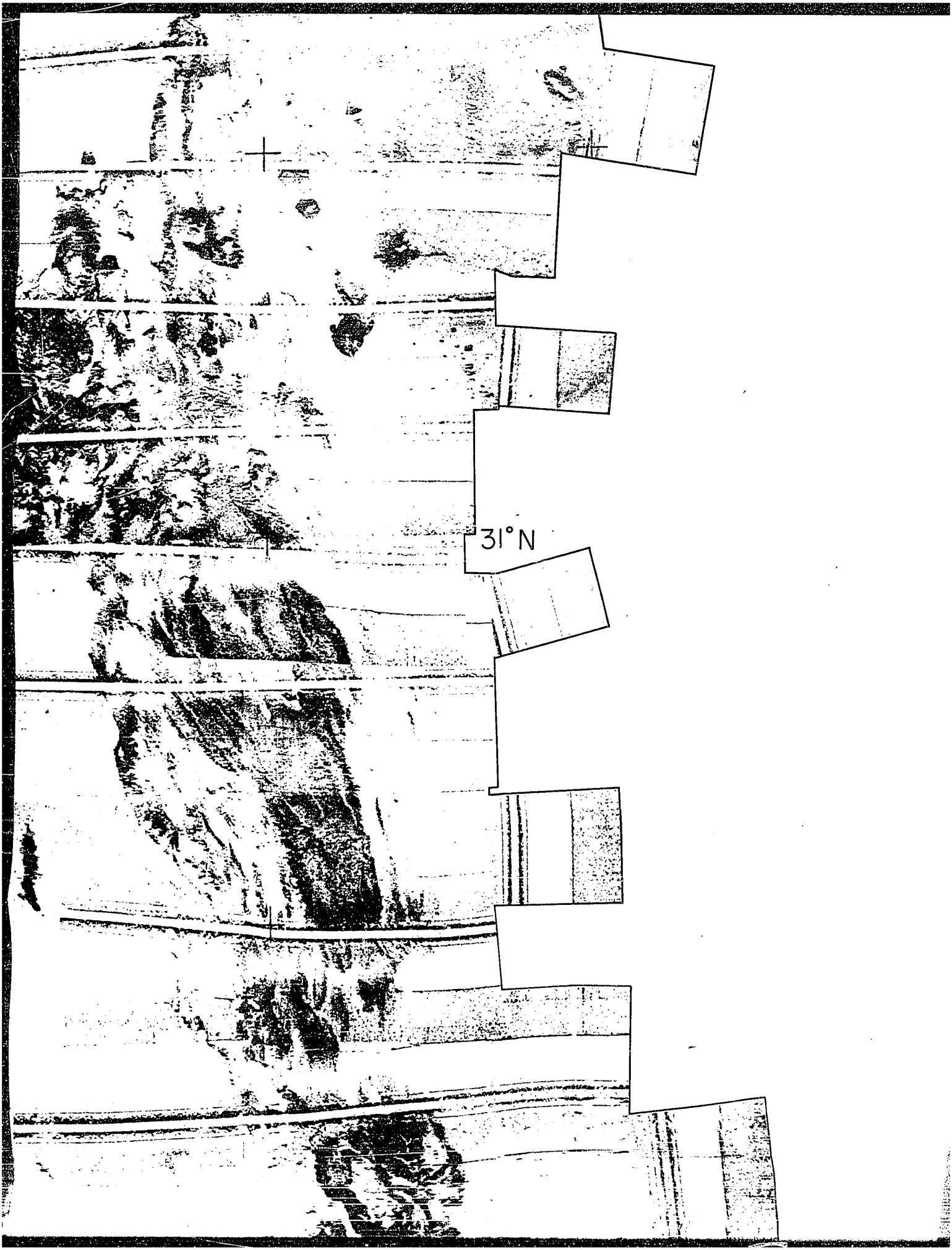
31°N

Micro-reflectors are backscatter from rough bottoms occurring when surface roughness is close to the wavelength of the SeaMARC II signal (approx. 10 cm).

Navigation was based on transit satellite and LORAN-C fixes. Additional minor adjustments to vehicle navigation were based on the match of geological features. The imagery mosaics were prepared at a scale of 1:78,740 using a Transverse Mercator projection with a principal meridian of 141°E north of 30°40'N and 139°E to the south.

The SeaMARC II imagery data have been corrected for bottom detection and recording errors. Reflections off the water surface and uneven gain along track have been removed from data south of 30°40'N. Funding for data collection and processing was provided by the United States National Science Foundation.

BLACKINTON, G. (1986) Bathymetric mapping with Sea MARC II: An elevation angle measuring side-scan sonar system. Ph.D. Diss., Univ. of Hawaii. 145pp.

ハワイ大学地球物理学研究所によるSeaMARC II 調査測線

Hawaii Institute of Geophysics tracks in SeaMARC II survey area

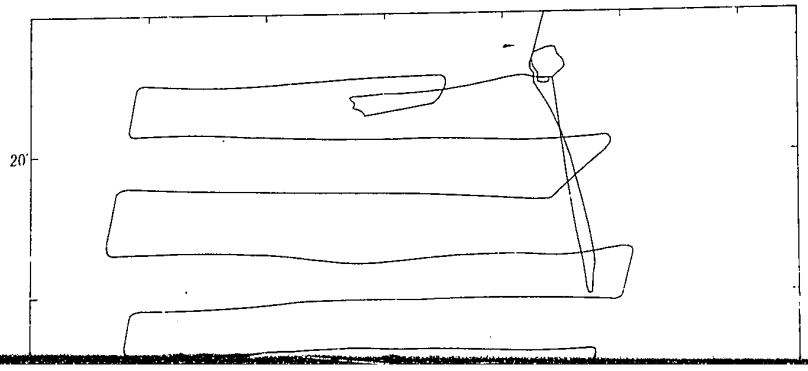

30°20'N

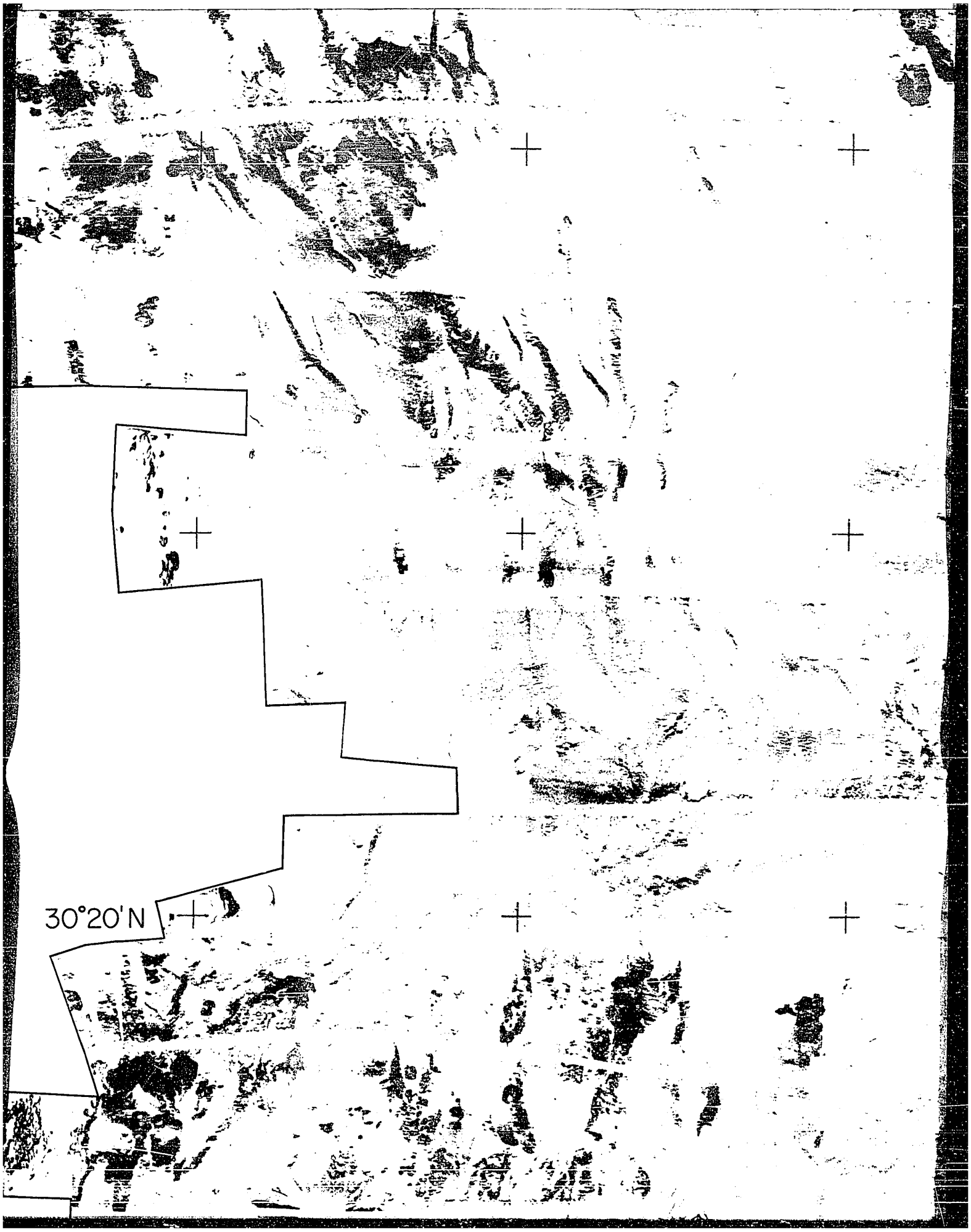
30°20'N

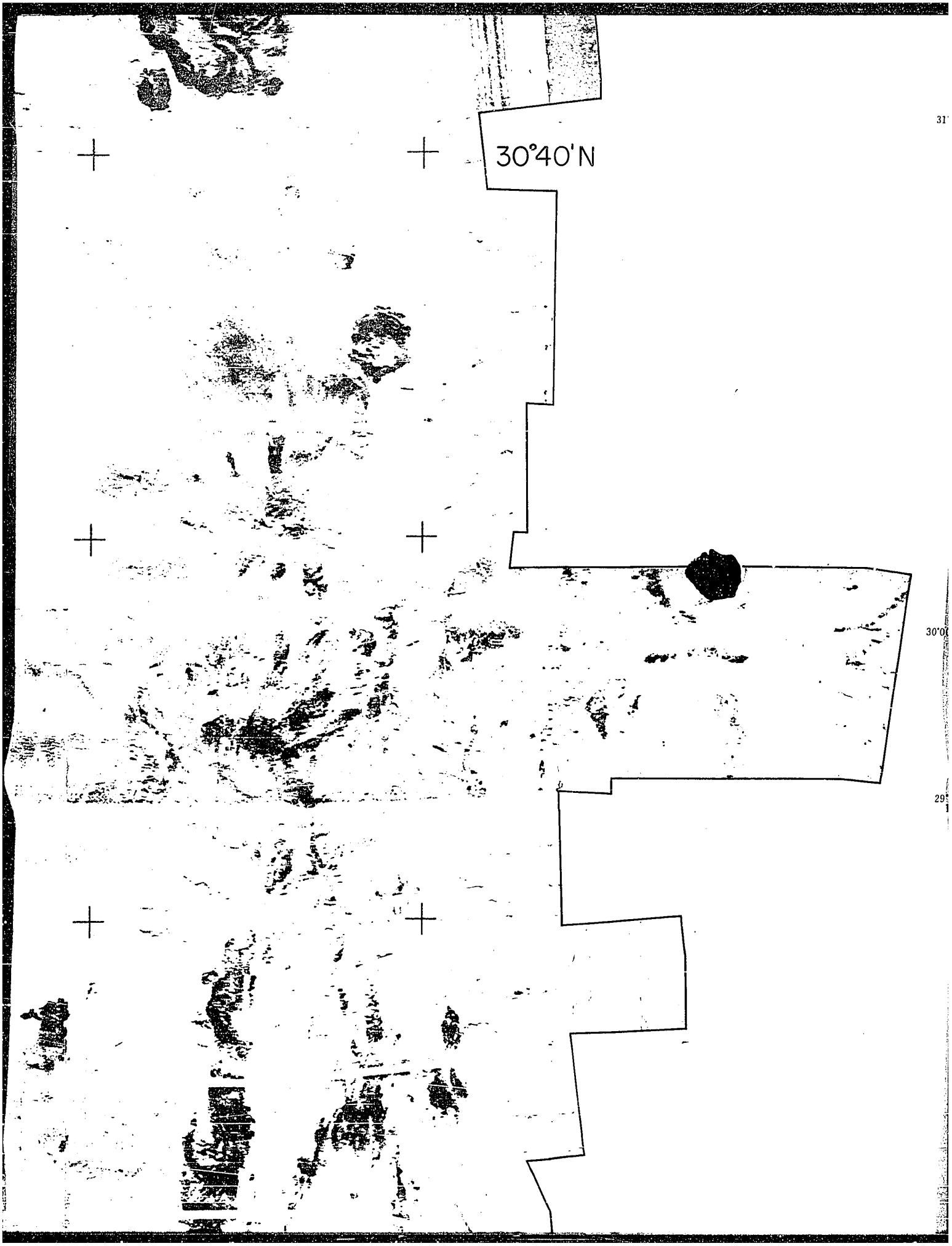
30°40'N
31
30°0
29

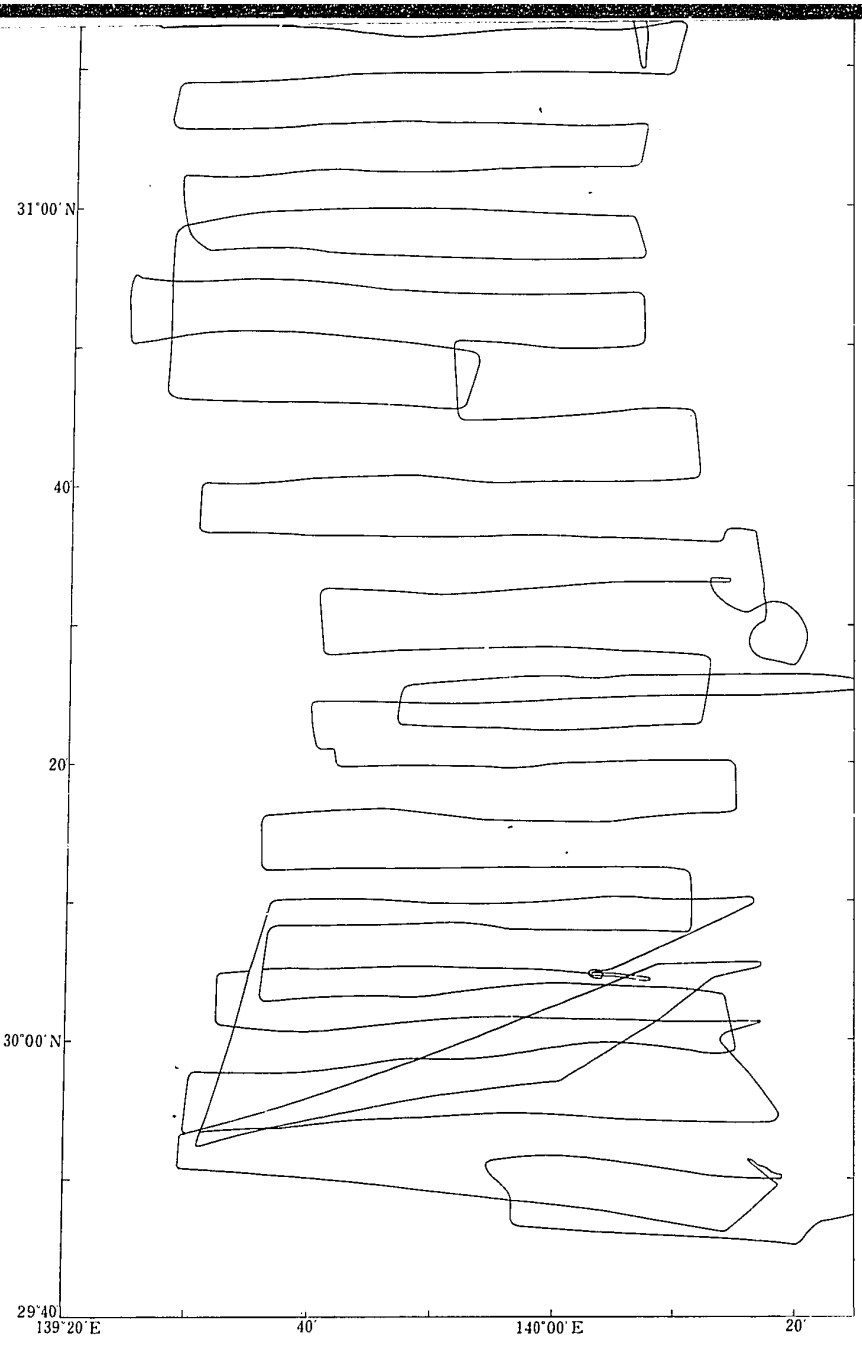
31°00′N
40
20
30°00′N
29°40
139°20′E
40′
140°00′E
20′

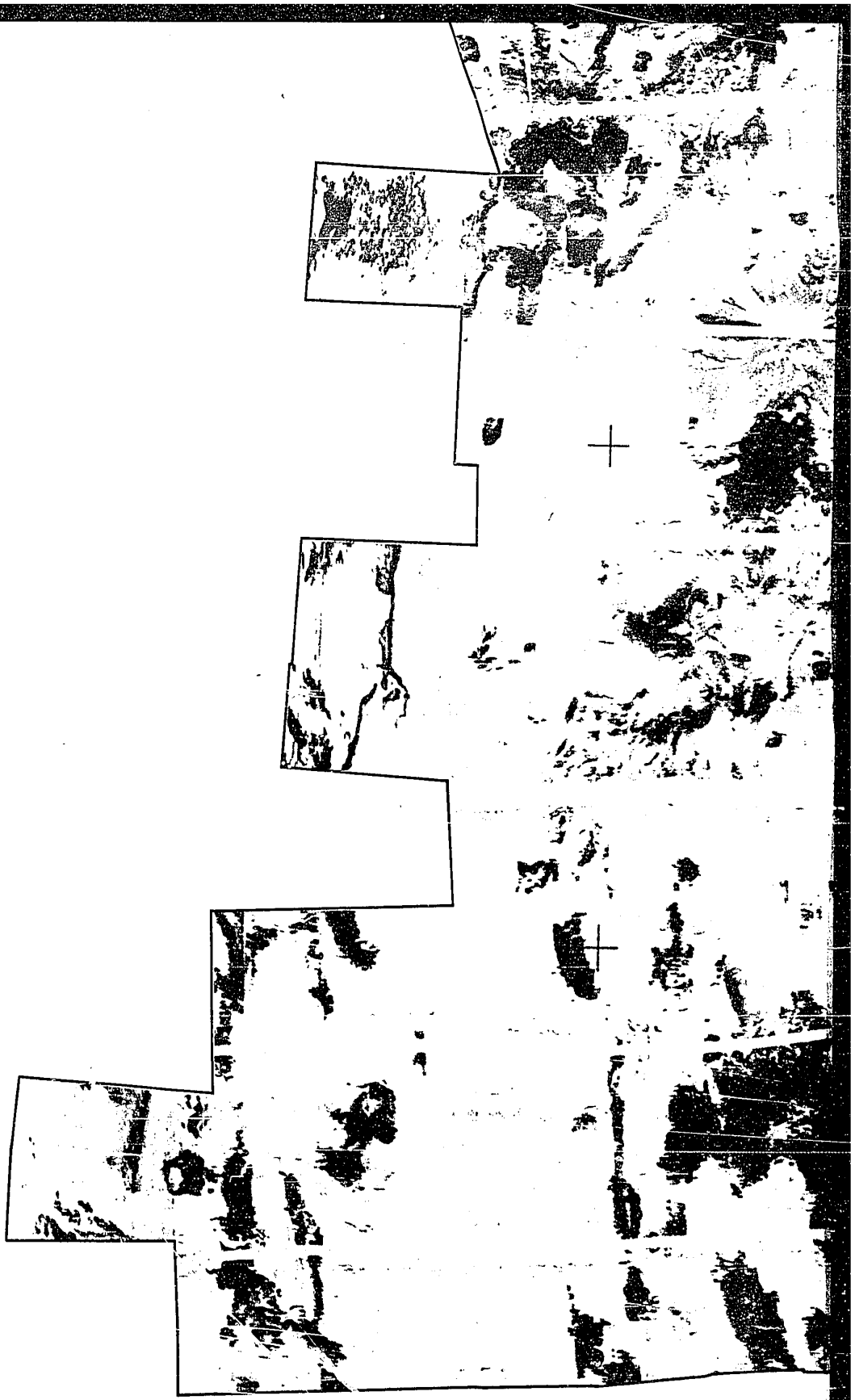

国土地図株式会社印刷（1色刷）

139°50'E

1 : 200,000

5 0 5 10 15 20km

15 20km

PLEASE NOTE:

Oversize maps and charts are filmed in sections in the following manner:

LEFT TO RIGHT, TOP TO BOTTOM, WITH SMALL OVERLAPS

The following map or chart has been refilmed in its entirety at the end of this dissertation (not available on microfiche). A xerographic reproduction has been provided for paper copies and is inserted into the inside of the back cover.

Black and white photographic prints (17" x 23") are available for an additional charge.

University Microfilms International

Appendix C

海 洋 地 質 図 31
MARINE GEOLOGY MAP SERIES 31

TORI

B. テイラー・G. ブラウン・D. ハッソン・P. フライヤー
ハワイ大学

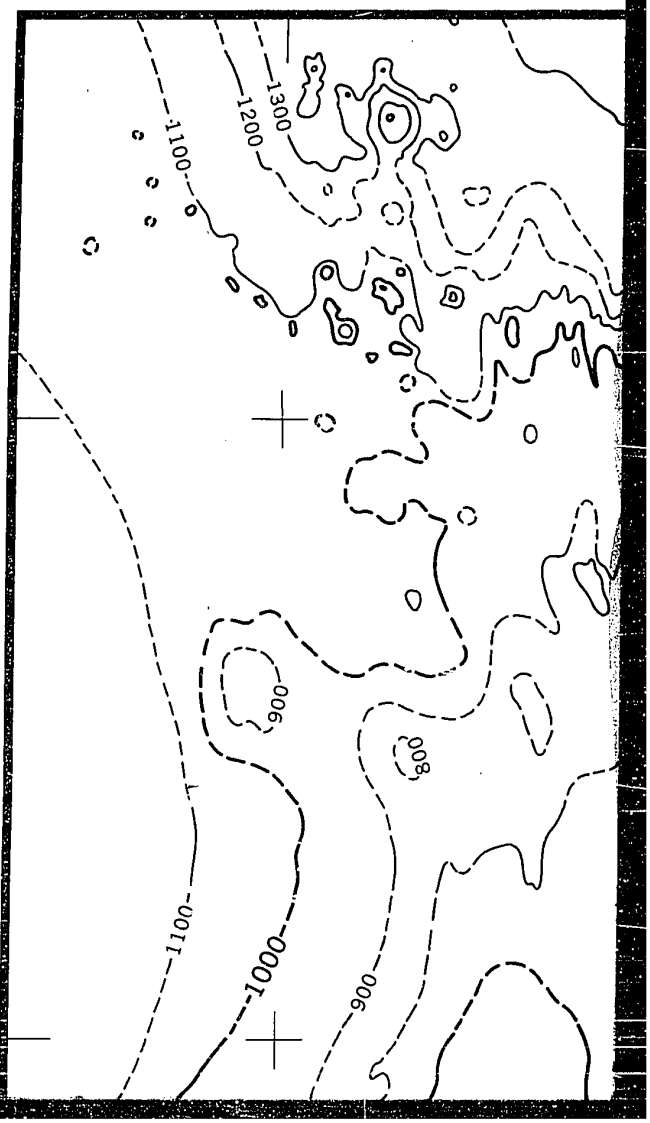

スミスリフト及び鳥島リフト地形図

BATHYMETRY OF SUMISU AN
TORISHIMA RIFTS, IZU-OGASAWARA

1：200,000

D. ハッソン・P. フライヤー

Brian TAYLOR, Glen
Hawaii Institute of

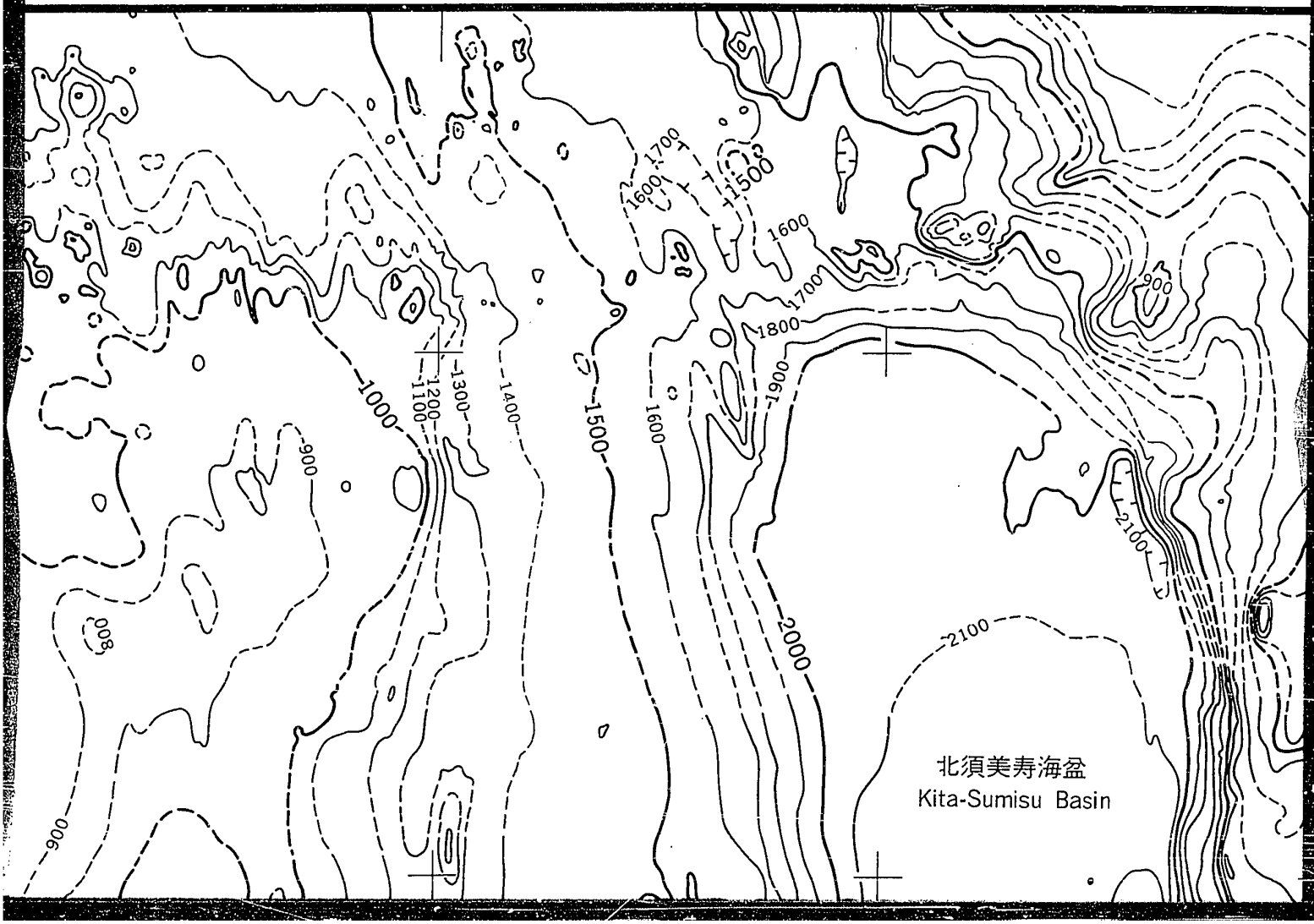

フト地形図

MISU AND
ASAWARA ARC

Brian TAYLOR, Glenn BROWN, Donald HUSSONG and Patricia FRYER
Hawaii Institute of Geophysics, University of Hawaii

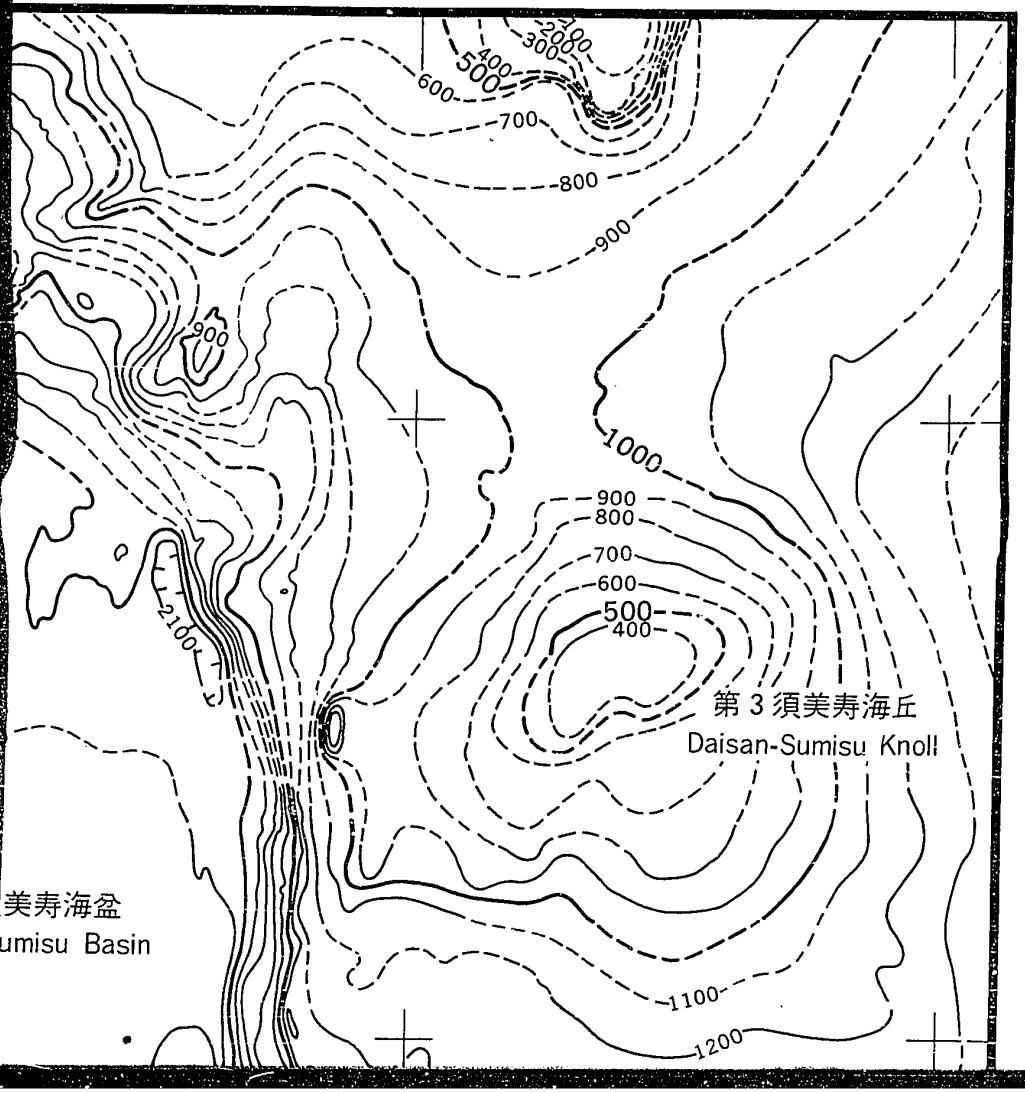

付　　記

SeaMARC II 装置は，曳航体の両側に2組ずつ配置されたトランスデューサ・アレイの反射波の位相差を用いて，もどってくる波の到来角を測定している（Blackinton, 1986）．SeaMARC II による海底地形データが得られなかったところでは，GSJ と HIG による数値化された3.5kHzサブボトムプロファイラ・データが用いられた（図の点線部分）．

Notes

To resolve bathymetry the SeaMARC II instrument measures the arrival angle of returning echoes, using the difference in echo phase at two transducer arrays, one on each side of the instrument (Blackinton, 1986). In areas lacking SeaMARC II bathymetric data, digitized 3.5-kHz data from the Geological Survey of Japan and the Hawaii Institute of Geophysics were used (dashed lines). Collection and processing of SeaMARC II data was funded by the United States National Science Foundation.

BLACKINTON, G. (1986) Bathymetric mapping with Sea MARC II: An elevation angle measuring side-scan sonar system. Ph.D.Diss., Univ. of Hawaii, 145pp.

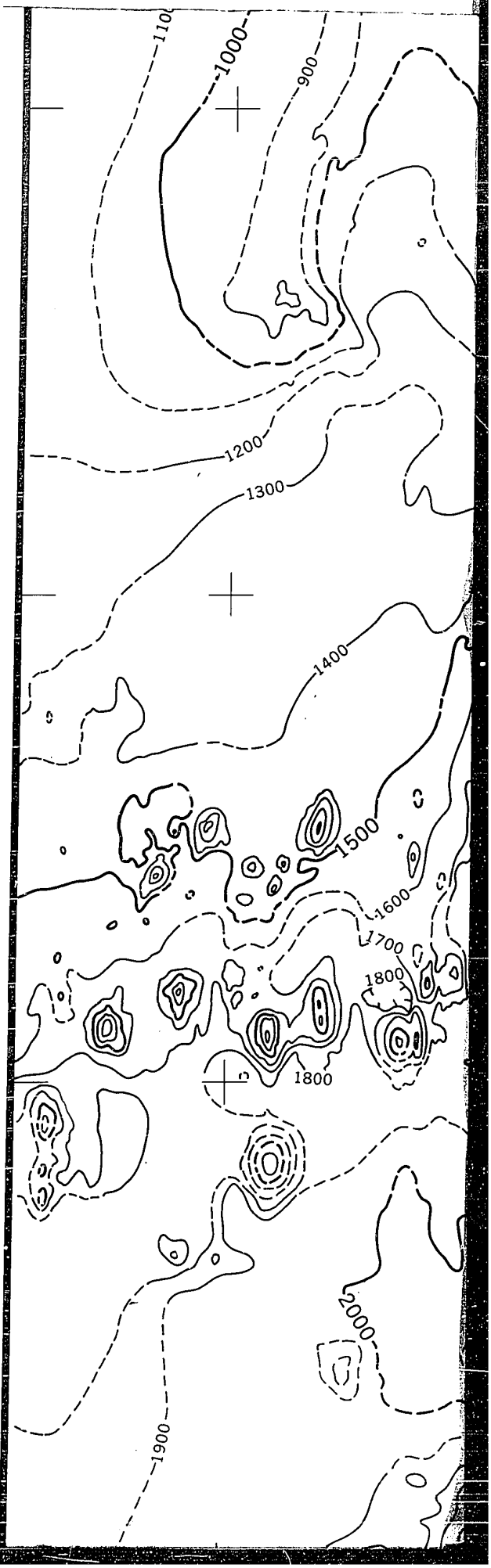
1100
1000
900
1200
1300
1400
1500
1600
1700
1800
1800
2000
1900


Kita-Sumisu Basin
南須美寿海盆
Minami-Sumisu Basin
900
1000
1100
1200
1300
1400
1500
1600
1700
1800
1900
2000
2100
2200

BLACKINT
MARC
sonar

BLACKINTON, G. (1986) Bathymetric mapping with Sea MARC II: An elevation angle measuring side-scan sonar system. Ph.D. Diss., Univ. of Hawaii, 145pp.

31°N

30°40'N

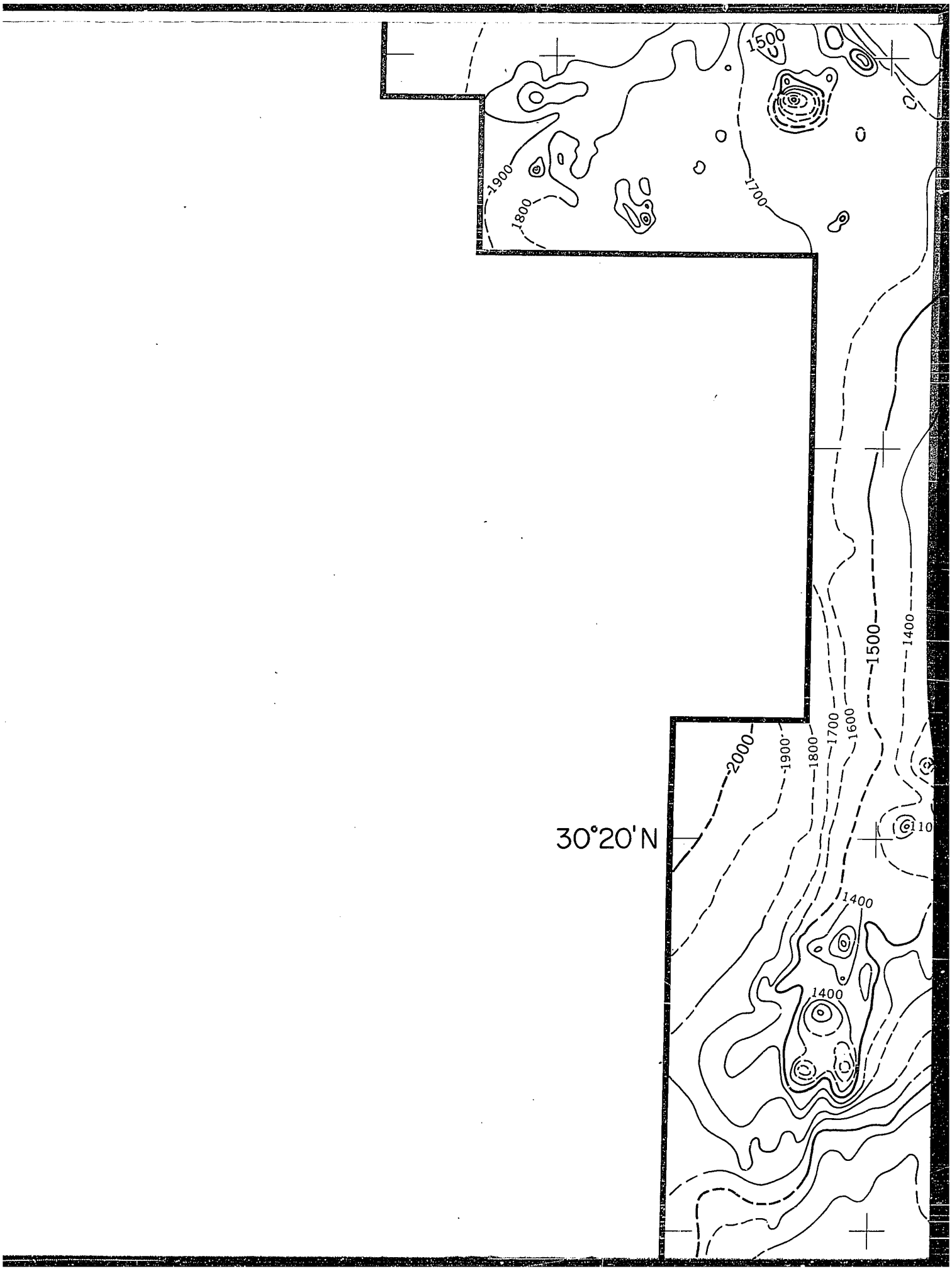
1500
1900
1800
1700
2000
1900
1800
1700
1600
1500
1400
30°20'N
1400
1400

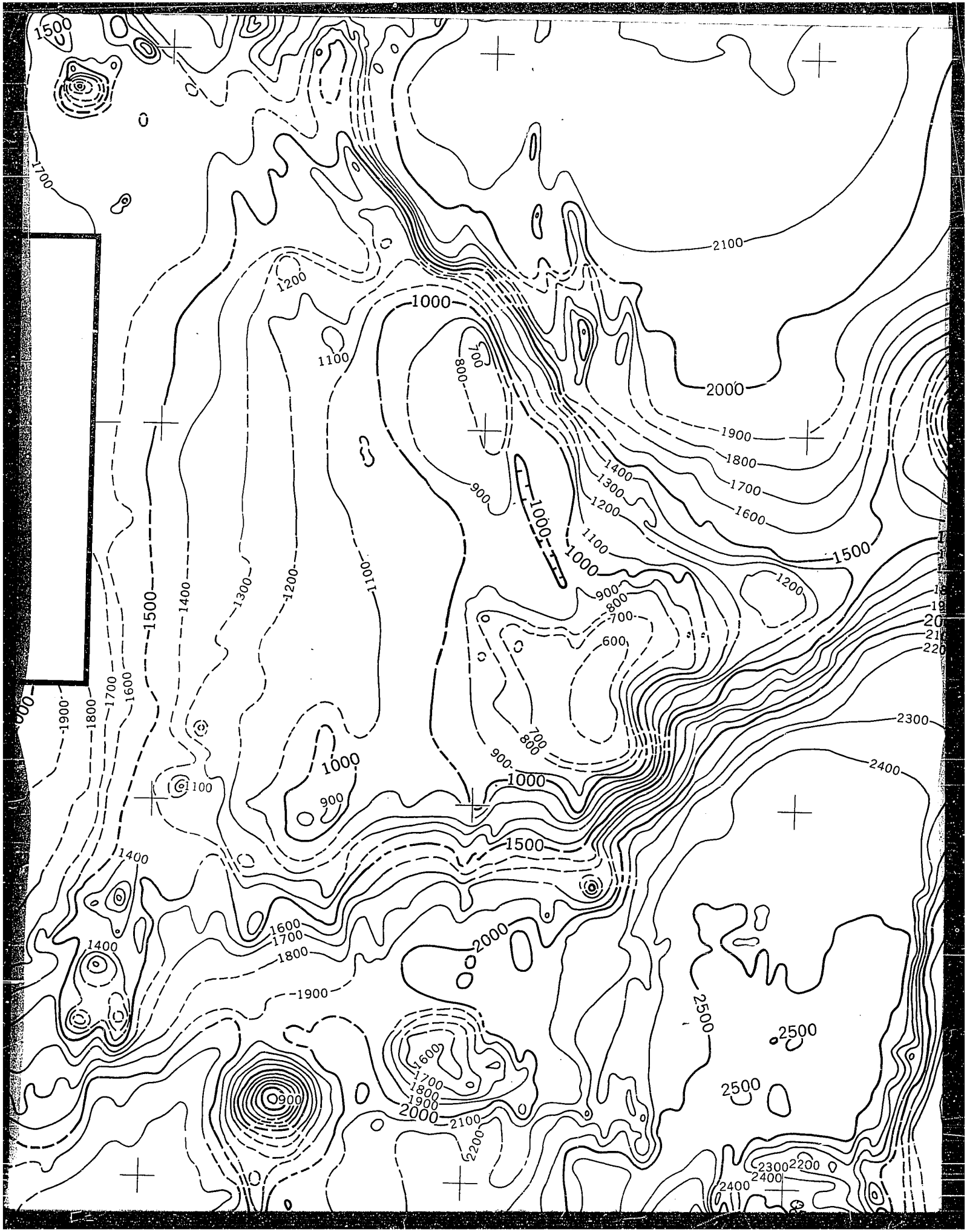
1500
1700
2100
1200
1000
1100
800
2000
1900
1800
1400
1300
1200
1700
1600
900
1000
1100
1000
1500
1200
900
800
700
600
1500
1400
1300
1200
1100
1900
1800
1700
1600
2300
2400
1000
900
1100
1000
900
700
800
1500
1400
1600
1700
1800
1900
2000
2500
2500
2500
1600
1700
1800
1900
2000
2100
2200
2300
2200
2400
2400

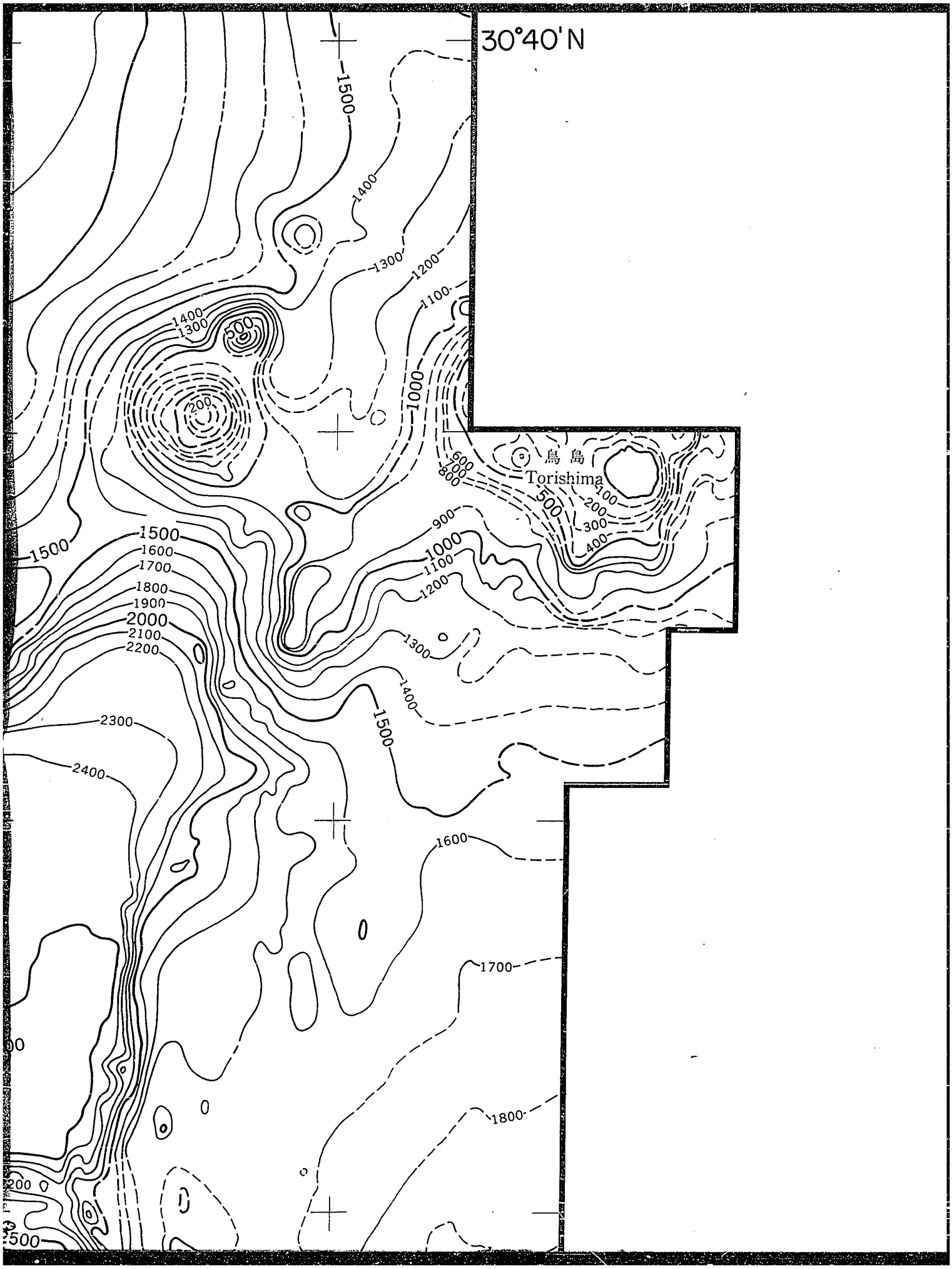
30°40'N
鳥島
Torishima
1500
1400
1300
1200
1100
1000
900
800
500
200
100
300
400
1600
1700
1800
1900
2000
2100
2200
2300
2400
0

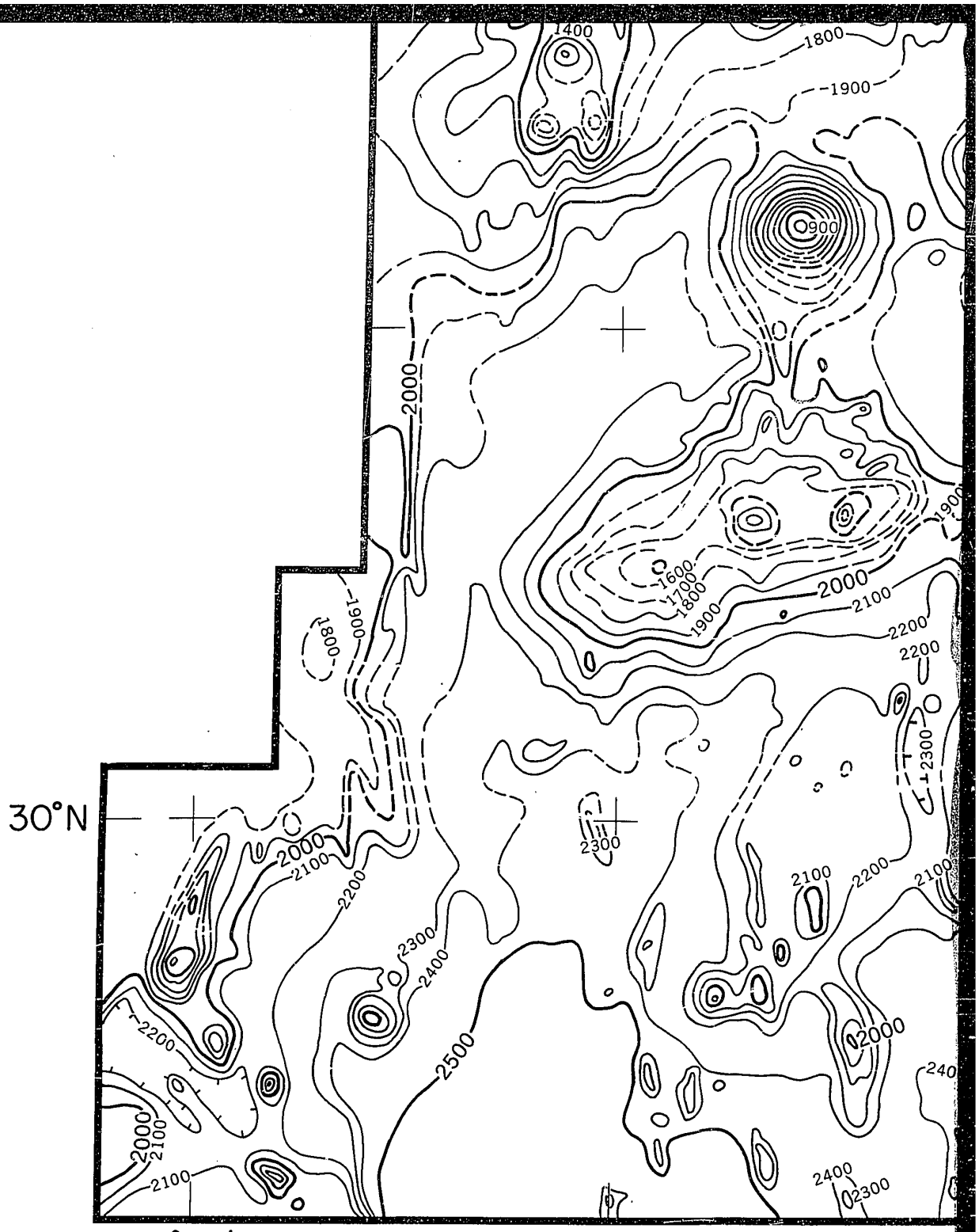

昭和63年3月25日発行

海上保安庁許可 第632508号

国土地図株式会社印刷（1色刷）

5

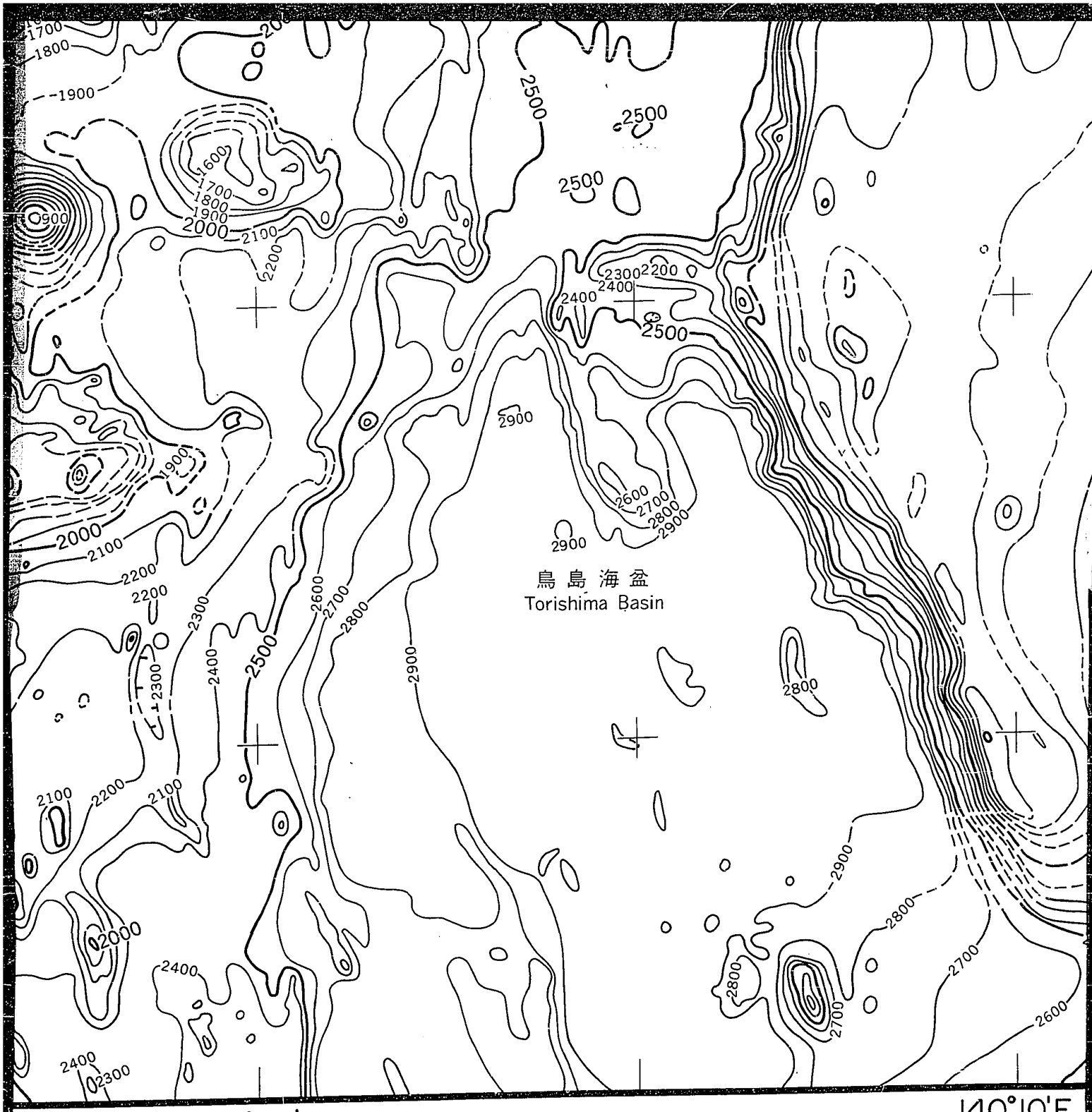

GEOLOGICAL

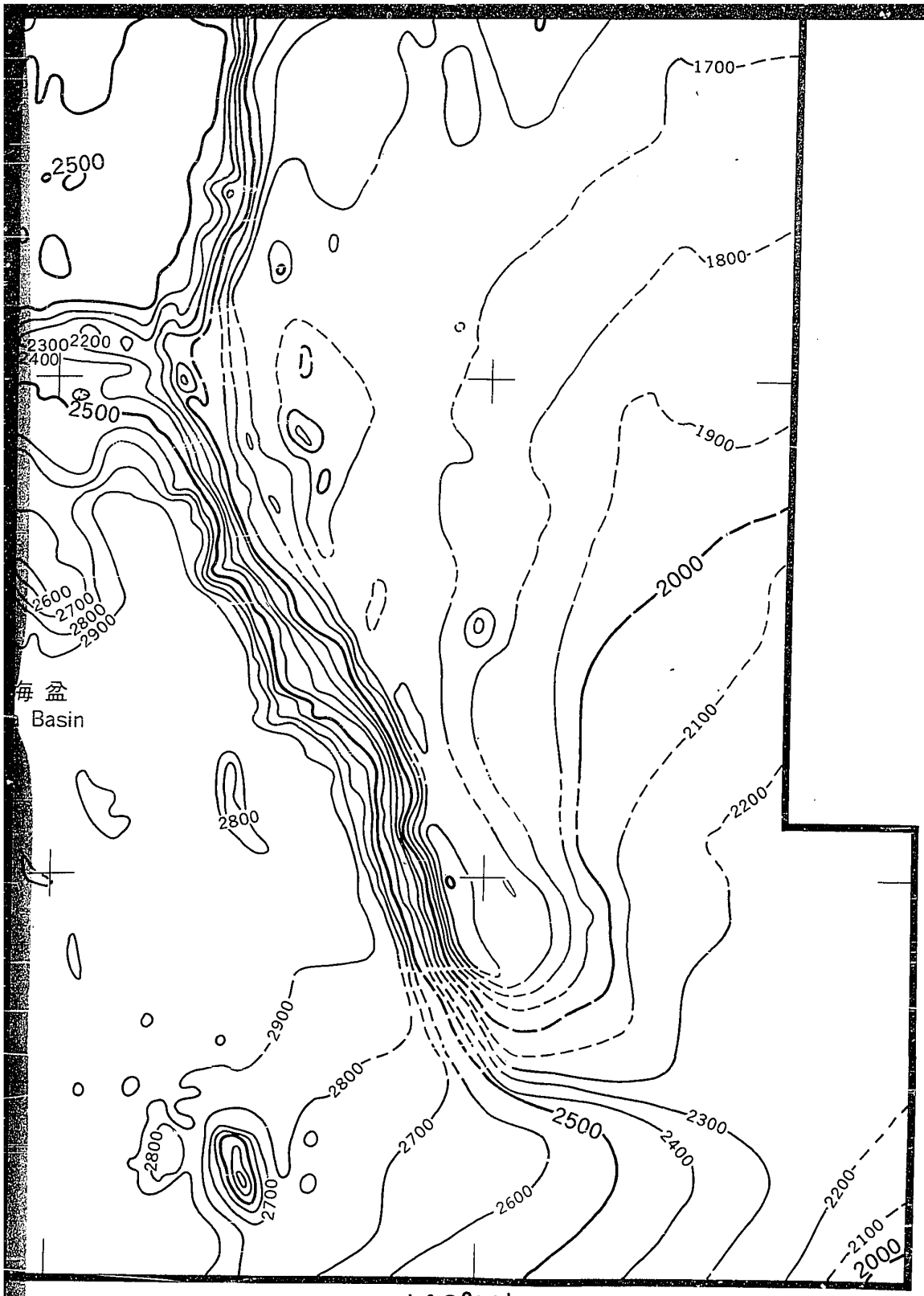

水深……メートル
Soundings in meters

PLEASE NOTE:

Oversize maps and charts are filmed in sections in the following manner:

LEFT TO RIGHT, TOP TO BOTTOM, WITH SMALL OVERLAPS

The following map or chart has been refilmed in its entirety at the end of this dissertation (not available on microfiche). A xerographic reproduction has been provided for paper copies and is inserted into the inside of the back cover.

Black and white photographic prints (17" x 23") are available for an additional charge.

University Microfilms International

Appendix D

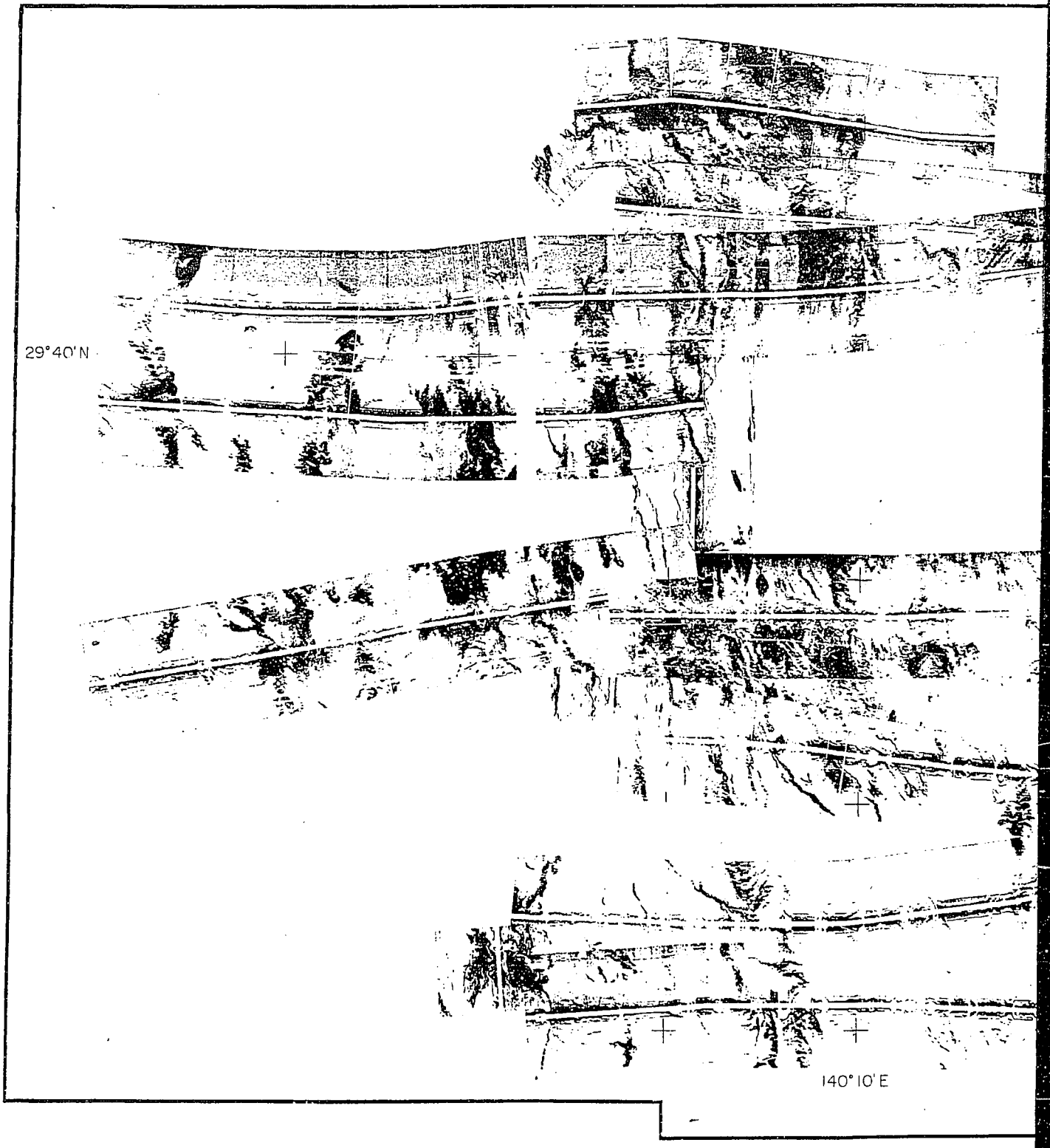
29°40'N
140°10'E

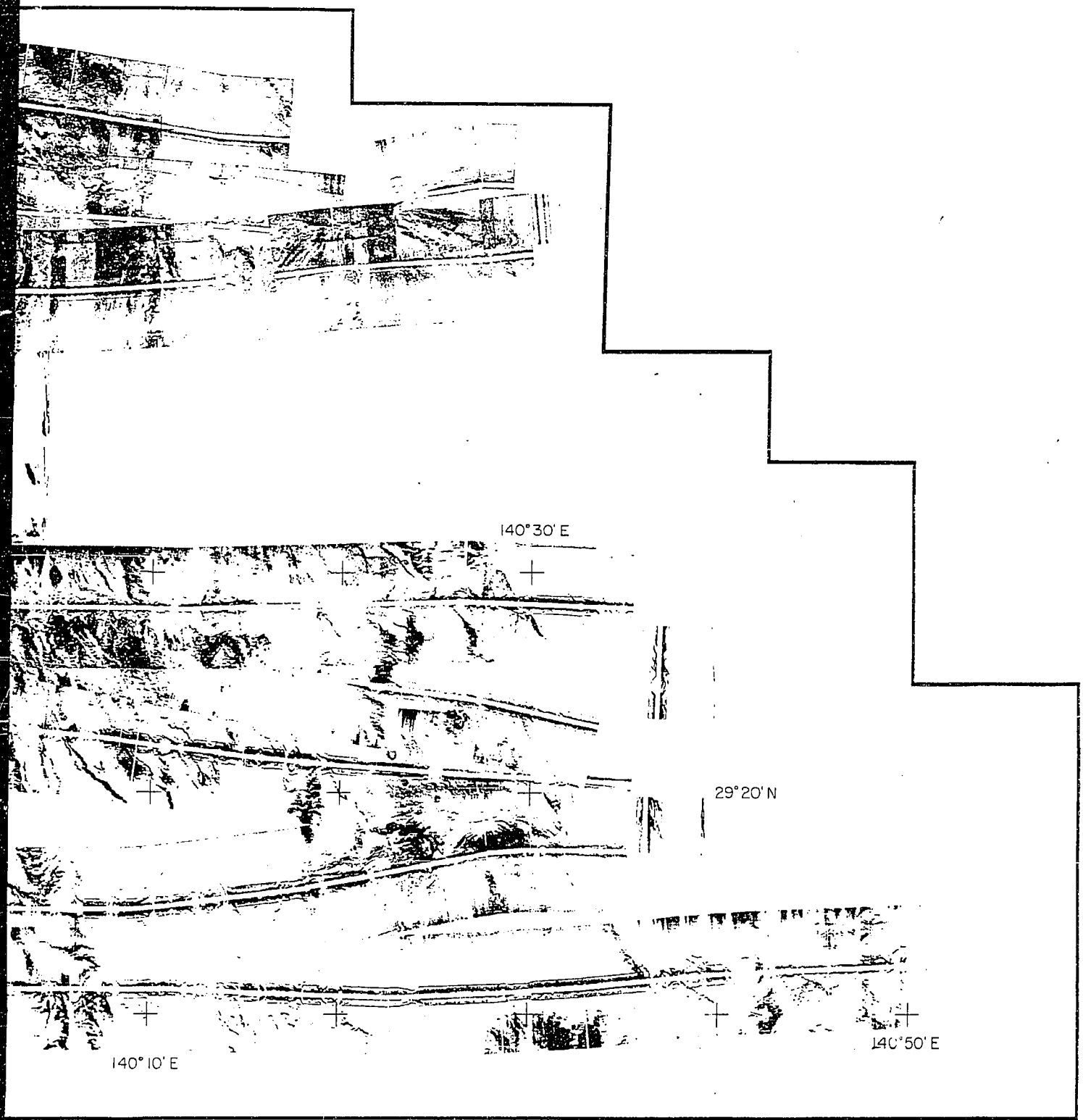
140°30' E
29°20' N
140°10' E
140°50' E